SUBSYSTEM QUANTUM MECHANICS

AND

ITS APPLICATIONS TO CRYSTALLINE SYSTEMS

By

Peng Fei Zou, M.Sc.

A Thesis

Submitted to the School of Graduate Studies

in Partial Fulfillment of the Requirements

for the Degree

Doctor of Philosophy

McMaster University

SUBSYSTEM QUANTUM MECHANICS AND ITS APPLICATIONS

DOCTOR OF PHILOSOPHY (1993) McMASTER UNIVERSITY

(Chemistry) Hamilton, Ontario, Canada

TITLE: SUBSPACE QUANTUM MECHANICS

AND ITS APPLICATIONS IN CRYSTALLINE SYSTEMS

AUTHOR: Peng Fei Zou, M.Sc. (Jilin University, China)

SUPERVISOR: Professor R. F. W. Bader

NUMBER OF PAGES: xii, 249

ABSTRACT

This thesis reports results of the author's investigations along the theme that both dynamic and static properties of molecules and solids can be expressed in terms of their parts from theoretical and applied aspects. Specifically, the following four main results are obtained: (1) A topological analysis of the charge density in crystals has been developed. This is an extension of the theory of molecular structure to crystalline systems. Relationships between the bulk properties of a crystal and its topological structure have been established. A comparison of the topological properties of molecules and crystals have been made. (2) The theory of atoms in molecules has been extended to a crystal and yields a variational definition of a Wigner-Seitz cell. This definition maximizes the relation of the cell to the physical form exhibited by the charge density and the derived structure factors that account, in a natural way, for the observed intensities of scattered electrons and X-rays. It has been demonstrated that the theory of atoms in molecules and crystals can provide a way to model the behaviour of solids. This is done through the use of the fact that atomic properties are often transferable from one system to another. (3) The subsystem variational principle has been reformulated in terms of quantum field theoretical language and the subsystem Feynman path integrals of electrons have been obtained using the coherent representation. This part contributes to the foundation of the

theory of atoms in molecules and crystals. (4) Both dynamic and static quantum mechanical subspace techniques have been extensively investigated. A new variational method has been derived for embedding one system in another using the R-matrix formalism within the density functional approach. A formal subspace perturbation scheme has been proposed. These methods aim to obtain the charge distribution of a subsystem starting from known reference systems.

Before I came here I was confused about this subject. Having listened to your lecture, I am still confused, but on a higher level.——Enrico Fermi

Acknowledgements

I wish to thank all the members of the Theoretical Chemistry Laboratory for their assistance, cooperation, encouragement and friendship during my stay at McMaster. In chronological order they are: Cheng Chang, Keith Laidig, Danny Legare, Jim Cheeseman, Paul Krug, Todd Keith, Paul Popelier, Ian Bytheway and Richard Bone. Particularly, I would like to thank Keith Laidig and Cheng Chang for their help in my early time here.

I would like to thank my English tutors Alice Hwang and Pam Doering. Pam contributed a lot of her precious time in proof-reading this thesis and helping me to correct the grammar.

I also wish to thank my wife Jie Tao, my son Albert and those many friends who don't know the first thing about chemistry but who have contributed so much to my time in Hamilton. Without Albert's understanding of the phrase "Daddy's working", I was probably still writing the Chapter N of this thesis.

I would like to give my special thanks to Richard Bader, my supervisor. I am grateful for many encouraging, inspiring and enthusiast discussions. I thank him for providing me a way of thinking, that is to understand things in terms their parts.

My education and the opportunity to do scientific research have been made possible through the generosity of many people and institutions. These patrons are: my parents, my sisters, Jiaying University, Jilin University, University of Sciences and Technologies of China and McMaster University. I am grateful for their help and support.

This Thesis Is Dedicated to My Parents.

Table of Contents

List of Figures

List of Tables

INTRODUCTION

What's a wave function for? A wave function is a scheme keeping track of all that happened in the past——a time integral over the past and you get a present function, which subsumes all the details from the past motion (of course, when you take an expection you can think of something for the future, or whatever). And, the real point is, that the quantities you are interested in are, in some respect, not sensitive to the details of the past if you only can remember enough in the form of the wave function. Now, in field theory, what's going on here and what's going on over there and all over space is more or less the same. Why do we have to keep track in our functional of all the things that are going on over there while we are looking at the things that are going on over here? In other words, we should only write down a wave function telling us how things will vary if we concentrate on the fields $A(\vec{x})$ in a certain region. How does it depend upon the $A(\vec{x})$ in this general region? Then we can see how the wave functions vary except for those variations coming from the values of $A(\vec{x})$ over there. But somehow or other we almost know that from what we know here. So, is there a way of keeping track of things that are going on in other places as well as in the past, so we don't have so many variables to drag up? It's really quite insane, actually: we are trying to find the energy by taking the expectation of an operator which is located here and we present ourselves with a functional which is dependent on everything all over the map. That's something wrong. Maybe there is some way to surround the object, or the region where we want to calculate things, by a surface and describe what things are coming in across the surface. It tells us everything that's going on outside.

——Richard P. Feynman, 1987

There emerged two distinguishable ways of setting out to explain the behaviour of solids: the macroscopic way and the atomistic way. Today these two ways supplement each other. For example, you can distinguish macroscopic and atomistic approaches toward crystalline symmetry, as toward the rest of the physics of solids, and the two make an interesting contrast. From the macroscopic point of view, the symmetry of a crystal is the symmetry of its observable properties. From the atomistic point of view, the symmetry of a crystal is that of its constituent atoms and that of the arrangement of these atoms. Since all the observable properties of a crystal are contributed by its atoms, the two points of view must yield results that are consistent with each other.

Before much was known about atoms and their behaviour, only the macroscopic approach was available. This way of thinking, sometimes called the phenomenological way, does not inquire into the ultimate construction of a solid. It reaches its conclusions without needing to know that construction. Nature is so diverse that she can provide exceptions to any but rigorous rule. But the macroscopic approach, from which a solid appears to be a structureless piece of matter, can do little in finding the exceptions and nothing to explain them (Holden, 1965). The ideal of the microscopic or atomistic approach is to penetrate deeply into the behaviour of solids and to deduce their observed properties from a knowledge of the way they are constructed by their constituent atoms and from a knowledge of the physical behaviour of those atoms. The goal of atomistic approach is not only qualitatively understanding the physical behaviour but also quantitatively predicting the properties of solids.

Historically, the realization of the role of atoms and the interactions between them in the behaviour of solids can be traced back to Sir Isaac Newton, even before the development of the concept of a chemical bond:

The Parts of all homogeneal hard Bodies which fully touch one another, stick together very strongly. And for explaining how this may be, some have invented hooked Atoms, which is begging the Question .... I had rather infer from their Cohesion, that their particles attract one another by some Force, which in immediate Contact is exceeding strong, at small Distances performes the chymical Operations above-mention'd and reaches not far from the Particles with sensible Effect .... There are therefore Agents in Nature able to make the Particles of Bodies stick together by very strong Attractions (Sir Isaac Newton, *Optics*, 1704).

About a century after Newton, Dalton proposed the atomic hypothesis that marked the birth of chemistry as a branch of science. In the atomic hypothesis, substances are identified and distinguished one from another by the elements they contain. The properties of each element are determined by the atoms unique to that element. Chemistry is the study of matter at the atomic level. Before the close of Dalton's century, there had evolved from his atomic hypothesis the concept of molecular structure. A molecular structure is a notion that the molecule consists of a collection of atoms linked by a network of bonds, the bonds imparting the structure. With the knowledge of the molecular structure of a system, a chemist is able to bring to bear all the knowledge of modern chemistry——the determination of molecular structure and the study of the change of one structure into another, for he understands the properties of a substance in terms of the properties of its constituent atoms and of the bonds that link them. The molecular structure hypothesis has been remarkably successful, through the use of relatively simple models of bonds, in characterizing and rationalizing chemical observations. A great body of structural, spectroscopic and thermochemical data is rationalized in terms of the bonds assigned in this manner through empirically defined quantities such as bond energies and bond force constants.

It took about 50 years after the discovery of quantum mechanics to realize the physical basis for the molecular structure hypothesis (Bader and

Nguyen-Dang, 1981; Bader, Nguyen-Dang and Tal, 1981). Given a state function, or a good approximation to it, how does one obtain from it a description of a system's properties in terms of its atoms and bonds which, from a chemists' point of view, summarize in a concise manner its important chemical properties? In the 1970s, Bader and his coworkers developed a theory of molecular structure based on the topological properties of the observable charge density. This theory provides rigorous definitions of structural elements: atom, bond, ring and cage. The atom so defined leads to a variational definition (Schwinger, 1952) of its average properties and can be identified as the chemical atom which exhibits characteristic sets of properties and these properties are, in many instances, transferable between different systems. The molecular structure defined in the theory reveals that the structure is a generic property of a system. The generic property of a structure is the essential understanding and original intent associated with the notion of structure in chemistry.

The central theme of the history of the theories of molecular structures is to understand molecular behaviour in terms of structure elements. The principal elements of a structure are the atoms and the bonds. A bond represents the interaction between the atoms in a molecule. An atom represents the smallest carrier of a set of properties characteristic of the element. These properties are often transferable from one system to another if the atom in both systems has a similar first neighbour environment. The transferable property of an atom implies that the quantities we are interested in are not sensitive to the long range environment or that "*what's going on here and what's going on over there*" is "*more or less the same*". Therefore "*we should only write down a wave function telling us how things will vary if we concentrate on the*" electronic field in an atom. However, in the quantum mechanics of molecules and crystals, "*we are trying to find the energy by taking the expectation of an operator which is located here and we present ourselves with a functional which is dependent on everything all over the map. That's something wrong*" (Feynman, 1988). One part of this thesis is dedicated to the development of a way to "*write down a wave function telling us how things will vary if we concentrate on*" an atom or a functional group.

The concepts of an atom, bond, ring and cage play the central role in the understanding of crystal properties. In pursuing the understanding of the behaviour of solids, a solid state scientist first separates out a particular phenomenon for study and makes an educated guess at what atomic behavior is largely responsible. He then sets up a model which embodies that behaviour and neglects all the confusing details he considers to be unimportant. He calculates how the model will behave and compares his answer with the results of experiments on actual solids. When constructed from first principle, mathematical equations describing the behaviour of a collection of particles become very difficult to solve and, on the other hand, the results of the solutions are too opaque to give insight. The reason for this is that the physical basis of the structural elements for solid systems has not been realized and, therefore, rigorous definitions for the structure elements cannot be given. Another part of this thesis aims to establish a theory of crystal structure. This theory is an extension of the theory of atoms in molecules. The theory of atoms in crystals provides a way to qualitatively understand and quantitatively predict the properties of solids in terms of the atoms in the solids. This fulfills the goal of atomistic approach.

The central theme of this thesis is to demonstrate the role of a subsystem (region) in both the dynamic and static behaviour of molecules and solids from theoretical and applied aspects. This theme is unfolded through:

(1) The Atomic Variational Principles

The atomic variational principles show that Dalton's atomic hypothesis has a quantum mechanical basis (Bader and Nguyen-Dang, 1981). This is done by demonstrating that atoms are objects in real space and are defined through a

partitioning of real space as determined by the ›pological properties exhibited by a charge distribution (Srebrenik and Bader, 1975; Srebrenik et al, 1978; Bader, 1990). This partition scheme leads to a variational definition of the average properties of an atom in a molecule or a solid.

(2) The Subsystem Quantum Mechanical Techniques

The subsystem quantum mechanical techniques are developed in response to Feynman's intuitive statement: "*Maybe there is some way to surround the object, or the region where we want to calculate things, by a surface and describe what things are coming in across the surface. It tells us everything that's going on outside.*"(Feynman, 1988).

(3) The Topological Structures of Crystals

The topological theory of molecular structure (Bader, Nguyen-Dang and Tal, 1981; Lader, 1990) is extended to crystalline systems. The theory rigorously define all the structural elements: an atom, bond, ring and cage based on the experimentally and theoretically determinable charge density of a system. The topological properties of charge density are exemplified by crystals diamond, silicon and zinc blende compounds: AlP, BN, BP and SiC. Applications of the theory are developed.

(4) The Role of Atoms in Crystals in Electron and X-Ray Scattering Theory

The theory of atoms in crystals is applied to interpret electron and X-ray diffraction intensities. The theory is able to provide a model and quantitatively predict the diffraction amplitudes.

The thesis is written in a way such that every chapter is relatively independent and pursues the central theme in different aspects.

1. ATOMIC VARIATIONAL PRINCIPLE

The opponents of the atom are generally content to point to its contradictions and reject it as unfruitful for science. A rash form of caution, for without the atom science falls.

——Hans Vaihinger, *The Philosophy of As If*

1.1 Introduction

Most of chemical and physical knowledge of molecules is classified based on the concept of an atom and functional grouping of atoms. The chemical atom or functional group is characterized by a set of properties that can be transferred from one system to another similar system. Examples of these transferable properties are X-ray atomic scattering factors, electric and magnetic polarizabilities, chemical reactivities, etc (Pauling, 1960; Bader 1990). A lot of chemical and physical information about atoms in molecules was known long ago from the great body of chemical facts. Modern experimental and theoretical methods are able to provide precise knowledge of nuclear geometries and electronic charge distributions of molecules or crystals.

Based on the electronic charge distribution of a molecule, an atom is defined by a region in real space bounded by the zero flux surface of the

gradient vector field of the electronic charge density (Bader, 1990), that is the atomic surface is defined by

$\nabla\rho(\mathbf{r})\cdot\mathbf{n}(\mathbf{r}) = 0$ for any point $\mathbf{r}$ on the surface

where $\mathbf{n}(\mathbf{r})$ is the unit vector normal to the surface. Bader and his research group have shown that an atom defined in this way not only recovers the atom in the chemical sense, but also behaves as an open quantum subsystem which obeys Schwinger's variational principle. The purpose of this chapter is to generalize the previously established atomic variational principle in the Shrödinger picture to the quantum particle field formulation which allows one to create and annihilate particles in a subsystem. The introduction of creation and annihilation operators into the theory enables one to study dynamic processes for an atom in a molecule. Using the coherent state representation of Fermions, the Feynman path integrals for an atom in a molecule are also investigated in this chapter. We show that the atomic path integrals in the coherent representation are related to the total system by the multiplicative law. The initial purpose of the construction of Feynman path integrals for an atom is to obtain an integral form for the differential atomic variational principle. Historically, two formulations of quantum mechanical variational principles were invented, respectively, by Schwinger and Feynman. Schwinger (1951) created the differential form of the quantum variational principle, and Feynman (1948) invented the integral form.

Variational principles exist in almost all branches of physics: in optics, classical mechanics, electrodynamics, hydrodynamics, quantum mechanics (Yourgrau and Mandelstam, 1979), quantum field theory (Schwinger, 1948 and 1952; Feynman, 1948 and 1949; Mandl and Shaw, 1990) and solid state physics

(Greiner and Mahler, 1992), etc. Fermat's principle of least time in geometrical optics was probably the first variational principle realized in physics. The variational principles as well as the principles of symmetry are the two basic guidelines for the establishment of modern quantum field theory. The importance of variational principles in physics may be best summarized by Planck, the father of quantum theory, in his philosophical view on the unique principle in physics. He said: "As long as there exists a physical science, it has as its highest and most coveted aim the solution of the problem to condense all natural phenomena which have been observed and are still to be observed into one simple principle, that allows the computation of past and more especially of future processes from present ones. ... Amid the more or less general laws which mark the achievements of physical science during the course of the past centuries, the principle of least action is perhaps that which, as regards form and content, may claim to come nearest to that ideal final aim of theoretical research." (Planck, 1915)

A paper describing the field theoretic development of the variational principle and of the path integrals for atoms in molecules has been published and appended at the end of this chapter. Sections 2-4 of this chapter provide the introduction to and the development of the work summarized in the paper. Section 2 describes the recipe for the second quantization of Fermions. Section 3 introduces the coherent representation of Fermions. The mathematical basis of Grassmann algebra is also given in this section. Section 4 gives the general quantum variational principle for the Fermion field and discuss its physical consequences.

1.2 Second Quantization of Fermions

A quantum particle is characterized by: (1) The commutator $[x_i, p_j] = i\hbar\delta_{ij}$ where $\mathbf{r}=(x_1,x_2,x_3)$ and $\mathbf{p}=(p_1,p_2,p_3)$ are, respectively, the position and momentum operators; (2) The time dependence for a physical operator $Q(\mathbf{r},\mathbf{p})$ is given by Heisenberg equation $i\hbar\dot{Q} = [Q,H]$ and the state vector evolves according to Shrödinger's equation $i\hbar|\dot{\Psi}\rangle = H|\Psi\rangle$. The eigenvalues of the position operator $\mathbf{r}$ are identified as the points in real space. Real space enters quantum mechanics through the use of the representation of the eigenvectors of the position operator. Point properties, which are those properties determined at each point in real space, for example, the electronic charge density, can be discussed only in this representation. For an N-particle (N > 1) system, the configuration space with 3N (4N if including spin) coordinates are needed to represent the quantum mechanics of the system. The evaluation of a point property requires the integrations for the N-1 particle coordinates. This inconvenience can be easily overcome, however, if one makes use of particle field theory. The field operators in field theoretical formulation are described by a complete basis set and by the creation and annihilation operators. The basis set in the field operators takes real space into consideration and the creation and annihilation operators give the quantum statistics of the particles. All of the observable operators can be expressed in terms of field operators, and the number of particles in a specific system does not enter into the formalisms of the operators. The natural combination of quantum particles and space produces a convenient tool to discuss the point properties for a many-particle system.

This is part of the motivation to introduce the particle field formulation of quantum mechanics into the theory of atoms in molecules. Another purpose is to introduce creation and annihilation operators to characterize the nonconservative particle number in a subsystem for a dynamic process. The total particle number (i.e. including electrons and nuclei) is conserved in a chemical or other low energy dynamic processes for the total system. However, for a subsystem the particle number is not necessarily conserved.

In order to develop the particle field formulation, we first need to introduce the creation and annihilation operators. For a complete set of state vectors ($|\alpha\rangle$), there is a creation operator $a_\alpha^\dagger$ and an annihilation operator a_α related to the vector $|\alpha\rangle$ by

$$|\alpha\rangle = a_\alpha^\dagger|0\rangle \text{ and } a_\alpha|\alpha\rangle = |0\rangle \qquad (1)$$

where $|0\rangle$ is the vacuum state which is defined as a normalized no-particle state and therefore $a_\alpha|0\rangle = 0$ for any α. The Fermion creation and annihilation operators satisfy the following equations which determine the statistical properties of Fermions:

$$a_\alpha a_\beta + a_\beta a_\alpha = 0, \quad a_\alpha^\dagger a_\beta^\dagger + a_\beta^\dagger a_\alpha^\dagger = 0$$

$$[a_\alpha, a_\beta^\dagger]_+ = a_\alpha a_\beta^\dagger + a_\beta^\dagger a_\alpha = \delta_{\alpha\beta}, \qquad (2)$$

The Fock space for the many Fermions is

$$|0\rangle, \quad (a_\alpha^\dagger|0\rangle), \quad (a_{\alpha_1}^\dagger a_{\beta_2}^\dagger|0\rangle), \quad \ldots, \quad (a_{\alpha_1}^\dagger \ldots a_{\alpha_N}^\dagger|0\rangle), \ldots$$

The N Fermion states is a vector in the space expanded by the basis $(a_{\alpha_1}^\dagger \ldots a_{\alpha_N}^\dagger|0\rangle)$. In terms of creation and annihilation operators one particle and two particle operators can be expressed as

$$T = \sum_{\alpha\beta} T_{\alpha\beta} a_\alpha^\dagger a_\beta \qquad (3)$$

$$V = \frac{1}{2} \sum_{\alpha\beta\mu\nu} V_{\alpha\beta,\mu\nu} a_\alpha^\dagger a_\beta^\dagger a_\nu a_\mu \qquad (4)$$

where

$T_{\alpha\beta} = \langle\alpha|T|\beta\rangle$, and $V_{\alpha\beta,\mu\nu} = \langle\alpha(1)\beta(2)|V(1,2)|\mu(1)\nu(2)\rangle$

Field operators are defined in terms of the creation and annihilation operators and also of the single-particle state functions ($\langle\mathbf{x}|\alpha\rangle$)

$$\Phi(\mathbf{x}) = \sum_\alpha \langle\mathbf{x}|\alpha\rangle\, a_\alpha \text{ and } \Phi^\dagger(\mathbf{x}) = \sum_\alpha \langle\alpha|\mathbf{x}\rangle\, a_\alpha^\dagger \qquad (5)$$

where $\mathbf{x} = (s, \mathbf{r})$ is a point in spin-space. The commutation relationships for the field operators are obtained from eqn (2) and the completeness of the state vectors

$$[\Phi^\dagger(\mathbf{x}), \Phi^\dagger(\mathbf{x}')]_+ = [\Phi(\mathbf{x}), \Phi(\mathbf{x}')]_+ = 0$$

$$[\Phi^\dagger(\mathbf{x}), \Phi(\mathbf{x}')]_+ = \delta(\mathbf{x} - \mathbf{x}') \qquad (6)$$

In terms of the field operators the one- and two-particle operators of eqns (3) and (4) can be written as

$$T = \int d\mathbf{x} \Phi^+(\mathbf{x}) T(\mathbf{x}) \Phi(\mathbf{x}) \qquad (7)$$

$$V = \frac{1}{2} \int d\mathbf{x} d\mathbf{y} \Phi^+(\mathbf{x}) \Phi^+(\mathbf{y}) V(\mathbf{x},\mathbf{y})) \Phi(\mathbf{y}) \Phi(\mathbf{x}) \qquad (8)$$

1.3 Fermion Coherent States and Grassmann Algebra

The Slater determinants provide a natural and oft used basis for the Fock space. Another useful basis of the Fock space is that obtained from coherent states of fermions. A coherent state is defined as the eigenstate of a fermion annihilation operators. According to the definition of a coherent state $|\xi_\alpha\rangle$ which is related to an annihilation operator a_α, we have

$$a_\alpha |\xi_\alpha\rangle = \xi_\alpha |\xi_\alpha\rangle \quad (9)$$

where the eigenvalue ξ_α is a non-zero "number" to be specified. For Fermions the annihilation operators (a_α) satisfy the anticommutation relations

$$a_\alpha a_\beta + a_\beta a_\alpha = 0 \quad (10)$$

If $|\xi_\alpha \xi_\beta\rangle$ is the coherent state of both a_α and a_β, then from eqn (10) and the coherent state definition eqn (9), we have

$$\xi_\alpha \xi_\beta + \xi_\beta \xi_\alpha = 0 \quad (11)$$

Equation (11) shows that the nonzero *numbers* ξ_α and ξ_β anticommute! These anticommuting numbers are called Grassmann numbers (or variables) which originate from the work of mathematician Grassmann in the 19th century. The systematic use of Grassmann algebra in quantum field theory and statistics is however quite recent (Berezin, 1966; Negele and Orland, 1988; Itzykson and Drouffe, 1989). The Grassmann numbers are the "natural" numbers for the description of Fermions just as the commuting complex numbers are for Bosons. The necessary mathematical rules for Grassmann algebra and calculus (the mathematics of integration and differentiation) are introduced here for the use in the description of Fermions. The beauty of the use of Grassmann numbers is that this mathematical construction takes care of all the minus signs associated with permutational antisymmetry. Grassmann algebra is not only used in the quantization of Fermion fields, but is also widely used in solving statistical models. For example, in the Onsager's solution (1944) of two-dimensional Ising model (1925), he was able to turn the model into a Fermion free field theory.

1.3.1 Grassmann Algebra and Calculus

A Grassmann algebra is defined by a set of generators (η_α, $\alpha = 1,\ldots,N$)

which satisfy anticommuting relations

$$\eta_\alpha\eta_\beta + \eta_\beta\eta_\alpha=0 \tag{12}$$

where $\alpha,\beta = 1,\ldots,N$, in particular,

$$\eta_1^2 = \eta_2^2=\cdots= \eta_N^2 = 0 \tag{13}$$

Due to eqns(12) and (13), there are only 2^N independent elements obtained from the N generators

$$1,\ \eta_1,\ldots,\eta_N,\ \eta_1\eta_2,\ \ldots\ \eta_{N-1}\eta_N,\ \ldots\ \eta_1\eta_2\cdots\eta_N \tag{14}$$

The independent elements in eqn (14) serve as the basis for the Grassmann algebra. Any function in the Grassmann algebra can be linearly expanded into the basis given in eqn (14)

$$f(\eta) = f_0 + \sum_i^N f_i\eta_i + \sum_{i<j}^N f_{ij}\eta_i\eta_j +\cdots+ f_{1\ldots N}\eta_1\ldots\eta_N \tag{15}$$

where the coefficients $(f_{1\ldots k})$ are usual complex numbers. If $f_{i_1\cdots i_k}$ is chosen as an anticommuting function of $(i_1,\ldots,i_k)$, then eqn (15) can be rewritten as

$$f(\eta) = f_0 + \sum_i^N f_i\eta_i + \frac{1}{2!}\sum_{i,j}^N f_{ij}\eta_i\eta_j +\cdots+ \frac{1}{N!}\sum_{i_1\cdots i_N}^N f_{i_1\cdots i_N}\eta_{i_1}\cdots\eta_{i_N} \tag{16}$$

In particular, eqn(15) reduces to two terms for a function in the space spanned by one generator, that is

$$f(\eta) = f_0 + f_1\eta \tag{17}$$

The differentiation of a function of Grassmann variables is defined as a usual complex derivative except that in order for the derivative operator $\frac{\partial}{\partial\eta}$ to act on η, the variable η has to be anticommuted through the product until it is adjacent to $\frac{\partial}{\partial\eta}$. The following equations Eqns (18) and (19) serve as the

derivative definition equations of Grassmann variables. Equation (18) states the linear property for a derivative operator, and eqn (19) shows the anticommuting property of the Grassmann variables and the derivative action.

$$\frac{\partial}{\partial\eta}(c\ f(\eta) + d\ g(\eta)) = c\ \frac{\partial}{\partial\eta}f(\eta) + d\ \frac{\partial}{\partial\eta}g(\eta) \tag{18}$$

$$\frac{\partial}{\partial\eta_{i_k}}(c\ \eta_{i_1}\eta_{i_2}\cdots\eta_{i_k}\cdots\eta_{i_m}) = (-1)^{k-1}c\ \eta_{i_1}\eta_{i_2}\cdots\eta_{i_{k-1}}\eta_{i_{k+1}}\cdots\eta_{i_m} \tag{19}$$

where c is a complex number.

The definite integral is defined as the same as the derivative, that is

(i) linear property

$$\int d\eta(c\ f(\eta) + c'\ g(\eta)) = c\int d\eta f(\eta) + d\int d\eta\ g(\eta) \tag{20}$$

where c and c′ are complex numbers.

(ii) anticommuting and integrating

$$\int d\eta_{i_k}(c\eta_{i_1}\eta_{i_2}\cdots\eta_{i_k}\cdots\eta_{i_m}) = (-1)^{k-1}c\ \eta_{i_1}\eta_{i_2}\cdots\eta_{i_{k-1}}\eta_{i_{k+1}}\cdots\eta_{i_m} \tag{21}$$

Specifically, for one Grassmann variable, we have

$$\frac{\partial(1)}{\partial\eta} = 0 \qquad \int d\eta = 0$$

$$\frac{\partial\eta}{\partial\eta} = 1, \qquad \int d\eta\ \eta = \int(-\eta)d\eta = 1$$

It should be noted that the Grassmann integral is not a Riemann or Lebesgue integral which has a specific measure related to it. The integral defined in eqn (21) is completely formal, however this rule and the other rules in the Grassmann algebra take care of all antisymmetrical combinatorics and yield correct results!

The following lists some interesting properties of the calculus for the Grassman variables:

(1) $$\frac{\partial}{\partial\eta_i}\frac{\partial}{\partial\eta_j} = -\frac{\partial}{\partial\eta_j}\frac{\partial}{\partial\eta_i} \tag{22}$$

The proof of this property can be easily carried out by operating lhs of eqn (22) on a general function of Grassmann variables, such as the one in eqn (15).

(2) $$\int d\eta_i \frac{\partial}{\partial\eta_i} f(\eta_i) = 0 \tag{23}$$

From the definition of derivative and the function form of Grassmann variables, $\frac{\partial}{\partial\eta_i} f(\eta_i)$ does not contain η_i, eqn (23) holds from the integral rule.

(3) If $g_+(-\eta) = g_+(\eta)$ with $\eta=(\eta_1, \eta_2, \cdots, \eta_N)$, then we have the rule of integration by parts

$$\int d\eta_i\, g_+(\eta)\frac{\partial}{\partial\eta_i} f(\eta) = -\int d\eta_i \left(\frac{\partial}{\partial\eta_i} g_+(\eta)\right) f(\eta) \tag{24}$$

Similarly, if $g_-(-\eta) = -g_-(\eta)$, we have

$$\int d\eta_i\, g_-(\eta)\frac{\partial}{\partial\eta_i} f(\eta) = \int d\eta_i \left(\frac{\partial}{\partial\eta_i} g_-(\eta)\right) f(\eta) \tag{25}$$

Proof: From the general function form eqn (15) of Grassmann variables, function $g_+(\eta)$ contains those terms with only even number of variables (η_i) in eqn (15), and therefore $\frac{\partial}{\partial\eta_i} g_+(\eta)$ contains only odd number of variables. If we assume $\int d\eta_i f(\eta) = \frac{\partial}{\partial\eta_i} f(\eta) = \phi(\eta_1, \ldots, \eta_{i-1}, \eta_{i+1}, \ldots, \eta_n)$ (note without η_i) and

$\int d\eta_i g_*(\eta) = \frac{\partial}{\partial \eta_i} g_*(\eta) = \xi(\eta_1, \ldots, \eta_{i-1}, \eta_{i+1}, \ldots, \eta_N)$, then

$$\int d\eta_i \; g_*(\eta) \frac{\partial}{\partial \eta_i} f(\eta) = \xi \; \phi$$

$$\int d\eta_i \; (\frac{\partial}{\partial \eta_i} g_*(\eta)) \; f(\eta) = \int d\eta_i \; \xi(\eta_1, \ldots, \eta_{i-1}, \eta_{i+1}, \ldots, \eta_N) \; f(\eta) = -\xi \; \phi$$

This proves eqn (24). Eqn (25) can be similarly proved. #[1]

(4) The linear transformation of Grassmann variables gives

$$\int d\eta \; f(\eta) = \int d\xi \; (\det(\frac{\partial \eta}{\partial \xi}))^{-1} f(\xi(\eta)) \qquad (26)$$

Note that the appearance of the inverse of Jacobian determinant instead of the Jacobian for the usual complex variables. For example, for one variable η

$$\int d\eta \; f(c\eta) = cf' = c\int d\xi \; f(\xi) = \int d\xi \; (\frac{d\xi}{d\eta}) \; f(\xi)$$

The proof of this property can be found in Negele and Orland's book (1988).

(5) δ-Function The δ-function of Grassmann variables is defined as

$$f(\eta) = \int d\eta' \; \delta(\eta - \eta') f(\eta') \qquad (27)$$

where $d\eta' = d\eta_1' \cdots d\eta_N'$ for multi-Grassmann variables. This definition of δ-function is exactly the same as the δ-function of complex variables. For one variable Grassmann variable η, the general function form in this case can be written as $f = f_0 + f_1 \eta$ and therefore we have

$$\int d\eta' \; (\eta - \eta')(f_0 + f_1 \eta') = -(f_0 + f_1 \eta) = -f(\eta)$$

[1]The sign "#" denotes the end of a proof.

this yields the one dimensional δ-function

$\delta(\eta-\eta') = \eta' - \eta$

From the property of the usual δ-function, we may have the multi-dimensional δ-function of Grassmann variables

$$\delta(\eta-\eta') = \prod_{1}^{N}(\eta_i' - \eta_i) = (\eta_N' - \eta_N)\cdots(\eta_1' - \eta_1) \qquad (28)$$

note that the product order is from N (left) to 1 (right) which is the inverse of the order of $d\eta_1'\cdots d\eta_N'$ in eqn (27). It is interesting to note that the parity of the δ-function is determined by the number of the Grassmann variables.

Proof of eqn (28): Consider a general term $\eta_{i_k}\ldots\eta_{i_1}$ in the function given by eqn (15) and the following integration

$$\int(d\eta_1'\cdots d\eta_N') \prod_{1}^{N}(\eta_i' - \eta_i)\ \eta_{i_k}'\ldots\eta_{i_1}' \qquad (29)$$

Without loss of generality, $i_k < \cdots < i_1$ is assumed. After the expansion of the product, the integral of all the terms vanishes except one term $\eta_N'\ldots(-\eta_{i_k})\ldots(-\eta_{i_1})\ldots\eta_1'$, therefore eqn (29) yields

$$\int(d\eta_1'\cdots d\eta_N')\ \eta_N'\ldots(-\eta_{i_k})\ldots(-\eta_{i_1})\ldots\eta_1'\ \eta_{i_k}'\ldots\eta_{i_1}'$$

$$= \int\ (d\eta_1'\cdots d\eta_{i_k}')\ ((-\eta_{i_k})\ldots(-\eta_{i_1})\ldots\eta_1')\ \eta_{i_k}'\ldots\eta_{i_1}'$$

$$= (-1)^{i_k}(-\eta_{i_k}) \int\ (d\eta_1'\cdots d\eta_{i_k}')\ (\eta_{i_k-1}'\ldots(-\eta_{i_1})\ldots\eta_1')\ \eta_{i_k}'\ldots\eta_{i_1}'$$

where $(-1)^{i_k}$ comes from the exchange between η_{i_k} and $d\eta_1'\cdots d\eta_{i_k}'$. $(-1)^{i_k-1}$ will be generated by the exchange of $(\eta_{i_k-1}'\ldots(-\eta_{i_1})\ldots\eta_1')$ and η_{i_k}', therefore

after the integral with respect to η'_{i_k}, we have

$$\eta_{i_k} \int (d\eta'_1 \cdots d\eta'_{i_k-1}) \ (\eta'_{i_k-1} \ldots (-\eta_{i_1}) \ldots \eta'_1) \ \eta'_{i_{k-1}} \cdots \eta'_{i_1}$$

The left integral can be carried out as the same as the above procedure. The final result is

$$\eta_{i_k} \cdots \eta_{i_1}$$

Since all the terms in eqn (15) can be evaluated in a similar way, this concludes that eqn (28) is the satisfied δ-function for the multi Grassmann variables. #

(6) Fourier Transformation The Fourier transformation for the Grassmann variables is defined by

$$g(\xi) = \int (d\eta_1 \cdots d\eta_N) \ \exp\Big(\sum_1^N \eta_i \xi_i \Big) f(\eta) \tag{30}$$

where the exponential function $\exp\big(\sum_1^N \eta_i \xi_i \big)$ is defined by

$$\exp\Big(\sum_1^N \eta_i \xi_i \Big) = \prod_1^N (1+\eta_i \xi_i) = (1+\eta_N \xi_N) \ldots (1+\eta_1 \xi_1) \tag{31}$$

where (ξ) are Grassmann variables which anticommute with (η). The inverse Fourier transformation of eqn (30) is given by

$$f(\eta) = \int (d\xi_N \cdots d\xi_1) \ \exp\Big(\sum_1^N \xi_i \eta_i \Big) g(\xi) \tag{32}$$

Note the order of $d\xi_N \cdots d\xi_1$ is inverse of $d\eta_1 \cdots d\eta_N$ of eqn (30).

Proof of eqn (32): The correctness of eqn (32) can be proved by the following equation

$$g(\xi') = \int(d\eta_1\cdots d\eta_N)\ \exp(\sum_1^N \eta_i\xi_i)\int(d\xi'_N\cdots d\xi'_1)\ \exp(\sum_1^N \xi'_i\eta_i)g(\xi') \qquad (33)$$

Rhs of eqn (33) can be written as

$$(-1)^{N^2}\int(d\xi'_N\cdots d\xi'_1)\ \int(d\eta_1\cdots d\eta_N)\ \exp(\sum_1^N \eta_i(\xi_i-\xi'_i))g(\xi') \qquad (34)$$

where $(-1)^{N^2}$ comes from the order exchange of $(d\eta_1\cdots d\eta_N)$ and $(d\xi'_N\cdots d\xi'_1)$. The integration of η_N of eqn (34) yields

$$\int(d\eta_1\cdots d\eta_N)\ \exp(\sum_1^N \eta_i(\xi_i-\xi'_i)) = \int(d\eta_1\cdots d\eta_{N-1})\ (\xi_N-\xi'_N)\ \prod_1^{N-1}(1+\eta_i(\xi_i-\xi'_i))$$

Noting that the change of both $(d\eta_1\cdots d\eta_{N-1})(\xi_N-\xi'_N)$ to $(\xi_N-\xi'_N)\ (d\eta_1\cdots d\eta_{N-1})$ and $d\xi'_N\ (d\xi'_{N-1}\cdots d\xi'_1)$ to $(d\xi'_{N-1}\cdots d\xi'_1)\ d\xi'_N$ will not yield any sign change, eqn (34) yields

$$(-1)^{N^2}\int(d\xi'_{N-1}\cdots d\xi'_1)\ d\xi'_N(\xi_N-\xi'_N)\int(d\eta_1\cdots d\eta_{N-1})\ \prod_1^{N-1}(1+\eta_i(\xi_i-\xi'_i))g(\xi')$$

Similar procedure can be used to finish all η integrals and gives

$$(-1)^{N^2}\int d\xi'_1\cdots\ d\xi'_N\ \prod_1^N(\xi_i-\xi'_i)g(\xi') = (-1)^{N^2}\int d\xi'_1\cdots\ d\xi'_N\ (-1)^N\prod_1^N(\xi'_i-\xi_i)g(\xi')$$

$$= \int d\xi'_1\cdots\ d\xi'_N\ \prod_1^N(\xi'_i-\xi_i)g(\xi')$$

The use of the δ-function given in eqn (29) shows that eqn(33) holds. #

(7) Conjugation: The conjugation of a Grassmann generator η_i is associated with another Grassmann generator (and therefore anticommuting to η_i) denoted as η_i^*. The conjugating operations of Grassmann variables are defined through the following three properties:

$$(1)\ (\eta_i)^* = \eta_i^*,\ (\eta_i^*)^* = \eta_i \qquad (35)$$

$$(2)(c\eta_i)^* = c^*\eta_i^* \tag{36}$$

where c is a complex number.

$$(3)(\eta_1\cdots\eta_N)^* = \eta_N^*\cdots\eta_1^* \tag{37}$$

By introducing the conjugation on a set of N Grassmann variables $\{\eta_i\}$, a set with 2N anticommuting Grassmann variables $\{\eta_i^*, \eta_i^*\}$ is generated. The function form of eqn (15), the integral, the derivative, and other mathematical operations defined for $\{\eta_i\}$ can be generated to the set of $\{\eta_i^*, \eta_i^*\}$. For example, we have integral formula

$$\int d\eta_{i_k}^*(c\eta_{i_1}\eta_{i_2}\cdots\eta_{i_k}^*\cdots\eta_{i_m}) = (-1)^{k-1}c\ \eta_{i_1}\eta_{i_2}\cdots\eta_{i_{k-1}}\eta_{i_{k+1}}\cdots\eta_{i_m}$$

1.3.2 Coherent Representation of Fermions

In order to introduce the coherent state representation into the quantum mechanics of Fermions, anticommuting relationships between a Grassmann variable η_i and Fermion creation or annihilation operator are required

$$\eta_i a_\alpha + a_\alpha \eta_i = 0, \quad \eta_i a_\alpha^+ + a_\alpha^+ \eta_i = 0 \tag{38}$$

The coherent state of operators $\{a_\alpha\}$ is

$$|\eta\rangle = \exp\{-\sum \eta_\alpha a_\alpha^+\}|0\rangle = \prod\{1 - \eta_\alpha a_\alpha^+\}|0\rangle \tag{39}$$

where $\{\eta_\alpha\}$ is a set of Grassmann variables.

Proof: We first prove $\exp\{-\eta_\alpha a_\alpha^+\}|0\rangle = \{1 - \eta_\alpha a_\alpha^+\}|0\rangle$ is an eigenstate of a_α

$a_\alpha \exp\{-\eta_\alpha a_\alpha^+\}|0\rangle = a_\alpha\{1 - \eta_\alpha a_\alpha^+\}|0\rangle = \eta_\alpha a_\alpha a_\alpha^+|0\rangle = \eta_\alpha|0\rangle$

$= \eta_\alpha\{1 - \eta_\alpha a_\alpha^+\}|0\rangle = \eta_\alpha \exp\{-\eta_\alpha a_\alpha^+\}|0\rangle$

$|\eta\rangle$ is an eigenfunction of a_β with eigenvalue η_β follows

$$a_\beta(\prod{}' \{1 - \eta_\alpha a_\alpha^+\})(1 - \eta_\beta a_\beta^+)(\prod{}'' \{1 - \eta_\alpha a_\alpha^+\})|0\rangle$$

$$= (\prod{}' (1 - \eta_\alpha a_{\alpha'}))a_\beta(1 - \eta_\beta a_{\beta'})(\prod{}'' (1 - \eta_\alpha a_{\alpha'}))|0\rangle = \eta_\beta|\eta\rangle \ \#$$

The coherent state $|\eta\rangle$ is also an eigenstate of the field operator $\Phi(\mathbf{x})$ given in eqn (5) with eigenvalue $\sum_\alpha \langle \mathbf{x}|\alpha\rangle\ \eta_\alpha$, because

$$\Phi(\mathbf{x})|\eta\rangle = \sum_\alpha \langle \mathbf{x}|\alpha\rangle\ a_\alpha|\eta\rangle = \sum_\alpha \langle \mathbf{x}|\alpha\rangle\ \eta_\alpha|\eta\rangle \tag{40}$$

Conjugate $a_\alpha|\eta\rangle = \eta_\alpha|\eta\rangle = |\eta\rangle\eta_\alpha$ yields

$$\langle\eta|a_\alpha^\dagger = \langle\eta|\eta_\alpha^* = \eta_\alpha^*\langle\eta| \tag{41}$$

Since

$$a_\alpha^\dagger \exp\{-\eta_\alpha a_{\alpha'}\}|0\rangle = a_{\alpha'}\{1 - \eta_\alpha a_{\alpha'}\}|0\rangle = a_{\alpha'}|0\rangle = -\frac{\partial}{\partial\eta_\alpha}\exp\{-\eta_\alpha a_{\alpha'}\}|0\rangle$$

we have

$$a_\alpha^\dagger|\eta\rangle = -\frac{\partial}{\partial\eta_\alpha}|\eta\rangle \tag{42}$$

The overlap integral of two coherent states is

$$\langle\eta'|\eta\rangle = \langle 0|\prod\{1+\eta'^*_\alpha a_\alpha\}\{1-\eta_\alpha a_\alpha^\dagger\}|0\rangle = \langle 0|\prod(1+\eta'^*_\alpha\eta_\alpha)|0\rangle = \exp\{\sum\eta'^*_\alpha\eta_\alpha\} \tag{43}$$

The unity resolution of the coherent states is

$$\int\prod(d\eta_\alpha^* d\eta_\alpha)\exp\{-\eta_\alpha^*\eta_\alpha\}|\eta\rangle\langle\eta| = 1 \tag{44}$$

This identity is established through the proof of $\langle\Phi|\ I\ |\Psi\rangle = \langle\Phi|\Psi\rangle$ where I is the lhs of the above equation(Negele and Orland, 1988). Using this identity, we have coherent state representation for a state

$$|\Psi\rangle = \int\prod(d\eta_\alpha^* d\eta_\alpha)\exp\{-\eta_\alpha^*\eta_\alpha\}\langle\eta|\Psi\rangle\ |\eta\rangle \tag{45}$$

Especially, for an N fermion state $|\Phi\rangle = a_{\alpha_1}^{+}\ldots a_{\alpha_N}^{+}|0\rangle$, we have

$$|\Phi\rangle = \int \prod (d\eta_\alpha^{*} d\eta_\alpha) \exp(-\eta_\alpha^{*}\eta_\alpha)\eta_{\alpha_1}^{*}\ldots\eta_{\alpha_N}^{*}|\eta\rangle \tag{46}$$

where $\langle\eta|a_{\alpha_1}^{+}\ldots a_{\alpha_N}^{+}|0\rangle = \eta_{\alpha_1}^{*}\ldots\eta_{\alpha_N}^{*}$ has been used.

A normal-ordered operator is the operator with creation operators standing on the left and annihilation operators on the right. The coherent representation for a normal-ordered operator $A(a_\alpha^{+}, a_\alpha)$ is

$$\langle\eta|A(a_\alpha^{+}, a_\alpha)|\eta'\rangle = \exp(\sum \eta_\alpha^{*}\eta'_\alpha) A(\eta_\alpha^{*}, \eta'_\alpha) \tag{47}$$

The proof of eqn (47) is straightforward since a general term of $A(a_\alpha^{+}, a_\alpha)$ can be written as $a_{\alpha_1}^{+}\ldots a_{\alpha_n}^{+} a_{\beta_1}\ldots a_{\beta_m}$.

$\langle\eta|a_{\alpha_1}^{+}\ldots a_{\alpha_n}^{+} a_{\beta_1}\ldots a_{\beta_m}|\eta'\rangle = \eta_{\alpha_1}^{*}\ldots\eta_{\alpha_n}^{*}\eta_{\beta_1}'\ldots\eta_{\beta_m}'\langle\eta|\eta'\rangle$ #

1.3.3. Path Integrals of Fermions

For a quantum system, the state vector $|\Psi\rangle$ satisfies Shrödinger equation

$$i\hbar \frac{d|\Psi\rangle}{dt} = H\,|\Psi\rangle \tag{48}$$

If the Hamiltonian H is time independent, then the time dependence for a state vector can be explicitly written down as

$$|\Psi(t)\rangle = \exp(-i/\hbar H(t-t'))|\Psi(t')\rangle \tag{49}$$

In ($|q\rangle$) representation, eqn (49) can be written as

$$\langle q|\Psi(t)\rangle = \langle q|\exp(-i/\hbar H(t-t'))|\Psi(t')\rangle$$

$$= \int dq' \langle q|\exp(-i/\hbar H(t-t'))f(q')|q'\rangle\langle q'|\Psi(t')\rangle$$

$$= \int dq' K(q,t;q',t')\ \Psi(q',t') \tag{50}$$

where the identity resolution for the complete set { $|q\rangle$ }

$$\int dq' f(q') |q'\rangle\langle q'| = 1 \tag{51}$$

is used, and the propagator $K(q,t;q',t')$ is

$$K(q,t;q',t') = \langle q|\exp(-i/\hbar H(t-t'))f(q')|q'\rangle \tag{52}$$

Therefore if the propagator is known, the temporal evolution of a state vector is completely determined from some initial state. The Feynman path integral technique is a method for obtaining the propagator. In addition, it also provides a unified view of quantum mechanics, field theory, and statistical models (Itzykson and Zuber, 1986). Through the use of Feynman path integrals, the propagator $K(q,t;q',t')$ can be understood as the summation of the quantum amplitudes $\{\exp(i/\hbar W(q,t;q',t'))\}$ of all the possible paths from initial point (q',t') to the final point (q,t) where $\{ W(q,t;q',t')\}$ are the classical actions of the paths. In the case of a Fermion system, the anticommuting character for the exchange of two particles makes it difficult to express the path integrals in terms the usual coordinate representation. However, the coherent representation introduced in the last section provides a natural mathematical technique to take care of the anticommuting property of Fermions. The path integrals for a single Fermion state is considered here. Paper *I* gives path integrals for the many Fermion states.

For a single Fermion state $|\alpha\rangle$, we have an annihilation operator a and creation operator $a^\dagger$. The Hamiltonian is

$$H = \omega\, a^\dagger a \tag{53}$$

The coherent state $|\eta\rangle$ of the annihilation operator a satisfies

$$\int d\eta' d\eta \exp(-\eta^{*}\eta) |\eta><\eta| = 1 \tag{54}$$

(note there is only one Grassmann generator) and for any normal-ordered operator A

$$<\eta|A(a^{\dagger},a)|\eta'> = \exp(\eta^{*}\eta')A(\eta^{*},\eta') \tag{55}$$

The propagator is

$$K(\eta,t;\eta',t') = <\eta|\exp(-i/\hbar H(t-t'))\exp(-\eta'^{*}\eta')|\eta'> \tag{56}$$

In order to express $\exp(-i/\hbar H(t-t'))$ in terms of normal-ordered operator, (t-t') is divided into N equal distance slices $(t-t') = N\varepsilon$, and in every slice we have expansion

$$\exp(-i/\hbar H\varepsilon) = 1 - i\varepsilon/\hbar H + O(\varepsilon^2) \tag{57}$$

as $\varepsilon \longrightarrow 0$, the above expansion becomes normal-ordered operator. In terms of the time slicing technique the propagator can be written as

$$K(\eta,t;\eta',t') = <\eta|\exp(-i\varepsilon/\hbar H)\ldots\exp(-i\varepsilon/\hbar H)\exp(-\eta'^{*}\eta')|\eta'> \tag{58}$$

Inserting the identity resolution eqn (58) into every time slicing point, we have

$$K(\eta,t;\eta',t') = \int \prod (d\eta_i^{*}d\eta_i)<\eta|\exp(-i\varepsilon/\hbar H)\exp(-\eta_N^{*}\eta_N)|\eta_N><\eta_N|\ldots$$

$$\exp(-\eta_1^{*}\eta_1)|\eta_1><\eta_1|\exp(-i\varepsilon/\hbar H)\exp(-\eta'^{*}\eta')|\eta'> \tag{59}$$

Using eqn (57), a general factor $<\eta_{i+1}|\exp(-i\varepsilon/\hbar H)\exp(-\eta_i^{*}\eta_i)|\eta_i>$ in the eqn (59) can be written as

$$<\eta_{i+1}|\exp(-i\varepsilon/\hbar H)\exp(-\eta_i^{*}\eta_i)|\eta_i> = \exp(i\varepsilon/\hbar L_i) \tag{60}$$

where L_i is the Lagrangian at time $t' + i\varepsilon$

$$L_i = \hbar/i\frac{(\eta_{i+1}^{*}-\eta_i^{*})}{\varepsilon}\eta_i - H(\eta_{i+1},\eta_i) \tag{61}$$

Finally, the propagator is expressed in terms of path integrals

$$K(\eta,t;\eta',t') = \int \prod_{0}^{N} (d\eta_i d\eta_i) \exp\{i\varepsilon/\hbar \sum_{0}^{N} L_i\} \tag{62}$$

where L_0 and L_N are defined by

$$L_0 = \hbar/i \frac{(\eta_1^{\cdot} - \eta'^{\cdot})}{\varepsilon} \eta' - H(\eta_1, \eta')$$

$$L_N = \hbar/i \frac{(\eta^{\cdot} - \eta_N^{\cdot})}{\varepsilon} \eta_N - H(\eta, \eta_N)$$

1.4. Lagrangian of Fermions and Its Associated Variational Principle

Schwinger's variational principle (Schwinger, 1951) is the differential form of the Feynman path integrals. The fundamental quantum dynamic principle is stated as a variational equation for the transformation function connecting eigenvectors associated with different spacelike surfaces in the Schwinger variational principle. The action for a dynamic system is expressed in terms of a Lagrangian of the system. The total change of the action from the alterations of the field operators for a system is determined by the end points on time or the surface in real space. In this section the Schwinger variational principle for a Fermion system will be demonstrated. The Lagrangian of fermion field is taken to be

$$L[\Phi,\dot{\Phi},\nabla\Phi] = \frac{i\hbar}{2} (\Phi^{\dagger}\cdot\dot{\Phi} - \dot{\Phi}^{\dagger}\cdot\Phi) - \frac{\hbar^2}{2m} \nabla\Phi^{\dagger}\cdot\nabla\Phi - \Phi^{\dagger} V \Phi$$
$$- \frac{1}{2} \int d\mathbf{x}' \Phi^{\dagger}(\mathbf{x}) \Phi^{\dagger}(\mathbf{x}') g(\mathbf{r},\mathbf{r}') \Phi(\mathbf{x}') \Phi(\mathbf{x}) \tag{63}$$

where $\mathbf{x}$ denotes spin-space coordinates. The Fermion field operators Φ and $\Phi^{\dagger}$ are given in eqn (5), the integral $\int d\mathbf{x}$ denotes the summation of spin and the integral over the total space, i.e. $\sum_{\text{spin}} \int d\mathbf{r}$, and $\dot{\Phi}$ denotes a time derivative of Φ. The correctness of the form for the Lagrangian is justified by showing

that the variational principle yields the correct equation of motion. This will be demonstrated in this section. We will also show that the continuity equations of charge density and energy density can be derived from the variations of this Lagrangian. The action integral in a region is given by

$$W[\Omega] = \int_{t_1}^{t_2} dt \int_{\Omega} d\mathbf{x}\ L[\Phi, \dot{\Phi}, \nabla\Phi] \tag{64}$$

where the integral $\int_{\Omega} d\mathbf{x}$ is the abbreviation of $\sum_{spin} \int_{\Omega} d\mathbf{r}$. The variation of the field operators is

$$\delta\Phi(\mathbf{x}) = \Phi'(\mathbf{x}) - \Phi(\mathbf{x}) = \sum_{\alpha} \delta\Phi_{\alpha}(\mathbf{x})\ a_{\alpha}, \text{ and } \delta\Phi^{\dagger}(\mathbf{x}) = \sum_{\alpha} \delta\Phi_{\alpha}^{*}(\mathbf{x})\ a_{\alpha}^{\dagger} \tag{65}$$

The field $\Phi(\mathbf{x})$ and its hermitian complex conjugate $\Phi^{\dagger}(\mathbf{x})$ are treated as two independent variables. Note that the variation $\delta\Phi(\mathbf{x})$ of eqn (65) is the change of the field at a fixed point $\mathbf{x}$ in the spin-space. Under the coordinate transformation $\mathbf{x}'=\mathbf{x}+\delta\mathbf{x}$ and field transformation $\Phi'(\mathbf{x})=\Phi(\mathbf{x}) + \delta\Phi(\mathbf{x})$, we have the total change of field (a detail discussion of this variation is referenced to Goldstein's book, 1980)

$$\Delta\Phi(\mathbf{x}) = \Phi'(\mathbf{x}') - \Phi(\mathbf{x}) \tag{65a}$$

The resulting change of action integral from the variation of eqn (65a) is

$$\begin{aligned}\delta W[\Omega] &= \int_{t_1'}^{t_2'} dt' \int_{\Omega'} d\mathbf{x}'\ L[\Phi'(\mathbf{x}'), \dot{\Phi}'(\mathbf{x}'), \nabla'\Phi'(\mathbf{x}')] - \int_{t_1}^{t_2} dt \int_{\Omega} d\mathbf{x}\ L[\Phi, \dot{\Phi}, \nabla\Phi] \\ &= \int_{t_1'}^{t_2'} dt \int_{\Omega'} d\mathbf{x}\ L[\Phi'(\mathbf{x}), \dot{\Phi}'(\mathbf{x}), \nabla\Phi'(\mathbf{x})] - \int_{t_1}^{t_2} dt \int_{\Omega} d\mathbf{x}\ L[\Phi, \dot{\Phi}, \nabla\Phi] \qquad (66)'\end{aligned}$$

Explicitly, we have

$$\begin{aligned}\delta W[\Omega] &= \int_{t_1}^{t_2} dt \int_{\Omega} d\mathbf{x}\ (\delta L[\Phi, \dot{\Phi}, \nabla\Phi] + \int_{\Omega} d\mathbf{x}\ L\delta t \Big|_{t_1}^{t_2} + \int_{t_1}^{t_2} dt \int_{\Sigma} dS\ L\delta\Sigma \\ &= \int_{t_1}^{t_2} dt \int_{\Omega} d\mathbf{x}\ \left(\delta L[\Phi, \dot{\Phi}, \nabla\Phi] + \frac{\partial(L\delta t)}{\partial t} + \frac{\partial}{\partial \mathbf{r}} \cdot (L\delta\mathbf{r})\right)\end{aligned} \tag{66}$$

where Σ is the boundary of Ω, $\delta L[\Phi,\dot{\Phi},\nabla\Phi]$ is the change in L due to the variation of the fields (that is the variation given in eqn (65)), the remaining terms on the rhs are due to the variation of the time end points (i.e. t_1 and t_2) and the boundary of Ω. The second step of eqn (66) is obtained by using Gauss' divergence theorem. The rhs first term of eqn (66) can be written as

$$\int_{t_1}^{t_2}dt\int_{\Omega}dx\ \{\delta L[\Phi,\dot{\Phi},\nabla\Phi] = \int_{t_1}^{t_2}dt\int_{\Omega}dx\{\ \frac{\delta L}{\delta\Phi}\delta\Phi + \frac{\delta L}{\delta\dot{\Phi}}\delta\dot{\Phi} + \frac{\delta L}{\delta(\nabla\Phi)}\delta(\nabla\Phi) + CC\}$$

$$= \int_{t_1}^{t_2}dt\int_{\Omega}dx\{\ \frac{\delta L}{\delta\Phi} - \frac{d}{dt}(\frac{\delta L}{\delta\dot{\Phi}}) - \nabla\cdot(\ \frac{\delta L}{\delta(\nabla\Phi)})\delta\Phi + CC\ \}$$

$$\int_{t_1}^{t_2}dt\int_{\Omega}dx\ \frac{\partial}{\partial t}\{\frac{\delta L}{\delta\dot{\Phi}}\delta\Phi + CC\} + \nabla\cdot(\ \frac{\delta L}{\delta(\nabla\Phi)}\delta\Phi + CC)\} \qquad (67)$$

where CC denotes the hermitian complex conjugate. Inserting eqn (67) into eqn (66), we obtain the total variation of the action

$$\delta W[\Omega] = = \int_{t_1}^{t_2}dt\int_{\Omega}dx\{\ \frac{\delta L}{\delta\Phi} - \frac{d}{dt}(\frac{\delta L}{\delta\dot{\Phi}}) - \nabla\cdot(\ \frac{\delta L}{\delta(\nabla\Phi)})\delta\Phi + CC\ \}$$

$$\int_{t_1}^{t_2}dt\int_{\Omega}dx\ \Big\{\ \frac{\partial}{\partial t}\{(\frac{\delta L}{\delta\dot{\Phi}}\delta\Phi + CC) + L\delta t\} + \nabla\cdot\{(\ \frac{\delta L}{\delta(\nabla\Phi)}\delta\Phi + CC) + L\delta x\}\ \Big\} \qquad (68)$$

According to Schwinger's action principle, the variation of $\delta W[\Omega]$ is determined by the time end point or the space boundary variations. Therefore we can infer that the equation of motion is given by

$$\frac{\delta L}{\delta\Phi} - \frac{d}{dt}(\frac{\delta L}{\delta\dot{\Phi}}) - \nabla\cdot(\ \frac{\delta L}{\delta(\nabla\Phi)}) = 0 \qquad (69)$$

By substitution of L into eqn (69), the Shrödinger equation for the field Φ is obtained

$$i\hbar\dot{\Phi} = -\frac{\hbar^2}{2m}\nabla^2\Phi + V\,\Phi + \int dx'\Phi^{\dagger}(x')g(x,x')\Phi(x')\Phi(x) \qquad (70)$$

The momentum conjugate fields of Φ and $\Phi^\dagger$ are defined in the usual way, that is

$$\Pi = \frac{\delta L}{\delta \dot{\Phi}} = \frac{i\hbar}{2}\Phi^\dagger, \text{ and } \Pi^\dagger = \frac{\delta L}{\delta \dot{\Phi}^\dagger} = -\frac{i\hbar}{2}\Phi \tag{71}$$

The Hamiltonian of the system is

$$H = \int dx\,(\Pi\dot{\Phi} + \dot{\Phi}^\dagger\Pi^\dagger - L)$$

$$= \int dx\,(\frac{\hbar^2}{2m}\nabla\Phi^\dagger\cdot\nabla\Phi + \Phi^\dagger V \Phi + \frac{1}{2}\int dx'\Phi^\dagger(x)\Phi^\dagger(x')g(x,x')\Phi(x')\Phi(x))$$

$$= \int dx\,(-\frac{\hbar^2}{2m}\Phi^\dagger\nabla^2\Phi + \Phi^\dagger V \Phi + \frac{1}{2}\int dx'\Phi^\dagger(x)\Phi^\dagger(x')g(x,x')\Phi(x')\Phi(x)) \tag{72}$$

The commutator of the field operator and Φ and the Hamiltonian H is given by

$$[\Phi,H] = [\Phi(x), \int dx''(-\frac{\hbar^2}{2m}\Phi^\dagger\nabla^2\Phi + \Phi^\dagger V \Phi + \frac{1}{2}\int dx'\Phi^\dagger(x'')\Phi^\dagger(x')g(x'',x')\Phi(x')\Phi(x''))]$$

$$= -\frac{\hbar^2}{2m}\nabla^2\Phi + V\Phi + \int dx'\Phi^\dagger(x')g(x,x')\Phi(x')\Phi(x)$$

where operator identities

$[A,BC] = [A,B]C + B[A,C]$ and $[A,BC] = [A,B]_+C - B[A,C]_+$

and the commutation relationship for the fields eqn (6) have been used. A comparison of this result with the rhs of eqn (70) shows that the field operator Φ obeys Heisenberg equation

$$i\hbar\dot{\Phi} = [\Phi,H] \tag{73}$$

Using this equation of Φ, we obtain the equation of motion for any observable operator Q

$$i\hbar\dot{Q}(x) = [Q(x),H] \tag{74}$$

where $Q(x) = \Phi^\dagger(x)Q\Phi(x)$. This shows that the equations of motion for field operators and observables are contained in Schwinger's variational principle.

Substituting eqn (69) into eqn (66), the variation of action integral can

be written as

$$\delta W[\Omega] = \int_{t_1}^{t_2} dt \int_{\Omega} dx \left\{ \frac{\partial}{\partial t} \left(\left(\frac{\delta L}{\delta \dot{\Phi}} \delta\Phi + CC \right) + L\delta t \right) + \nabla \cdot \left(\left(\frac{\delta L}{\delta(\nabla\Phi)} \delta\Phi + CC \right) + L\delta r \right) \right\} \tag{75}$$

The conservation laws and continuity equations followed from the invariance of the Lagrangian under a variation can be derived from eqn (75). This will be demonstrated in the following special variations.

If L is invariant to a transformation of the field without changing the end points, i.e. δt and $\delta \Sigma$ vanish

$$\Phi \longrightarrow \Phi'(x') = \Phi'(x) = \Phi(x) + \delta\Phi(x) \tag{76}$$

then we obtain continuity equation from eqn (75)

$$\frac{d}{dt} \left\{ \frac{\delta L}{\delta \dot{\Phi}} \delta\Phi + CC \right\} + \nabla \cdot \left\{ \frac{\delta L}{\delta(\nabla\Phi)} \delta\Phi + CC \right\} = 0 \tag{77}$$

For the Lagrangian given in eqn (63), the continuity equation reads

$$\frac{i\hbar}{2} \frac{d}{dt} \left\{ (\Phi^{\dagger} \delta\Phi - \delta\Phi^{\dagger} \cdot \Phi) \right\} - \frac{\hbar^2}{2m} \nabla \cdot \left\{ (\nabla\Phi^{\dagger}) \delta\Phi + \delta\Phi^{\dagger} (\nabla\Phi) \right\} = 0 \tag{78}$$

Integrating eqn (77) over the total space, we have

$$\frac{d}{dt} \int dr \left\{ \frac{\delta L}{\delta \dot{\Phi}} \delta\Phi + CC \right\} = - \int dr \nabla \cdot \left\{ \frac{\delta L}{\delta(\nabla\Phi)} \delta\Phi + CC \right\} \tag{79a}$$

Using Gauss' divergence theorem on the rhs of eqn (79) and noting that both $\delta\Phi$ or $\Phi \longrightarrow 0$ at infinity, we obtain

$$\frac{d}{dt} \int dr \left\{ \frac{\delta L}{\delta \dot{\Phi}} \delta\Phi + CC \right\} = 0 \tag{79}$$

This is the Noether's theorem in the case of the field variation without coordinate transformation. Noether's theorem states that the physical

quantity represented by the operator $\int d\mathbf{r}\ (\frac{\delta L}{\delta \dot{\Phi}}\delta\Phi + CC\ )$ is conserved if the Lagrangian is invariant to the variation $\delta\Phi$ and $\delta\Phi^{\dagger}$. For example, the Lagrangian of eqn (63) is invariant under the phase change of the field $\Phi \longrightarrow \Phi' = \exp(i\varepsilon)\Phi \cong (1+i\varepsilon)\Phi$, that is

$$L[\Phi',\dot{\Phi}',\nabla\Phi'] = L[\Phi,\dot{\Phi},\nabla\Phi] \tag{80}$$

The conserved quantity corresponding to this invariance is

$$\int d\mathbf{r}\ (\frac{\delta L}{\delta \dot{\Phi}}\delta\Phi + \delta\Phi^{\dagger}\ \frac{\delta L}{\delta \dot{\Phi}^{\dagger}}\ )$$

$$=\int d\mathbf{r}[\frac{i\hbar}{2}\ \Phi^{\dagger}(i\varepsilon)\Phi + \{(-i\varepsilon)\Phi^{\dagger}\}(-\ \frac{i\hbar}{2}\ \Phi)\ ]=-\varepsilon\hbar\int d\mathbf{r}\Phi^{\dagger}\Phi \tag{81}$$

which corresponds to the conservation of the total charge. The corresponding continuity equation is

$$-\varepsilon\hbar\frac{d}{dt}(\Phi^{\dagger}\Phi) +(\ -\ \frac{\hbar^2}{2m}\ \nabla\Phi^{\dagger})(i\varepsilon\Phi) + (-i\varepsilon\Phi^{\dagger})(\ -\ \frac{\hbar^2}{2m}\ \nabla\Phi) = 0$$

or

$$\frac{d}{dt}(\Phi^{\dagger}\Phi) + \frac{1}{2m}\{(\frac{\hbar}{i}\nabla\Phi)^{\dagger}\Phi + \Phi^{\dagger}(\frac{\hbar}{i}\nabla\Phi)\} = 0 \tag{82}$$

This is the charge density continuity equation.

For the translation of time $t' = t + \varepsilon$, $\delta\Sigma = 0$. If the field operators are assumed to be invariant under this transformation, that is, $\Phi'(t') = \Phi(t)$, then the resulting change of the field at t is $\delta\Phi = \Phi'(t) - \Phi(t)$ and can be calculated in the following way:

$$\Phi'(t+\varepsilon) - \Phi(t) = \Phi'(t) + \varepsilon\dot{\Phi}'(t) - \Phi(t) + O(\varepsilon^2) = \varepsilon\dot{\Phi}'(t) + \delta\Phi(t) + O(\varepsilon^2) = 0,$$

and

$$\dot{\Phi}(t) = \frac{d\Phi'(t')}{dt'} = \frac{d\Phi'(t')}{dt} = \frac{d\Phi'(t)}{dt} + O(\varepsilon)$$

therefore to the first order of ε we have

$$\delta\Phi = \Phi'(t) - \Phi(t) = -\varepsilon\dot{\Phi}'(t) = -\varepsilon\dot{\Phi}(t) \tag{83}$$

Using this result, we have the total change of Lagrangian

$$\Delta L = \frac{d}{dt}\{\frac{\delta L}{\delta\dot{\Phi}}\delta\Phi + CC\} + \nabla\cdot\{\frac{\delta L}{\delta(\nabla\Phi)}\delta\Phi + CC\} + \frac{\partial L}{\partial t}\delta t$$

$$= \varepsilon\frac{d}{dt}\{L - \frac{i\hbar}{2}(\Phi^{\dagger}\dot{\Phi} - \dot{\Phi}^{\dagger}\cdot\Phi)\} + \nabla\cdot\{\frac{\delta L}{\delta(\nabla\Phi)}\delta\Phi + CC\} = 0 \tag{84}$$

Therefore the conserved quantity corresponding to the time translation is

$$\int d\mathbf{r}\{\frac{i\hbar}{2}(\Phi^{\dagger}\dot{\Phi} - \dot{\Phi}^{\dagger}\cdot\Phi) - L\} \tag{85}$$

this is the Hamiltonian operator given in eqn (72). Therefore the invariance of the Lagrangian under a time translation yields conservation of the energy. The continuity equation for the energy density is given by eqn (84) and can be written as

$$\frac{dE(\mathbf{r})}{dt} + \nabla\cdot J_E = 0 \tag{86}$$

where energy density operator E is

$$E = \frac{i\hbar}{2}(\Phi^{\dagger}\dot{\Phi} - \dot{\Phi}^{\dagger}\cdot\Phi) - L\} \tag{87}$$

and the energy current operator is

$$J_E = -\frac{\hbar^2}{2m}\{(\nabla\Phi)^{\dagger}\dot{\Phi} + \dot{\Phi}^{\dagger}(\nabla\Phi)\} \tag{88}$$

Equation (86) can also be directly obtained from the equation of motion of the field operators eqn (70). Differentiation of the Hamiltonian density in eqn (87) with respect to time t yields

$$\dot{E} = \frac{\hbar^2}{2m}(\nabla\dot{\Phi}^{\dagger}\cdot\nabla\Phi + \nabla\Phi^{\dagger}\cdot\nabla\dot{\Phi}) + \dot{\Phi}^{\dagger}V\Phi + \Phi^{\dagger}V\dot{\Phi}$$

$$= \frac{\hbar^2}{2m}\nabla\cdot(\dot{\Phi}^{\dagger}\nabla\Phi + \nabla\Phi^{\dagger}\dot{\Phi}) - \frac{\hbar^2}{2m}(\dot{\Phi}^{\dagger}\nabla^2\Phi + \nabla^2\Phi^{\dagger}\dot{\Phi}) + \dot{\Phi}^{\dagger}V\Phi + \Phi^{\dagger}V\dot{\Phi}$$

$$= \frac{\hbar^2}{2m}\nabla\cdot(\dot{\Phi}^\dagger\nabla\Phi + \nabla\Phi^\dagger\dot{\Phi}) + \dot{\Phi}^\dagger(-\frac{\hbar^2}{2m}\nabla^2\Phi + V\Phi) + (-\frac{\hbar^2}{2m}\nabla^2\Phi^\dagger + \Phi^\dagger V)\dot{\Phi}$$

Equation (86) is obtained from the above equation by using eqn (70) and its conjugate.

Similarly, for the invariance of a Lagrangian under the translation of spatial coordinates, the induced field change is $\delta\Phi = \Phi'(\mathbf{r}) - \Phi(\mathbf{r}) \cong -\boldsymbol{\varepsilon}\cdot\nabla\Phi$, the corresponding conserved quantity is momentum

$$\int d\mathbf{r}\{\frac{\delta L}{\delta\dot{\Phi}}\delta\Phi + \delta\Phi^\dagger\frac{\delta L}{\delta\dot{\Phi}^\dagger}\} = -\frac{i\hbar}{2}\boldsymbol{\varepsilon}\cdot\int d\mathbf{r}\Phi^\dagger\nabla\Phi - (\nabla\Phi^\dagger)\Phi = \frac{1}{2}\boldsymbol{\varepsilon}\cdot\int d\mathbf{r}[\Phi^\dagger\mathbf{p}\Phi + (\mathbf{p}\Phi)^\dagger\Phi] \qquad (89)$$

If the Lagrangian is not invariant under the variation of field operators, we have

$$\int d\mathbf{r}\delta L = \int d\mathbf{r}\frac{d}{dt}\{\frac{\delta L}{\delta\dot{\Phi}}\delta\Phi + CC\} + \int d\mathbf{r}\nabla\cdot\{\frac{\delta L}{\delta(\nabla\Phi)}\delta\Phi + CC\} \qquad (90)$$

where the explicit time variation is omitted and the variation of coordinates at infinity is set to 0. The equation of motion eqn (69) has been used for the derivation of eqn (90). If we denote quantity $\int d\mathbf{r}\{\frac{\delta L}{\delta\dot{\Phi}}\delta\Phi + CC\}$ as Q, then we have

$$\frac{dQ}{dt} = \int d\mathbf{r}\delta L \qquad (91)$$

where we have used $\delta\Phi \longrightarrow 0$ at infinity to eliminate the rhs second term of eqn (90). By using Heisenberg equation, we obtain a relationship between the change of Lagrangian and the commutator of the Hamiltonian and observable operator Q

$$[H,Q] = (i/\hbar) \int d\mathbf{r}\delta L \qquad (92)$$

As an example of the application of eqn (92), we consider the transformation of coordinate scaling $\mathbf{r} \longrightarrow \mathbf{r}' = (1+\varepsilon)\mathbf{r} = \mathbf{r}+\varepsilon\mathbf{r}$. Under this transformation, the variation of the field is $\delta\Phi = \Phi'(\mathbf{r},s) - \Phi(\mathbf{r},s) \cong -\varepsilon\mathbf{r}\cdot\nabla\Phi$

$$\int d\mathbf{r}\delta L = \int d\mathbf{r} \frac{i\hbar}{2} \frac{d}{dt}\{(\Phi^{\dagger}\delta\Phi - \delta\Phi^{\dagger}\cdot\Phi)\}$$

$$= -\int d\mathbf{r} \frac{i\hbar}{2} \frac{d}{dt}\{(\Phi^{\dagger}(\varepsilon\mathbf{r}\cdot\nabla\Phi) - (\varepsilon\mathbf{r}\cdot\nabla\Phi)^{\dagger}\cdot\Phi)\} = \int d\mathbf{r} \frac{\varepsilon}{2} \frac{d}{dt}\{(\Phi^{\dagger}\mathbf{r}\cdot\mathbf{p}\Phi) + (\mathbf{r}\cdot\mathbf{p}\Phi)^{\dagger}\cdot\Phi)\}$$

The commutator of lhs of eqn (92) can be worked out by replacing the second quantized operators by the operators in usual coordinate representation, that is

$$H \longrightarrow \sum \frac{\mathbf{p}_i^2}{2m} + V$$

$$Q \longrightarrow \varepsilon \sum \mathbf{r}_i\cdot\mathbf{p}_i$$

this yields

$$[\sum \frac{\mathbf{p}_i^2}{2m} + V,\ \varepsilon \sum \mathbf{r}_i\cdot\mathbf{p}_i] = \varepsilon(-i\hbar)\sum \frac{\mathbf{p}_i^2}{m} + \varepsilon(i\hbar)\sum \mathbf{r}_i\cdot(\nabla_i V) \qquad (93)$$

In terms of field operators, eqn (93) gives $(i\hbar)\varepsilon\int d\mathbf{r}(-2\Phi^{\dagger}\frac{\mathbf{p}^2}{2m}\Phi + \Phi^{\dagger}\mathbf{r}\cdot\nabla V\Phi^{\dagger})$.

Finally, we obtain equation for the coordinate scaling transformation

$$\int d\mathbf{r}(-2\Phi^{\dagger}\frac{\mathbf{p}^2}{2m}\Phi + \Phi^{\dagger}\mathbf{r}\cdot\nabla V\Phi^{\dagger}) = \int d\mathbf{r} \frac{\varepsilon}{2} \frac{d}{dt}\{(\Phi^{\dagger}\mathbf{r}\cdot\mathbf{p}\Phi) + (\mathbf{r}\cdot\mathbf{p}\Phi)^{\dagger}\cdot\Phi)\} \qquad (93)$$

For a stationary state, the rhs of eqn (93) vanishes, therefore this equation

gives virial theorem (Bader and Nguyen-Dang, 1981).

In conclusion, by using one variational principle, we are able to show that the Fermion Lagrangian given in eqn (63) not only yields the equation of motion, but also produces the continuity equations for the conserved quantities. The continuity equations derived from the variational principle are identical to those directly obtained from the equation of motion. These consistencies not only demonstrate the beauty of the variational principle but also justify the correctness of the Lagrangian given in eqn (63). The atomic variational principle derived in Paper *I* uses this Lagrangian.

INTERNATIONAL JOURNAL OF QUANTUM CHEMISTRY, VOL. 43, 677–699 (1992)

Variational Principle and Path Integrals for Atoms in Molecules

P. F. ZOU AND R. F.W. BADER

Department of Chemistry, McMaster University, Hamilton, Ontario L8S 4M1, Canada

Abstract

Two things were done in this paper: (i) A generalization of Schwinger's variational principle to a subsystem was developed within the framework of quantum field theory and applied to the theory of atoms in molecules. This work generalizes the previous derivation given in the Schrödinger formulation. (ii) It is demonstrated that Feynman's path integral, when expressed in terms of the coherent-state representation, can be constructed for a subsystem of a many-electron system if a divergence term, which serves as a variational constraint in the definition of an atom in a molecule, is added to the Lagrangian. This formulation is equivalent to the atomic statement of the variational principle if the divergence term is suitably constructed. It is shown that the path integral can be expressed as a product of the individual atomic contributions to the steps along the paths with the action being determined by a corresponding sum of the atomic contributions to the action integral. © 1992 John Wiley & Sons, Inc.

1. Introduction

The classic papers of Wigner and Seitz in 1933 and 1934 on "a calculation of the chemical properties of metallic sodium" [1] introduced the concept of a subsystem into quantum mechanics. They did this by calculating the wave function for the single-valence electron in a sodium atom in the crystal subject to the boundary condition that there be a zero flux in the derivative of the function through the surface of the atom. This boundary condition defines the Wigner–Seitz cell in body-centered and face-centered cubic structures [2]. These authors adopted the atomic approach because of the great increase in difficulty of a quantum mechanical calculation that accompanies an increase in the number of atoms present in a system. One may, however, introduce the concept of a subsystem in the study of a system of any size by again identifying a subsystem with an atom, and in this manner recover, in an operational sense, the essence of chemistry—that the properties of any system are predicted and understood in terms of the characteristic and additive contributions made by every atom in the system. It is this recovery of the atomic concept from physics that is the purpose and motivation of the research reported here.

The approach followed by Wigner and Seitz, of solving for the wave function with periodic boundary conditions over connected cells, cannot be generalized to the many-electron case. Quantum mechanics can, however, be extended to obtain a definition of the properties of a particular class of subsystems [3–5] through a

 CCC 0020-7608/92/050677-23$04.00

generalization of Schwinger's derivation [6] of the principle of stationary action. The generalization of this principle demands the satisfaction of the variational constraint that the subsystem be bounded by a surface of zero flux in the gradient vector field of the system's charge density [3, 7], a condition that has been shown to define an atom in a molecule [8]. For a one-electron system, this constraint is identical to the Wigner–Seitz boundary condition. The imposition of the zero-flux atomic constraint generalizes the definition of the Wigner–Seitz cell to yield a unique decomposition of a system into a set of space-filling disjoint domains, even in the absence of symmetry. The present paper reports the derivation of the atomic statement of the principle of stationary action using quantum field theory and its corresponding statement in terms of Feynman path integrals [9]. Later papers will report on the application of these ideas to specific problems using a regional embedding technique [10].

A field theoretic development of the subsystem action principle was given earlier [4]. The present derivation introduces the variational constraint that defines a subsystem in a different manner and sets the stage for the path integral derivation that follows. It also avoids a somewhat arbitrary definition of the two-electron contribution to the subsystem Lagrangian used in the original development. It was pointed out there that, since all subsystem properties are obtained as averages over effective single-particle densities. field theory, because of its basic single-particle nature [6], appears to be the natural language to use in the description of a subsystem. In addition, both the Schrödinger and Heisenberg descriptions of a quantum system can be recovered from the field theoretic derivation of the variational principle. Most important, the subsystem variational principle gives a consistent and intuitive description of the subsystem equation of motion.

Auerbach and Kivelson [11] developed a technique for the decomposition of path integrals into subsystem contributions, called the path decomposition expansion. The method deals with the dynamics of a single particle and provides a clear physical picture of its motion through the different regions of configuration space. We are concerned with the many-electron case. If one proceeds in the manner of Auerbach and Kivelson, it is difficult to express the propagator, that is, the path integrals, as contributions from different regions. This difficulty arises because of the anticommutation relations between the creation or annihilation operators, as required in the description of a system of Fermions. To overcome these difficulties, one uses the so-called coherent-state representation to express the subspace path integrals. The discussion of the definition and properties of this representation given in the text is sufficient to enable a novice reader to follow the course of the argument, if not its detail. In recent years, an increasing number of papers have appeared that use the coherent-state representation in the study of many-Fermion systems [12–14].

The derivation of the subsystem variational principle using field theory is presented first and related to the theory of atoms in molecules. It is straightforward to recover the previous wave-function formulation of this theory and the associated boundary condition as stated in terms of a property of the atom's surface [3, 5]. This is followed by the development of the path integral technique for a

subsystem using the coherent representation. Basic information about coherent states, Grassman algebra, and path integrals in the coherent space is also given in the same section.

2. Field Theoretic Approach to the Subsystem Variation Principle

2.1. Subsystem Operators

The first requirement in the development of the mechanics of a subsystem is to define one- and two-particle field operators for a subsystem Ω, a bounded region of three-dimensional space. A subsystem operator is defined as

$$\hat{F}_\Omega(\mathbf{r}) = \chi_\Omega(\mathbf{r})\hat{F}(\mathbf{r}), \tag{1}$$

where the subsystem projector $\chi_\Omega(\mathbf{r})$ is defined as [3,4]

$$\chi_\Omega(\mathbf{r}) = \begin{cases} 1 & \mathbf{r} \in \Omega \\ 0 & \mathbf{r} \notin \Omega \end{cases}$$

The average value of an observable $\hat{F}$ over the subsystem Ω is then given by

$$\langle \hat{F} \rangle_\Omega = \int d\mathbf{x}_1 \cdots d\mathbf{x}_n \Psi^* \sum_i \hat{F}_\Omega(\mathbf{r}_i)\Psi, \tag{2}$$

where Ψ is the many-particle wave function of the system and the integration is over the space ($\mathbf{r}_i$) and spin (σ_i) coordinates of each electron, with $\mathbf{x}_i = \mathbf{r}_i\sigma_i$. The field theoretic expression for an operator $\hat{F}_\Omega$, all of which are considered to be functions only of the spatial variables, is defined in terms of the field operators $\hat{\Phi}^\dagger(\mathbf{x})$ and $\hat{\Phi}(\mathbf{x})$ as

$$\hat{F}_\Omega = \int d\mathbf{x}\hat{\Phi}^\dagger\hat{F}_\Omega(\mathbf{r})\hat{\Phi} = \sum_{\text{spin}} \int_\Omega d\mathbf{r}\hat{\Phi}^\dagger\hat{F}(\mathbf{r})\hat{\Phi}, \tag{3}$$

where we have performed the usual separation of integration over the space and spin coordinates [15]. The average value of the operator over the subsystem Ω, as given in the Schrödinger formulation by Eq. (2), is equivalently expressed as

$$\langle \hat{F} \rangle_\Omega = \langle \Psi | \hat{F}_\Omega | \Psi \rangle. \tag{4}$$

Accordingly, the field theoretic expressions for some important subsystem operators are the number operator:

$$\hat{N}_\Omega = \int d\mathbf{x}\hat{\Phi}^\dagger\hat{\chi}_\Omega(\mathbf{r})\hat{\Phi}; \tag{5}$$

the moment operator:

$$\hat{\mathbf{R}}_\Omega = \int d\mathbf{x}\hat{\Phi}^\dagger\mathbf{r}\hat{\chi}_\Omega(\mathbf{r})\hat{\Phi}; \tag{6}$$

the kinetic energy operator:

$$\hat{K}_\Omega = \frac{\hbar^2}{2m} \int d\mathbf{x}(\nabla\hat{\Phi}^\dagger \cdot \nabla\hat{\Phi})\hat{\chi}_\Omega(\mathbf{r}); \tag{7}$$

and for a two-body interaction denoted by $g(\mathbf{r}, \mathbf{r}')$, the operator is

$$\hat{V}_\Omega = \frac{1}{2} \iint dx\, dx' \Phi^\dagger(x)\Phi^\dagger(x') g(\mathbf{r}, \mathbf{r}') \hat{\Phi}(x')\hat{\Phi}(x)\hat{\chi}_\Omega(\mathbf{r}) . \tag{8}$$

It is important to note that in a two-body interaction, one particle is created over the entire system, while the second is created only over the subsystem. Thus, the subsystem average of such an operator includes the interaction of the subsystem with the remainder of the system, as well as the interactions arising from within the subsystem.

Subsystem operators possess the following properties:

(1) If $\Omega = \Omega_1 + \Omega_2$ and $\Omega_1 \cap \Omega_2 = \partial\Omega_1 \cap \partial\Omega_2$, that is, Ω_1 and Ω_2 share a common surface or the cross set is empty, then

$$\hat{F}_\Omega = \hat{F}_{\Omega_1} + \hat{F}_{\Omega_2}. \tag{9}$$

(2) If $[\hat{F}, \hat{G}] = \hat{B}$, then

$$[\hat{F}, \hat{G}]_\Omega = [\hat{F}_\Omega, \hat{G}_\Omega] = \hat{B}_\Omega , \tag{10}$$

since the commutator equation is satisfied locally.

2.2. *Principle of Stationary Action for a Subsystem*

Schwinger [6] postulated that the infinitesimal change in the transformation function connecting the eigenstates $|q_1, t_1\rangle$ and $|q_2, t_2\rangle$ is $(i/\hbar)$ times the matrix element of the variation of the action integral operator $\hat{W}$ connecting the two states:

$$\delta\langle q_2 t_2 | q_1 t_1\rangle = \frac{i}{\hbar}\langle q_2 t_2 | \delta\hat{W}_{12} | q_1 t_1\rangle = \frac{i}{\hbar}\langle q_2 t_2 | \delta \int \hat{\mathcal{L}}\, dt | q_1 t_1\rangle , \tag{11}$$

where $\hat{\mathcal{L}}$, the Lagrange function operator, is an invariant Hermitian function of the variable q and its first derivatives. If the parameters of a system are not altered, then the variation of the action integral in Eq. (11) arises only from infinitesimal changes of the sets of commuting observables at the times t_1 and t_2. The same change in transformation function can be expressed in terms of the action of infinitesimal generating operators $\hat{G}(t_1)$ and $\hat{G}(t_2)$ acting on the two eigenvectors:

$$\delta\langle q_2 t_2 | q_1 t_1\rangle = \frac{i}{\hbar}\langle q_2 t_2 | \hat{G}(t_2) - \hat{G}(t_1) | q_1 t_1\rangle , \tag{12}$$

and a comparison of Eqs. (11) and (12) yields the operator principle of stationary action:

$$\delta\hat{W}_{12} = \hat{G}(t_2) - \hat{G}(t_1) . \tag{13}$$

It states that the action integral operator is unaltered by infinitesimal variations in the state functions between the times t_1 and t_2, being affected only by the action of generators at the two time endpoints.

In the principle of stationary action, the variation of the action integral does not vanish as it does in Hamilton's principle, but, instead, equals the difference in the effects of infinitesimal generators acting at the two time endpoints. This result requires that the variation of the action integral in Eq. (11) be generalized to include the variations of the state function and of the time at the time endpoints. The principle of stationary action then implies the equation of motion of the system as obtained in Hamilton's principle, and the endpoint variations define the generators of the infinitesimal canonical transformations that induce changes in the dynamical properties of the system. In this way, a single dynamical principle recovers not only the equation of motion, but also defines the observables and their equations of motion and makes possible the derivation of the Heisenberg commutation relations.

The generators $\hat{G}(t)$ are introduced via the infinitesimal unitary operator $\hat{U}$:

$$\hat{U} = \hat{1} - \frac{i\varepsilon}{\hbar}\hat{G}, \tag{14}$$

where ε is an infinitesimal number. We consider only those generators that induce spatial or temporal changes, independent of spin. Such unitary operators induce an infinitesimal transformation on either an observable $\hat{F}$:

$$\delta\hat{F} = \hat{U}\hat{F}\hat{U}^{\dagger} - \hat{F} = \left(-\frac{i\varepsilon}{\hbar}\right)[\hat{G}, \hat{F}], \tag{15}$$

or on the field operator $\hat{\Phi}$:

$$\delta\hat{\Phi} = \hat{U}\hat{\Phi} - \hat{\Phi} = \left(-\frac{i\varepsilon}{\hbar}\right)\hat{G}\hat{\Phi}. \tag{16}$$

The latter variation may be considered to arise from the action of the generator on the coordinate representation wave function $\Phi_i(\mathbf{x})$ of the i'th single-particle state:

$$\delta\hat{\Phi} = \left(-\frac{i\varepsilon}{\hbar}\right)\sum_i [\hat{G}\Phi_i(\mathbf{x})]\hat{a}_i, \tag{17}$$

or through its action on the annihilation operator:

$$\delta\hat{\Phi} = \left(-\frac{i\varepsilon}{\hbar}\right)\sum_i \Phi_i(\mathbf{x})\,[\hat{G}, \hat{a}_i]. \tag{18}$$

The two modes of action of the generator are equivalent.

The action integral operator for a subsystem is defined to be

$$\hat{W}_{12}[\hat{\Phi}, \Omega] = \int_{t_1}^{t_2} \hat{\mathfrak{L}}[\hat{\Phi}, t, \Omega]\, dt, \tag{19}$$

where the subsystem Lagrangian function operator, following the rules laid down above, is given by the subsystem integration of the Lagrangian density:

$$\hat{\mathcal{L}}[\hat{\Phi}, t, \Omega] = \sum_{\text{spin}} \int_{\Omega} d\mathbf{r} \hat{L}[\hat{\Phi}, \nabla\hat{\Phi}, \dot{\hat{\Phi}}]$$
$$= \sum_{\text{spin}} \left\{ \frac{i\hbar}{2} \int_{\Omega} d\mathbf{r} (\hat{\Phi}^{\dagger} \cdot \dot{\hat{\Phi}} - \dot{\hat{\Phi}}^{\dagger} \cdot \hat{\Phi}) - \frac{\hbar^2}{2m} \int_{\Omega} d\mathbf{r} \nabla\hat{\Phi}^{\dagger} \cdot \nabla\hat{\Phi} - \int_{\Omega} d\mathbf{r} \hat{\Phi}^{\dagger} \hat{V} \hat{\Phi} \right.$$
$$\left. - \frac{1}{2} \int_{\Omega} d\mathbf{r} \int d\mathbf{x}' \hat{\Phi}^{\dagger}(\mathbf{x}) \hat{\Phi}^{\dagger}(\mathbf{x}') g(\mathbf{r}, \mathbf{r}') \hat{\Phi}(\mathbf{x}') \hat{\Phi}(\mathbf{x}) \right\}. \tag{20a}$$

The Lagrangian density appearing in Eq. (20a) is

$$\hat{L}[\hat{\Phi}, \nabla\hat{\Phi}, \dot{\hat{\Phi}}] = \frac{i\hbar}{2} (\hat{\Phi}^{\dagger} \cdot \dot{\hat{\Phi}} - \dot{\hat{\Phi}}^{\dagger} \cdot \hat{\Phi}) - \frac{\hbar^2}{2m} \nabla\hat{\Phi}^{\dagger} \cdot \nabla\hat{\Phi} - \hat{\Phi}^{\dagger} \hat{V} \hat{\Phi}$$
$$- \frac{1}{2} \int d\mathbf{x}' \hat{\Phi}^{\dagger}(\mathbf{x}) \hat{\Phi}^{\dagger}(\mathbf{x}') g(\mathbf{r}, \mathbf{r}') \hat{\Phi}(\mathbf{x}') \hat{\Phi}(\mathbf{x}), \tag{20b}$$

where $\hat{V}$ is the external one-body, and $g(\mathbf{r}, \mathbf{r}')$, the two-body potential energy operator. The generalized variation of the action integral is one that retains the variations in the field operators at the time endpoints along with a variation of these endpoints. For a subsystem, one also includes a variation of the surface $S(\hat{\Phi}, \Omega)$ that bounds the subsystem and one obtains

$$\delta\hat{W}_{12}[\hat{\Phi}, \Omega] = \sum_{\text{spin}} \left\{ \int_{t_1}^{t_2} dt \int_{\Omega} d\mathbf{r} \left\{ \left(\frac{\delta\hat{L}}{\delta\hat{\Phi}} - \nabla \cdot \frac{\delta\hat{L}}{\delta\nabla\hat{\Phi}} - \frac{d}{dt} \frac{\delta\hat{L}}{\delta\dot{\hat{\Phi}}} \right) \delta\hat{\Phi} + cc \right\} \right.$$
$$+ \left\{ \int_{\Omega} d\mathbf{r} \hat{L}\, \delta t + \int_{\Omega} d\mathbf{r} \left(\frac{\delta\hat{L}}{\delta\dot{\hat{\Phi}}} \delta\hat{\Phi} + cc \right) \right\} \Big|_{t_1}^{t_2}$$
$$+ \int_{t_1}^{t_2} dt \left\{ \oint d\mathbf{S} \cdot \vec{n} \hat{L}\, \delta S + \oint d\mathbf{S} \cdot \left(\frac{\delta\hat{L}}{\delta\nabla\hat{\Phi}} \delta\hat{\Phi} + cc \right) \right\}$$
$$\left. + \int_{t_1}^{t_2} dt \left\{ (-i\hbar/2) \oint d\mathbf{S} (\partial S/\partial t) \hat{\Phi}^{\dagger}\, \delta\Phi + cc \right\} \right\}. \tag{21}$$

The first set of terms in Eq. (21) results from changes in action within the subsystem Ω between the times t_1 and t_2; the second set results from the changes occurring within Ω at the two time endpoints and the two final terms from the changes in and within the surface of Ω over time. The final term in the second set arises from the use of an integration by parts to rid the expression of terms involving $\delta\dot{\hat{\Phi}}$ [8]. The first set of terms represents changes in the space–time volume; the next two sets are due to changes in the surface of this volume—the first from changes in the time and the final ones from changes in the spatial surface.

According to Schwinger's principle of stationary action [Eq. (13)], the contribution to the variation of the action from the space–time volume must vanish, and

in this manner, one obtains the equation of motion for the field

$$\frac{\delta \hat{L}}{\delta \hat{\Phi}} - \nabla \cdot \frac{\delta \hat{L}}{\delta \nabla \hat{\Phi}} - \frac{d}{dt}\frac{\delta \hat{L}}{\delta \dot{\hat{\Phi}}} = 0, \tag{22}$$

that is,

$$-i\hbar\dot{\hat{\Phi}}^{\dagger} = -\frac{\hbar^2}{2m}\nabla^2\hat{\Phi}^{\dagger} + \hat{\Phi}^{\dagger}V + \hat{\Phi}^{\dagger}(\mathbf{x})\int d\mathbf{x}'\hat{\Phi}^{\dagger}(\mathbf{x}')g(\mathbf{r},\mathbf{r}')\hat{\Phi}(\mathbf{x}'). \tag{23}$$

The variation of the two-body interaction in L [see Eq. (20b)] yields the contribution

$$\frac{1}{2}\hat{\Phi}^{\dagger}(\mathbf{x})\int d\mathbf{x}'\hat{\Phi}^{\dagger}(\mathbf{x}')g(\mathbf{r},\mathbf{r}')\hat{\Phi}(\mathbf{x}')\,\delta\hat{\Phi}(\mathbf{x}) + \frac{1}{2}\hat{\Phi}^{\dagger}(\mathbf{x})\int d\mathbf{x}'\hat{\Phi}^{\dagger}(\mathbf{x}')g(\mathbf{r},\mathbf{r}')\frac{\delta\hat{\Phi}(\mathbf{x}')}{\delta\hat{\Phi}(\mathbf{x})}\hat{\Phi}(\mathbf{x})\,\delta\hat{\Phi}(\mathbf{x}) + cc, \tag{24}$$

and the second term in this contribution may be written as

$$\frac{1}{2}\hat{\Phi}^{\dagger}(\mathbf{x})\int d\mathbf{x}'\hat{\Phi}^{\dagger}(\mathbf{x}')g(\mathbf{r},\mathbf{r}')\hat{\Phi}(\mathbf{x}')\,\delta\hat{\Phi}(\mathbf{x}) \tag{25}$$

to yield the result given in Eq. (23) for the two-body interaction.

The total variation in $\hat{\Phi}$ denoted by $\Delta\hat{\Phi}$ is composed of a change in $\hat{\Phi}(\mathbf{x})$ at $\mathbf{x}$, $\delta\hat{\Phi}(\mathbf{x})$, and of the changes in $\hat{\Phi}$ resulting from temporal and spatial displacements, that is,

$$\Delta\hat{\Phi}(\mathbf{x}) = \delta\hat{\Phi}(\mathbf{x}) + \dot{\hat{\Phi}}\,\delta t + \partial_{\mathbf{r}}\hat{\Phi}(\mathbf{x})\,\delta\mathbf{r}. \tag{26}$$

If we restrict ourselves to changes in space–time, we have

$$\delta\hat{\Phi}(\mathbf{x}) = -\dot{\hat{\Phi}}\,\delta t - \partial_{\mathbf{r}}\hat{\Phi}(\mathbf{x})\,\delta\mathbf{r}. \tag{27}$$

Using Eq. (27) and the equation of motion [Eq. (24)], the variation of the subsystem action in Eq. (21) is given by

$$\delta\hat{W}_{12}[\hat{\Phi},\Omega] = \sum_{\text{spin}}\left\{-\int_{\Omega}d\mathbf{r}\{\hat{H}\,\delta t + (\hat{\Pi}\,\partial_{\mathbf{r}}\hat{\Phi}(\mathbf{x}) + cc)\,\delta\mathbf{r}\}\Big|_{t_1}^{t_2} - \int_{t_1}^{t_2}dt\oint d\mathbf{S}\cdot\left\{-\frac{\hbar^2}{2m}\nabla\hat{\Phi}\dot{\hat{\Phi}}\,\delta t + cc + \hat{P}_i\,\delta S\right\} + \int_{t_1}^{t_2}dt\left\{(-i\hbar/2)\oint d\mathbf{S}(\partial S/\partial t)\hat{\Phi}^{\dagger}\,\delta\hat{\Phi} + cc\right\}\right\}, \tag{28}$$

where the following definitions have been introduced:

$\hat{\Pi}(\mathbf{x})$, the momentum conjugate to the field variable $\hat{\Phi}(\mathbf{x})$ is

$$\hat{\Pi}(\mathbf{x}) = \frac{\delta\hat{L}}{\delta\dot{\hat{\Phi}}} = \frac{i\hbar}{2}\hat{\Phi}^{\dagger}(\mathbf{x}). \tag{29}$$

$\hat{H}$, the Hamiltonian, in analogy with classical particle mechanics, is

$$\hat{H} = (\hat{\Pi}\dot{\hat{\Phi}} + cc) - \hat{L}. \tag{30}$$

$\hat{P}_i$, the diagonal elements of energy-momentum tensor, is

$$\hat{P}_i = \left(-\frac{\hbar^2}{2m}\nabla\hat{\Phi}^\dagger\partial_i\hat{\Phi}(\mathbf{x}) + cc\right) - \vec{n}\hat{L}. \tag{31}$$

Equation (28) resolves the variations of the action for the subsystem into two parts. The first describes the contributions arising from variations in time and in the spatial coordinates over the space of the subsystem at the two time endpoints, while the second gives contributions from corresponding changes over the spatial surface of the subsystem integrated over the time. The variations in $\mathbf{r}$ that cause a displacement in the surface are denoted by $\partial_i\Phi(\mathbf{x})\,\partial S$. Equation (28) identifies $-\hat{H}\,\delta t$ as the generator of temporal changes within a system. The properties of interest for a subsystem are obtained as a result of spatial variations, the time dependence of a subsystem property being obtainable from the field equation. Thus, δt is set equal to zero in Eq. (28) to yield the following statement of the principle of stationary action for a subsystem:

$$\delta\hat{W}_{12}[\hat{\Phi}, \Omega] = \hat{G}_\varepsilon(t_2, \Omega) - \hat{G}_\varepsilon(t_1, \Omega) - \sum_{\text{spin}}\int_{t_1}^{t_2} dt \oint d\mathbf{S} \cdot \{\hat{P}_i\,\delta S + [(i\hbar/2)(\partial S/\partial t)\hat{\Phi}^\dagger\delta\hat{\Phi} + cc]\}, \tag{32}$$

where

$$\hat{G}_\varepsilon(t, \Omega) = \sum_{\text{spin}}\int_\Omega d\mathbf{r}(\hat{\Pi}\,\delta\hat{\Phi}(\mathbf{x}) + cc) = \sum_{\text{spin}}\frac{\varepsilon}{2}\left\{\int_\Omega d\mathbf{r}\hat{\Phi}^\dagger(\hat{G}\hat{\Phi}) + cc\right\}. \tag{33}$$

Differentiation of Eq. (32) with respect to t yields

$$\delta\hat{\mathcal{L}}[\hat{\Phi}, t, \Omega] = \frac{d\hat{G}_\varepsilon}{dt} + \sum_{\text{spin}}\oint d\mathbf{S} \cdot \left\{\left(-\frac{\hbar^2}{2m}\nabla\hat{\Phi}^\dagger\delta\hat{\Phi} + cc\right) + \vec{n}\hat{L}\,\delta S - [(i\hbar/2)(\partial S/\partial t)\hat{\Phi}^\dagger\delta\hat{\Phi} + cc]\right\}. \tag{34}$$

Using the field equation and Eq. (33) for the definition of $\hat{G}_\varepsilon(t, \Omega)$, the Heisenberg equation of motion for a subsystem operator is

$$\frac{d\hat{G}_\varepsilon}{dt} = \frac{\varepsilon}{2}\{(-i/\hbar)\langle\hat{\Phi}|[\hat{G}, \hat{H}]|\hat{\Phi}\rangle_\Omega + cc\} + \sum_{\text{spin}}\left\{\oint d\mathbf{S} \cdot \left\{\frac{\varepsilon\hbar}{4mi}(\nabla\hat{\Phi}^\dagger\hat{G}\hat{\Phi} - \hat{\Phi}^\dagger\nabla(\hat{G}\hat{\Phi})) + cc\right\} + \left\{(1/2)\oint d\mathbf{S}(\partial S/\partial t)\hat{\Phi}^\dagger\hat{G}\hat{\Phi} + cc\right\}\right\}. \tag{35}$$

Substitution of this result into Eq. (34), recalling Eq. (16) for the relation between the generator $\hat{G}$ and the variation in Φ, yields

$$\delta\hat{\mathcal{L}}[\hat{\Phi}, t, \Omega] = -(\varepsilon/2)\{(i/\hbar)\langle\hat{\Phi}|[\hat{G}, \hat{H}]|\hat{\Phi}\rangle_\Omega + cc)\} - \frac{\hbar^2}{4m}\sum_{\text{spin}}\oint d\mathbf{S}\cdot\{(\hat{\Phi}^\dagger\nabla(\delta\hat{\Phi}) + \nabla\hat{\Phi}^\dagger\delta\hat{\Phi} + cc)\} + \oint d\mathbf{S}\cdot\vec{n}\hat{L}\delta S. \tag{36}$$

Using again the equation of motion, one finds that the Lagrangian density, as it appears in Eq. (36) and defined in Eq. (20b) at the point of variation, that is, where the field equation applies, is given by

$$\hat{L} = -\frac{\hbar^2}{4m}\nabla^2(\hat{\Phi}^\dagger\hat{\Phi}), \tag{37}$$

and substitution of this result into Eq. (36) yields the expression for the variation of the subsystem Lagrangian function operator for a subsystem

$$\delta\hat{\mathcal{L}}[\hat{\Phi}, t, \Omega] = -(\varepsilon/2)\left\{(i/\hbar)\langle\hat{\Phi}|[\hat{G}, \hat{H}]|\hat{\Phi}\rangle_\Omega + cc\right\} - \frac{\hbar^2}{4m}\sum_{\text{spin}}\oint d\mathbf{S} \cdot\{(\hat{\Phi}^\dagger\nabla(\delta\hat{\Phi}) + \delta\hat{\Phi}^\dagger\nabla\hat{\Phi} + cc) + \vec{n}\nabla^2(\hat{\Phi}^\dagger\hat{\Phi})\delta S\}. \tag{38}$$

For a total system with boundaries at infinity, that is, a closed isolated system, there are no contributions to the change in the Lagrangian from displacements in the surface of the system and the expression for the variation of the Lagrange function Eq. (38) reduces to

$$\delta\hat{\mathcal{L}}[\hat{\Phi}, t] = -(i\varepsilon/\hbar)\langle\hat{\Phi}|[\hat{G}, \hat{H}]|\hat{\Phi}\rangle_{(\mathcal{R})}. \tag{39}$$

What we demonstrate next is that when the surface of the subsystem is chosen so that a particular variational constraint, as determined by the topology of the charge density is satisfied, the subsystem expression for the change in the Lagrangian [Eq. (38)] assumes the form corresponding to that given in Eq. (39) for the total system. Thus, the change in the Lagrange function for an atom in a molecule is entirely determined by variations within the atom with no contributions from its surface, as it is for the total system within which the atom is found. The expression for the change in the atomic action integral exhibits corresponding properties [4,5,8].

2.3. *Definition of an Atom in a Molecule*

The atomic form is imposed on the structure of matter as a consequence of the principal topological property exhibited by a molecular electronic charge distribution—that, in general, it possesses local maxima only at the positions of the nuclei. Because of this morphological feature of $\rho(\mathbf{r})$, the nuclei act as attractors in the gradient vector field of the charge density, leading to the definition of an atom as the union of an attractor and its associated basin. This definition leads to the disjoint partitioning of the total space of a system into regions, each of which, in general, contains a single attractor (see Fig. 1). The atoms, as well as

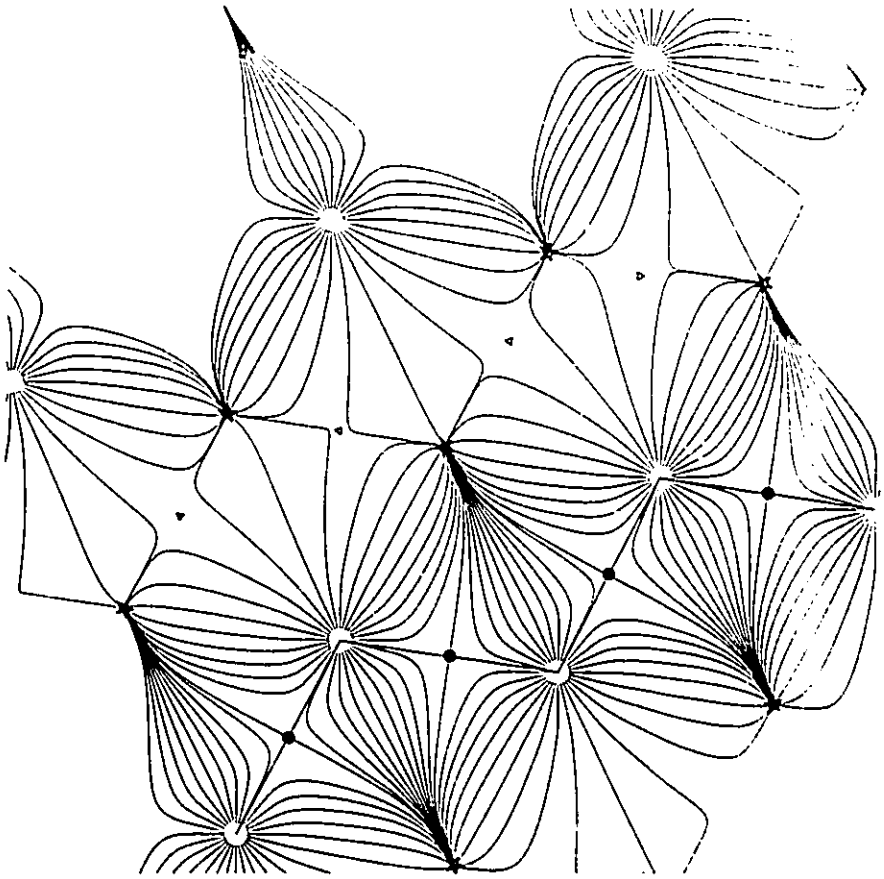

Figure 1. Portion of the gradient vector field of the charge density in diamond for the (1, 1, 0) plane. All the trajectories shown terminate at the positions of the carbon nuclei (denoted by small open circles) where the charge density is a local maximum, except for the pairs that terminate at each of the (3, −1) critical points (denoted by dots) and that define the intersection of the interatomic surfaces with the plane of the diagram. The two trajectories that originate at each (3, −1) critical point define the lines of maximum charge density—the bond paths—linking neighboring carbon nuclei. Also appearing in this plane in the boundary of each atom are (3, +3) or cage critical points (denoted by a star) and (3, +1) or ring critical points (denoted by a triangle). In this plane, the bond and ring critical points both appear as (2, 0) critical points. The electronic charge density was calculated using the program CRYSTAL 88 [16].

dominating the physical form of a system, also determine its behavior, since the atomic properties sum to give the corresponding properties of the total system. The dynamics of the gradient vector field of the charge density, as caused by motions of the nuclei, forms the basis for a theory of molecular structure and structural stability [8]. An application of the structural aspects of the theory to the properties of metals has recently appeared [17].

It is clear from Figure 1 that each atomic basin exhibits the property of zero flux in the gradient vector field of the charge density, that is, it is bounded by a surface that satisfies the condition

$$\langle\Psi|\mathbf{n}\cdot\nabla\hat{\rho}(\mathbf{r}_s)|\Psi\rangle = \nabla\rho(\mathbf{r}_s)\cdot\mathbf{n}(\mathbf{r}_s) = 0 \qquad \mathbf{r}_s \in \partial\Omega\,, \tag{40}$$

where the density operator $\hat{\rho}(\mathbf{r})$ is defined as

$$\hat{\rho}(\mathbf{r}) = \sum_{\text{spin}} \hat{\Phi}^\dagger(\mathbf{x})\hat{\Phi}(\mathbf{x})\,. \tag{41}$$

The basins of two neighboring atoms are separated by an interatomic surface that is defined by the set of trajectories of the gradient vector field of ρ that terminate at a particular type of critical point: a $(3,-1)$ critical point (Fig. 1). The vector $\nabla\rho(\mathbf{r})$ is thus tangent at every point on such a surface and Eq. (40) is necessarily satisfied. The surface bounding linked groupings of atoms up to and including the total system also satisfies Eq. (40).

The definition of an atom given in Eq. (40) is equivalent to demanding the satisfaction of the variational constraint

$$\delta\left\{\int_\Omega d\mathbf{r}\nabla^2\rho(\mathbf{r})\right\} = 0\,. \tag{42}$$

Since this variation equals a surface integral of the integrand multiplied by the variation of the surface plus a volume integral of the variation of the integrand, the constraint leads to the identification of the integral arising from the variation of the surface in Eq. (38) with the negative of that arising from the variation of the integrand:

$$\begin{aligned}\oint d\mathbf{S}\cdot\vec{n}\nabla^2\rho(\mathbf{r})\,\delta S &= -\int_\Omega d\mathbf{r}\,\delta\{\nabla^2\rho(\mathbf{r})\} \\ &= -\sum_{\text{spin}}\int d\mathbf{r}'\oint d\mathbf{S}\cdot\{(\Psi^\dagger\nabla(\delta\Psi) + \delta\Psi^\dagger\nabla\Psi + cc)\}\,,\end{aligned} \tag{43}$$

where the integral over $d\mathbf{r}'$ implies an integration over the coordinates of all electrons but the one whose coordinate $\mathbf{r}$ is integrated over the basin of atom Ω. The possibility of introducing the constraint into the variation of the action and Lagrangian integrals is a result of the property possessed by the Lagrangian density given in Eq. (37): That at the point of variation it reduces to a term proportional to $\nabla^2\rho(\mathbf{r})$. Thus, substituting the identity in Eq. (43) into Eq. (38) for a system in a state $|\Psi\rangle$ yields the atomic statement of the variational principle

$$\langle\Psi|\delta\hat{\mathcal{L}}[\hat{\Phi},t,\Omega]|\Psi\rangle = \delta\mathcal{L}[\Psi,t,\Omega] = (\varepsilon/2)\{(i/\hbar)\langle\Psi|[\hat{H},\hat{G}]|\Psi\rangle_\Omega + cc\}\,. \tag{44}$$

This result is identical in form and content to that given Eq. (39) for a total system. Thus, the principle of stationary action defines the observables (by identifying the variations in the field operator $\hat{\Phi}$ with the generators $\hat{G}$), their average values, and their equations of motion for an atom in a molecule in the same manner as it does for the total system and the theorems derived from this principle,

such as the Ehrenfest and virial theorems, apply to the atoms as well as to the total system of which they are a part. Indeed, the region Ω may refer to the total system and Eq. (44) generalizes the usual quantum description of a system to its subsystems.

3. Subsystem Path Integrals

3.1. Path Integrals for Electrons

Feynman's path integral method [9], like Schwinger's quantum action principle Eq. (11), is concerned with the determination of the transformation function, or transition amplitude, which gives the wave function at one time in terms of the wave function at an earlier time. Schwinger's principle is, in fact, a differential form of Feynman's formulation for the determination of the transformation function, a function that in the path integral method is referred to as the propagator $K(\mathbf{r}, t; \mathbf{r}', t')$ and whose role is defined in Eq. (45):

$$\langle \mathbf{r}, t \,|\, \Psi \rangle = \int d\mathbf{r}' K(\mathbf{r}, t; \mathbf{r}', t') \langle \mathbf{r}', t' \,|\, \Psi \rangle . \tag{45}$$

Feynman states that the amplitude $K(\mathbf{r}, t; \mathbf{r}', t')$ is the sum of contributions from each path connecting $\mathbf{r}', t'$ to $\mathbf{r}, t$. Each of these contributions has the same modulus, but its phase is proportional to the classical action evaluated along the path in question, that is,

$$K(\mathbf{r}, t; \mathbf{r}', t') = \int \prod_i (A_i d\mathbf{r}_i) \exp\left\{ \frac{i}{\hbar} \sum_i L(t_i)\varepsilon \right\}, \tag{46}$$

where A_i is the normalization constant.

It is difficult to formulate Feynman's path integrals in a space–time representation for many-fermion systems, because of the required permutational antisymmetry. It is the classical action that is evaluated in the path integral technique and the Fermion antisymmetry must be embodied in the classical expression for the action. This presents no problem for Bosons since the associated operator commutation relation $[\hat{b}, \hat{b}^\dagger] = 1$ becomes $[b, b^\dagger] = 0$ in the classical limit and the action $\mathcal{W}$ can be expressed in terms of ordinary complex numbers b and b^*. For Fermions, on the other hand, one has the anticommutation relationship $[\hat{a}, \hat{a}^\dagger]_+ = 1$, and transferring this result to the classical limit demands that $[a, a^\dagger]_+ = 0$. This unusual property forces one to introduce a set of anticommuting variables called Grassmann numbers. These numbers are obtained as the eigenvalues of a set of states defined to be the eigenstates of the annihilation operators [12]: the coherent states. The coherent states form a basis for the Fock space. They may be regarded as the analog of the basis of position states $|\mathbf{r}\rangle$ defined as the eigenstates of the position operator $\hat{\mathbf{r}}$. Their associated eigenvalues generate an anticommuting set of numbers that obey Grassman algebra, and through their use, one is able to meet the antisymmetry requirement resulting from the exchange of fermions. The construction of Fermion coherent states and the algebras of anticommuting numbers, Grassmann algebras, are admirably treated in [12].

For a state $|\alpha\rangle$, there exists annihilation and creation operators $\hat{a}_\alpha$ and $\hat{a}_\alpha^\dagger$, respectively, and, thus, for the complete set of states $\{|\alpha\rangle\}$, one has the corresponding set of operators $\{\hat{a}_\alpha, \hat{a}_\alpha^\dagger\}$. A coherent state $|a\rangle$ is defined as one that is an eigenfunction of the annihilation operator

$$\hat{a}_\alpha|a\rangle = a_\alpha|a\rangle . \tag{47}$$

Since the annihilation operators anticommute, so do the eigenvalues:

$$a_\alpha a_\beta + a_\beta a_\alpha = 0 . \tag{48}$$

Thus, the eigenvalues $\{a_\alpha\}$ of $\{\hat{a}_\alpha\}$ obey Grassman algebra and there exists a one-to-one correspondence between the operators $\{\hat{a}_\alpha, \hat{a}_\alpha^\dagger\}$ and the Grassman algebra $\{a_\alpha, a_\alpha^\dagger\}$:

$$\hat{a}_\alpha \longrightarrow a_\alpha \quad \text{and} \quad \hat{a}_\alpha^\dagger \longrightarrow a_\alpha^\dagger .$$

The resolution of the identity may be expressed as

$$\int \prod_\alpha (da_\alpha^\dagger\, da_\alpha) \exp\left[-\sum_\alpha a_\alpha^\dagger a_\alpha\right] |a\rangle\langle a| = 1 .$$

Thus, any state $|\Psi\rangle$ can be resolved as follows:

$$|\Psi\rangle = \int \prod_\alpha (da_\alpha^\dagger\, da_\alpha) \exp\left[-\sum_\alpha a_\alpha^\dagger a_\alpha\right] |a\rangle\langle a|\Psi\rangle , \tag{50}$$

where $\langle a|\Psi\rangle$ is the wave function in the coherent-state representation.

The propagator $K(a_f, a_i)$ in the coherent-state representation is defined as

$$\langle a_f|\Psi\rangle = \int K(a_f, a_i) \prod_\alpha (da_{i\alpha}^\dagger da_{i\alpha}) \langle a_i|\Psi\rangle , \tag{51}$$

where the subscripts i and f denote initial and final times. From Schrödinger's equation, one has

$$\begin{aligned}\langle a_f|\Psi\rangle &= \langle a_f|\exp\left\{-\frac{i}{\hbar}\hat{H}(t_f - t_i)\right\}|\Psi\rangle \\ &= \int \langle a_f|\exp\left\{-\frac{i}{\hbar}\hat{H}(t_f - t_i)\right\} \exp\left[-\sum_\alpha a_{i\alpha}^\dagger a_{i\alpha}\right] \prod_\alpha (da_{i\alpha}^\dagger da_{i\alpha})|a_i\rangle\langle a_i|\Psi\rangle ,\end{aligned} \tag{52}$$

and from this equation and Eq. (51), one obtains

$$K(a_f; a_i) = \langle a_f|\exp\left\{-\frac{i}{\hbar}\hat{H}(t_f - t_i)\right\} \exp\left[-\sum_\alpha a_{i\alpha}^\dagger a_{i\alpha}\right]|a_i\rangle . \tag{53}$$

The matrix element of a normal-ordered operator between two coherent states can be written as [18]

$$\langle a|\hat{F}(\hat{a}^\dagger, \hat{a})|a'\rangle = \exp\left[\sum_\alpha a_\alpha^\dagger a_\alpha'\right] F(a^\dagger, a') . \tag{54}$$

It should be noted that $\exp\{-i/\hbar\,\hat{H}\varepsilon\} \approx 1 - i/\hbar\,\hat{H}\varepsilon$, for $\varepsilon \to 0$, is a normal-ordered operator. Use of this result in Eq. (53) yields the following expression for the path integrals, with k denoting the time ordering:

$$\begin{aligned} K(a_f, a_i) = \lim_{\varepsilon \to 0} \int \prod_k \prod_\alpha (da^\dagger_{k\alpha} da_{k\alpha}) \langle a_f | \exp\left\{-\frac{i}{\hbar}\hat{H}\varepsilon\right\} |a_n\rangle \exp\left[-\sum_\alpha a^\dagger_{n\alpha} a_{n\alpha}\right] \\ \cdots \langle a_{(k+1)}| \exp\left\{-\frac{i}{\hbar}\hat{H}\varepsilon\right\} |a_k\rangle \exp\left[-\sum_\alpha a^\dagger_{k\alpha} a_{k\alpha}\right] \\ \cdots \langle a_1| \exp\left\{-\frac{i}{\hbar}\hat{H}\varepsilon\right\} |a_i\rangle \exp\left[-\sum_\alpha a^\dagger_{i\alpha} a_{i\alpha}\right] \\ = \lim_{\varepsilon \to 0} \int \prod_k \prod_\alpha (da^\dagger_{k\alpha} da_{k\alpha}) \exp\left\{\frac{i}{\hbar}\sum_k^n L^k \varepsilon\right\}, \end{aligned} \tag{55}$$

where

$$\begin{aligned} L^1 &= -i\hbar \sum_\alpha \frac{a^\dagger_{1\alpha} - a^\dagger_{i\alpha}}{\varepsilon} a_{i\alpha} - H^1(a^\dagger, a) \\ L^k &= -i\hbar \sum_\alpha \frac{a^\dagger_{k\alpha} - a^\dagger_{(k-1)\alpha}}{\varepsilon} a_{(k-1)\alpha} - H^k(a^\dagger, a) \\ L^{n+1} &= -i\hbar \sum_\alpha \frac{a^\dagger_{f\alpha} - a^\dagger_{n\alpha}}{\varepsilon} a_{n\alpha} - H^{n+1}(a^\dagger, a) \end{aligned} \tag{56}$$

and

$$H^k(a^\dagger, a) = H(a^\dagger_{k\alpha}, a_{(k-1)\alpha})\,. \tag{57}$$

The Hamiltonian appearing in these expressions expresses the kinetic energy in its classical form, that is,

$$H(\hat{a}^\dagger, \hat{a}) = \sum_{\alpha,\beta} (T_{\alpha\beta} + V_{\alpha\beta}) \hat{a}^\dagger_\alpha \hat{a}_\beta, \tag{58}$$

where

$$T_{\alpha\beta} = (\hbar^2/2m) \int \nabla\Phi^\dagger_\alpha(\mathbf{x}) \cdot \nabla\Phi_\beta(\mathbf{x})\, d\mathbf{x}\,.$$

The contribution of a typical term to the final expression for the propagator in Eq. (55) is derived in the Appendix.

A change in basis to one expressed in terms of the coordinates $\mathbf{x}$ enables one to recast the expressions for the Lagrangian in Eq. (56) into Grassman field variables $\Phi(\mathbf{x})$ and $\Phi^\dagger(\mathbf{x})$ and thereby obtain forms analogous to the more familiar ones expressed in terms of field operators. The change in variable, from index α to $\mathbf{x}$, is given by

$$\begin{aligned} \Phi(\mathbf{x}, t) &= \sum_\alpha \Phi_\alpha(\mathbf{x}) a_\alpha \\ \Phi^\dagger(\mathbf{x}, t) &= \sum_\alpha \Phi^\dagger_\alpha(\mathbf{x}) a^\dagger_\alpha\,, \end{aligned} \tag{59}$$

where $\{\Phi_\alpha(\mathbf{x})\}$ is a complete set and

$$\int d\mathbf{x}\Phi_\beta^\dagger(\mathbf{x})\Phi_\alpha(\mathbf{x}) = \delta_{\alpha\beta}. \tag{60}$$

The transformation given in Eq. (59) is unitary because of the orthogonality constraint expressed in Eq. (60). Its use in Eq. (56) yields

$$\begin{aligned}\mathcal{L}^k &= -i\hbar\int d\mathbf{x}\frac{\Phi^\dagger(\mathbf{x},t_k) - \Phi^\dagger(\mathbf{x},t_{(k-1)})}{\varepsilon}\Phi(\mathbf{x},t_{(k-1)}) - \int d\mathbf{x}H^k(\Phi^\dagger,\Phi)\\ &= -i\hbar\int d\mathbf{x}\dot{\Phi}^\dagger(\mathbf{x},t_k)\Phi(\mathbf{x},t_{(k-1)}) - \int d\mathbf{x}H^k(\Phi^\dagger,\Phi),\end{aligned} \tag{61}$$

where

$$\dot{\Phi}^\dagger(\mathbf{x},t_k) = \frac{\Phi^\dagger(\mathbf{x},t_k) - \Phi^\dagger(\mathbf{x},t_{(k-1)})}{\varepsilon}. \tag{62}$$

One notes that

$$\sum_k\sum_\alpha \frac{a_{k\alpha}^\dagger - a_{(k-1)\alpha}^\dagger}{\varepsilon}a_{(k-1)\alpha} = -\sum_k\sum_\alpha a_{k\alpha}^\dagger\frac{a_{k\alpha} - a_{(k-1)\alpha}}{\varepsilon} \tag{63}$$

is a result that is used to obtain the expression for the L^k summed over the succession of time intervals:

$$\begin{aligned}\sum_k^n \mathcal{L}^k &= \sum_k^n\int d\mathbf{x}\frac{i\hbar}{2}\{\Phi^\dagger(\mathbf{x},t_k)\dot{\Phi}(\mathbf{x},t_{(k-1)}) - \dot{\Phi}^\dagger(\mathbf{x},t_k)\Phi(\mathbf{x},t_{(k-1)})\}\\ &\quad - \sum_k^n\int d\mathbf{x}H^k(\Phi^\dagger,\Phi),\end{aligned} \tag{64}$$

as required in the expression for the path integrals. Therefore, the expression for the path integrals in the coherent-state representation can be written as

$$\begin{aligned}K(\Phi_f,\Phi_i) &= \lim_{\varepsilon\to 0}\int\prod_k\prod_\alpha(d\Phi^\dagger(\mathbf{x}_\alpha,t_k)\,d\Phi(\mathbf{x}_\alpha,t_k))\exp\left[\frac{i}{\hbar}\sum_k^n\mathcal{L}^k\varepsilon\right]\\ &= \int\mathfrak{D}[\Phi^\dagger(\mathbf{x},t)]\mathfrak{D}[\Phi(\mathbf{x},t)]\exp\left[\frac{i}{\hbar}\int dt\mathcal{L}[\Phi,t]\right],\end{aligned} \tag{65}$$

where

$$\mathcal{L}[\Phi,t] = \int d\mathbf{x}\left\{\frac{i\hbar}{2}\{\Phi^\dagger\dot{\Phi} - \dot{\Phi}^\dagger\Phi\} - H(\Phi^\dagger,\Phi)\right\} \tag{66}$$

and $H(\Phi^\dagger,\Phi)$ is the Hamiltonian given in Eq. (58) expressed in terms of the Grassman field variables:

$$H(\Phi^\dagger,\Phi) = (\hbar^2/2m)\int\nabla\Phi^\dagger\cdot\nabla\Phi\,d\mathbf{x} + \int d\mathbf{x}\hat{V}\Phi^\dagger\Phi.$$

Equation (65) is a formal statement of the desired expression. In Feynman's expression for the propagator in the single-particle case [Eq. (46)], the classical La-

grangian is summed over each time interval. In the many-Fermion case [Eq. (65)], every space–time point $(\mathbf{x}_\alpha, t_k)$ is related to a Grassman field variable $\Phi(\mathbf{x}_\alpha, t_k)$ and the "summation over history" in this case implies a summation of the Lagrangian over space and spin, as well as over time. This same point is implied in Schwinger's field theory formulation of the action principle.

3.2. *Path Integrals for an Atom in a Molecule*

In analogy with Eq. (40), the zero flux surface condition defining an atom in a molecule is given in terms of the field operators $\hat{\Phi}^\dagger(\mathbf{x})$, $\hat{\Phi}(\mathbf{x})$ by

$$\mathbf{n}_s \cdot \nabla_s \langle \Psi | \hat{\Phi}^\dagger(\mathbf{x}) \hat{\Phi}(\mathbf{x}) | \Psi \rangle = 0 , \tag{67}$$

and the corresponding constraint that must be imposed during the variation of the action is

$$\delta \sum_{\text{spin}} \int_\Omega d\mathbf{r} \nabla^2 \langle \Psi | \hat{\Phi}^\dagger(\mathbf{x}) \hat{\Phi}(\mathbf{x}) | \Psi \rangle = 0 . \tag{68}$$

The construction of the path integrals for a subsystem requires the definition of an appropriate subsystem or atomic Lagrangian. It must be such that its variation gives the correct equation of motion and the equivalent of the atomic statement of the principle of stationary action [Eq. (44)].

By restricting the derivation to a particular state $|\Psi\rangle$, the constraint in Eq. (68) can be expressed in the form

$$\delta \sum_{\text{spin}} \int_\Omega d\mathbf{r} \nabla^2 \{ \Phi^\dagger(\mathbf{x}) \Phi(\mathbf{x}) \} = 0 . \tag{69}$$

This constraint is introduced into the Lagrangian through the use of the undetermined multiplier λ to give

$$\begin{aligned} \mathcal{L}_\lambda[\Phi, t, \Omega] = \sum_{\text{spin}} \Bigg\{ & \frac{i\hbar}{2} \int_\Omega d\mathbf{r} (\Phi^\dagger \dot{\Phi} - \dot{\Phi}^\dagger \Phi) - \frac{\hbar^2}{2m} \int_\Omega d\mathbf{r} \nabla \Phi^\dagger \cdot \nabla \Phi - \int_\Omega d\mathbf{r} \Phi^\dagger V \Phi \\ & - \frac{1}{2} \int_\Omega d\mathbf{r} \int d\mathbf{x}' \Phi^\dagger(\mathbf{x}) \Phi^\dagger(\mathbf{x}') g(\mathbf{r}, \mathbf{r}') \Phi(\mathbf{x}') \Phi(\mathbf{x}) \\ & + \lambda \int_\Omega d\mathbf{r} \nabla^2 \{ \Phi^\dagger(\mathbf{x}) \Phi(\mathbf{x}) \} \Bigg\} \\ = \sum_{\text{spin}} & \left\{ \int_\Omega d\mathbf{r} L[\Phi, \nabla\Phi, t] + \lambda \int_\Omega d\mathbf{r} \nabla^2 \{ \Phi^\dagger(\mathbf{x}) \Phi(\mathbf{x}) \} \right\} , \end{aligned} \tag{70}$$

where

$$\begin{aligned} L[\Phi, \nabla\Phi, t] = & \frac{i\hbar}{2} (\Phi^\dagger \dot{\Phi} - \dot{\Phi}^\dagger \Phi) - \frac{\hbar^2}{2m} \nabla \Phi^\dagger \cdot \nabla \Phi - \Phi^\dagger V \Phi \\ & - \frac{1}{2} \int d\mathbf{x}' \Phi^\dagger(\mathbf{x}) \Phi^\dagger(\mathbf{x}') g(\mathbf{r}, \mathbf{r}') \Phi(\mathbf{x}') \Phi(\mathbf{x}) . \end{aligned}$$

As previously pointed out, the Laplacian of the charge density appearing in Eq. (69) is a divergence expression, that is, its variation yields only surface terms.

Thus, introduction of the constraint in this manner will still yield Schrödinger's equation of motion in the variation of $\mathcal{L}_\lambda[\Phi, t, \Omega]$. The atomic path integral in Eq. (65) is now given by

$$K^\Omega(\Phi_f^\dagger, \Phi_i) = \lim_{\varepsilon \to 0} \int \prod_\lambda \prod_{x \in \Omega} d\Phi^\dagger(\mathbf{x}, t_\lambda)\, d\Phi(\mathbf{x}, t_\lambda) \exp\left[\frac{i}{\hbar} \int dt \mathcal{L}_\lambda[\Phi, t, \Omega]\right], \quad (71)$$

where the index x in the product $\Pi_{x \in \Omega}$ denotes a coordinate r in Ω and its spin components.

The variation of $\mathcal{L}_\lambda[\Phi, t, \Omega]$, including a variation of the surface and retaining the variations in Φ at the time endpoints, yields a result equivalent to that obtained for the variation of $\hat{\mathcal{L}}[\hat{\Phi}, t, \Omega]$ in the field theoretic approach. Using the fact that Schrödinger's equation is satisfied, the variation in $\mathcal{L}_\lambda[\Phi, t, \Omega]$ yields

$$\begin{aligned}\delta\mathcal{L}_\lambda[\Phi, t, \Omega] = \sum_{\text{spin}} \Bigg\{ & \frac{d}{dt} \int_\Omega d\mathbf{r} \left\{ \frac{i\hbar}{2} \Phi^\dagger(x)\, \delta\Phi(\mathbf{x}) + cc \right\} \\ & - \left(\frac{\hbar^2}{2m} - \lambda \right) \oint d\mathbf{S} \cdot \{(\nabla\Phi^\dagger\, \delta\Phi + cc)\} + \lambda \oint d\mathbf{S} \\ & \cdot \{(\Phi^\dagger \nabla(\delta\Phi) + cc)\} + \oint d\mathbf{S} \\ & \cdot \vec{n}\, \delta S[L[\Phi, \nabla\Phi, t] + \lambda\nabla^2\{\Phi^\dagger(\mathbf{x})\Phi(\mathbf{x})\}] \Bigg\}. \end{aligned} \quad (72)$$

The term involving $(\partial S/\partial t)$ is omitted from this derivation for reasons of clarity and brevity, since it cancels once one introduces the generator into the final expression. It behaves in the same manner as in the variation of the field theoretic expressions.

As previously discussed in the field theoretic development of the theory, the Lagrangian density is proportional to the Laplacian of the charge density at the point of variation where Schrödinger's equation obtains [Eq. (37)]. The density $L[\Phi, \nabla\Phi, t]$ [Eq. (70)], appearing in Eq. (72) and resulting from the variation in the surface of the subsystem behaves similarly. Thus, one has

$$L[\Phi, \nabla\Phi, t] = -\frac{\hbar^2}{4m} \nabla^2(\Phi^\dagger\Phi). \quad (73)$$

Using Eq. (73), one obtains for the variation of $\mathcal{L}_\lambda[\Phi, t, \Omega]$,

$$\begin{aligned}\delta\mathcal{L}_\lambda[\Phi, t, \Omega] = \sum_{\text{spin}} \Bigg\{ & \frac{d}{dt} \int_\Omega d\mathbf{r} \left\{ \frac{i\hbar}{2} \Phi^\dagger(\mathbf{x})\, \delta\Phi(\mathbf{x}) + cc \right\} \\ & - \left(\frac{\hbar^2}{2m} - \lambda \right) \oint d\mathbf{S} \cdot \{(\nabla\Phi^\dagger\, \delta\Phi + cc)\} \\ & + \lambda \oint d\mathbf{S} \cdot \{(\Phi^\dagger \nabla(\delta\Phi) + cc)\} \\ & - \left(\frac{\hbar^2}{4m} - \lambda \right) \oint d\mathbf{S} \cdot \vec{n}\, \delta S\{\nabla^2(\Phi^\dagger\Phi)\} \Bigg\}. \end{aligned} \quad (74)$$

To determine the constraint parameter λ, one first varies the Lagrangian in Eq. (70) with λ set equal to zero and then imposes the variational constraint given in Eq. (69) in the manner followed in the field theoretic derivation of the principle of stationary action. Variation of the Lagrangian given in Eq. (70) with λ set equal to zero, a functional denoted as $\mathcal{L}[\Phi, t, \Omega]$, yields

$$\delta\mathcal{L}[\Phi, t, \Omega] = \sum_{\text{spin}} \left\{ \frac{d}{dt} \int_\Omega d\mathbf{r} \left\{ \frac{i\hbar}{2} \Phi^\dagger(\mathbf{x})\, \delta\Phi(\mathbf{x}) + cc \right\} - \frac{\hbar^2}{2m} \oint d\mathbf{S} \cdot \{(\nabla\Phi^\dagger\, \delta\Phi + cc)\} - \frac{\hbar^2}{4m} \oint d\mathbf{S} \cdot \vec{n}\, \delta S\{\nabla^2(\Phi^\dagger\Phi)\} \right\}. \tag{75}$$

The variational constraint stated in Eq. (69) and including a variation of the surface yields

$$\delta \int_\Omega d\mathbf{r} \nabla^2\{\Phi^\dagger(\mathbf{x})\Phi(\mathbf{x})\} = \oint d\mathbf{S} \cdot \vec{n}\, \delta S\{\nabla^2(\Phi^\dagger\Phi)\} + \int_\Omega d\mathbf{r}\, \delta[\nabla^2\{\Phi^\dagger(\mathbf{x})\Phi(\mathbf{x})\}] = 0 \tag{76}$$

or

$$\oint d\mathbf{S} \cdot \vec{n}\, \delta S\{\nabla^2(\Phi^\dagger\Phi)\} = -\int_\Omega d\mathbf{r}\, \delta[\nabla^2\{\Phi^\dagger(\mathbf{x})\Phi(\mathbf{x})\}]. \tag{77}$$

This constraint is to be imposed at every stage of the variation that limits the subsystems to those bounded by a zero flux in the gradient vector field of the charge density. The constraint enables one to replace the term involving the variation of the surface in Eq. (76) with the RHS of the constraint equation [Eq. (77)] to obtain

$$\delta\mathcal{L}[\Phi, t, \Omega] = \sum_{\text{spin}} \left\{ \frac{d}{dt} \int_\Omega d\mathbf{r} \left\{ \frac{i\hbar}{2} \Phi^\dagger(\mathbf{x})\, \delta\Phi(\mathbf{x}) + cc \right\} - \frac{\hbar^2}{4m} \oint d\mathbf{S} \cdot \{(\nabla\Phi^\dagger\, \delta\Phi + cc)\} + \frac{\hbar^2}{4m} \oint d\mathbf{S} \cdot \{(\Phi^\dagger\, \delta(\nabla\Phi) + cc)\} \right\}. \tag{78}$$

Proceeding as in the theoretic derivation of Schwinger's principle of stationary action, the variation in Φ is replaced by the action of an infinitesimal generator $\hat{G}$, as in Eq. (16), and this substitution, coupled with the use of the Heisenberg equation of motion for the generator, demonstrates that the expression given for $\delta\mathcal{L}[\Phi, t, \Omega]$ in Eq. (78) is indeed Schwinger's principle. Thus, Eq. (78) with these substitutions yields

$$\delta\mathcal{L}[\Phi, t, \Omega] = (\varepsilon/2)\{(i/\hbar)\langle\Phi|[\hat{H}, \hat{G}]|\Phi\rangle_\Omega + cc\}. \tag{79}$$

The result given in Eq. (75) for $\delta\mathcal{L}[\Phi, t, \Omega]$, which is a variation without constraints on the surface, represents the most general variation of a subsystem. However, to recover Schwinger's principle from this general result as given by the

expression for $\delta\mathcal{L}[\Phi, t, \Omega]$ in Eq. (79), one must limit the subsystems to those which satisfy the variational constraint, that is, to those systems bounded by a surface of zero flux in the gradient vector field of the charge density.

A comparison of Eq. (78) with Eq. (74) shows that $\lambda = (\hbar^2/4m)$ and the Lagrangian appearing in the atomic expression for the path integrals is

$$\mathcal{L}_\lambda[\Phi, t, \Omega] = \sum_{\text{spin}} \int_\Omega d\mathbf{r} \left\{ \frac{i\hbar}{2}(\Phi^\dagger \cdot \dot{\Phi} - \dot{\Phi}^\dagger \cdot \Phi) - \frac{\hbar^2}{2m} \nabla\Phi^\dagger \cdot \nabla\Phi - \Phi^\dagger V \Phi \right.$$
$$- \frac{1}{2} \int dx' \Phi^\dagger(\mathbf{x}) \Phi^\dagger(\mathbf{x}') g(\mathbf{r}, \mathbf{r}') \Phi(\mathbf{x}') \Phi(\mathbf{x})$$
$$\left. + \frac{\hbar^2}{4m} \nabla^2(\Phi^\dagger \Phi) \right\}. \tag{80}$$

Using this result, the expression for the path integral given in Eq. (71) becomes, using the usual notation for the integration,

$$K^\Omega(\Phi_f, \Phi_i) = \lim_{\varepsilon \to 0} \int \prod_k \prod_{\mathbf{x} \in \Omega} (d\Phi^\dagger(\mathbf{x}, t_k)\, d\Phi(\mathbf{x}, t_k)) \exp\left[\frac{i}{\hbar} \int dt \mathcal{L}_\lambda[\Phi, t, \Omega] \right]$$
$$= \int \mathcal{D}[\Phi^\dagger(\Omega, t)] \mathcal{D}[\Phi(\Omega, t)] \exp\left[\frac{i}{\hbar} \int dt \mathcal{L}_\lambda[\Phi, t, \Omega] \right]. \tag{81}$$

The justification of Eq. (81) rests upon the Lagrangian $\mathcal{L}_\lambda[\Phi, t, \Omega]$ exhibiting correct behavior: (i) It yields Schrödinger's equation when used in the expression for the equation of motion for the field [Eq. (22)], and (ii) its variation yields Schwinger's principle of stationary action [Eq. (79)].

One can express the path integral for the total system, the quantity $K(\Phi_f; \Phi_i]$ [Eq. (65)], in terms of the individual atomic contributions given in Eq. (81). This step in made possible by a fundamental property of transformation functions. Dirac [19] was the first to show that this property, the multiplicative law of transformation functions, forms the basis for the Lagrangian approach to quantum mechanics, the approach subsequently used by Feynman and Schwinger. The multiplicative law enables one to express the propagator connecting states at two times as

$$K(\mathbf{r}_f, t_f; \mathbf{r}_i, t_i) = \int K(\mathbf{r}_f, t_f; \mathbf{r}_m, t_m)\, d\mathbf{r}_m K(\mathbf{r}_m, t_m; \mathbf{r}_i, t_i). \tag{82}$$

Through repeated use of Eq. (82), Dirac was able to express the propagator for a single path by a sequence of transformation functions for times intermediate between the initial and final times. Taken to the limit of successive intermediate times differing by only an infinitesimal one from the next, the multiplicative law yields a product of all the transformation functions associated with the successive increments of time. Dirac then stated that the transformation function associated with the time displacement from t to $t + dt$ corresponds to $\exp[(i/\hbar)L dt]$, where the classical Lagrangian was considered to be a function of the coordinates and time at the two time limits, a step that enables one to sum the action at each step

and show that the propagator for a single path is proportional to $\exp[(i/\hbar)W]$, where W, the action, is equal to the integral of L between the initial and final times. Feynman [9] extended this work by considering all the paths that connect the initial and final states (rather than just the single path that describes the classical limit of quantum mechanics considered by Dirac) to obtain the expression for the propagator as the sum over all possible paths.

The fundamental property of the probability amplitude of a path being determined by the product of contributions from successive steps and by the sum of the actions for each step is nicely summarized by Feynman in the statement [9], "We shall see that it is the possibility of expressing S [the action] as a sum, and hence Φ [the probability amplitude for a single path] as a product of contributions from successive sections of the path, which leads to the possibility of defining a quantity having the properties of a wave function." We now demonstrate that the total propagator can be expressed as a product of the individual atomic contributions to the steps along the paths with the action being determined by a corresponding sum of the atomic action integrals.

According to Eq. (65), one can write the Grassman field propagator in the form

$$K(\Phi_f, \Phi_i) = \lim_{\varepsilon \to 0} \int \prod_{t_k} \prod_{\mathbf{x}} (d\Phi^\dagger(\mathbf{x}, t_k)\, d\Phi(\mathbf{x}, t_k)) \exp\left[\frac{i}{\hbar} \int dt \mathcal{L}[\Phi, t]\right], \quad (83)$$

where the product $\Pi_{\mathbf{x}}$ is over the Cartesian space and spin and Π_{t_k} is over the time intervals (t_i, t_f). Since Cartesian space can be divided into finite connected subspaces, one has

$$\mathcal{L}[\Phi, t] = \int d\mathbf{x} L[\Phi, \nabla\Phi, \dot{\Phi}] = \sum_{\alpha} \sum_{\text{spin}} \int_{\Omega_\alpha} d\mathbf{r} L[\Phi, \nabla\Phi, \dot{\Phi}], \quad (84)$$

where the summation is over all atoms in the system. Using Eq. (84), Eq. (83) yields

$$\begin{aligned} K(\Phi_f, \Phi_i) &= \lim_{\varepsilon \to 0} \int \prod_{\alpha} \left\{ \prod_{\mathbf{x}_\alpha} \prod_{t_k} (d\Phi^\dagger(\mathbf{x}_\alpha, t_k)\, d\Phi(\mathbf{x}_\alpha, t_k)) \right\} \\ &\quad \cdot \exp\left[\frac{i}{\hbar} \sum_{\alpha} \int dt \sum_{\text{spin}} \int_{\Omega_\alpha} d\mathbf{r} L[\Phi, \nabla\Phi, \dot{\Phi}]\right] \\ &= \lim_{\varepsilon \to 0} \int \prod_{t_k} \prod_{\alpha} \left\{ \prod_{\mathbf{x}_\alpha} (d\Phi^\dagger(\mathbf{x}_\alpha, t_k)\, d\Phi(\mathbf{x}_\alpha, t_k)) \right\} \\ &\quad \cdot \exp\left[\frac{i}{\hbar} \sum_{\text{spin}} \int dt \int_{\Omega_\alpha} d\mathbf{r} L[\Phi, \nabla\Phi, \dot{\Phi}]\right] \Bigg\} \\ &= \lim_{\varepsilon \to 0} \int \prod_{t_k} \prod_{S} (d\Phi^\dagger(\mathbf{x}_s, t_k)\, d\Phi(\mathbf{x}_s, t_k)) \\ &\quad \cdot \prod_{\alpha} K^{\Omega_\alpha}(\Phi(\mathbf{x}_f, t_k), \Phi(\mathbf{x}_i, t_i)), \end{aligned} \quad (85)$$

where $\mathbf{x}_s = \mathbf{r},\sigma$ and $\mathbf{r}_s$ is a point on the interatomic surface and the product Π_α is over all the subsystems. One can symbolically rewrite this relation between subsystem propagators K^{Ω_α} and that for the total system as

$$K(\Phi_f, \Phi_i) = K^{\Omega_1} \otimes K^{\Omega_2} \otimes \cdots \otimes K^{\Omega_N}. \tag{86}$$

Equation (86) is an atomic statement of the multiplicative composition law of transformation functions. As pointed out by Schwinger [6], the multiplicative law requires that the corresponding total change in the action be additive. It follows from Eq. (84) that this is indeed the case, with the total action being given by the sum of the separate atomic contributions:

$$W[\Phi]_{12} = \sum_\alpha W[\Phi, \Omega_\alpha]_{12} = \sum_\alpha \int_{t_1}^{t_2} \sum_{\text{spin}} \int_{\Omega_\alpha} d\mathbf{r} L[\Phi, \nabla\Phi, \dot{\Phi}]\,. \tag{87}$$

Equations (86) and (87) are the atomic statements of the multiplicative and summation principles, respectively.

It is also possible to obtain an atomic statement of the fundamental dynamical principle postulated by Schwinger [Eq. (11)]. As first pointed out by Dyson [20], this principle and Feynman's path integral expression [Eq. (46)] are equivalent, with Schwinger's principle being a differential form of Feynman's statement. Thus, one can recover Schwinger's fundamental principle expressed in terms of the Grassman field variables by a variation of the path integral expression given for the propagator in Eq. (65), a process that yields

$$\delta K(\Phi_f, \Phi_i) = \langle \Phi_f | (i/\hbar)\, \delta W[\Phi] | \Phi_i \rangle\,. \tag{88}$$

Because of the atomic additivity of the action given in Eq. (87), this can be re-expressed as

$$\delta K(\Phi_f, \Phi_i) = \langle \Phi_f | (i/\hbar) \sum_\alpha \delta W[\Phi, \Omega_\alpha] | \Phi_i \rangle\,. \tag{89}$$

The same result can be obtained through the variation of Eq. (85): the atomic statement of Feynman's path integral expression. Equations (85) and (89) provide the basis for extending the theory of atoms in molecules to problems involving a change in state.

Appendix

The evaluation of the matrix element of the temporal generator for an infinitesimal time interval appearing in the expression for the propagator in Eq. (55) is derived. Consider the term

$$T_{k+1,k} = \langle a_{k+1} | \exp\left\{ -\frac{i}{\hbar} \hat{H} \varepsilon \right\} | a_k \rangle \exp\left[-\sum_\alpha a^\dagger_{k\alpha} a_{k\alpha} \right], \tag{A.1}$$

where $\hat{H} \equiv H(\hat{a}^\dagger, \hat{a})$. Expanding the generator to first-order gives

$$T_{k+1,k} = \langle a_{k+1}|1 - \frac{i}{\hbar}\hat{H}\varepsilon|a_k\rangle \exp\left[-\sum_\alpha a_{k\alpha}^\dagger a_{k\alpha}\right]$$
$$= \left[\langle a_{k+1}|a_k\rangle - \frac{i}{\hbar}\varepsilon\langle a_{k+1}|\hat{H}(\hat{a}^\dagger, \hat{a})|a_k\rangle\right] \exp\left[-\sum_\alpha a_{k\alpha}^\dagger a_{k\alpha}\right]. \quad \text{(A.2)}$$

The use of Eq. (54) in the RHS of Eq. (A.2) yields

$$T_{k+1,k} = \left\{\exp\left[\sum_\alpha a_{k+1\alpha}^\dagger a_{k\alpha}\right] - \frac{i}{\hbar}\varepsilon\hat{H}(a_{k+1}^\dagger, a_k) \exp\left[\sum_\alpha a_{k+1\alpha}^\dagger a_{k\alpha}\right]\right\}$$
$$\cdot \exp\left[-\sum_\alpha a_{k\alpha}^\dagger a_{k\alpha}\right]$$
$$= \exp\left\{-\frac{i}{\hbar}\varepsilon\hat{H}(a_{k+1}^\dagger, a_k)\right\} \exp\left[\sum_\alpha \{a_{k+1\alpha}^\dagger a_{k\alpha} - a_{k\alpha}^\dagger a_{k\alpha}\}\right]$$
$$= \exp\left\{(i\varepsilon/\hbar)\left[\sum_\alpha (-i\hbar)\frac{a_{k+1\alpha} - a_{k\alpha}}{\varepsilon} a_{k\alpha} - H(a_{k+1}^\dagger, a_k)\right]\right\},$$

to give finally a typical term appearing in Eq. (55):

$$T_{k+1,k} = \exp\{(i\varepsilon/\hbar)L^k\}. \quad \text{(A.3)}$$

Bibliography

[1] E. Wigner and F. Seitz, Phys. Rev. **43**, 804 (1933); *Ibid.* **46**, 509 (1934).
[2] C. Kittel, *Introduction to Solid State Physics* (Wiley, New York, 1965). J. C. Slater, *Quantum Theory of Molecules and Solids* (McGraw-Hill, New York, 1965), Vol. 2.
[3] S. Srebrenik and R. F.W. Bader, J. Chem. Phys. **63**, 3945 (1975). S. Srebrenik, R. F.W. Bader, and T.T. Nguyen-Dang, J. Chem. Phys. **68**, 3667 (1978).
[4] R. F.W. Bader, S. Srebrenik, and T.T. Nguyen-Dang, J. Chem. Phys. **68**, 3680 (1978).
[5] R. F.W. Bader and T.T. Nguyen-Dang, Adv. Quantum Chem. **14**, 63 (1981).
[6] J. Schwinger, Phys. Rev. **82**, 914 (1951).
[7] R. F.W. Bader and P. M. Bedall, J. Chem. Phys. **56**, 3320 (1972).
[8] R. F.W. Bader, *Atoms in Molecules—A Quantum Theory* (Oxford University Press, Oxford, 1990).
[9] R. P. Feynman, Rev. Mod. Phys. **20**, 367 (1948).
[10] P. F. Zou, submitted.
[11] A. Auerbach and S. Kivelson, Nucl. Phys. **B257**, 799 (1985).
[12] J.W. Negele and H. Orland, *Quantum Many-Particle Systems* (Addison-Wesley, Reading, MA, 1988).
[13] W.-M. Zhang, D. H. Feng, and R. Gilmore, Rev. Mod. Phys. **62**, 867 (1990).
[14] S. Samuel, J. Math. Phys. **21**, 2806 (1980).
[15] J. Linderberg and Y. Öhrn, *Propagators in Quantum Chemistry* (Academic Press, New York, 1973), Chap. 4.
[16] C. Pisani, R. Dovesi, and C. Roetti, *Hartree–Fock Ab Initio Treatment of Crystalline Systems*, Lecture Notes in Chemistry, Vol. 48 (Springer-Verlag, Heidelberg, 1988).
[17] M. E. Eberhart, M. M. Donovan, J. McLaren, and D. P. Clougherty, Prog. Surf. Sci. **36**, 1 (1991).
[18] D. E. Soper, Phys. Rev. D **18**, 4590 (1978).

[19] P. A. M. Dirac, Physik. Zeits. Sowjetunion 3, 64 (1945). P. A. M. Dirac, *The Principles of Quantum Mechanics*, 2nd ed. (University of Oxford Press, Oxford, 1935).
[20] F. J. Dyson, Phys. Rev. 75, 486 (1949).

Received September 27, 1991
Revised manuscript received February 19, 1992
Accepted for publication March 7, 1992

2. SUBSYSTEM QUANTUM MECHANICAL TECHNIQUES

Physics always develops in two directions. One front pushes forward towards phenomena which do not yet fit into the general picture, and the victories on this front are marked by important changes in our fundamental concepts.... But, in addition to this search for new concepts, there is constant effort directed toward the deepening and broadening of our knowledge of phenomena which, we believe, can be understood on the basis of existing concepts and theories.

——E. P. Wigner, Scientific Monthly, Jan. 1936

2.1 Introduction

Intuitively and conveniently, many systems should be treated in terms of open systems besides atoms in molecules or in crystals. Among them are surfaces, interfaces, adsorbates, defects, ect. The chemically and physically important properties of these systems are determined by their parts. For example, the properties of chemical reactivity, structural reconstruction, and low energy electron scattering of a surface are determined by the atoms on the top several layers. These top layers are openly connected to the interior,

that is the electrons and energy can be exchanged between the complementary subsystems. The strong interaction and the free exchange of matter and energy between a subsystem and its environment are the basic characteristics for an open system with which we are dealing here.

In a closed system, there are two fundamental problems and these same problems exist in an open subsystem: the static and dynamic problems. The static properties of a subsystem are determined by its electronic charge density according to density functional theory, therefore the fundamental static problem for a subsystem reduced to the determination of the charge density. The determination of dynamic properties is involved not only with the charge density but also with the electronic current density in the subsystem. The conventional methods for solving Shrödinger equation in a closed system are not appropriate for a subsystem. There are at least three reasons for the development of open quantum mechanical techniques: (1) The total system of interest is usually large, therefore it is practically impossible to solve the Shrödinger equation for the total system, and even if it is possible it is not efficient; (2) The chemical and physical properties of a subsystem are interesting themselves. Because the properties of a system can be expressed in terms of its constituted parts, it will be significant if one is able to directly calculate the properties of the interested part without solving the total system; And (3), probably the most important reason is to obtain a desired property for a subsytem through controlling the interaction of the subsystem and its environment. The aim of this chapter is to develop the dynamic and static quantum mechanical treatments suitable to a subsystem. At present only the formal solution is given and the practical

implementations or applications remain to be developed. The original purpose of this project is to determine the charge distribution of an atom or a chemical group without solving the Shrödinger equation of the total molecule. Bader and his research group have observed that in many situations, an atom or a chemical group is relatively transferable from one molecule to another. This observation provides a way to predict the properties of a new molecule. At the same time this brings up two theoretical questions: (1) how to determine the degree of transferability and the conditions which control this; and (2) how to predict the change of the properties of the atom or group when placed in a new molecule. Even though the original purpose of the project has not been fully realized in practice, the subsystem quantum mechanical techniques developed in this chapter will be useful in the studies of defects, surface sciences, quantum wells, and quantum control of a subsystem.

Many techniques have been and are being developed for the treatment of a subsystem based on Green's function. Garcia-Moliner and Velasco (1991) developed matching methods to solve a variety of physical problems of single and multiple interfaces within some models. Dobrynski (1986-1989) used an interface response function to obtain the electronic and phonon structures of composite systems. The common feature of these two approaches is that the surface response function is used to match the environment of the sybsystem we are interested in. The surface response function can be approximated from the known substrate Green's function and the interaction between the subsystem and its environment. These two methods can be classified as a perturbation method. In the last decade Inglsfield (1981-1988) developed a variational

embedding method which also used Green's function. In his approach a special Green's function with zero derivative on the surface is used to enforce the matching of the wave function on the surface. The enforcement of the wave function matching yields an extra effective potential to the subsystem Hamiltonian. The solution of the Shrödinger equation with the effective subsystem Hamiltonian gives the charge distribution of the subsystem.

Since Wigner and Eisenbud proposed the R-matrix technique for the use in solving scattering problems, the R-matrix has been widely used for obtaining the dynamic properties (such as scattering cross sections, threshold peaks, etc) for a scattering system. In 1984, based on the R-matrix expression derived from the variational principle, Nesbet suggested a method for the determination of energy bands of a crystal. The R-matrix was used to match the wave function on the surface enclosing a region with its external part. Using the periodic boundary condition for a crystal, in conjunction with the defining equation of the R-matrix for a translational unit cell, Nesbet obtained a secular equation for the energy bands. Based on the work of Nesbet and Inglesfield, a new embedding procedure is proposed by the author (Paper II). In the new method, the variational procedure eliminates the use of the periodic condition in Nesbet's implementation, while the use of R-matrix overcomes the constraint of the zero derivative on the surface for the Green's function used in the Inglesfield's approach. Therefore our formalism may provide a more flexible and computationally efficient way to treat the subsystem problems for non-crystalline systems.

While much effort has been devoted to the development of the stationary charge and energy spectrum distributions of a subsystem, the implementation of

the parallel quantum dynamic behaviour has not been fully developed. The properties related to electron transport or tunneling are determined by the dynamics of a subsystem. In an open and far-from equilibrium situation one has the opportunity to create many quantum coherence phenomena, such as the quantum-well resonant-tunneling, bond-selective chemical reaction, etc. Auerbach, Kivelson and Nicole (1984, 1985) developed a path decomposition technique and used it in the discussion of tunneling between two different regions in multidimensional configuration space. In that method the Feynman path integrals are decomposed into the contributions from different configuration and the dynamics of the full system is expressed in terms of its parts. The advantage of the decomposition for configuration space is that different approximations can be made for different regions in solving Schrödinger equation and the results can be related through the path decomposition formula. Frensley (1986-1990) used boundary conditions of the density matrix for an open system to discuss the one-dimensional tunneling problems which originated from the device of the semiconductor heterostructure resonant-tunneling diode (Chang, Esaki and Tsu, 1974; Sollner et al, 1974). In his approach, Frensley demonstrated that spatial boundary conditions can be used to introduce irreversibility in a way similar to that by which temporal conditions do so in the time domain. Another important approach to the dynamics of an open system is the method advocated by Landauer (1970, Büttiker et al., 1985). This method was successfully used in the description of a number of quantum conductance phenomena, for example universal conductance fluctuations and Aharonov-Bohm oscillations (Stone and Szafer, 1988; Szafer and Stone, 1989 (coherent book)). In Landauer's approach, the conductance due

to elastic scattering of a region (obstacle) are obtained through the transmission and reflection coefficients.

There are other kinds of quantum systems that are often called open systems in literature. These quantum systems are coupled to a reservoir so that an exchange of energy is permitted (see, for example, Chester, 1963; Louisell, 1973; Haken, 1975; Davies, 1976; Oppenheim, Shuler, and Weiss, 1977; Li, 1986), or the quantum systems are in purely thermal contact with two or more reservoirs (Lebowitz, 1959). The difference between our subsystems and these open systems is the possibility of particle exchange and a boundary condition in real space. Most of the analyses in these quantum systems are modelled by the problems of damping which was motivated by the development of optical technology (Louisell, 1973; Haken, 1975). In laser physics, for example, the degrees of freedom of greatest interest are the normal modes of the radiation fields. A single theoretical model, the damped harmonic oscillator, is used to describe both the loss of energy (photons) to the gain medium within the cavity and the loss of photons to the output beam (Gordon, 1967; Scully and Lamb, 1967).

Sections 2.2 and 2.3 of this chapter devote for the development of the dynamics contributed from a subsystem, and sections 2.4 and 2.5 describe the perturbation and variational techniques for obtaining stational charge density and energy for a subsystem.

2.2 Path Decomposition Technique

In the time domain, the propagation of a particle from time $t=t_1$ to $t=t_2$ can be clearly decomposed according to an intermediate time, say t_m ($t_1<t_m<t_2$). The particle first propagates from the initial point $(\mathbf{r}_1,t_1)$ to

the intermediate time t_m, and then to the final point $(\mathbf{r}_2,t_2)$. This propagating relation in the time domain can be expressed as

$$K(\mathbf{r}_2,t_2;\mathbf{r}_1,t_1) = \int d\mathbf{r}_m K(\mathbf{r}_2,t_2;\mathbf{r}_m,t_m)K(\mathbf{r}_m,t_m;\mathbf{r}_1,t_1) \qquad (1)$$

where the propagator $K(\mathbf{r}_2,t_2;\mathbf{r}_1,t_1)$ of time dependent Shrödinger equation satisfies following equations (Feynman and Hibbs, 1965)

$$i\hbar\frac{\partial K(\mathbf{r}_2,t_2;\mathbf{r}_1,t_1)}{\partial t_2} - H_2K(\mathbf{r}_2,t_2;\mathbf{r}_1,t_1) = i\hbar\delta(\mathbf{r}_2-\mathbf{r}_1)\delta(t_2-t_1) \qquad (2)$$

$$-i\hbar\frac{\partial K(\mathbf{r}_2,t_2;\mathbf{r}_1,t_1)}{\partial t_1} - H_1K(\mathbf{r}_2,t_2;\mathbf{r}_1,t_1) = -i\hbar\delta(\mathbf{r}_2-\mathbf{r}_1)\delta(t_2-t_1) \qquad (2)'$$

and

$$K(\mathbf{r}_2,t;\mathbf{r}_1,t) = \delta(\mathbf{r}_2-\mathbf{r}_1) \qquad (3)$$

where H_i is the Hamiltonian of the system and operates on variables $\mathbf{r}_i$ and t_i (i=1,2). The analog of eqn (1) in probability theory is known as the Chapman-Kilmogoroff equation, and in diffusion theory, the Smoluchowsky equation (Sakurai, 1985)

Similar to the propagation explanation of eqn (1) in the time domain, in real space a quantum particle at a initial position $\mathbf{r}_1$ is first propagated to a intermediate surface and then to the final point $\mathbf{r}_2$. In this section we will seek an expression similar to eqn (1) which will describe the particle propagation in the space. This will clarify the contribution of a region in real space to the dynamics of a particle. It is a fundamental question in subsystem quantum mechanics, as to how a region in real space contributes to the propagation of a particle from one point $\mathbf{r}_1$ at time t_1 to another $\mathbf{r}_2$ at time t_2. This question was first investigated by Auerbach et al (1984, 1985). This section will give a new derivation for the formula obtained by Auerbach

et al. and some explicit examples. The aim of the development is to decompose the propagator or Feynman path integrals of a total system into the contributions from different regions of space. This decomposition directly yields an interpretation of the contribution of a region to a particle's dynamic behaviour.

Consider the case in which the real space is divided into two complementary regions, say Ω and $\bar{\Omega}$, separated by a 2-dimensional surface Σ. If the initial position $\mathbf{r}_1$ of a particle is in region Ω, and the final position $\mathbf{r}_2$ in $\bar{\Omega}$, then any path from $\mathbf{r}_1$ to $\mathbf{r}_2$ must cross the surface Σ at least once. We can therefore divide every path into two pieces according to the last crossing time t through the surface: a piece that goes from $\mathbf{r}_1$ to the crossing point $\mathbf{r}$ on Σ in time t, and a piece that in the remaining time t_2-t goes directly from $\mathbf{r}$ to $\mathbf{r}_2$ without crossing Σ again. Before time t, the particle propagates according to $K(\mathbf{r},t;\mathbf{r}_1,t_1)$ which satisfies equation

$$i\hbar\frac{\partial K(\mathbf{r},t;\mathbf{r}_1,t_1)}{\partial t} - HK(\mathbf{r},t;\mathbf{r}_1,t_1) = i\hbar\delta(\mathbf{r}-\mathbf{r}_1)\delta(t-t_1) \qquad (4)$$

where the Hamitonian $H = H(\mathbf{r},t)$. After time t the particle is committed to the condition that it will not come back to region Ω during the remaining time. Therefore the particle propagates according to the restricted propagator $K^r(\mathbf{r}',\mathbf{r}_2;t)$ which satisfies equation

$$-i\hbar\frac{\partial K^r(\mathbf{r}_2,t_2;\mathbf{r},t)}{\partial t} - HK^r(\mathbf{r}_2,t_2;\mathbf{r},t) = -i\hbar\delta(\mathbf{r}-\mathbf{r}_2)\delta(t-t_2) \qquad (5)$$

and the boundary condition

$$K^r(\mathbf{r}_2,t_2;\mathbf{r},t) = 0 \text{ if } \mathbf{r} \text{ or } \mathbf{r}_2 \text{ is in } \Omega \qquad (6)$$

The boundary condition for the restricted propagator given in eqn (6) is equivalent to replacing the surface Σ with an infinite barrier so that the

particle has no chance to cross the wall.

Within the period $t_1<t<t_2$, eqns (4) and (5) give

$$i\hbar\frac{\partial K(\mathbf{r},t;\mathbf{r}_1,t_1)}{\partial t} - HK(\mathbf{r},t;\mathbf{r}_1,t_1) = 0 \tag{7}$$

$$-i\hbar\frac{\partial K^r(\mathbf{r}_2,t_2;\mathbf{r},t)}{\partial t} - HK^r(\mathbf{r}_2,t_2;\mathbf{r},t) = 0 \tag{8}$$

Both sides of eqn (7) multiplied by $K^r(\mathbf{r}_2,t_2;\mathbf{r},t)$ and of eqn (5) by $K(\mathbf{r},t;\mathbf{r}_1,t_1)$, the first result minus the second one yields

$$K^r(\mathbf{r}_2,t_2;\mathbf{r},t)\{i\hbar\frac{\partial K(\mathbf{r},t;\mathbf{r}_1,t_1)}{\partial t} - HK(\mathbf{r},t;\mathbf{r}_1,t_1)\}$$

$$-K(\mathbf{r},t;\mathbf{r}_1,t_1)\{-i\hbar\frac{\partial K^r(\mathbf{r}_2,t_2;\mathbf{r},t)}{\partial t} - HK^r(\mathbf{r}_2,t_2;\mathbf{r},t)\}$$

$$=i\hbar\frac{\partial(K^r(\mathbf{r}_2,t_2;\mathbf{r},t)K(\mathbf{r},t;\mathbf{r}_1,t_1))}{\partial t}$$

$$- \{K^r(\mathbf{r}_2,t_2;\mathbf{r},t)HK(\mathbf{r},t;\mathbf{r}_1,t_1)-K(\mathbf{r},t;\mathbf{r}_1,t_1)HK^r(\mathbf{r}_2,t_2;\mathbf{r},t)\} = 0 \tag{9}$$

Integrating $\mathbf{r}$ of eqn (9) over region $\bar{\Omega}$ and t over t_1 to t_2 gives

$$i\hbar\int_{\bar{\Omega}}d\mathbf{r}\ \{K^r(\mathbf{r}_2,t_2;\mathbf{r},t_2)K(\mathbf{r},t_2;\mathbf{r}_1,t_1)\ -K^r(\mathbf{r}_2,t_2;\mathbf{r},t_1)K(\mathbf{r},t_1;\mathbf{r}_1,t_1)\ \} =$$

$$-\frac{\hbar^2}{2m}\int_{\bar{\Omega}}d\mathbf{r}\int_{t_1}^{t_2}dt\{K^r(\mathbf{r}_2,t_2;\mathbf{r},t)\nabla^2K(\mathbf{r},t;\mathbf{r}_1,t_1)-K(\mathbf{r},t;\mathbf{r}_1,t_1)\nabla^2K^r(\mathbf{r}_2,t_2;\mathbf{r},t)\} \tag{10}$$

Using eqn (4), the lhs of eqn (9) reduces to $i\hbar K(\mathbf{r}_2,t_2;\mathbf{r}_1,t_1)$ because we are assuming $\mathbf{r}_1 \in \Omega$, $K(\mathbf{r},t_1;\mathbf{r}_1,t_1) = \delta(\mathbf{r}-\mathbf{r}_1) = 0$ for $\mathbf{r} \in \bar{\Omega}$. Therefore we have

$K(\mathbf{r}_2,t_2;\mathbf{r}_1,t_1)$

$$=\frac{i\hbar}{2m}\int_{t_1}^{t_2}dt\int_{\Sigma}d\mathbf{S}\cdot\{K^r(\mathbf{r}_2,t_2;\mathbf{r}_s,t)\nabla K(\mathbf{r}_s,t;\mathbf{r}_1,t_1)-K(\mathbf{r}_s,t;\mathbf{r}_1,t_1)\nabla K^r(\mathbf{r}_2,t_2;\mathbf{r}_s,t)\} \tag{11}$$

where Gauss divergence theorem has been used to transfer the volume integral to the surface integral. Noting that $K^r(\mathbf{r}_2,t_2;\mathbf{r},t) = 0$ when $\mathbf{r}$ is on the

surface, we have

$$K(\mathbf{r}_2,t_2;\mathbf{r}_1,t_1) = \frac{i\hbar}{2m}\int_{t_1}^{t_2}dt\int_{\Sigma}d\mathbf{S}\cdot(-K(\mathbf{r}_s,t;\mathbf{r}_1,t_1)\nabla K^r(\mathbf{r}_2,t_2;\mathbf{r},t)\,|_{\mathbf{r}=\mathbf{r}_s}) \qquad (12)$$

where the direction of the surface Σ is chosen as directing to Ω (the surface of $\bar{\Omega}$). Equation (12) is the desired result for the case that the particle propagates from one region to another. This formula shows that a particle in Ω must cross the surface of region $\bar{\Omega}$ in order to propagate to $\bar{\Omega}$. The formula similar to eqn (12) in probability theory is interpreted in terms of conditional probability (de Broglie, 1990).

There is another case in which both the initial position $\mathbf{r}_1$ and final position $\mathbf{r}_2$ of the particle are in region $\bar{\Omega}$. The propagating process can be thought as consisting of two parts. One is the paths which do not cross the surface during (t_1,t_2). The amplitude representing these paths is the restricted propagator $K^r(\mathbf{r}_2,t_2;\mathbf{r}_1,t_1)$. The other consists of the paths which cross the surface Σ at least once. These paths again can be classified according to the last crossing time as we have discussed in the case of $\mathbf{r}_1$ in Ω and $\mathbf{r}_2$ in $\bar{\Omega}$. Therefore we should have

$$K(\mathbf{r}_2,t_2;\mathbf{r}_1,t_1) = K^r(\mathbf{r}_2,t_2;\mathbf{r}_1,t_1) + \frac{i\hbar}{2m}\int_{t_1}^{t_2}dt\int_{\Sigma}d\mathbf{S}\cdot(-K(\mathbf{r}_s,t;\mathbf{r}_1,t_1)\nabla K^r(\mathbf{r}_2,t_2;\mathbf{r},t)\,|_{\mathbf{r}=\mathbf{r}_s}) \qquad (13)$$

Indeed, eqn (13) can be straightforwardly obtained from eqn (10) by noting that both $\mathbf{r}_1$ and $\mathbf{r}_2$ are in $\bar{\Omega}$. When the particle starts from surface, i.e. $\mathbf{r}_1 \in \Sigma$ at t_1, then eqns (13) and (12) become equivalent because K^r vanishes on the surface. The results in eqns (12) and (13) are first obtained by Auerbach and Kivelson(1985) with the explicit Feynman path integrals technique. The

derivation given here is new and straightforward and seems more simple.

As an example, we consider the decomposition of a free particle propagator. The propagator for a free particle in one dimension is

$$K(x_2,t_2;x_1,t_1) = \frac{1}{(2\pi\hbar)}\int dp\ \exp\{\frac{i}{\hbar}p(x_2-x_1) - \frac{ip^2}{2m\hbar}(t_2-t_1)\}$$

$$= (\frac{m}{2\pi i\hbar(t_2-t_1)})^{1/2}\exp\{\frac{im(x_2-x_1)^2}{2\hbar(t_2-t_1)}\} \qquad (14)$$

If we divide the space into two regions: $\Omega = (-\infty,0)$ and $\bar{\Omega} = (0,\infty)$, then the surface Σ is the origin O, and the normal of the surface of $\bar{\Omega}$ is directed toward to negative x. The restricted propagator is

$$K^r(x_2,t_2;x_1,t_1) = \frac{2}{(2\pi\hbar)}\int dp\ \sin(\frac{p}{\hbar}x_2)\sin(\frac{p}{\hbar}x_1)\ \exp\{-\frac{ip^2}{2m\hbar}(t_2-t_1)\} =$$

$$-\frac{1}{2(2\pi\hbar)}\int dp\{\exp\{\frac{ip}{\hbar}x_2)-\exp\{-\frac{ip}{\hbar}x_2)\}\{\exp\{\frac{ip}{\hbar}x_1)-\exp\{-\frac{ip}{\hbar}x_1)\}\exp\{-\frac{ip^2}{2m\hbar}(t_2-t_1)\}$$

$$= -\frac{1}{2}\{K(x_2,t_2;-x_1,t_1) - K(x_2,t_2;x_1,t_1) - K(x_2,t_2;x_1,t_1) + K(x_2,t_2;-x_1,t_1)\}$$

$$= K(x_2,t_2;x_1,t_1)-K(x_2,t_2;-x_1,t_1) \qquad (15)$$

Assuming $x_1 < 0$ and $x_2 > 0$, the rhs of eqn (12) yields

$$\frac{i\hbar}{2m}\int_{t_1}^{t_2} dt\{K(0,t;x_1,t_1)\partial_x K^r(x_2,t_2;x,t)|_{x=0}\} \qquad (16)$$

where

$$K(0,t;x_1,t_1) = (\frac{m}{2\pi i\hbar(t-t_1)})^{1/2}\exp\{\frac{imx_1^2}{2\hbar(t-t_1)}\}$$

and

$$\partial_x K^r(x_2,t_2;x,t)|_{x=0} = \partial_x\{K(x_2,t_2;x,t)-K(x_2,t_2;-x,t)\}|_{x=0}$$

$$= 2\partial_x[(\frac{m}{2\pi i\hbar(t_2-t)})^{1/2}\exp(\frac{im(x_2-x)^2}{2\hbar(t_2-t)})]|_{x=0}$$

Therefore we have

$$\frac{i\hbar}{m}\int_{t_1}^{t_2}dt(\frac{m}{2\pi i\hbar(t-t_1)})^{1/2}\exp(\frac{imx_1^2}{2\hbar(t-t_1)})\partial_x[(\frac{m}{2\pi i\hbar(t_2-t)})^{1/2}\exp(\frac{im(x_2-x)^2}{2\hbar(t_2-t)})]|_{x=0} \quad (17)$$

Set $\tau = i(t-t_1)$, $\rho=i(t_2-t_1)$, eqn (17) gives

$$\frac{\hbar}{m}\int_0^{\rho}d\tau(\frac{m}{2\pi\hbar\tau})^{1/2}\exp(-\frac{mx_1^2}{2\hbar\tau})\partial_x[(\frac{m}{2\pi\hbar(\rho-\tau)})^{1/2}\exp(-\frac{m(x_2-x)^2}{2\hbar(\rho-\tau)})]|_{x=0} \quad (18)$$

When $x_1<x = 0 <x_2$, the integral in eqn (18) can be proved to be (Auerbach and Kivelson, 1985)

$$(\frac{m}{2\pi\hbar\rho})^{1/2}\exp(-\frac{m(x_2-x_1)^2}{2\hbar\rho})$$

which is the propagator $K(x_2,t_2;x_1,t_1)$. This shows that eqn (12) holds for the case of free particle.

In the case x_1 and $x_2 > 0$ (i.e. in region $\bar{\Omega}$), eqn (18) yields

$$(\frac{m}{2\pi\hbar\rho})^{1/2}\exp(-\frac{m(x_2-(-x_1))^2}{2\hbar\rho}) = K(x_2,t_2;-x_1,t_1)$$

Rhs of eqn (13) yields

$$K^r(\mathbf{r}_2,t_2;\mathbf{r}_1,t_1) + K(x_2,t_2;-x_1,t_1) = K(x_2,t_2;x_1,t_1)$$

where the expression for $K^r(x_2,t_2;x_1,t_1)$, eqn (15), has been used.

An interesting application of eqn (12) is the diffusion of a wave packet in region Ω. We assume that we have a wave packet which has the following form at the initial time t_1:

$$\Psi(\mathbf{r},t_1) = \begin{cases}\Phi(\mathbf{r},t_1) & \text{if } \mathbf{r}\in\Omega\\ 0 & \text{elsewhere}\end{cases}$$

At time t the wave function can be expressed as

$$\Psi(\mathbf{r},t) = \int d\mathbf{r}_1 K(\mathbf{r},t;\mathbf{r}_1,t_1)\Psi(\mathbf{r}_1,t_1) = \int_{\Omega} d\mathbf{r}_1 K(\mathbf{r},t;\mathbf{r}_1,t_1)\Phi(\mathbf{r}_1,t_1) \qquad (19)$$

Using eqn (12), we obtain a relation for the wave function on the surface of region $\bar{\Omega}$ and inside the region $\bar{\Omega}$

$$\Psi(\mathbf{r}_2,t_2) = = \frac{i\hbar}{2m}\int_{t_1}^{t_2} dt \int_{\Sigma} d\mathbf{S}\cdot\{-\Psi(\mathbf{r}_s,t)\nabla K^r(\mathbf{r}_2,t_2;\mathbf{r},t)|_{\mathbf{r}=\mathbf{r}_s}\} \qquad (20)$$

where $\mathbf{r}_2 \in \bar{\Omega}$. Equation (20) shows that the wave function inside $\bar{\Omega}$ can be obtained from the wave function on the surface and the restricted propagator.

2.3 Quantum Extinction Theorem

The extinction theorem originated from physical optics and has been widely used in that area(Born and Wolf, 1980; Nieto-Vesperinas, 1991). The optical extinction theorem states that when an electromagnetic wave is incident on a homogeneous medium with a sharp boundary, it is extinguished inside the medium in the process of interaction and is replaced by a wave propagated in the medium with a velocity different from that of the incident wave. In mathematical terms the theorem may be expressed in the form (Born and Wolf, 1980)

$$\mathbf{E}^i(\mathbf{r}_2) - \frac{1}{k^2}\nabla_2\times\nabla_2\times\int_{\Sigma} d\Sigma\{\mathbf{E}(\mathbf{r})\partial_n G_0(\mathbf{r}_2,\mathbf{r}) - G_0(\mathbf{r}_2,\mathbf{r})\partial_n\mathbf{E}(\mathbf{r})\} = 0 \qquad (21)$$

valid at every point $\mathbf{r}_2$ inside the volume bounded by a surface Σ occupied by the medium, where the integral is over surface Σ, $\mathbf{r} \in \Sigma$, $\mathbf{E}^i$ and $\mathbf{E}$ represent the Fourier transforms (for frequency components (ω)) of the incident electric field and of the total electric field generated inside the medium respectively, and G_0 is the outgoing free-space Green's function of the Helmholtz equation

$$G_0(\mathbf{r},\mathbf{r}') = -\frac{1}{4\pi}\exp\{ik|\mathbf{r}-\mathbf{r}'|\}/|\mathbf{r}-\mathbf{r}'| \tag{22}$$

which satisfies

$$(\nabla^2 + k^2)G_0(\mathbf{r},\mathbf{r}') = \delta(\mathbf{r}-\mathbf{r}') \tag{23}$$

In this section we will show that there is a strict analog of eqn (21) in non-relativitic quantum mechanical potential scattering theory.

Consider the scattering of a free particle with momentum $\mathbf{p}$ by a potential $V(\mathbf{r})$ in real space. The Schrodinger equation for this problem may be written as

$$(\nabla^2 + k^2)\ \Psi(\mathbf{r}) = U(\mathbf{r})\Psi(\mathbf{r}) \tag{24}$$

where $k^2 = 2mE/\hbar^2$ and $U(\mathbf{r}) = 2mV(\mathbf{r})/\hbar^2$. The solution of eqn (24) is given by the Lippmann-Schwinger equation

$$\Psi(\mathbf{r}) = \phi(\mathbf{r}) + \int d\mathbf{r}' G_0(\mathbf{r},\mathbf{r}')U(\mathbf{r}')\Psi(\mathbf{r}') \tag{25}$$

where $\phi(\mathbf{r})$ is the incident wave function and satisfies

$$(\nabla^2 + k^2)\ \phi(\mathbf{r}) = 0 \tag{26}$$

We divide the space into two complementary subsystems Ω and $\bar{\Omega}$ as we have discussed in the last section. Equation (23) multiplied by $\Psi(\mathbf{r})$ minus eqn (24) by $G_0(\mathbf{r},\mathbf{r}')$ yields

$$\Psi(\mathbf{r})\nabla^2 G_0(\mathbf{r},\mathbf{r}') - G_0(\mathbf{r},\mathbf{r}')\nabla^2\Psi(\mathbf{r}) = \delta(\mathbf{r}-\mathbf{r}')\Psi(\mathbf{r}) - G_0(\mathbf{r},\mathbf{r}')U(\mathbf{r})\Psi(\mathbf{r}) \tag{27}$$

Integrating eqn(27) over an arbitrary region Ω', we have

$$\int_{\Omega'} d\mathbf{r}' \{\delta(\mathbf{r}-\mathbf{r}')\Psi(\mathbf{r}') - G_0(\mathbf{r},\mathbf{r}')U(\mathbf{r}')\Psi(\mathbf{r}')\}$$

$$= \int_{\Sigma'} dS\{\Psi(\mathbf{r}_s)\partial_s G_0(\mathbf{r}_s,\mathbf{r}) - G_0(\mathbf{r}_s,\mathbf{r})\partial_s\Psi(\mathbf{r}_s)\} \tag{28}$$

where Σ' is the surface of region Ω'. Let Ω' be the whole space and note that Ψ satisfy Lippmann-Schwinger equation, we obtain the relation between the incident wave and the scattered wave at the infinity

$$\phi(\mathbf{r}) = \lim_{R\to\infty} \int_{\Sigma_R} dS\{\Psi(\mathbf{r}_s)\partial_s G_0(\mathbf{r}_s,\mathbf{r}) - G_0(\mathbf{r}_s,\mathbf{r})\partial_s\Psi(\mathbf{r}_s)\} \tag{29}$$

where the surface integral is over the surface Σ_R of a large sphere with radius R (R is so large that the surface is far from the potential).

Set $\Omega' = \Omega$ in eqn (28), if $\mathbf{r} \in \Omega$, then we have

$$\Psi(\mathbf{r}_i) = \int_\Omega d\mathbf{r}'\{G_0(\mathbf{r}_i,\mathbf{r}')U(\mathbf{r}')\Psi(\mathbf{r}')\}$$

$$+ \int_\Sigma dS\{\Psi(\mathbf{r}_s)\partial_s G_0(\mathbf{r}_s,\mathbf{r}_i) - G_0(\mathbf{r}_s,\mathbf{r}_i)\partial_s\Psi(\mathbf{r}_s)\} \tag{30}$$

where $\mathbf{r}_i$ denotes a point in the region Ω and Σ is the surface. Equation (30) shows that the scattered wave inside a region is composed of the wave scattered from the boundary surface and the wave scattered from the potential of the region. If $\mathbf{r} \notin \Omega$, then eqn (28) yields

$$\int_\Omega d\mathbf{r}'\{G_0(\mathbf{r}_o,\mathbf{r}')U(\mathbf{r}')\Psi(\mathbf{r}')\} + \int_\Sigma dS\{\Psi(\mathbf{r}_s)\partial_s G_0(\mathbf{r}_s,\mathbf{r}_o) - G_0(\mathbf{r}_s,\mathbf{r}_o)\partial_s\Psi(\mathbf{r}_s)\} = 0 \tag{31}$$

where $\mathbf{r}_o$ is a point outside of the region Ω.

In particular, if the scattering potential has a finite and sharp boundary, that is

$$U(\mathbf{r}) = \begin{cases} 2mV(\mathbf{r})/\hbar^2 & \text{if } \mathbf{r} \in \Omega \\ 0 & \text{elsewhere} \end{cases} \tag{32}$$

then eqn (30) yields *quantum extinction theorem* (Wolf, 1973)

$$\phi(\mathbf{r}) = \int_{\Sigma} dS\{\Psi(\mathbf{r}_s)\partial_s G_0(\mathbf{r}_s,\mathbf{r}) - G_0(\mathbf{r}_s,\mathbf{r})\partial_s\Psi(\mathbf{r}_s)\} \qquad (33)$$

for $\mathbf{r} \in \Omega$. Equation (33) is the quantum mechanical analog for the optical extinction theorem eqn (21) (Lax, 1952; Wolf, 1973). This equation has the similar explanation to the optical correspondence. In the present special case, setting $\Omega' = \bar{\Omega}$ in eqn (28) and noting that the volume integral with the potential term vanishes in the region $\bar{\Omega}$, we have

$$\Psi(\mathbf{r}_o) = \int_{\bar{\Sigma}} dS\{\Psi(\mathbf{r}_s)\partial_s G_0(\mathbf{r}_s,\mathbf{r}_o) - G_0(\mathbf{r}_s,\mathbf{r}_o)\partial_s\Psi(\mathbf{r}_s)\} \qquad (34)$$

where the surface $\bar{\Sigma}$ includes two parts: one is the part interfacing the region Ω, another is at the infinity. The part from infinity gives the incident wave because of eqn (29). Therefore we have the wave function in the outside of the scattering potential

$$\Psi(\mathbf{r}_o) = \phi(\mathbf{r}_o) - \int_{\Sigma} dS\{\Psi(\mathbf{r}_s)\partial_s G_0(\mathbf{r}_s,\mathbf{r}_o) - G_0(\mathbf{r}_s,\mathbf{r}_o)\partial_s\Psi(\mathbf{r}_s)\} \qquad (35)$$

Wolf (1973) showed that eqn (33) can be used as a non-local boundary condition to solve the Shrödinger equation inside the potential region, and eqn (35) can be used to propagate the surface wave function to the outside. This approach to the scattering problem is equivalent to the solution of Lippmann-Schwinger equation. However, the new formulation given in eqn (35) involves only a surface integral for obtaining the wave function in the outside region, not a volume integral as it does in the conventional approach.

3.4 Subsystem Perturbation Technique

In a calculation of quantum chemistry, generally, one starts from bare electrons and nuclei without using the knowledge of atoms or fragments in

molecules. This approach is computationally not economic, also chemically not intuitive. Chemically, a knowledge of a molecule is always considered to be made up from the atoms or functional groups of atoms, and the products of a chemical reaction are always related to the reactants through the transferred atoms or functional groups. The object of this section is to formulate a chemically intuitive and hopefully computationally economic approach to construct the charge density of A-B from the knowledge of the fragments A in A-C and B in B-D. According to the density functional theory, the local potential of the subsystems A and B can be written as

$$V_A(\mathbf{r}) = V_{N_A}(\mathbf{r}) + V_{e_A}[\rho_A(\mathbf{r})] \tag{36}$$

$$V_B(\mathbf{r}) = V_{N_B}(\mathbf{r}) + V_{e_B}[\rho_B(\mathbf{r})] \tag{37}$$

where $V_N(\mathbf{r})$ is the single-electron nuclear attractive potential, $V_e[\rho(\mathbf{r})]$ is electron-electron interaction potential derived from the density functional theory, for example $V_e[\rho(\mathbf{r})]$ may be approximated by the classical Coulomb electron-electron repulsive interaction and the local exchange potential $\alpha\rho^{1/3}$. The Green's functions for the subsystems A and B can be obtained from the total systems A-C and B-D. The subsystem Green's functions $G_A(\mathbf{r},\mathbf{r}')$ and $G_B(\mathbf{r},\mathbf{r}')$ satisfy

$$(-\nabla^2 + V_A - E)\, G_A(\mathbf{r},\mathbf{r}') = \delta(\mathbf{r}-\mathbf{r}') \tag{38}$$

for $\mathbf{r}$ and $\mathbf{r}' \in A$;

$$(-\nabla^2 + V_B - E)\, G_B(\mathbf{r},\mathbf{r}') = \delta(\mathbf{r}-\mathbf{r}') \tag{39}$$

for $\mathbf{r}$ and $\mathbf{r}' \in B$.

Explicitly, the subsystem Green's functions $G_A(\mathbf{r},\mathbf{r}')$ and $G_B(\mathbf{r},\mathbf{r}')$ can be expressed in terms of the eigenfunctions of the original systems:

$$G_A(\mathbf{r},\mathbf{r}') = \sum \Phi_i^{AC*}\ \Phi_i^{AC}/(E_i^{AC}-E) \tag{40}$$

$$G_B(\mathbf{r},\mathbf{r}') = \sum \Phi_i^{BD*}\ \Phi_i^{BD}/(E_i^{BD}-E) \tag{41}$$

For the new system A-B, the potential is $V(\mathbf{r})$ and the corresponding Green's function satisfy

$$(-\nabla^2 + V - E)\ G(\mathbf{r},\mathbf{r}') = \delta(\mathbf{r}-\mathbf{r}') \tag{42}$$

Equation (42) multiplied by $G_A(\mathbf{r},\mathbf{r}')$ minus eqn (3) multiplied by $G(\mathbf{r},\mathbf{r}')$ and then integrated variable $\mathbf{r}$ over region Ω_A yields

$$\int_{\Omega_A} d\mathbf{r}\delta(\mathbf{r}-\mathbf{r}')\{G_A(\mathbf{r},\mathbf{r}')-G(\mathbf{r},\mathbf{r}')\} = \int_{\Omega_A} d\mathbf{r}\{G(\mathbf{r},\mathbf{r}')\nabla^2 G_A(\mathbf{r},\mathbf{r}')-G_A(\mathbf{r},\mathbf{r}')\nabla^2 G(\mathbf{r},\mathbf{r}')\}$$

$$+ \int_{\Omega_A} d\mathbf{r}\Delta V_A(\mathbf{r})\ G(\mathbf{r},\mathbf{r}')G_A(\mathbf{r},\mathbf{r}') \tag{43}$$

where

$$\Delta V_A(\mathbf{r}) = V(\mathbf{r}) - V_A(\mathbf{r}) \quad \text{for } \mathbf{r} \in \Omega_A \tag{44}$$

is the potential difference in the region Ω_A between the new system A-B and the system A-C. If the charge density difference in region Ω_A between the two systems is small, then we expect that the potential difference $\Delta V_A(\mathbf{r})$ can be seen as a small perturbation.

If $\mathbf{r}$ and $\mathbf{r}' \in \Omega_A$, then eqn (43) reduces to

$$G(\mathbf{r},\mathbf{r}) = G_A(\mathbf{r},\mathbf{r}) - \int_{\Sigma_A} d\sigma\{G(\mathbf{r}'_\sigma,\mathbf{r})\partial'_s G_A(\mathbf{r}'_\sigma,\mathbf{r}) - G_A(\mathbf{r}'_\sigma,\mathbf{r})\partial'_s G(\mathbf{r}'_\sigma,\mathbf{r})\}$$

$$- \int_{\Omega_A} d\mathbf{r}'\Delta V_A(\mathbf{r}')\ G(\mathbf{r}',\mathbf{r})G_A(\mathbf{r}',\mathbf{r}) \tag{45}$$

where the surface integral (variable $\mathbf{r}'_\sigma$) is over the boundary of Ω_A. As the

same way as deriving eqn (45), we can obtain the Green's function in the region Ω_B

$$G(\mathbf{r},\mathbf{r}) = G_B(\mathbf{r},\mathbf{r}) - \int_{\Sigma_B} d\sigma \{G(\mathbf{r}'_\sigma,\mathbf{r})\partial'_s G_B(\mathbf{r}'_\sigma,\mathbf{r}) - G_B(\mathbf{r}'_\sigma,\mathbf{r})\partial'_s G(\mathbf{r}'_\sigma,\mathbf{r})\}$$

$$- \int_{\Omega_B} d\mathbf{r}' \Delta V_B(\mathbf{r}')\ G(\mathbf{r}',\mathbf{r}) G_B(\mathbf{r}',\mathbf{r}) \qquad (46)$$

where $\mathbf{r} \in \Omega_B$, Σ_B is the boundary of Ω_B and

$$\Delta V_B(\mathbf{r}) = V(\mathbf{r}) - V_B(\mathbf{r}), \quad \text{for } \mathbf{r} \in \Omega_B \qquad (47)$$

Similarly, $\Delta V_B(\mathbf{r})$ may be seen as a small perturbation if the charge distribution in region Ω_B for the system A-B changes little from the system B-D.

The charge distribution for a system can be expressed through the Green's function by

$$\rho(\mathbf{r}) = \frac{1}{\pi} \int^{E_f} dE \lim_{\varepsilon \to 0} \mathrm{Im}\{G(\mathbf{r},\mathbf{r};E+i\varepsilon)\} \qquad (48)$$

where E_f is determined by the normalization condition of $\rho(\mathbf{r})$

$$\int \rho(\mathbf{r}) d\mathbf{r} = N \qquad (49)$$

where N is the total number of electrons, and the integral is over the whole space.

From eqns (45) and (46), we can write down the charge distribution of the new system A-B

$$\rho(\mathbf{r}) = \begin{cases} \rho_A(\mathbf{r}) + \rho_{\sigma_A}(\mathbf{r}) + \rho_{\Delta_A}(\mathbf{r}) & \text{if } \mathbf{r} \in \Omega_A \\ \rho_B(\mathbf{r}) + \rho_{\sigma_B}(\mathbf{r}) + \rho_{\Delta_B}(\mathbf{r}) & \text{if } \mathbf{r} \in \Omega_B \end{cases} \qquad (50)$$

where $\rho_A(\mathbf{r})$ is the unperturbed charge distribution of the old system A-C which

can be written as

$$\rho_A(\mathbf{r}) = \frac{1}{\pi}\int^{E_f} dE \lim_{\varepsilon\to 0} \mathrm{Im}(G_A(\mathbf{r},\mathbf{r};E+i\varepsilon)) \tag{51}$$

$\rho_{\sigma_A}(\mathbf{r})$ is the contribution of the change of the Green's function on the surface due to the mis-match of charge distribution on the surface

$$\rho_{\sigma_A}(\mathbf{r}) = -\frac{1}{\pi}\int^{E_f} dE \lim_{\varepsilon\to 0} \mathrm{Im}\int_{\Sigma_A} d\sigma (G(\mathbf{r}'_\sigma,\mathbf{r})\partial'_s G_A(\mathbf{r}'_\sigma,\mathbf{r}) - G_A(\mathbf{r}'_\sigma,\mathbf{r})\partial'_s G(\mathbf{r}'_\sigma,\mathbf{r})) \tag{52}$$

and $\rho_{\Delta_A}(\mathbf{r})$ is the charge distribution change caused mainly by the potential difference in the region Ω_A

$$\rho_{\Delta_A}(\mathbf{r}) = -\frac{1}{\pi}\int^{E_f} dE \lim_{\varepsilon\to 0} \mathrm{Im}\int_{\Omega_A} d\mathbf{r}'\Delta V_A(\mathbf{r}')\ G(\mathbf{r}',\mathbf{r})G_A(\mathbf{r}',\mathbf{r}) \tag{53}$$

Similar equations can be written down for $\rho_B(\mathbf{r})$, $\rho_{\sigma_B}(\mathbf{r})$ and $\rho_{\Delta_B}(\mathbf{r})$.

From the perturbation expression of charge distribution eqn(50), we can see that the charge density of the new system contains three parts: the unperturbed density, the change caused by the discontinuity of the surface derivatives of G and G_A, and the change caused by the potential difference. As an approximation, setting $G = G_A$ in region Ω_A or G_B in region Ω_B in the rhs of eqn (50) yields the first-order charge distribution

$$\rho(\mathbf{r}) = \begin{cases} \rho_A(\mathbf{r}) + \rho^0_{\Delta_A}(\mathbf{r}) & \text{if } \mathbf{r}\in\Omega_A \\ \rho_B(\mathbf{r}) + \rho^0_{\Delta_B}(\mathbf{r}) & \text{if } \mathbf{r}\in\Omega_B \end{cases} \tag{54}$$

where

$$\rho^0_{\Delta_A}(\mathbf{r}) = -\frac{1}{\pi}\int^{E_f} dE \lim_{\varepsilon\to 0} \mathrm{Im}\int_{\Omega_A} d\mathbf{r}'\Delta V_A(\mathbf{r}')\ G_A(\mathbf{r}',\mathbf{r})G_A(\mathbf{r}',\mathbf{r}) \tag{55}$$

Therefore in the first-order approximation, there is no surface contribution.

The above discussion is a formal perturbation theory in subsystem quantum

mechanics. Although no practical applications have been made, this method could provide a chemically intuitive theoretical tool to understand and predict the changes of the electronic charge density caused by transferring a fragment from one system to another.

2.5 Subsystem Energy Variational Methods

2.5.1. R-matrix approach

The R-matrix method was first introduced by Wigner and Eisenbud (1947) and used in the theory of nuclear reactions. Since then many applications have been made in physics (Burke and Gillan, 1990; Connerade and Lane 1990) and chemical dynamics (Light and Walker, 1976; Webster and Light, 1989). The essential idea of the method is that the configuration space describing the scattered particle and the target is divided into two regions: the internal region and the external region. In the internal region, the interaction is many-body and strong. In the external region, the interaction is weak and in many cases is exactly solvable in terms of plane waves or of Coulomb waves (Burke and Robb, 1975; Sakurai, 1985). Since the interaction is strong and many-body in the internal region, the Shrödinger equation is difficult to solve by imposing the logarithmic boundary conditions on the surface of this region. By knowing the R-matrix of the surface and the known solution in the external region, the S-matrix and the cross section can be calculated (Burke and Robb, 1975; Lane and Thomas, 1958). However, the R-matrix is relative easy to construct, this makes the method for calculating a broad range of physical and chemical processes in an accurate and economical way.

2.5.1.1 Definition and Derivation of R-matrix and Its Inverse

The R-matrix is defined on a surface and is used to relate the derivative of a wave function to the wave function itself on the surface. The detailed definition of R-matrix used here can be found in Nesbet's paper (1984) or in *Paper II* attached at the end of this section. There are many derivations for the R-matrix. Nesbet gave a variational method for the construction of the R-matrix (1984) and its inverse (1986, 1988). We have used a surface identity to yield the R-matrix and its inverse in Paper *II*. Here we give a standard derivation (Lane and Thomas, 1958; Burke and Robb, 1975) for a single-particle system.

The Shrödinger equation of the system is written as

$$\{-\frac{\hbar^2}{2m}\nabla^2 + V(\mathbf{r})\ \}\ \Psi(\mathbf{r}) = E\ \Psi(\mathbf{r}) \tag{56}$$

We divide real space into two regions: Ω and its complement $\bar{\Omega}$. Inside the region Ω, we assume that the complete set $\{\ \Phi_i\ \}$ is the solution of Shrödinger equation

$$\{-\frac{\hbar^2}{2m}\nabla^2 + V(\mathbf{r})\ \}\ \Phi_i(\mathbf{r}) = \varepsilon_i\ \Phi_i(\mathbf{r}) \tag{57}$$

with boundary conditions

$$\partial_n\Phi_i(\mathbf{r}_s) = 0 \qquad \mathbf{r}_s \in \Sigma \tag{58}$$

where Σ is the boundary of Ω, $\partial_s = \mathbf{n}_s\cdot\nabla$ with the normal $\mathbf{n}_s$ of Σ. This set can be assumed to be orthogonal inside the region, that is

$$\int_\Omega d\mathbf{r}\Phi_i^*(\mathbf{r})\Phi_j(\mathbf{r}) = \delta_{ij} \tag{59}$$

The solution to the Shrödinger equation eqn (56) at any energy may now be expanded in the region Ω in terms of $(\Phi_i(\mathbf{r}))$:

$$\Psi(\mathbf{r}) = \sum c_i \Phi_i(\mathbf{r}) \tag{60}$$

where

$$c_i = \int_\Omega d\mathbf{r} \Phi_i^*(\mathbf{r}) \Psi(\mathbf{r}) \tag{61}$$

For the determination of the expansion coefficients c_i, eqn (56) is multiplied by $\Phi_i^*(\mathbf{r})$ and the complex conjugate of eqn(57) by $\Psi(\mathbf{r})$, and the difference is then integrated in the region Ω

$$\int_\Omega d\mathbf{r} \{\Phi_i^*(\mathbf{r}) (-\frac{\hbar^2}{2m} \nabla^2)\Psi(\mathbf{r}) - \Psi(\mathbf{r}) (-\frac{\hbar^2}{2m} \nabla^2)\Phi_i^*(\mathbf{r})\} = (E-\varepsilon_i) \int_\Omega d\mathbf{r} \Phi_i^*(\mathbf{r}) \Psi(\mathbf{r}) \tag{62}$$

Using the Green's theorem and eqn (61) and noting the boundary condition eqn (58), one thereby obtains the relation

$$c_i = \frac{\hbar^2}{2m} \int_\Sigma d\sigma \{ \Phi_i^*(\mathbf{r}_s) \partial_n \Psi(\mathbf{r}_s) \} / (\varepsilon_i - E) \tag{63}$$

Inserting eqn (63) into eqn (60) yields

$$\Psi(\mathbf{r}) = \int_\Sigma d\sigma \{ G(\mathbf{r}, \mathbf{r}_s) \partial_n \Psi(\mathbf{r}_s) \} \tag{64}$$

where

$$G(\mathbf{r}, \mathbf{r}_s) = \frac{\hbar^2}{2m} \sum \Phi_i(\mathbf{r}) \Phi_i^*(\mathbf{r}_s) / (\varepsilon_i - E) \tag{65}$$

It is obvious that $G(\mathbf{r}, \mathbf{r}_s)$ is the Green's function of the Shrödinger equation with boundary condition eqn (58). This function(or matrix) relates the value of the wave function in the internal region to its derivative on the surface. The R-matrix is defined as a matrix function relating the wave function on the surface and its surface derivative $\partial_n \Psi(\mathbf{r}_s)$

$$\Psi(\mathbf{r}_s') = \int_\Sigma d\sigma\{\ R(\mathbf{r}_s', \mathbf{r}_s)\partial_n\Psi(\mathbf{r}_s)\ \} \tag{66}$$

From eqn (64) and the definition equation of the R-matrix, we have

$$R(\mathbf{r}_s', \mathbf{r}_s) = G(\mathbf{r}_s', \mathbf{r}_s) = \frac{\hbar^2}{2m}\sum \Phi_i(\mathbf{r}_s')\Phi_i^*(\mathbf{r}_s)\ /(\varepsilon_i - E) \tag{67}$$

Similarly, one can obtain the inverse of the R-matrix, $R^{-1}(\mathbf{r}_s', \mathbf{r}_s)$. The inverse matrix is defined by equation

$$\partial_n\Psi(\mathbf{r}_s') = \int_\Sigma d\sigma\{\ R^{-1}(\mathbf{r}_s', \mathbf{r}_s)\Psi(\mathbf{r}_s)\ \} \tag{68}$$

Instead of using the complete set $\{\ \Phi_i\ \}$ which satisfies the boundary condition (58), we use another complete set $\{\ \varphi_i\ \}$ which is the solutions of Shrödinger equation eqn (69) in region Ω with the boundary condition given in eqn (70)

$$\{-\frac{\hbar^2}{2m}\nabla^2 + V(\mathbf{r})\ \}\ \varphi_i(\mathbf{r}) = \varepsilon_i\ \varphi_i(\mathbf{r}) \tag{69}$$

$$\varphi_i(\mathbf{r}_s) = 0 \qquad \mathbf{r}_s \in \Sigma \tag{70}$$

$\{\varphi_i\}$ is also assumed to satisfy the orthogonal relation in the region Ω

$$\int_\Omega d\mathbf{r}\varphi_i^*(\mathbf{r})\varphi_j(\mathbf{r}) = \delta_{ij} \tag{71}$$

Equation (56) multiplied by φ_i^* minus the complex of eqn (69) multiplied by Ψ, integrating the result in the region Ω yields

$$\int_\Omega d\mathbf{r}\{\varphi_i^*(\mathbf{r})(-\frac{\hbar^2}{2m}\nabla^2)\Psi(\mathbf{r}) - \Psi(\mathbf{r})(-\frac{\hbar^2}{2m}\nabla^2)\varphi_i^*(\mathbf{r})\} = (E-\varepsilon_i)\int_\Omega d\mathbf{r}\varphi_i^*(\mathbf{r})\Psi(\mathbf{r}) \tag{72}$$

Using the Green's theorem and boundary condition eqn(70) in eqn (72) gives

$$\int_{\Omega} d\mathbf{r}\varphi_i^*(\mathbf{r})\Psi(\mathbf{r}) = \frac{\hbar^2}{2m}\int_{\Sigma} d\sigma\{\ \Psi(\mathbf{r}_s)\partial_n\varphi_i^*(\mathbf{r}_s)\ \}/(E-\varepsilon_i) \tag{73}$$

Since the wave function Ψ can be expanded by basis set (φ_i) and the expansion coefficients (c_i') are

$$c_i' = \int_{\Omega} d\mathbf{r}\varphi_i^*(\mathbf{r})\Psi(\mathbf{r})$$

from eqn (73) we have the expansion equation of Ψ

$$\Psi(\mathbf{r}) = \sum\frac{\hbar^2}{2m}\int_{\Sigma} d\sigma\{\ \Psi(\mathbf{r}_s)\partial_n\varphi_i^*(\mathbf{r}_s)\ \}\varphi_i(\mathbf{r})/(E-\varepsilon_i) \tag{74}$$

This equation, in conjunction with the definition equation of R^{-1}, eqn (68), yields

$$R^{-1}(\mathbf{r}_s',\mathbf{r}_s) = \frac{\hbar^2}{2m}\sum \partial_n\varphi_i(\mathbf{r}_s')\partial_n\varphi_i^*(\mathbf{r}_s)\ /(E-\varepsilon_i) \tag{75}$$

2.5.1.2 Relations Between Volume Integrals and Surface Integrals

Physically, for a particle scattered from a region Ω, the particle must pass through the boundary of the region. Therefore it is intuitively understandable that the scattering cross section for the process can be written as a function of the surface matrix $R(\mathbf{r}_s',\mathbf{r}_s)$. However, some volume integrals, for example the overlap of two eigenfunctions Ψ_1 and Ψ_2 of eqn (56) for the total space, can also be written as a surface integral. Physically, this conclusion seems not so obvious. In this section, we show that the volume integral of a region Ω for the eigenfunction product $\Psi_1\Psi_2$ and the matrix element $\Psi_1 Q\Psi_2$ can be written as a surface integral in terms of the R-matrix and the boundary condition, where Q is an observable operator.

The Shrödinger equations for Ψ_1 and Ψ_2 are repeated here for convenience

$$(-\frac{\hbar^2}{2m}\nabla^2 + V(\mathbf{r})\ )\ \Psi_1(\mathbf{r}) = E_1\ \Psi_1(\mathbf{r}) \tag{76}$$

$$(-\frac{\hbar^2}{2m}\nabla^2 + V(\mathbf{r})\ )\ \Psi_2(\mathbf{r}) = E_2\ \Psi_2(\mathbf{r}) \tag{77}$$

Equation (76) multiplied $\Psi_2^*(\mathbf{r})$ minus the complex of eqn (77) multiplied by $\Psi_1(\mathbf{r})$, the result integrated over region Ω gives

$$\int_\Omega d\mathbf{r}\{\Psi_2^*(\mathbf{r})(-\frac{\hbar^2}{2m}\nabla^2)\Psi_1(\mathbf{r}) - \Psi_1(\mathbf{r})(-\frac{\hbar^2}{2m}\nabla^2)\Psi_2^*(\mathbf{r})\} = (E_1-E_2)\int_\Omega d\mathbf{r}\Psi_2^*(\mathbf{r})\Psi_1(\mathbf{r}) \tag{78}$$

Using the Green's theorem on lhs and dividing both sides by E_1-E_2 if $E_1 \neq E_2$, eqn (78) yields

$$\int_\Omega d\mathbf{r}\Psi_2^*(\mathbf{r})\Psi_1(\mathbf{r}) = -\frac{\hbar^2}{2m}\int_\Sigma d\sigma\{\Psi_2^*(\mathbf{r}_s)\ \partial_n\Psi_1(\mathbf{r}_s) - \Psi_1(\mathbf{r}_s)\partial_n\Psi_2^*(\mathbf{r}_s)\}/(E_1-E_2) \tag{79}$$

Using the defining equation eqn (66) of the R-matrix in conjunction with the explicit expression for the R-matrix given in eqn (67), eqn (79) yields

$$\int_\Omega d\mathbf{r}\Psi_2^*(\mathbf{r})\Psi_1(\mathbf{r}) = \frac{\hbar^2}{2m}\int_\Sigma d\sigma d\sigma'\{\partial_n\Psi_2^*(\mathbf{r}_s')R_{12}(\mathbf{r}_s',\mathbf{r}_s)\partial_n\Psi_1(\mathbf{r}_s)\ \} \tag{80}$$

where

$$R_{12}(\mathbf{r}_1,\mathbf{r}_2) = \frac{R(\mathbf{r}_s',\mathbf{r}_s;E_1) - R^*(\mathbf{r}_s',\mathbf{r}_s;E_2)}{E_1 - E_2} \tag{81}$$

Equation (80) shows that the overlap integral in a region can be expressed in terms of a surface integral which involves only the boundary condition and the R-matrix on the surface.

For the case of $\Psi_2(\mathbf{r}) = \Psi_1(\mathbf{r}) = \Psi(\mathbf{r})$, eqn (64) yields

$$\int_\Omega d\mathbf{r}\Psi^*(\mathbf{r})\Psi(\mathbf{r}) = \int_\Omega d\mathbf{r}\int_\Sigma d\sigma\{\ G^*(\mathbf{r},\mathbf{r}_s')\partial_n\Psi^*(\mathbf{r}_s')\}\ \int_\Sigma d\sigma\{\ G(\mathbf{r},\mathbf{r}_s'')\partial_n\Psi(\mathbf{r}_s'')\} \tag{82}$$

Inserting the Green's function, eqn (65), into eqn (82) and noting that the

basis set is orthogonal in the region, we obtain

$$\int_\Omega d\mathbf{r}\Psi^*(\mathbf{r})\Psi(\mathbf{r}) = \int_\Sigma d\sigma\{\partial_n\Psi^*(\mathbf{r}_s')\}\int_\Sigma d\sigma\{\partial_n\Psi(\mathbf{r}_s'')\}\frac{\hbar^2}{2m}\sum\Phi_i^*(\mathbf{r}_s'')\Phi_i(\mathbf{r}_s')/(\varepsilon_i-E)$$

$$= \int_\Sigma d\sigma' d\sigma''\{\partial_n\Psi^*(\mathbf{r}_s')\}\frac{\partial R(\mathbf{r}_s',\mathbf{r}_s'';E)}{\partial E}\{\partial_n\Psi(\mathbf{r}_s'')\} \qquad (83)$$

Equation (802) can be derived in a similar way. The correctness of eqn (83) can also be checked by substituting the explicit expression of R-matrix into eqn (81). Equation (83) shows that the probability for a particle to stay in the region Ω is determined by the boundary value of $\partial_n\Psi(\mathbf{r}_s)$ and the R-matrix on the surface.

Now we will consider the volume integral $\int_\Omega d\mathbf{r}\Psi^*(\mathbf{r})Q\Psi(\mathbf{r})$. If operator Q commutes with the Hamiltonian H, then $\{\Phi_i\}$ can be assumed also to diagonize Q. It is straightforward to prove that the average value of Q in the region Ω in the state Ψ can be written as

$$\int_\Omega d\mathbf{r}\Psi^*(\mathbf{r})Q\Psi(\mathbf{r}) = \int_\Sigma d\sigma' d\sigma''\{\partial_n\Psi^*(\mathbf{r}_s')\}\frac{\partial R_Q(\mathbf{r}_s',\mathbf{r}_s'';E)}{\partial E}\{\partial_n\Psi(\mathbf{r}_s'')\} \qquad (84)$$

where

$$R_Q(\mathbf{r}_s',\mathbf{r}_s'';E) = QR(\mathbf{r}_s',\mathbf{r}_s'';E) = \frac{\hbar^2}{2m}\sum\Phi_i^*(\mathbf{r}_s'')\Phi_i(\mathbf{r}_s')\,Q_i/(\varepsilon_i-E) \qquad (85)$$

where Q_i is the eigenvalue of Q in the basis set $\{\Phi_i\}$. Generally, if Q does not commute with Hamiltonian, a equation as similar to eqn (84) can be derived as

$$\int_\Omega d\mathbf{r}\Psi^*(\mathbf{r})\hat{A}\Psi(\mathbf{r}) = \int_\Sigma d\sigma' d\sigma''\{\partial_n\Psi^*(\mathbf{r}_s')\}G_Q(\mathbf{r}_s',\mathbf{r}_s'';E)\{\partial_n\Psi(\mathbf{r}_s'')\} \qquad (86)$$

where

$$G_Q(\mathbf{r}_s', \mathbf{r}_s''; E) = \frac{\hbar^2}{2m} \sum_{ij} \Phi_i^*(\mathbf{r}_s'') \Phi_j(\mathbf{r}_s') \; Q_{ij} / ((\varepsilon_i - E)(\varepsilon_j - E)) \qquad (87)$$

where

$$Q_{ij} = \int_\Omega d\mathbf{r} \Phi_i^*(\mathbf{r}) Q \Phi_j(\mathbf{r})$$

The results given in eqns (80) ,(83) ,(84) and (86) are expressed in terms of the R-matrix and the surface derivative on the boundary. If the boundary condition of the region is stated in terms of the wave function Ψ itself instead of the surface derivative, then one may use the inverse of the R-matrix and the boundary condition to accomplish the volume integral by equations similar to eqns (81)-(87). The equations governing the relations between the volume and surface integrals are essential to obtain the formulation of the regional embedding method given in Paper *II*.

2.5.1.3 Determination of the Electronic Structure of a Crystal Using the R-Matrix

Nesbet (1984) was the first to advocate the application of the R-matrix for the determination of the electronic structure of a complex system, for example a crystalline material. He derived the formal theory for the application of the method to crystals in 1984. Since then he has made some other developments (Nesbet, 1986,1988) for practical implementation and applied the method to obtain the energy bands of fcc Cu (Nesbet, 1986) and an empty-lattice test (Sun and Nesbet, 1987). In this section the basic principle of the R-matrix method for the determination of band structures of a crystal is given. The subsystem in this application is chosen to be a cell

which is invariant with respect to the lattice translations. The method is advantaged if an economical way can be found for the calculation of R-matrix.

The translational invariance of a crystal requires that the surface Σ of a cell Ω should consist of sets of paired facets Σ_α, Σ_β that can be labeled such that points on Σ_β are obtained from matched points on Σ_α by a translational vector $\mathbf{T}_{\alpha\beta}$. The translational symmetry determines the boundary conditions of the unit cell Ω. The single electron wavefunction satisfies the Bloch periodic condition (Kittel)

$$\Phi(\mathbf{r} + \mathbf{T}_{\alpha\beta}) = \exp(i\mathbf{k}\cdot\mathbf{T}_{\alpha\beta})\Phi(\mathbf{r}) \tag{88}$$

where $\mathbf{k}$ is a vector in the reciprocal space (for details, see next chapter). Equation (88) yields the condition for the surface derivative

$$\partial_n\Phi(\mathbf{r} + \mathbf{T}_{\alpha\beta}) = -\exp(i\mathbf{k}\cdot\mathbf{T}_{\alpha\beta})\partial_n\Phi(\mathbf{r}) \tag{89}$$

The surface normal of rhs of eqn (89) is opposite to the normal on lhs, this accounts for the negative sign in the equation.

We divide the surface Σ into two half-surfaces A (all facets Σ_α) and B (all facets Σ_β). Using the translational conditions eqns (88) and (89) and the definition of R-matrix, we obtain

$$\Phi(A) = \int_{\Sigma_A} d\sigma'_A \, [R(A,A') - \exp(i\mathbf{k}\cdot\mathbf{T}'_{\alpha\beta})R(A,B')]\partial_n\Phi(A') \tag{90}$$

and

$$\Phi(A) = \exp(-i\mathbf{k}\cdot\mathbf{T}_{\alpha\beta})\Phi(B)$$

$$= \exp(-i\mathbf{k}\cdot\mathbf{T}_{\alpha\beta})\int_{\Sigma_A} d\sigma'_A \, [R(B,A') - \exp(i\mathbf{k}\cdot\mathbf{T}'_{\alpha\beta})R(B,B')]\partial_n\Phi(A') \tag{91}$$

where B and A denote a point on half-surface Σ_B and Σ_A, respectively, and the

surface integral is over the surface Σ_A. Consistency between eqns (90) and (91) requires

$$\int_{\Sigma_A} d\sigma'_A \; [R(A,A') - \exp(i\mathbf{k}\cdot\mathbf{T}'_{\alpha\beta})R(A,B') - \exp(-i\mathbf{k}\cdot\mathbf{T}_{\alpha\beta})R(B,A') - \exp(-i\mathbf{k}\cdot\mathbf{T}_{\alpha\beta})\exp(i\mathbf{k}\cdot\mathbf{T}'_{\alpha\beta})R(B,B')]\partial_n\Phi(A') = 0 \qquad (92)$$

This integral equation can be converted to algebraic equations by expanding functions and the R-matrix in a basis of surface functions or finite elements. The vector $\mathbf{k}$ is to chosen so that the determinant of these algebraic equations is zero. This determines $\partial_n\Phi$ on the half-surface Σ_A, except for normalization. Then $\partial_n\Phi$ on Σ_B is determined by translation, and the surface values of Φ are determined by the R-matrix defining equation. Thus a full solution of the periodic potential problem is obtained, except for normalization, if the R-matrix is known and $\mathbf{k}(\varepsilon)$ is chosen so that the secular determinant of eqn (92) vanishes.

2.5.1.4 Subsystem Embedding Method

From eqn (80) or eqn (83) we see that the finite volume integral for two eigenfunctions of a system can be expressed in terms of the surface integral. The relation between the surface and volume integrals is obtained through the energy derivative of the R-matrix. By making use of this property, a regional variational embedding method is developed in *Paper II*. In that paper it has been shown that,at least in principle, the Shrödinger equation for a piece of a large system can be solved through embedding the piece in its environment through the use of the R-matrix. Techniquely, in order to apply this method in a real situation, one needs to know how to characterize the environment through the R-matrix or its inverse. Hopefully, this method can be developed

into a practical and efficient approach for the determination of electronic structures of large molecules, the surfaces and defects in crystals.

As an explicit application of *Paper II*, the well potential model will be considered. This potential can be written as

$$V(r) = \begin{cases} 0 & r>r_0 \\ V_0 & \text{elsewhere} \end{cases} \tag{93}$$

The solution of the Shrodinger equation in the outer region is

$$\Psi_K(r) = \frac{1}{\sqrt{4\pi}} \frac{e^{-K(r-r_0)}}{r} \tag{94}$$

where the constant is chosen such that $\Psi_K(r)$ is normalized on the sphere surface $r=r_0$

$$\int \Psi_K^2(r)\ r_0^2\ d\Omega = 1 \tag{95}$$

The energy for this solution is $\varepsilon=-K^2/2$. The question here is to find the inner region solution which matches the outer region solution on the surface $r=r_0$.

According to the formula given in *Paper II*, the R-matrix and its inverse can be calculated as

$$R(\mathbf{r}_s', \mathbf{r}_s) = \sum_{\alpha\beta} \phi_\alpha(\mathbf{r}_s')\ (A^{-1})_{\alpha\beta}\ \phi_\beta(\mathbf{r}_s) \tag{96}$$

$$R^{-1}(\mathbf{r}_s', \mathbf{r}_s) = \sum_{\alpha\beta} \frac{\partial\phi_\alpha(\mathbf{r}_s')}{\partial n_s}\ (A^{-1})_{\alpha\beta}\ \frac{\partial\phi_\beta(\mathbf{r}_s)}{\partial n_s} \tag{97}$$

where $\{\phi\}$ is any basis set. The Nesbet matrix element $\mathbf{A}_{\alpha\beta}$ is defined by

$$\mathbf{A}_{\alpha\beta} = \int_{\mathcal{R}} \left\{ \frac{1}{2} \nabla\phi_\alpha^* \cdot \nabla\phi_\beta + \phi_\alpha^* \left(V(\mathbf{r}) - \varepsilon \right) \phi_\beta \right\} d\mathbf{r} \tag{98}$$

If basis functions are chosen as the solutions of Shrödinger's equation

in the outer region, then the Nesbet matrix element can be written as

$$\langle\Psi_K|A|\Psi_{K'}\rangle_o = \int_o dr\Psi_K\left(-\frac{1}{2}\nabla^2 - \varepsilon\right)\Psi_{K'} + \int d^2r_s\Psi_K\frac{1}{2}\frac{\partial\Psi_{K'}}{\partial n_s}$$

$$= -(K'^2/2 + \varepsilon)\frac{1}{K+K'} + \int d^2r_s\Psi_K\frac{1}{2}\frac{\partial\Psi_{K'}}{\partial n_s} \qquad (99)$$

where the 'o' denotes region $r \le r_0$ and the surface integral can be evaluated as

$$\int d^2r_s\Psi_K\frac{1}{2}\frac{\partial}{\partial n_s}\Psi_{K'} = \frac{1}{4\pi}\int r_0^2 d\Omega\frac{e^{-K(r-r_0)}}{r}\frac{1}{2}[1+K'r]\left(\frac{1}{r^2}\right)e^{-K'(r-r_0)}$$

$$= \frac{1+K'r_0}{2\,r_0} \qquad (100)$$

Combine eqn (99) and (100), we obtain the Nesbet matrix element in this special basis set

$$\langle\Psi_K|A|\Psi_{K'}\rangle_o = -(K'^2/2 + \varepsilon)\frac{1}{K+K'} + \frac{1+K'r_0}{2\,r_0} \qquad (101)$$

If the outer region solution $\Psi_K(r)$ of the Shrödinger equation is required to connect the inner region solution, $\Psi_K(r)$ can be chosen as the only basis function to construct the R-matrix and its inverse matrix. In this case, the energy is known to be $\varepsilon=-K^2/2$, the A matrix element in eqn (101) yields

$$\langle\Psi_K|A|\Psi_K\rangle_o = \frac{1+Kr_0}{2\,r_0} \qquad (102)$$

Using this result and eqns (96) and (97), we obtain the R-matrix and its inverse for connecting the outer and inner solutions

$$R(r_0,\varepsilon) = \frac{1}{4\pi}\frac{e^{-2K(r_0-r_0)}}{r_0^2}\langle\Psi_K|A|\Psi_K\rangle_o^{-1}$$

$$= \frac{1}{2\pi}\frac{1}{r_0(1+Kr_0)} \qquad (103)$$

$$R^{-1}(r_0,\varepsilon) = \frac{1}{4\pi}\frac{1+Kr_0}{2\,r_0^3} \qquad (104)$$

The energy derivative of $\partial R^{-1}/\partial \varepsilon$ can be obtained from eqn (104)

$$\partial R^{-1}/\partial \varepsilon = - \frac{1}{4\pi} \frac{1}{2Kr_0^2} \qquad (105)$$

After R^{-1} and $\partial R^{-1}/\partial \varepsilon$ are obtained, the variational embedding procedure given in *Paper II* can proceed. It is interesting to note that R^{-1} and $\partial R^{-1}/\partial \varepsilon$ given, respectively, in eqns (104) and (105) are the same as the corresponding Green's functions obtained by Inglesfield (1971 and 1981). Therefore Inglsfield's variational results will be exactly recovered for this model (1981).

2.5.2 Variational Cellular Method (VCM)

The original cellular method was first proposed by Wigner and Seitz (1933) in solving the crystal-wave equation for a realistic crystal model. The starting point is the partitioning of a crystal into space-filling atomic polyhedra (Wigner-Seitz cell). The crystal potential in the polyhedra is approximated by its spherical average with respect to the center of the cell. In recent years this method has been revived by using the variational procedure(Ferraz, et al ,1982, 1984; Lino, et al, 1987; Nesbet, 1988). The variational cellular method (VCM) has been successfully and efficiently used in solving the single particle or the local-density-functional wavefunction of molecules (Ferreira and Leite, 1978, 1979) and solids(Ferraz, et al, 1984, 1982). The subsystem of the method is chosen as the primitive cell for a crystalline system. A basis set is chosen to expand the single-particle wavefunction in the cell. The expansion coefficients are obtained through the variational principle which is constructed by the consideration of boundary conditions for the primitive unit cell. At present, this method is limited to

the systems with one or two atoms in a primitive cell (for example, sodium or silicon). It would be useful to combine the VCM with the embedding procedure to obtain a more effective and realistic model for the treatment of molecular and crystalline systems. In the following we will outline the principal features of the variational cellular method.

For a given one-electron potential energy function $V(\mathbf{r})$, periodic in a given space lattice, i.e., $V(\mathbf{r}+\mathbf{T}) = V(\mathbf{r})$, where $\mathbf{T}$ is a lattice translational vector, we seek solutions of the Schrödinger equation,

$$H\Psi = \varepsilon\Psi \tag{106}$$

to obtain a description of the bulk properties of the solid. With the use of periodic boundary conditions of the crystal, the problem may be reduced to finding the solutions of Schrödinger's equation in a single primitive cell of the lattice which satisfies the cellular boundary conditions given by the following two equations

$$\Psi(\mathbf{r}+\mathbf{T},\mathbf{k}) = \exp(i\mathbf{k}\cdot\mathbf{T})\ \Psi(\mathbf{r},\mathbf{k}) \tag{107}$$

$$\partial_n\Psi(\mathbf{r}+\mathbf{T},\mathbf{k}) = -\partial_n\exp(i\mathbf{k}\cdot\mathbf{T})\ \Psi(\mathbf{r},\mathbf{k}) \tag{108}$$

where n refers to the outward normal on the cell boundary, and the solutions are classified by the wavevector $\mathbf{k}$, which gives the change in phase of the wave function and its gradient on crossing the cell. For each $\mathbf{k}$, solutions of the Schrödinger equation form a discrete set of eigenfunctions $\Psi_\nu(\mathbf{r},\mathbf{k})$, and the corresponding eigenvalues give the energies $\varepsilon_\nu(\mathbf{k})$. For each value of the band index ν, the energy as a function of $\mathbf{k}$ is referred to as the νth energy band.

The key point of the VCM is to write down the composite representation for the trial wave function, i.e. different functions are chosen for different

cells. The basis functions chosen in this way may be discontinuous on the boundaries. Thefore one should consider this discontinuous effect in the variation. The variational functional is chosen as (Schlosser and Marcus, 1963; Ferreira and Leite, 1978)

$$\varepsilon\sum_i\int_\Omega d\mathbf{r}\Psi_i^*\Psi_i = \sum_i\int_\Omega d\mathbf{r}\Psi_i^*\hat{H}\Psi_i - \frac{1}{4}\sum_{ij}\int_{\Sigma_{ij}} d\sigma(\Psi_i^* + \Psi_j^*)(\partial_n\Psi_j - \partial_n\Psi_i)$$

$$- \frac{1}{4}\sum_{ij}\int_{\Sigma_{ij}} d\sigma(\Psi_i - \Psi_j)(\partial_n\Psi_i^* + \partial_n\Psi_j^*) \qquad (109)$$

where the volume integrals are performed in each cell i and the surface integrals on each boundary Σ_{ij} between cells i and j; the summations (i) run over cells and (ij) over the boundaries of the neighboring cells i and j, $\partial_n\Psi$ denotes the outward normal derivative to the cell surface Σ_{ij}, from cell i. There are three reasons for choosing this variational functional form: (1) ε in this equation is always real for any trial function, (2) the variation is stationary with respect to the solution of Schrödinger equation, and (3) the variation of Ψ^* yields the conditions for which ε is stationary

$$\left(-\frac{1}{2}\nabla^2 + V \right)\Psi_i = \varepsilon\,\Psi_i \qquad (110)$$

$$\Psi_i|_{\Sigma_{ij}} = \Psi_j|_{\Sigma_{ij}} \qquad (111)$$

$$\partial_n\Psi_i|_{\Sigma_{ij}} = \partial_n\Psi_j|_{\Sigma_{ij}} \qquad (112)$$

Equations (111) and (112) imply that the variationally derived wave function and its normal derivative have to be continuous through the cell boundaries. The following is a proof of these three properties.

Proof: (1) From Green's theorem, we have

$$-\int_\Omega d\mathbf{r}\Phi\nabla^2\Psi = \int_\Omega d\mathbf{r}\nabla\Phi\cdot\nabla\Psi - \int_\Sigma d\sigma\Phi\partial_n\Psi \tag{113}$$

Using eqn (113), the Hamiltonian matrix element can be written as

$$\sum_i\int_\Omega d\mathbf{r}\Psi_i^*\hat{H}\Psi_i = \sum_i\int_\Omega d\mathbf{r}\left(\frac{1}{2}\nabla\Psi_i^*\cdot\nabla\Psi_i + \Psi_i^*\hat{V}\Psi_i\right) - \frac{1}{2}\sum_{ij}\int_{\Sigma_{ij}} d\sigma(\Psi_i^*\partial_n\Psi_i - \Psi_j^*\partial_n\Psi_j) \tag{114}$$

where we have used the fact that a surface Σ_{ij} is shared by two neighboring cells i and j. Inserting eqn (114) into (109) gives

$$\varepsilon\sum_i\int_\Omega d\mathbf{r}\Psi_i^*\Psi_i = \sum_i\int_\Omega d\mathbf{r}\left(\frac{1}{2}\nabla\Psi_i^*\cdot\nabla\Psi_i + \Psi_i^*\hat{V}\Psi_i\right) - \frac{1}{2}\sum_{ij}\int_{\Sigma_{ij}} d\sigma(\Psi_i^*\partial_n\Psi_i - \Psi_j^*\partial_n\Psi_j)$$

$$- \frac{1}{4}\sum_{ij}\int_{\Sigma_{ij}} d\sigma(\Psi_i^* + \Psi_j^*)(\partial_n\Psi_j - \partial_n\Psi_i) - \frac{1}{4}\sum_{ij}\int_{\Sigma_{ij}} d\sigma(\Psi_i - \Psi_j)(\partial_n\Psi_i^* + \partial_n\Psi_j^*)$$

$$= \sum_i\int_\Omega d\mathbf{r}\left(\frac{1}{2}\nabla\Psi_i^*\cdot\nabla\Psi_i + \Psi_i^*\hat{V}\Psi_i\right) + \frac{1}{4}\sum_{ij}\int_{\Sigma_{ij}} d\sigma\left\{(\Psi_j\partial_n\Psi_j^* + \Psi_j^*\partial_n\Psi_j) - (\Psi_i\partial_n\Psi_i^* + \Psi_i^*\partial_n\Psi_i)\right.$$

$$\left. - (\Psi_i\partial_n\Psi_j^* + \Psi_i^*\partial_n\Psi_j) + (\Psi_j^*\partial_n\Psi_i + \Psi_j\partial_n\Psi_i^*)\right\}$$

$$= \sum_i\int_\Omega d\mathbf{r}\left(\frac{1}{2}\nabla\Psi_i^*\cdot\nabla\Psi_i + \Psi_i^*\hat{V}\Psi_i\right) + \frac{1}{2}\,\mathrm{Re}\left\{\sum_{ij}\int_{\Sigma_{ij}} d\sigma\,(\Psi_j - \Psi_i)(\partial_n\Psi_j^* + \partial_n\Psi_i^*)\right\} \tag{115}$$

This proves the first property of the variational form eqn(96): ε is always real.

(2) For the second property, we need to prove that the variational form is stationary for the true wave function. That is, if Ψ_0 is the solution of Schrödinger equation with energy ε_0, then the first-order change in energy $\delta\varepsilon = 0$ for the variation

$$\Psi_i = \Psi_0 + \delta\Psi_i \tag{116}$$

and its complex conjugate. From eqn (109) and Schrödinger equation, it is straightforward to write down the first order change of energy as

$$\delta\varepsilon = \sum_i \int_\Omega d\mathbf{r}\{\Psi_0^*(\hat{H}-\varepsilon_0)\delta\Psi_i + \delta\Psi_i^*(\hat{H}-\varepsilon_0)\Psi_0\}$$

$$- \frac{1}{2}\sum_{ij}\int_{\Sigma_{ij}} d\sigma\Psi_0^*(\partial_n\delta\Psi_j - \partial_n\delta\Psi_i) - \frac{1}{2}\sum_{ij}\int_{\Sigma_{ij}} d\sigma(\delta\Psi_i - \delta\Psi_j)\partial_n\Psi_0^*$$

$$= \sum_i \int_\Omega d\mathbf{r}\Psi_0^*(\hat{H}-\varepsilon_0)\delta\Psi_i$$

$$+ \frac{1}{2}\sum_{ij}\int_{\Sigma_{ij}} d\sigma\Psi_0^*(\partial_n\delta\Psi_i - \partial_n\delta\Psi_j) - \frac{1}{2}\sum_{ij}\int_{\Sigma_{ij}} d\sigma(\delta\Psi_i - \delta\Psi_j)\partial_n\Psi_0^* \qquad (117)$$

Using the identity

$$\Psi\nabla^2\delta\Phi = \nabla\cdot(\Psi\nabla\delta\Phi) - \nabla\cdot(\nabla\Psi\delta\Phi) + (\nabla^2\Psi)\delta\Phi$$

and Green's theorem, the first term in the second step of eqn (117) can be written as

$$\sum_i \int_\Omega d\mathbf{r}\Psi_0^*(\hat{H}-\varepsilon_0)\delta\Psi_i = \sum_i \int_\Omega d\mathbf{r}(\hat{H}-\varepsilon_0)\Psi_0^*\delta\Psi_i$$

$$- \frac{1}{2}\sum_{ij}\int_{\Sigma_{ij}} d\sigma\{\Psi_0^*(\partial_n\delta\Psi_i - \partial_n\delta\Psi_j) - \partial_n\Psi_0^*(\delta\Psi_i - \delta\Psi_j)\} \qquad (118)$$

Inserting eqn (11ε) into eqn (117), we obtain $\delta\varepsilon=0$.

(3) Varying Ψ_i^* on both sides of eqn (109) yields

$$\varepsilon\sum_i \int_\Omega d\mathbf{r}\delta\Psi_i^*\Psi_i = \sum_i \int_\Omega d\mathbf{r}\delta\Psi_i^*\hat{H}\Psi_i - \frac{1}{4}\sum_{ij}\int_{\Sigma_{ij}} d\sigma(\delta\Psi_i^* + \delta\Psi_j^*)(\partial_n\Psi_j - \partial_n\Psi_i)$$

$$-\frac{1}{4}\sum_{ij}\int_{\Sigma_{ij}} d\sigma(\Psi_i - \Psi_j)(\partial_n\delta\Psi_i^* + \partial_n\delta\Psi_j^*) \qquad (119)$$

Noting that the variations of Ψ_i^* are unconstrained throughout Ω and on the surface Σ_{ij}, property (3) (i.e. eqns (110)-(112)) follows from eqn (119). #

By choosing appropriate basis sets and using the boundary conditions in eqns (111) and (112) for a cell, the variation of eqn (109) yields the secular equation for the cell in a crystal. Leite and his coworkers (Ferraz, et al, 1982) use the solutions of the Schrödinger equation in a spherical potential as the basis set to expand the cell trial function Ψ_i. They have successfully applied the VCM in solving molecular and crystalline systems. The practical implementation of this method can be found in the paper of Ferraz, Takahashi and Leite, 1982.

Appendix

A.1, The Paradox of the R-matrix Method

There is obvious paradox in eqns (64) or (66). If one tries to obtain the surface derivative of Ψ by differentiating the individual terms of the sum for $G(\mathbf{r},\mathbf{r}_s)$ of eqn (64), one obtains a null result for the lhs, because derivatives of the individual terms are all zero according to the boundary condition for the basis eqn (58). However, the surface derivative does not necessarily vanish. The explanation for this paradox is that the derivative series thus obtained is not uniformly convergent in the vicinity of the surface. A comprehensive proof is given in Lane and Thomas' review article (1958). Actually, this kind of problem also exists in a series expansion.

For example, the function x^2 can be expanded as cosine function in [0,1]

$$x^2 = \sum a_n \cos(2\pi n x)$$

The derivative on lhs is 2 at x=1, however the rhs yields a null result.

A.2, Relation between R-matrix and Scattering Cross Section

In this section we give the relation of R-matrix and scattering cross section for the central potential scattering. Detailed discussions on the general scattering problems can be found in Lane and Thomas(1958) and Burke and Robb(1975). For a two-body scattering, the relative motion is govened by Shrödinger equation eqn (24). In spherical coordinates we have

$$\{\frac{1}{r^2}\frac{\partial}{\partial r}r^2\frac{\partial}{\partial r} + \frac{1}{r^2}(\frac{1}{\sin^2\theta}\frac{\partial^2}{\partial\phi^2} + \frac{1}{\sin\theta}\frac{\partial}{\partial\theta}\sin\theta\frac{\partial}{\partial\theta})\} - \frac{2m}{\hbar^2}(V(r) - E)\}\Psi = 0 \qquad (A\text{-}1)$$

For a potential with spherical symmetry, the angular momentum operator L^2 commutes with the Hamiltonian, therefore the angular part in eqn (A-1) can be separated. Set $\Psi = \Psi_l(r)Y_{lm}(\theta,\phi)$, from eqn (A-1) we have

$$\{\frac{1}{r^2}\frac{d}{dr}r^2\frac{d}{dr} + \frac{l(l+1)}{r^2} - \frac{2m}{\hbar^2}(V(r) - E)\}\Psi_l = 0 \qquad (A\text{-}2)$$

Set

$$\Psi_l = \chi_l(r)/r \qquad (A\text{-}3)$$

where χ_l satisfies $\chi_l(0) = 0$. Inserting (A-3) into (A-2), we have

$$\frac{d^2\chi''}{dr^2} + \{\frac{l(l+1)}{r^2} - \frac{2m}{\hbar^2}(V(r) - E)\}\chi_l = 0 \qquad (A\text{-}4)$$

In the external region $r \longrightarrow \infty$ and $V(r) = 0$, the solution of eqn (A-4) in this region is

$$F_l(kr) = (\frac{\pi kr}{2})^{1/2}J_{l+1/2}(kr) \longrightarrow \sin(kr - l\pi/2) \text{ as } r\longrightarrow\infty \qquad ((A\text{-}5)$$

$$G_l(kr) = \frac{1}{\cos(\pi l)}(\frac{\pi kr}{2})^{1/2}J_{-l-1/2}(kr) \longrightarrow \cos(kr - l\pi/2) \text{ as } r\longrightarrow\infty$$

where $k = (\frac{2m}{\hbar^2}E)^{1/2}$. Therefore a general solution for (A-4) can be written in terms of the incoming and outgoing spherical waves

$$\chi_l \sim \exp(-ikr) - (-1)^l S_l \exp(ikr) \qquad \text{(A-6)}$$

The scattering cross section is given by

$$\sigma(\theta) = |f(\theta)|^2 = |\frac{1}{2ik}\sum_0^\infty (2l+1)(S_l - 1)P_l(\cos\theta)|^2 \qquad \text{(A-7)}$$

The R-matrix for (A-6) is defined by

$$X_l(a) = R_l \frac{d\chi_l}{da} \qquad \text{(A-8)}$$

where a is some r value. Explicitly, we have

$$\exp(-ika) - (-1)^l S_l \exp(ika) = iRk\,\{-\exp(-ika) - (-1)^l S_l \exp(ika)\} \qquad \text{(A-8)'}$$

This yields the S_l expression in terms of R-matrix:

$$S_l = (-1)^l \frac{1+iRk}{1-iRk} \exp(-2ika) \qquad \text{(A-9)}$$

(A-9) shows that once R-matrix is known, the S_l can be calculated and therefore the cross section can be obtained.

INTERNATIONAL JOURNAL OF QUANTUM CHEMISTRY, VOL. 44, 997-1013 (1992)

A Regional Embedding Method

P. F. ZOU

Department of Chemistry, McMaster University, Hamilton, Ontario, Canada, L8S 4M1

Abstract

A new variational embedding method is derived. This method couples Nesbet's use of the R-matrix in the determination of the electronic structure of a crystal with the energy variational technique. The procedure is based on the observation that in many cases the properties for a spatial region of a system change by relatively small amounts when the region is transferred to another system. The transfer of the region from one system to another is accomplished by the embedding potential that is obtained by the inversion of the R-matrix and its energy derivative. It is shown that the interaction between two connected regions can be written as a surface term that is obtained by the continuity conditions on the wave function and its derivative on the surface. The existence of an identity resolution on the surface is demonstrated and this result is used to derive the R-matrix and its inverse. An application of this method to H_2^+ is given, which shows that the method is accurate and reliable if one chooses the appropriate basis set to construct the R-matrix and to perform the variation. © 1992 John Wiley & Sons, Inc.

1. Introduction

Many large molecules, particularly biomolecules and solids, are composed of repeating units. It is also true, as has been demonstrated [1], that functional groups or molecular fragments defined by special boundary conditions in real space can frequently be transferred between systems with little change in their properties, as evidenced by the observation of additive schemes for various properties. It should be possible to develop a method that takes advantage of the observation that fragments frequently change by what are relatively small amounts when transferred between systems. A simple example of a method that takes advantage of transferability at the orbital level is the pseudopotential method for the treatment of core orbitals of a heavy atom. This method is concerned mainly with the transferability near the nuclear regions: the core region. However, transferable properties not only occur in the core regions, but also for an atom or a group of atoms that is bounded by a zero gradient field condition, as has been demonstrated by Bader [1]. A general approach to this regional embedding problem is to consider the effect on the properties of one region when it is embedded in another, i.e., to calculate the properties of a region of a total system. The idea of breaking up a system into several pieces in real space and calculating the pieces separately has been widely discussed in recent years [1–7].

Auerbach et al. [6] developed a path decomposition technique for doing this and applied it to the studies of tunneling between different regions of configuration space. Dobrzynski [7] developed a formal interface response theory and ap-

CCC 0020-7608/92/060997-17

plied it to solve lattice dynamics, electronic structure within the tight-binding approximation, and other physical problems for composite systems. This theory enables one to calculate the response function of composite system from the separate pieces. Inglesfield and Benesh [3] used Green's function to obtain the effective potential from the environment caused by the continuity conditions on the boundary surface. However, this method requires that the surface satisfy the zero derivative of the Green's function. This is a very strong condition. In practice, the surface is replaced by an effective flat surface. Inglesfield's method is useful in solving surface and solid defect problems [3]. The zero derivative surfaces are, however, difficult to determine and manipulate, a problem that is partly alleviated through the use of an effective surface. All these methods have been proved to be successful in some applications. The motivation of the present paper is to develop an embedding method that can be used in molecular systems. This can be done through Inglesfield's embedding procedure and the **R**-matrix method that enables one to connect the wave function and its derivative on a boundary surface.

The **R**-matrix has been widely used in the study of dynamical processes in both chemistry and physics [2, 8]. Since Wigner and Eisenbud [9] introduced the **R**-matrix method, it has been widely used in the studies of nuclear scattering and electron scattering by atoms and molecules [10, 11]. Webster and Light [8] introduced this method in the study of chemical reactions. They used the **R**-matrix propagation to solve the unbound motion along a scattering coordinate. The essential idea in applying this procedure to a reactive system is to divide configuration space into reactant, intermediate, and product regions. The **R**-matrix method then enables one to correctly match the wave function on the surfaces separating the reactant–intermediate and intermediate–product region pairs in real space and obtain the scattering cross section. Nesbet [2] developed a variational principle to determine the **R**-matrix and extended the method to the determination of the electron energy-band structure of a crystal, one that makes use of the periodic boundary condition characteristic of such systems.

The present paper combines the ideas of Nesbet's use of the **R**-matrix [2] and Inglesfield's regional embedding method [3] to yield a new embedding procedure, one that is based on the **R**-matrix method rather than on the zero derivative Green's function technique. The **R**-matrix method enables one to match the derivatives on a surface of any shape and, thus, the method proposed here can be used in a single-particle model for any geometry of the region. The method must be used in conjunction with density functional theory in the treatment of a many-particle system to avoid the problems introduced by exchange (the nonlocal potential). The present procedure uses one basis set in the region of interest, and the environmental effect is considered by the embedding potential, while, in comparison, the variational cellular method [2, 12, 13] uses composite basis sets in the consideration of the whole system. In Section 2, an equation for the resolution of the identity on the surface is obtained by expanding a wave function into a complete basis set in the region. Through the use this identity, one is not only able to derive the **R**-matrix, but also its inverse $\mathbf{R}^{-1}$. It is also pointed out that one can obtain the inverse matrix $\mathbf{R}^{-1}$ directly from the **R**-matrix by eliminating the

overcompleteness of the basis set on the surface. The R-matrix and its inverse developed in Section 2 are used in Section 3 to yield a new variational embedding equation where the potential is written in two parts: one is a local part; the other is a surface term that expresses the interaction between the environment and the region. The last section shows how this theory might be used in practice. We demonstrate this by applying this new procedure to the molecule H_2^+. A discussion about future possible applications in chemistry and surface science is also given in this section.

2. The R-Matrix and Its Inverse Matrix

The R-matrix, $\mathbf{R}(\mathbf{r}_s, \mathbf{r}_s'; \varepsilon)$, is defined as a matrix that has continuous indices and connects the derivative of a wave function on a surface to the wave function itself [2]:

$$\Psi(\mathbf{r}_s) = \oint \mathbf{R}(\mathbf{r}_s, \mathbf{r}_s'; \varepsilon) \cdot \frac{\partial \Psi}{\partial n_s}(\mathbf{r}_s')\, d\mathbf{r}_s', \tag{1}$$

where Ψ is a solution of Schrödinger's equation with energy ε:

$$-\frac{1}{2}\nabla^2\Psi + V\Psi = \varepsilon\Psi, \tag{2}$$

and $(\partial\Psi)/(\partial n_s)(\mathbf{r}_s) = \mathbf{n}_s \cdot \nabla\Psi(\mathbf{r}_s)$; $\mathbf{n}_s$ is the normal to the surface. The integral in Eq. (1) is over the surface forming the boundary of a region, say the $\mathfrak{R}$-region, in real space. The indices $\mathbf{r}_s$ and $\mathbf{r}_s'$ are restricted to the surface. The inverse of the R-matrix is defined on the surface by Eq. (3):

$$\oint d\mathbf{r}_s \mathbf{R}(\mathbf{r}_s', \mathbf{r}_s; \varepsilon) \cdot \mathbf{R}^{-1}(\mathbf{r}_s, \mathbf{r}_s''; \varepsilon) = \delta(\mathbf{r}_s' - \mathbf{r}_s''). \tag{3}$$

Thus, through the use of Eqs. (1) and (3), one finds that $\mathbf{R}^{-1}$ yields the inverse of the relationship between Ψ and $\partial\Psi/\partial\mathbf{n}$, as defined by $\mathbf{R}$ itself:

$$\frac{\partial \Psi}{\partial n_s}(\mathbf{r}_s) = \oint \mathbf{R}^{-1}(\mathbf{r}_s, \mathbf{r}_s'; \varepsilon) \cdot \Psi(\mathbf{r}_s')\, d\mathbf{r}_s'. \tag{4}$$

This equation also serves as the definition of $\mathbf{R}^{-1}$.

To construct the R-matrix and its inverse, one chooses a complete, linearly independent set of functions $\{\Phi_i\}$ in the region, in terms of which the wave function can be expanded as

$$\Psi = \sum_i c_i \Phi_i. \tag{5}$$

The coefficients $\{c_i\}$ are defined by the Schrödinger's equation if Ψ is a solution of the equation. Following Nesbet's method, we first define his matrix $\mathbf{A}$ with element $\mathbf{A}_{ij}$ given by [2]

$$\mathbf{A}_{ij} = \int_{\mathfrak{R}} \left\{ \frac{1}{2}\nabla\Phi_i^* \cdot \nabla\Phi_j + \Phi_i^*(V(\mathbf{r}) - \varepsilon)\Phi_j \right\} d\mathbf{r}, \tag{6}$$

where ε is a parameter, which has the unit of energy, and $V(\mathbf{r})$ is the local potential of the system and the integral is over the region $\mathcal{R}$. We denote the expansion of the surface derivative $\partial\Psi/\partial\mathbf{n}_s$ by the function

$$\xi(\mathbf{r}_s) = \sum_i c_i \partial\Phi_i/\partial\mathbf{n}_s(\mathbf{r}_s)\,. \tag{7}$$

Specifically, if Ψ is the solution of Schrödinger's equation with energy ε, then we have

$$\langle\Psi|H - \varepsilon|\Psi\rangle_{\mathcal{R}} = \int_{\mathcal{R}} \Psi^*\left(-\frac{1}{2}\nabla^2 + V - \varepsilon\right)\Psi d\mathbf{r} = 0\,. \tag{8}$$

This equation can be expressed as

$$\sum_{ij} c_i c_j^* A_{ij} = \frac{1}{2}\sum_i c_i \oint \xi^*(\mathbf{r}_s)\Phi_i(\mathbf{r}_s)\,d\mathbf{r}_s\,, \tag{9}$$

where the rhs integral is over the surface of the region $\mathcal{R}$. From Eq. (7) and the fact that the basis functions are linearly independent and also by that $\{c_i\}$ satisfy a variational condition [2], one can obtain the coefficients $\{c_i\}$ in Eq. (5) as

$$c_i = \frac{1}{2}\sum_j A_{ij}^{-1} \oint \xi(\mathbf{r}_s)\Phi_j^*(\mathbf{r}_s)\,d\mathbf{r}_s\,. \tag{10}$$

By combining Eqs. (7) and (10), one may obtain an expression for the resolution of the identity on the surface

$$\frac{1}{2}\sum_{ij}\frac{\partial\Phi_j(\mathbf{r}_s)}{\partial n_s}\mathbf{A}(\varepsilon)_{ij}^{-1}\Phi_i^*(\mathbf{r}_s') = \delta(\mathbf{r}_s' - \mathbf{r}_s)\,. \tag{11}$$

This expression allows one to obtain the expansion coefficients in terms of the wave function or its derivative. One can see that the basis set $\{\Phi_i\}$ and its derivatives $\{\partial\Phi_j(\mathbf{r}_s)/\partial n_s\}$ on the surface are related through the inverse of the Nesbet matrix **A**. Therefore, the Nesbet matrix plays a key role in relating the wave function and the surface derivative on the boundary. By Eqs. (5) and (10), one has

$$\Psi(\mathbf{r}_s) = \frac{1}{2}\sum_{ij}\oint \Phi_i(\mathbf{r}_s)\mathbf{A}(\varepsilon)_{ij}^{-1}\Phi_j^*(\mathbf{r}_s')\xi(\mathbf{r}_s')\,d\mathbf{r}_s'. \tag{12}$$

Comparison of Eq. (12) with the definition of the **R**-matrix given in Eq. (1) yields an expansion for the **R**-matrix in terms of the basis set and its matrix elements:

$$\mathbf{R}(\mathbf{r}_s, \mathbf{r}_s'; \varepsilon) = \frac{1}{2}\sum_{ij}\Phi_i(\mathbf{r}_s)A(\varepsilon)_{ij}^{-1}\Phi_j^*(\mathbf{r}_s')\,. \tag{13}$$

The derivation of the **R**-matrix given here, although closely related to Nesbet's variational derivation, appears to be more direct. However, the present method assumes a knowledge of Ψ to be followed by the use of Schrödinger's equation [Eqs. (2) and (8)], whereas Nesbet's method is a variational derivation of the **R**-matrix itself. Through the use of the identity resolution given in Eq. (11) and the expansion in Eq. (5), one can express the coefficients $\{c_i\}$ into another form, one

in which the wave function rather than the derivative function $\xi(\mathbf{r}_s)$ appearing in Eq. (10) is known:

$$c_i = \frac{1}{2}\sum_j A(\varepsilon)^{-1}_{ij} \oint \frac{\partial \Phi_j^*}{\partial n_s}(\mathbf{r}_s)\Psi(\mathbf{r}_s)\, d\mathbf{r}_s . \tag{14}$$

Insertion of this result into the expansion for the surface derivative of the wave function given in the Eq. (7) and comparison of the definition equation for $\mathbf{R}^{-1}$ [Eq. (4)] enables one to write the inverse of the **R**-matrix as

$$\mathbf{R}^{-1}(\mathbf{r}_s, \mathbf{r}_s'; \varepsilon) = \frac{1}{2}\sum_{ij} \frac{\partial \Phi_i}{\partial n_s}(\mathbf{r}_s) A(\varepsilon)^{-1}_{ij} \frac{\partial \Phi_j^*}{\partial n_s}(\mathbf{r}_s') . \tag{15}$$

This equation parallels Eq. (13) for the **R**-matrix. Both of the equations can be obtained from the resolution of the identity on the surface [Eq. (11)]. The **R**-matrix and its inverse expressed by Eqs. (13) and (15) are evaluated through the use of a complete, linearly independent basis set for the region and of the inverse of the Nesbet matrix **A**. These two results are general and exact. One notes that the Hilbert space spanned by the function set $\{\Phi_i\}$ is used to expand the **R**-matrix on the surface of a region in real space and the surface derivative of the function set can be used to express the inverse of the **R**-matrix. An expression similar to Eq. (15) has been derived in the first paper [2].

The complete, linearly independent basis set of a region can be reduced to a smaller complete and linearly independent basis set on the surface. The reason for this reduction is that some different functions in the region can be the same function on the surface. This implies that the function $\Phi_i\Phi_j^*$ appearing in a term of the Eq. (13) can be equal to a corresponding function in some other term. Therefore, one can reorganize Eq. (13) according to the independent surface functions

$$\mathbf{R}(\mathbf{r}_s', \mathbf{r}_s) = \frac{1}{2}\sum_{\alpha,k} \eta_\alpha'(\mathbf{r}_s')\,(\mathscr{A}^{-1})_{\alpha k}\eta_k'(\mathbf{r}_s) , \tag{16}$$

where the surface function set $\{\eta_\alpha'(\mathbf{r}_s)\}$ is an independent function set that is obtained from the region complete basis set $\{\Phi_i\}$ when it is restricted to the surface of the region. Therefore, the index α in this equation represents a set of region functions:

$$\alpha = \{a, \text{ when } c_a\Phi_a(\mathbf{r}_s) = \eta_\alpha'(\mathbf{r}_s)\} , \tag{17}$$

where c_a is the surface normalized constant of function Φ_a. Therefore the reduced matrix $\mathscr{A}^{-1}$ in Eq. (16) is defined as

$$(\mathscr{A}^{-1})_{\alpha k} = \sum_{a\in\alpha}\sum_{b\in k}(c_a c_b)^{-1}(A^{-1})_{ab} . \tag{18}$$

The reduced matrix $\mathscr{A}$ is still a Hermitian matrix. One can now find the surface-normalized orthogonal set $\{\eta\}$ by doing a linear combination of $\{\eta'\}$

$$\eta_\alpha = \sum_k \mathscr{D}_{\alpha k}\eta_k' , \tag{19}$$

and the R-matrix can be expressed into this orthogonal set as

$$\mathbf{R}(\mathbf{r}_s', \mathbf{r}_s) = \frac{1}{2} \sum_{\alpha,\beta} \eta_\alpha(\mathbf{r}_s') (\tilde{\mathcal{A}}^{-1})_{\alpha\beta} \eta_\beta^*(\mathbf{r}_s), \tag{20}$$

where the matrix $\tilde{\mathcal{A}}^{-1}$ can be obtained from $\mathcal{A}^{-1}$ and the linear combination coefficients $\{\mathcal{D}_{\alpha\beta}\}$ of $\{\eta\}$ given in Eq. (19). By using the surface orthogonal property of $\{\eta_\alpha\}$, one can prove that the inverse of the R-matrix can be written as

$$\mathbf{R}^{-1}(\mathbf{r}_s', \mathbf{r}_s) = 2 \sum_{\alpha,\beta} \eta_\alpha(\mathbf{r}_s') (\tilde{\mathcal{A}})_{\alpha\beta} \eta_\beta^*(\mathbf{r}_s). \tag{21}$$

Therefore, one has two recipes to find $\mathbf{R}^{-1}$: After the Nesbet matrix A and its inverse are found, one can construct $\mathbf{R}^{-1}$ directly by Eq. (15) with matrix $\mathbf{A}^{-1}$ and the surface derivatives of the basis set $\{\Phi_i\}$, or one constructs the R-matrix followed by the determination of the surface orthogonal functions $\{\eta_i\}$ and the matrix $\tilde{\mathcal{A}}$, and then constructs the $\mathbf{R}^{-1}$-matrix with Eq. (21). These two recipes will be proved to be useful in different situations in the next two sections.

3. Embedding Variation

One can numerically use the R-matrix given in Eq. (13) and the periodic boundary conditions to obtain energy bands in a crystal, as Nesbet showed [2]. However, one can also use the R-matrix and its inverse as connecting conditions in the energy variational technique. We would like to discuss the energy variation in a special case in which the real space of the system is divided into two connected regions, the $\mathcal{L}$- and $\mathcal{R}$-regions, and the cross set of the two regions is a two-dimensional surface. However, this method is easily extended to a case having many regions. In many cases, the observable properties like the charge density, in a region, say the $\mathcal{R}$-region, change little from one system to another similar system. Therefore, one can reasonably make the assumption that the wave function Ψ in the $\mathcal{R}$-region is known approximately from the other system; then, one needs to determine the $\mathcal{L}$-region's wave function and do so that the two functions are correctly matched at the surface. This can be done by using the R-matrix and its inverse developed above, coupled with a variational technique that one needs to minimize an energy functional of the complete system.

The energy functional, which one needs to minimize, has contributions from the two regions $\mathcal{R}$ and $\mathcal{L}$. Therefore, one has

$$E[\Phi] = \frac{\displaystyle\int_{\mathcal{R}} \left\{ \frac{1}{2} \nabla\Psi^* \cdot \nabla\Psi + \Psi^* V \Psi \right\} d\mathbf{r} + \int_{\mathcal{R}} \left\{ \frac{1}{2} \nabla\Phi^* \cdot \nabla\Phi + \Phi^* V \Phi \right\} d\mathbf{r}}{\displaystyle\int_{\mathcal{R}} \Psi^* \Psi d\mathbf{r} + \int_{\mathcal{L}} \Phi^* \Phi \, d\mathbf{r}}, \tag{22}$$

where Φ is the trial function in $\mathcal{L}$-region and Ψ is the solution of the Schrödinger's equation [Eq. (2)] in the region $\mathcal{R}$. There are two conditions that the trial function Φ must satisfy on the surface: the continuity of the wave function

$$\Phi(\mathbf{r}_s) = \Psi(\mathbf{r}_s) \tag{23}$$

and the continuity of its first derivative on the surface

$$\frac{\partial \Phi}{\partial \mathbf{n}_s}(\mathbf{r}_s) = \frac{\partial \Psi}{\partial \mathbf{n}_s}(\mathbf{r}_s). \tag{24}$$

Using these two conditions, together with Schrödinger's Eq. (2), the variational function can be written as

$$E[\Phi] = \frac{\varepsilon \int_{\mathcal{R}} \Psi^* \Psi d\mathbf{r} + \frac{1}{2} \oint \Phi^*(\mathbf{r}_s) \cdot \frac{\partial \Phi}{\partial n_s}(\mathbf{r}_s) d\mathbf{r}_s + \int_{\mathcal{L}} \left\{ \frac{1}{2} \nabla \Phi^* \cdot \nabla \Phi + \Phi^* V \Phi \right\} d\mathbf{r}}{\int_{\mathcal{R}} \Psi^* \Psi d\mathbf{r} + \int_{\mathcal{L}} \Phi^* \Phi d\mathbf{r}}, \tag{25}$$

where $\oint d\mathbf{r}_s$ denotes the two-dimensional surface integral on the boundary of the region $\mathcal{R}$. The volume integral of $|\Psi|^2$ in Eq. (25) can be eliminated by using Eq. (26), which expresses the volume integral into the surface integral through using the energy derivative of $\mathbf{R}^{-1}$-matrix [10]

$$\int_{\mathcal{R}} \Psi^* \Psi d\mathbf{r} = -\frac{1}{2} \oint d\mathbf{r}_s \Phi(\mathbf{r}_s)^* \frac{\partial \mathbf{R}^{-1}(\varepsilon)}{\partial \varepsilon} \Phi(\mathbf{r}_s'). \tag{26}$$

Equation (26) is satisfied for any solution of Schrödinger's equation. One can obtain the final variational form of the functional by replacing the volume integral in $\mathcal{R}$-region with the surface integral on the boundary:

$$E[\Phi] = \frac{\frac{1}{2} \oint d\mathbf{r}_s \Phi^*(\mathbf{r}_s) \left(\mathbf{R}^{-1} - \varepsilon \frac{\partial \mathbf{R}^{-1}(\varepsilon)}{\partial \varepsilon} \right) \Phi(\mathbf{r}_s') d\mathbf{r}_s' + \int_{\mathcal{L}} \left\{ \frac{1}{2} \nabla \Phi^* \cdot \nabla \Phi + \Phi^* V \Phi \right\} d\mathbf{r}}{\frac{1}{2} \oint d\mathbf{r}_s \Phi^*(\mathbf{r}_s) \left(-\frac{\partial \mathbf{R}^{-1}(\varepsilon)}{\partial \varepsilon} \right) \Phi(\mathbf{r}_s') d\mathbf{r}_s' + \int_{\mathcal{L}} \Phi^* \Phi d\mathbf{r}}. \tag{27}$$

This variational functional expresses the total energy through the volume integral of the $\mathcal{L}$-region and the surface integral. The surface appearing in this equation is the interface between the $\mathcal{R}$-region and $\mathcal{L}$-region. The surface term expresses the effect that the $\mathcal{R}$-region, which is the environment of $\mathcal{L}$-region, has on the $\mathcal{L}$-region.

To determine the trial function, one may choose a complete basis set $\{\varphi_i\}$ in the region $\mathcal{L}$, which is not necessarily the same as the basis set $\{\Phi_i\}$ in the region $\mathcal{R}$, for the expansion of the trial function in the $\mathcal{L}$-region

$$\Phi = \sum_i c_i \varphi_i. \tag{28}$$

By substituting Eq. (28) into Eq. (27) and varying the coefficients, one obtains the secular equation

$$\mathbf{HC} = E\mathbf{SC}, \tag{29}$$

where the overlap matrix S is

$$S_{ij} = \int_{\mathcal{L}} \varphi_i^* \varphi_j \, d\mathbf{r} - \frac{1}{2} \oint \varphi_i^*(\mathbf{r}_s) \frac{\partial \mathbf{R}^{-1}(\mathbf{r}_s, \mathbf{r}_s'; \varepsilon)}{\partial \varepsilon} \varphi_j(\mathbf{r}_s') \, d\mathbf{r}_s \, d\mathbf{r}_s' \tag{30}$$

and the Hamiltonian matrix H is

$$\begin{aligned} \mathbf{H}_{ij} &= \int_{\mathcal{L}} \frac{1}{2} \nabla \varphi_i^* \cdot \nabla \varphi_j + \varphi_i^* V \varphi_j \, d\mathbf{r} + \frac{1}{2} \oint \varphi_i^*(\mathbf{r}_s) \left(\mathbf{R}^{-1} - \varepsilon \frac{\partial \mathbf{R}^{-1}(\varepsilon)}{\partial \varepsilon} \right) \varphi_j(\mathbf{r}_s') \, d\mathbf{r}_s \, d\mathbf{r}_s' \\ &= \int_{\mathcal{L}} \frac{1}{2} \nabla \varphi_i^* \cdot \nabla \varphi_j \, d\mathbf{r} + \mathbf{V}_{ij}^{\text{eff}}, \end{aligned} \tag{31}$$

with the effective potential matrix element

$$\mathbf{V}_{ij}^{\text{eff}} = \int_{\mathcal{L}} \varphi_i^* V \varphi_j \, d\mathbf{r} + \frac{1}{2} \oint \varphi_i^*(\mathbf{r}_s) \left(R^{-1} - \varepsilon \frac{\partial \mathbf{R}^{-1}(\varepsilon)}{\partial \varepsilon} \right) \varphi_j(\mathbf{r}_s') \, d\mathbf{r}_s \, d\mathbf{r}_s'.$$

This enables one to define an effective potential operator for the particle moving in the $\mathcal{L}$-region:

$$V^{\text{eff}} = V \chi_{\mathcal{L}}(\hat{\mathbf{r}}) + \oint |\mathbf{r}_s\rangle \, d\mathbf{r}_s \, V_s(\mathbf{r}_s, \mathbf{r}_s'; \varepsilon) \, d\mathbf{r}_s' \langle \mathbf{r}_s' |, \tag{32}$$

where $\chi_{\mathcal{L}}$ is the projecting operator, defined by

$$\chi_{\mathcal{L}}(\mathbf{r}) = \begin{cases} 1 & \text{if } \mathbf{r} \in \mathcal{L} \\ 0 & \text{else,} \end{cases}$$

and the embedding potential:

$$V_s(\mathbf{r}_s, \mathbf{r}_s'; \varepsilon) = \frac{1}{2} \left[\mathbf{R}^{-1}(\mathbf{r}_s, \mathbf{r}_s'; \varepsilon) - \varepsilon \frac{\partial \mathbf{R}^{-1}}{\partial \varepsilon}(\mathbf{r}_s, \mathbf{r}_s'; \varepsilon) \right]. \tag{33}$$

Equation (33) is the principal result of the paper. The embedding potential given in this equation determines the effect that the $\mathcal{R}$-region has on the remainder of the system. We see that the effect of the environment can be written as a surface term. Physically, this should be the case, as far as one is concerned with a local potential interaction, because any physical interaction between two connected regions in real space must be transmitted through the boundary surface. This result is analogous to that obtained from the quantum mechanics of a subsystem, where it has been shown [1] that the Ehrenfest force acting on a region of space bounded by a surface of zero flux in the gradient vector field of the charge density is completely determined by the pressure that the remainder of the system exerts on each element of this surface. One can use Eq. (32) to determine the effective potential that a small system, say a molecule, has on a large system, a molecule adsorbed on the surface of the solid, for example, or a defect within the solid.

Practically, to determine the matrices H and S, one needs to know not only $\mathbf{R}^{-1}$ but also its derivative with the energy. This derivative can be obtained by using

the explicit expression for $\mathbf{R}^{-1}$ [Eq. (15)] and the fact that

$$\frac{\partial \mathbf{A}^{-1}}{\partial \varepsilon} = -\mathbf{A}^{-1}\frac{\partial \mathbf{A}}{\partial \varepsilon}\mathbf{A}^{-1}. \tag{34}$$

By the definition of the Nesbet matrix [Eq. (6)], the energy derivative of the Nesbet matrix is

$$\frac{\partial \mathbf{A}}{\partial \varepsilon} = -S^{\mathfrak{R}}, \tag{35}$$

where $\mathbf{S}^{\mathfrak{R}}$ is the overlap matrix of the basis $\{\Phi_i\}$ in the region $\mathfrak{R}$ where matrix A is defined. One can introduce a new matrix B, which is defined as the energy derivative of matrix $\mathbf{A}^{-1}$:

$$\mathbf{B} \equiv \frac{\partial \mathbf{A}^{-1}}{\partial \varepsilon}. \tag{36}$$

From Eqs. (34) and (35), one obtains

$$\mathbf{B} = \mathbf{A}^{-1}\mathbf{S}^{\mathfrak{R}}\mathbf{A}^{-1}. \tag{37}$$

In terms of the matrix B, one can obtain the energy derivative of $\mathbf{R}^{-1}$ as

$$\frac{\partial \mathbf{R}^{-1}(\varepsilon)}{\partial \varepsilon} = \frac{1}{2}\sum_{ij}\frac{\partial \Phi_j}{\partial n_s}(\mathbf{r}_s)\mathbf{B}(\varepsilon)_{ij}\frac{\partial \Phi_i}{\partial n_s}(\mathbf{r}_s'). \tag{38}$$

Define a surface integral matrix G as

$$\mathbf{G}_{ij} = \frac{1}{2}\oint \varphi_i(\mathbf{r}_s)\frac{\partial \Phi_j^*}{\partial n_s}(\mathbf{r}_s)\,d\mathbf{r}_s. \tag{39}$$

From the definition, one sees that the matrix G is not Hermit. In terms of matrices $\mathbf{A}^{-1}$, B, and G, the embedding potential matrix $\mathbf{V}_s$ can be written as

$$\mathbf{V}_s = G(\mathbf{A}^{-1} - \mathbf{EB})\mathbf{G}^T, \tag{40}$$

where $\mathbf{G}^T$ is the transformed matrix of G. Therefore, one can calculate the matrix elements appearing in Eq. (29) as far as one has obtained the matrix B and $\mathbf{V}_s$. However, from Eqs. (37) and (40), we can see that there is no difficulty in calculating these two matrices if one has found the Nesbet matrix A. This implies that Eq. (29) is a practically realizable equation. More explicitly, one can write down Eq. (29) in terms of matrices B and $\mathbf{V}_s$ as

$$(\mathbf{T}^{\mathfrak{L}} + \mathbf{V}^{\mathfrak{L}} + \mathbf{V}_s)\mathbf{C} = \mathbf{E}(\mathbf{S}^{\mathfrak{L}} + \mathbf{GBG}^T)\mathbf{C}, \tag{41}$$

where $\mathbf{T}^{\mathfrak{L}}$, $\mathbf{V}^{\mathfrak{L}}$, and $\mathbf{S}^{\mathfrak{L}}$ are, respectively, the kinetic, potential $V(\mathbf{r})$, and overlap matrices in the region $\mathfrak{L}$. Equation (41) with the embedding potential given in Eq. (33) provides one the tool to solve problems. This result shows that one can study a region independent from the total system if one knows the effective interaction on the surface. This effective interaction can be written down with the inverse of the R-matrix and its energy derivative, and these two matrices can be explicitly obtained by Eqs. (15) and (38). Numerically, one is able to use the fi-

nite element method [14] to determine a solution of a region. In the finite element method, the iterative methods are accepted and the conjugate gradient method is used to handle the interaction across the surface that separates the regions. The present procedure is a fully variational method and handles the interaction between the two connected regions with an effective surface embedding potential. As these treatments are analytical, therefore, they should be easier to apply.

4. Application and Discussion

Equation (41) can be used to solve for the energy of any system within the one particle approximation if one is able to obtain the inverse R-matrix of the environment of a region. Here, we will demonstrate the application of the method by giving an explicit solution of the ground state of the molecule H_2^+. One can also explicitly solve some typical R-matrix model problems, like well-potentials. The potential in the molecule H_2^+ system is produced by the attraction between the electron and the nuclei and also by the repulsion between the two nuclei. The repulsive potential is a constant when the distance between the nuclei is fixed and it can be omitted. Therefore, one has

$$V(\mathbf{r}) = -\frac{1}{r_1} - \frac{1}{r_2}, \tag{42}$$

where $\mathbf{r}$ is the electron position, and r_1 and r_2 are, respectively, the distances between the electron and the nuclei 1 and 2 (see Fig. 1). The region $z \leq 0$ is chosen as the environmental region. We choose two Slater-type basis functions $\{\Phi_1, \Phi_2\}$ as

$$\Phi_1(\mathbf{r}) = \exp(-\alpha r_1) \tag{43}$$

$$\Phi_2(\mathbf{r}) = \exp(-\alpha r_2)\,. \tag{44}$$

Φ_1 is centered on the hydrogen 1 and Φ_2 is on hydrogen 2; the α is a parameter. These two functions will be used as an approximate complete basis set to construct the $\mathbf{R}$ and $\mathbf{R}^{-1}$ matrices and also to do the linear variation of the energy functional. According to Eq. (15), in this basis set, the $\mathbf{R}^{-1}$-matrix can be written as

$$\begin{aligned}\mathbf{R}^{-1}(\mathbf{r}_s', \mathbf{r}_s, \varepsilon) = \frac{1}{2}\Bigg\{&\frac{\partial\Phi_1}{\partial n_s}(\mathbf{r}_s')\mathbf{A}_{11}^{-1}\frac{\partial\Phi_1}{\partial n_s}(\mathbf{r}_s) + \frac{\partial\Phi_1}{\partial n_s}(\mathbf{r}_s')\mathbf{A}_{12}^{-1}\frac{\partial\Phi_2}{\partial n_s}(\mathbf{r}_s)\\ &+ \frac{\partial\Phi_2}{\partial n_s}(\mathbf{r}_s')\mathbf{A}_{21}^{-1}\frac{\partial\Phi_1}{\partial n_s}(\mathbf{r}_s) + \frac{\partial\Phi_2}{\partial n_s}(\mathbf{r}_s')\mathbf{A}_{22}^{-1}\frac{\partial\Phi_2}{\partial n_2}(\mathbf{r}_s)\Bigg\},\end{aligned} \tag{45}$$

where the Nesbet matrix $\mathbf{A}$ is given by Eq. (16) in terms of this basis set, i.e.,

$$\mathbf{A}_{ij} = \int_{z\leq 0} d\mathbf{r}\left\{\frac{1}{2}\nabla\Phi_i \cdot \nabla\Phi_j + \Phi_i V\Phi_j - \varepsilon\Phi_i\Phi_j\right\},$$

where the potential is given by Eq. (42) and ε is treated as a parameter. More

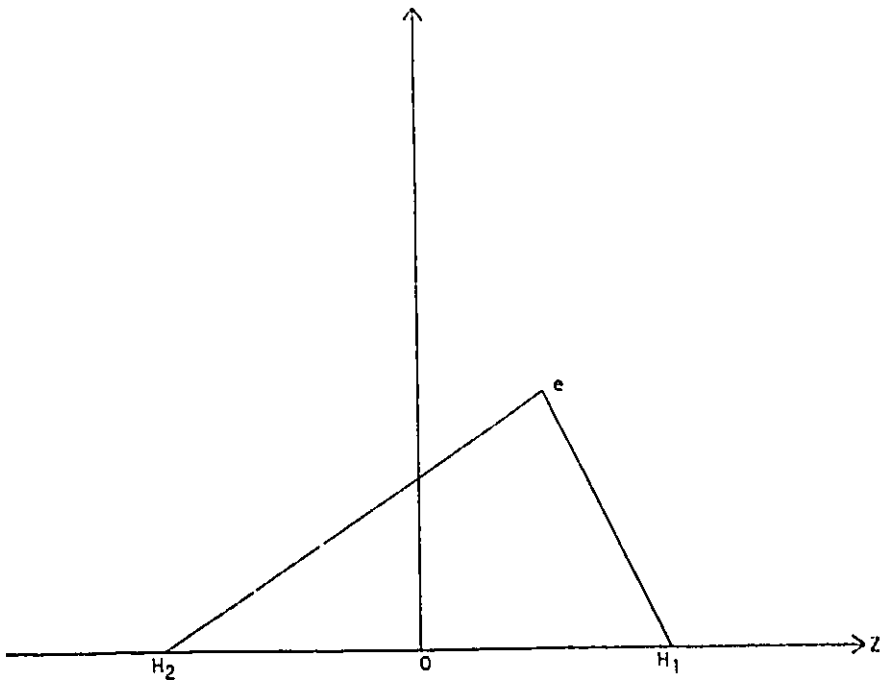

Figure 1. The coordinate system of H_2^+.

specifically, all the matrix elements of A can be obtained by using the integral formula given in Appendix 1:

$$A_{11} = \frac{\pi}{4\alpha}(1 + \alpha R)\exp(-2\alpha R) - \frac{\pi}{2\alpha^2}\exp(-2\alpha R)\left\{2 + \frac{1}{\alpha R} - 2\exp(-2\alpha R)\left(1 + \frac{1}{2\alpha R}\right)\right\} - \varepsilon\frac{4\pi}{(2\alpha)^3}(1 + \alpha R)\exp(-2\alpha R) \tag{46}$$

$$A_{12} = \pi\alpha R^2\exp(-2\alpha R)\left\{\frac{1}{2\alpha R} + \frac{1}{(2\alpha R)^2} - \frac{1}{3}\right\} - \frac{\pi R}{\alpha}\exp(-2\alpha R)\left\{2 + \frac{1}{\alpha R}\right\} - \varepsilon\frac{2\pi R^2}{\alpha}\exp(-2\alpha R)\left\{\frac{1}{3} + \frac{1}{2\alpha R} + \frac{1}{(2\alpha R)^2}\right\} \tag{47}$$

$$A_{22} = \frac{\pi}{4\alpha}\{2 - (1 + \alpha R)\exp(-2\alpha R)\} - \frac{\pi(1 + 2\alpha R)}{2\alpha^3 R}\{1 - \exp(-2\alpha R)\} - \varepsilon\frac{4\pi}{(2\alpha)^3}\{2 - (1 + \alpha R)\exp(-2\alpha R)\}, \tag{48}$$

where R is the distance between the center of the molecule to one of the hydrogens.

The derivative of $\mathbf{R}^{-1}$ to energy can be obtained from Eq. (38):

$$\frac{\partial \mathbf{R}^{-1}(\mathbf{r}_s', \mathbf{r}_s, \varepsilon)}{\partial \varepsilon} = \frac{1}{2}\left\{\frac{\partial \Phi_1}{\partial n_s}(\mathbf{r}_s')\mathbf{B}_{11}\frac{\partial \Phi_1}{\partial n_s}(\mathbf{r}_s) + \frac{\partial \Phi_1}{\partial n_s}(\mathbf{r}_s')\mathbf{B}_{12}\frac{\partial \Phi_2}{\partial n_s}(\mathbf{r}_s) + \frac{\partial \Phi_2}{\partial n_s}(\mathbf{r}_s')\mathbf{B}_{21}\frac{\partial \Phi_1}{\partial n_s}(\mathbf{r}_s) + \frac{\partial \Phi_2}{\partial n_2}(\mathbf{r}_s')\mathbf{B}_{22}\frac{\partial \Phi_2}{\partial n_s}(\mathbf{r}_s)\right\}, \quad (49)$$

where the matrix $\mathbf{B}$, which is defined in Eq. (36), can be obtained by using the matrix $\mathbf{A}$ given in Eqs. (46)–(48) and the overlap matrix $\mathbf{O}$ that can be easily obtained from the formulas given in Appendix 1. Since we choose the same basis set to construct the $\mathbf{R}$-matrix and to do the energy variation, the surface matrix $\mathbf{G}$ appearing in Eq. (40) can be written as

$$\mathbf{G}_{11} = \pi R \exp(-2\alpha R) \quad (50)$$

$$\mathbf{G}_{21} = \mathbf{G}_{11} = -\mathbf{G}_{12} = -\mathbf{G}_{22}. \quad (51)$$

With the results given in Eqs. (45)–(51) and the variational equation (41), one can solve for the energy of the system by requiring that the smaller one of the two eigenvalues, say ε_1, is equal to the parameter ε in the matrix $\mathbf{A}$. In this way, a total energy of -16.16 eV, which includes the nuclear–nuclear repulsion energy, is found when α and R are chosen, respectively, as the optimized value 1.24 and as the experimental value 1 au. This energy is lower than the usual variational energy of -15.96 eV for the total system but higher than the experimental value -16.39 eV. However, this result coincides with the symmetrized variational result -16.16 eV (see Appendix 2). Figure 2 shows that the eigenvalue ε_1 changes with parameter ε when the α and R are fixed to 1.24 and 1 au.

Although one can judge the accuracy of the present method, it is not easy to see the physical role of $\mathbf{R}^{-1}$ and $(\partial \mathbf{R}^{-1})/(\partial \varepsilon)$ using the above-constructed embedding potential. However, if one makes some reasonable approximation to the inverse of $\mathbf{R}$-matrix given in Eq. (20), one will clearly see an average interaction in the Hamiltonian from the environmental region $z \leq 0$ to the region $z \geq 0$. This interaction is actually from the result of the continuity conditions of the wave function on the boundary. According to Eq. (13) and in the basis set given in Eqs. (43) and (44), the $\mathbf{R}$-matrix can be written as

$$\mathbf{R}(\mathbf{r}_s, \mathbf{r}_s'; \varepsilon) = \frac{1}{2}\Phi_1(\mathbf{r}_s)\Phi_1(\mathbf{r}_s')\left(A_{11}^{-1} + 2A_{12}^{-1} + A_{22}^{-1}\right), \quad (52)$$

where we have used the fact that the two basis functions will be reduced to one function $\Phi_1(\mathbf{r}_s)$ on the surface. Therefore, the $\mathbf{R}^{-1}$ can be derived from this expression as

$$\mathbf{R}^{-1}(\mathbf{r}_s, \mathbf{r}_s', \varepsilon) = 2\mathcal{S}_{11}^{-2}\Phi_1(\mathbf{r}_s)\Phi_1(\mathbf{r}_s')\left(A_{11}^{-1} + 2A_{12}^{-1} + A_{22}^{-1}\right)^{-1}, \quad (53)$$

where $\mathcal{S}_{11}$ is a surface overlap integral that can be found from formulas in Appendix 1. As an approximation, one has

$$\mathbf{R}^{-1}(\mathbf{r}_s, \mathbf{r}_s'; \varepsilon) \simeq 2\mathcal{S}_{11}^{-2}\Phi_1(\mathbf{r}_s)\Phi_1(\mathbf{r}_s')\left(A_{11} + 2A_{12} + A_{22}\right). \quad (54)$$

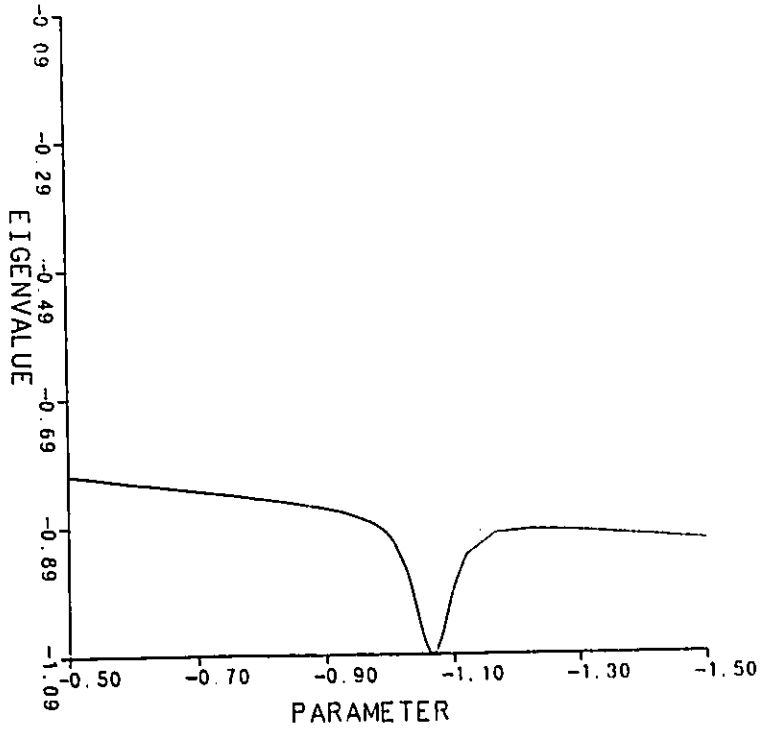

Figure 2. The change of the eigenvalue ε_1 with the parameter ε.

Therefore, the energy derivative of $\mathbf{R}^{-1}$ can be written as

$$\frac{\partial \mathbf{R}^{-1}}{\partial \varepsilon}(\mathbf{r}_1, \mathbf{r}_1'; \varepsilon) = -2\mathcal{S}_{11}^{-2}\Phi_1(\mathbf{r}_1)\Phi_1(\mathbf{r}_1')\,(\mathbf{O}_{11} + 2\mathbf{O}_{12} + \mathbf{O}_{22})\,, \tag{55}$$

where $\mathbf{O}_{ij}$ is the volume overlap integral

$$\mathbf{O}_{ij} = \int_{z\leq 0} \Phi_i \Phi_j d\mathbf{r}\,. \tag{56}$$

The matrix elements of $\mathbf{R}^{-1}$ and $\partial/(\partial\varepsilon)\mathbf{R}^{-1}$ are

$$(\mathbf{R}^{-1})_{ij} = 2(A_{11} + 2A_{12} + A_{22}) \tag{57}$$

$$\left(\frac{\partial}{\partial \varepsilon}\mathbf{R}^{-1}\right)_{ij} = -2(S_{11} + 2S_{12} + S_{22})\,. \tag{58}$$

Therefore, the embedding potential contribution to the linear variational matrix elements from the region $z \leq 0$ is

$$(\mathbf{R}^{-1})_{ij} - \varepsilon\left(\frac{\partial}{\partial \varepsilon}\mathbf{R}^{-1}\right)_{ij} = 2(H_{11} + 2H_{12} + H_{22})\,, \tag{59}$$

where the environmental Hamiltonian matrix H is given in Eq. (60):

$$H_{ij} = \int_{z\leq 0} d\mathbf{r}\left\{\frac{1}{2}\nabla\Phi_i \cdot \nabla\Phi_j + \Phi_i V\Phi_j\right\}. \tag{60}$$

By solving the linear variational equation, the energy -15.95 eV is found. This result is very close to the above "accurate" result and also close to the experimental and usual variational values. In the above approximation, one can see that the embedding potential given in Eq. (59) is equal to the summation of the Hamiltonian in the environmental region $z \leq 0$. This average result comes from approximating Eq. (53) by Eq. (54). However, this demonstrates that the effective potential given by this regional embedding method has some kind of average meaning and represents the interaction between regions.

The application of this embedding method to the molecule H_2^+ shows that the effective interaction between a region and its environment can be produced by choosing an appropriate analytical basis set to represent the R-matrix and its inverse. This effective interaction is produced from the continuity conditions of the wave function and its derivative on the surface. The accuracy given in the above example shows that there is no reason that the new embedding method cannot be applied to some more realistic and complex systems. There are obvious applications of this method to solving surface electronic structure problems and to calculating chemical adsorption energy on a surface. In these cases, one may divide the system into the surface and interior regions. The R-matrix and its inverse can be obtained for a similar system, like the corresponding crystal or some other appropriate approximation, and then if one uses the density functional potential, one would be able to use Eq. (41) to solve for the energy of the system. Inglesfield's Green's function method is similar to this R-matrix approach except that Inglesfield's method requires that the Green's function satisfy the zero derivative boundary condition and the R-matrix method allows any geometry surface. The success of Inglesfield's approach shows that this R-matrix procedure may be appropriate and efficient as a tool in solving the surface problems. Another way in which one can use this method is to study the electronic structure change within the density functional framework when an atom or a group in a large molecule is replaced by another. For example, the group ACH_2- in the molecule ACH_2-R is replaced by a new group BCH_2-. One can use the information in the molecule ACH_2-R to obtain the $\mathbf{R}^{-1}$-matrix and its energy derivative for the group $R-$ and then use this information to calculate the embedding potential in the new molecule BCH_2-R. In the local density functional approximation, the application to find the environmental group effect is straightforward. However, the computational implementation of this approach in a general case remains to be developed.

Acknowledgments

The author acknowledges Professor R. F.W. Bader for suggesting the problem and for many stimulating discussions.

Appendix 1

The following integrals can be obtained by choosing illiptic coordinates. The atoms are arranged as in Figure 1 and R is the distance between the center and one of the hydrogens:

$$\int_{z\le 0} \exp(-\alpha r_2)\, d\mathbf{r} = \frac{2\pi}{\alpha^3}\left\{4 - (2 + \alpha R)\exp(-\alpha R)\right\} \tag{A.1.1}$$

$$\int_{z\le 0} \exp(-\alpha r_1)\, d\mathbf{r} = \frac{2\pi}{\alpha^3}(2 + \alpha R)\exp(-\alpha R) \tag{A.1.2}$$

$$\int_{z\le 0} \exp\{-\alpha(r_1 + r_2)\}\, d\mathbf{r} = \frac{2\pi R^2}{\alpha}\exp(-2\alpha R)\left\{\frac{1}{3} + \frac{1}{2\alpha R} + \frac{1}{(2\alpha R)^2}\right\} \tag{A.1.3}$$

$$\int_{z\le 0} \frac{\exp(-\alpha r_1)}{r_1} d\mathbf{r} = \frac{2\pi}{\alpha^2}\exp(-\alpha R) \tag{A.1.4}$$

$$\int_{z\le 0} \frac{\exp(-\alpha r_2)}{r_1} d\mathbf{r} = \frac{2\pi}{\alpha^3 R}\left\{2 - (2 + \alpha R)\exp(-\alpha R)\right\} \tag{A.1.5}$$

$$\int_{z\le 0} \frac{\exp\{-\alpha(r_1 + r_2)\}}{r_1}) d\mathbf{r} = \frac{\pi R}{2\alpha}\exp(-2\alpha R)\left\{1 + \frac{1}{\alpha R}\right\} \tag{A.1.6}$$

$$\int_{z\le 0} \frac{\exp(-\alpha r_1)}{r_2} d\mathbf{r} = \frac{2\pi}{\alpha^2}\exp(-\alpha R)\left\{1 + \frac{2}{\alpha R} - 2\exp(-\alpha R)\left(1 + \frac{1}{\alpha R}\right)\right\} \tag{A.1.7}$$

$$\int_{z\le 0} \frac{\exp(-\alpha r_2)}{r_2} d\mathbf{r} = \frac{2\pi}{\alpha^2}\{2 - \exp(-\alpha R)\} \tag{A.1.8}$$

$$\int_{z\le 0} \frac{\exp\{-\alpha(r_1 + r_2)\}}{r_2} d\mathbf{r} = \frac{\pi R}{2\alpha}\exp(-2\alpha R)\left\{3 + \frac{1}{\alpha R}\right\} \tag{A.1.9}$$

$$\int_{z=0} \exp(-\alpha r_2)\, d\mathbf{r}_1 = \frac{2\pi}{\alpha^2}\exp(-\alpha R)\{1 + \alpha R\} \tag{A.1.10}$$

$$\int_{z=0} \exp(-\alpha r_2)\frac{\partial}{\partial z}\exp(-\alpha r_2)\, d\mathbf{r}_1 = -\pi R\exp(-2\alpha R)\,. \tag{A.1.11}$$

Appendix 2: The Symmetrized Variation

In this appendix, we describe an energy variational method in which the trial function is symmetrized before the energy functional is varied. The surprising result of this approach is that one can obtain a lower-energy result than the usual variational method using the same basis set. The symmetrized trial function of H_2^+ can be written as

$$\Psi_g(\mathbf{r}) = \begin{cases} c_1\Phi_1(\mathbf{r}) + c_2\Phi_2(\mathbf{r}) & z \ge 0 \\ c_1\Phi_2(\mathbf{r}) + c_2\Phi_1(\mathbf{r}) & z \le 0\,, \end{cases} \tag{A.2.1}$$

where the coordinate system is chosen as in Figure 1. One obvious solution for c_1 and c_2 is $c_1 = c_2$; this is the usual variational result. However, c_1 and c_2 are not necessarily equal in this variation. In this trial function, the energy can be written as

$$E[\Psi_g] = \frac{\mathcal{H}[\Psi_g]}{O[\Psi_g]}, \tag{A.2.2}$$

where the Hamiltonian $\mathcal{H}[\Psi_g]$ is written as

$$\mathcal{H}[\Psi_g] = \frac{1}{2}\int \nabla\Psi_g \cdot \nabla\Psi_g d\mathbf{r} + \int \Psi_g^2 V(\mathbf{r})\, d\mathbf{r}$$

$$= 2\left\{\frac{1}{2}\int_{z\le 0} \nabla\Psi_g \cdot \nabla\Psi_g d\mathbf{r} + \int_{z\le 0} \Psi_g^2 V(\mathbf{r})\, d\mathbf{r}\right\},$$

and the overlap integral as

$$O[\Psi_g] = \int \Psi_g^2 d\mathbf{r} = 2\left\{\int_{z\le 0} \Psi_g^2 d\mathbf{r}\right\}.$$

Therefore, one has

$$E[\Psi_g] = \frac{\left\{\frac{1}{2}\int_{z\le 0} \nabla\Psi_g \cdot \nabla\Psi_g d\mathbf{r} + \int_{z\le 0} \Psi_g^2 V(\mathbf{r})\, d\mathbf{r}\right\}}{\left\{\int_{z\le 0} \Psi_g^2 d\mathbf{r}\right\}}. \tag{A.2.3}$$

Inserting Eq. (A.2.1) into $E[\Psi_g]$, one has

$$E[\Psi_g] = \frac{c_{22}^2 H_{11} + 2c_1c_2H_{12} + c_1^2 H_{22}}{c_{22}^2 S_{11} + 2c_1c_2S_{12} + c_1^2 S_{22}}, \tag{A.2.4}$$

where

$$S_{ij} = \int_{z\le 0} \Phi_i \Phi_j d\mathbf{r}$$

$$H_{ij} = \frac{1}{2}\int_{z\le 0} \nabla\Phi_i \cdot \nabla\Phi_j d\mathbf{r} + \int_{z\le 0} \Phi_i \Phi_j V(\mathbf{r})\, d\mathbf{r}.$$

After one varies the coefficients $\{c_1, c_2\}$ in (A.2.4), one obtains a secular equation and then solves it to yield the energy of the system. We choose the Slater basis set given in Eqs. (43) and (44), with α and R chosen as 1.24 and 1 au, respectively. This yields an eigenvalue $\varepsilon_1 = -1.09376$ au. This eigenvalue yields a total energy for H_2^+ of -16.16 eV. The energy obtained here is higher than the experimental value but lower than the usual variational result.

Bibliography

[1] R. F.W. Bader, *Atoms in Molecules: A Quantum Theory* (Oxford University Press, Oxford, 1990); R. F.W. Bader, A. Larouche, C. Gatti, P. J. MacDougall, and K. B. Wiberg, J. Chem. Phys. **87**, 1142 (1987).

[2] R. K. Nesbet, Phys. Rev. A **38**, 4955 (1988); *Ibid.*, Phys. Rev. B **33**, 8027 (1986).
[3] J. E. Inglesfield and G. A. Benesh, Phys. Rev. B **37**, 6682 (1988).
[4] J. M. MacLaren, S. Crampin, and D. D. Vvedensky, Phys. Rev. B **40**, 12176 (1989).
[5] C. E. Dykstra and B. Kirtman, Annu. Rev. Phys. Chem. **41**, 155 (1990).
[6] A. Auerbach, S. Kivelson, and D. Nicole, Phys. Rev. Lett. **53**, 411 (1984).
[7] L. Dobrzynski, Surf. Sci. Rep. **11**, 139 (1990).
[8] F. Webster and J. C. Light, J. Chem. Phys. **90**, 265 (1989) and references cited therein.
[9] E. P. Wigner and L. Eisenbud, Phys. Rev. **72**, 29 (1947).
[10] A. M. Lane and R. G. Thomas, Rev. Mod. Phys. **30**, 257 (1958).
[11] P. G. Burke and W. D. Robb, Adv. At. Mol. Phys. **11**, 143 (1975).
[12] H. Schlosser and P. Marcus, Phys. Rev. **131**, 2529 (1963).
[13] L. G. Ferreira and J. R. Leite, Phys. Rev. A **18**, 335 (1978).
[14] P. E. Bjorstad and O. B. Widlund, SIAM J. Numer. Anal. **23**, 1097 (1986).

Received February 25, 1992
Revised manuscript received May 21, 1992
Accepted for publication June 3, 1992

3. Topological Structures of the Charge Density of Crystals

Since every solid substance contains parts that are crystalline, and since in many of them the whole is an aggregation of crystals, it will be readily understood that a knowledge of crystal structure often affords an explanation of the properties of the substance.

——Sir William Bragg, *The Universe of Light*

3.1 Introduction

Most of industrial materials are solids, and many of them contain repeating physical units, and therefore can be classified as crystals. The repeating unit cell is extremely small, typically 10 angstroms on a side, whereas the sides of crystals in a powder may be 1000 to 100,000 times larger, and in general a crystal contains in the order of 10^{23} atoms. The disparity in size between a unit cell and a crystal is so vast that we can model a crystal as if it contained an infinite number of unit cells in all directions.

This is the crystal model that we are going to accept for the description of solids even though real solids are almost always have a variety of defects and impurities.

Crystals are often empirically classified by their properties, for example conductivity, hardness or magnetism. This empirical classification is a reflection of the nature of the bonding which holds the chemical atoms or molecules together in a crystal. Essentially five types of solids can be distinguished according to the nature of the bonding between the atoms in the crystals. These are ionic, covalent, metallic, molecular and hydrogen-bonded crystals. The physical and chemical properties of a crystal are determined by the atoms or chemical groups, the bonds, and the arrangements of these two structure elements in space. In experiment, the geometrical positions of the nuclei in a crystal are directly measured. The structure for the crystal is obtained by empirically assigning bonds between the nuclei. Rings and cages, which are deduced from the arrangement of the nuclei and bonds in real space, always exist in crystals but not always in molecules. The appearance of rings and cages not only makes a crystal structure complex, but also accompanies a variety of fascinating properties for the crystal. For example, diamond is an insulator, and another form of carbon called γ-C, which has a face-centered cubic structure, is a conductor (Palatnik, et al, 1984) and was considered to be likely a candidate of high-T_c superconducting materials (Kvam, 1991).

The concepts of an atom, bond, ring and cage play the central role in the understanding of crystal properties. However, the rigorous definitions of these structural elements have not been established for the solid systems. Yet, the corresponding topological theory of molecular structure has been

developed for more than a decade (Bader, Nguyen-Dang and Tal, 1981). This chapter aims to extend the topological theory for the molecular systems to crystals. The theory is based on the topological analysis of experimentally measurable electronic charge density in a molecule or a crystal and provides unique definitions and precise meanings for the elements of the molecular and crystalline structures: atoms, bonds, rings and cages.

Since the establishment of the topological theory of molecular structure, the theory has been successfully used to provide the basis for many classical chemical models (Bader, MacDougall and Lau, 1984; Bader, 1990). These include the Lewis' model of localized pairs of electrons (Lewis, 1916) and the valence shell electron pair repulsive (VSEPR) model of molecular geometry (Gillespie, 1957 and 1972). Many other molecular properties have been related to the topological properties of the charge density (see, for example, Bader's book: *Atoms in Molecules - A quantum Theory*, 1990). We can expect that the topological theory of crystal structure will play a similar role in qualitatively understanding the chemical and physical properties of solids, identifying the nature of the bonding in crystals, on surfaces or defects, and predicting the chemical and physical behavior of electrons, atoms or chemical groups in a crystal. In a recent study, Eberhart, et al, (1991) used the topological bonding concept to identify the second neighbor bonds in bcc metals and successfully predict the structural selection between bcc or fcc structures for a metal. In another study (Eberhart, et al, 1992), Eberhart and his co-workers have shown that the the difference in diffusivity of O through Cu, Ag and Au can be consistently explained by associating the curvature of the charge density at the bond critical point normal to the inter

nuclear axis with the barrier to oxygen diffusion. A very interesting and important application of the topological theory of the charge density will be in the study of surface charge distribution. For example, there are 7×7 and 2×1 reconstructed structures for Si (111) surface. The bonds between the surface atoms are considered to play the central role in the reconstruction. Conventionally the dangling bond model is used to explain surface structures. This theory may not only provide a basis to the dangling bond model but also give precise nature of the bonding.

The organization of this chapter is as follows. In section 2, we give the rigorous mathematical definition for a crystal and its logical consequence to a single particle wave function—Bloch's theorem. The principles for the determinations of the charge density by both theoretical and experimental methods are also reviewed in this section. The geometrical structures of diamond and zinc-blende are given in section 3. This section points out the role of boat and chair conformations of a six-atom ring in the construction of a crystal structure. This role is applied to a discussion of the relative stability of diamond and hexagonal diamond (lonsdaleite). In section 4, the central ideas of the topological analysis of the charge density are given and the topological rule for a crystal—Poincaré-Hopf relationship for an infinite system——is established. In section 5, the electronic charge density structures of diamond, silicon, and zinc-blende structural compounds: AlP, BN, BP and SiC are explored in terms of the scalar fields $\rho(\mathbf{r})$ and $\nabla^2\rho$ and the gradient vector field $d\mathbf{r}/ds=\nabla\rho(\mathbf{r})$. Correlations between the physical properties (bulk modulus, transverse optical frequencies and binding energy) and the topological

properties at the critical points are developed in section 6. In the last section, the weak bonds in crystals are investigated in terms of the developed topological theory.

3.2 Principles of the Determination of the Charge Density of a Crystal—— ab initio Hartree-Fock and Experimental Methods

3.2.1. Crystals and the Bloch Theorem

A crystal is an idealized material state in which the atoms are periodically arranged in three-dimensional real space. Any crystal can be classified into one of 230 space groups (Koster, 1957; Lax, 1974; Burns and Glazer, 1990) even though there exists an infinite number of arrangements for the atoms in crystals. If the basic repeating unit or pattern (called primitive unit cell (Kittel, 1986)) is abstracted as a point in real space, conventionally called a lattice point, then these periodically arranged points can be classified into one of the 14 Bravais lattices. Mathematically the three dimensional lattice can be spanned by three linear independent vectors $\mathbf{a}_1$, $\mathbf{a}_2$ and $\mathbf{a}_3$

$$\mathbf{R}_n = n_1\mathbf{a}_1 + n_2\mathbf{a}_2 + n_3\mathbf{a}_3 \qquad (1)$$

where the n_i are integers. Physically all the lattice points in a crystal are equivalent, therefore any translation from one lattice point to another will leave the crystal unchanged. All of the translations define a group, called translational group $\mathcal{T}$. An operation $\mathcal{T}_n$ of the group $\mathcal{T}$ is defined by

$$\mathcal{T}_n(\mathbf{r}) = \mathbf{r} + \mathbf{R}_n \qquad (2)$$

If the periodic Born-von Karman boundary conditions are introduced, $\mathcal{T}$ becomes a cyclic group which is the direct product of three cyclic groups of order M, M being an arbitrarily large but fixed integer. The projection operators for

the irreducible one-dimensional representations of the group $\mathcal{T}$ are of the form

$$O(\mathbf{k}) = N^{-1/2} \sum_n exp(i\mathbf{k}\cdot\mathbf{R}_n)\mathcal{T}_n \qquad (3)$$

where $N = M^3$ and the general "reciprocal space vector (or point)" $\mathbf{k}$ belongs to a net of vectors, which reproduces the reciprocal lattice shrunk by a factor M. That is, if $\mathbf{B}_i$ are the fundamental reciprocal lattice vectors, related to the direct lattice fundamental vectors $\mathbf{a}_j$ by relation:

$$\mathbf{B}_j\cdot\mathbf{a}_i = 2\pi\delta_{ij} \quad (i,j = 1,2,3) \qquad (4)$$

then the $\mathbf{k}$ vectors, called the wave vector or propagation constant, are of the form

$$\mathbf{k} = 1/M\ (n_1\mathbf{B}_1 + n_2\mathbf{B}_2 + n_3\mathbf{B}_3) \qquad (5)$$

with integer n_i. It follows from the definition that projection operators are equivalent if they refer to $\mathbf{k}$ vectors that differ by a reciprocal lattice vector $\mathbf{K} = (i_1\mathbf{B}_1 + i_2\mathbf{B}_2 + i_3\mathbf{B}_3)$ with integer i_j. The set $\{\mathbf{k} \mid \mathbf{k} = 1/M\ (n_1\mathbf{B}_1 + n_2\mathbf{B}_2 + n_3\mathbf{B}_3)$ with $0 \le n_i < M\}$ is called the first Brillouin Zone of the representation, this set is also the Wigner-Seitz cell of reciprocal space.

By applying the projection operator $O(\mathbf{k})$ to an atomic basis $\varphi_\alpha(\mathbf{r})$ in the reference lattice point (0, 0, 0), a Bloch function Φ_α is generated that belongs to the $\mathbf{k}$-th irreducible representation of $\mathcal{T}$

$$\Phi_\alpha(\mathbf{k},\mathbf{r}) = N^{-1/2} \sum_n exp(i\mathbf{k}\cdot\mathbf{R}_n)\varphi_\alpha(\mathbf{r}-\mathbf{R}_n) \qquad (6)$$

where the summation is over all the N lattice points. From equation (6), we can see that

$$\Phi_\alpha(\mathbf{k},\mathbf{r}+\mathbf{R}_n) = exp(i\mathbf{k}\cdot\mathbf{R}_n)\ \Phi_\alpha(\mathbf{k},\mathbf{r}) \qquad (7)$$

Since $\Phi_\alpha(\mathbf{k},\mathbf{r})$ is an irreducible representation of the translational group $\mathcal{T}$,

the single particle wave function can be written as the linear combination of the functions of the same irreducible representation

$$\psi(\mathbf{k},\mathbf{r}) = \sum_{\alpha} c_{\alpha}\Phi_{\alpha}(\mathbf{k},\mathbf{r}) \tag{8}$$

where the summation is over the atomic basis in a unit cell. By eqn (7), we have

$$\psi(\mathbf{k},\mathbf{r}+\mathbf{R}_n) = exp(i\mathbf{k}\cdot\mathbf{R}_n)\ \psi(\mathbf{k},\mathbf{r}) \tag{9}$$

Equation (9) is the mathematical expression of the famous Bloch theorem, which states that one may write the solutions of the periodic potential problem in such a form that the value of the function, at a given point of the unit cell which is displaced from a given unit cell by the vector $\mathbf{R}_n$, equals the value of that function at the corresponding point of the undisplaced unit cell, multiplied by the factor $exp(i\mathbf{k}\cdot\mathbf{R}_n)$, where $\mathbf{k}$ is a real constant vector, called the crystal momentum because it is a natural extension of $\mathbf{p}/\hbar$ (Burns, 1985). This theorem is a direct result of the fact that the translational operations of group $\mathcal{T}$ commute with the Hamiltonian of the crystalline system, and eqn (8) states that the wave function chosen in this way simultaneously diagonalizes all the translational operations, as well as the Hamiltonian.

3.2.2 Hartree-Fock Method and Its Determination of Charge Density $\rho(\mathbf{r})$

As stated in the eqn (8), the single-particle state can be chosen as one of the irreducible representations of the translation group $\mathcal{T}$ of the crystal. Therefore the many-particle wave function can be approximated by a single Slater determinant

$$\Psi = \sum \nu_p \hat{P} \left\{ \prod_{k_i} \psi_1(k_1, x_{k_1}) \psi_2(k_2, x_{k_2}) \cdots \psi_n(k_n, x_{k_n}) \right\} \tag{10}$$

where x represents a spin-space coordinates, $\psi_i(k_i, x_{k_i})$ is the i-th band single-particle state, $\prod_{k_i}$ denotes the product of the occupied states with different k values in the corresponding band, and the summation is over all the permutations ($\hat{P}$) of the electrons, ν_p is -1 if $\hat{P}$ is a odd permutation else +1. The true many-electron states can be obtained through the configuration interaction technique, that is the linear combination of Slater determinants.

Assuming the orthogonal relation

$$\int \psi_i^*(k,x) \psi_j(k',x)\, dx = \delta(k-k')\delta_{ij} \tag{11}$$

With the constraint eqn(11), the variation of $E=\langle\Psi|\hat{H}|\Psi\rangle$ yields the Hartree-Fock equation

$$\hat{F}(k)\psi_i(k,x) = \varepsilon_i(k)\psi_i(k,x) \tag{12}$$

where $\hat{F}(k)$ is the Fock operator defined by

$$\hat{F}(k) = \hat{h} + \hat{V}_e^c - \hat{V}_e^e(k) \tag{13}$$

where $\hat{h}$ is the single particle operator including the kinetic and electron-nuclear attraction operators, $\hat{V}_e^c$ is coulomb electron-electron repulsion operator, and $\hat{V}_e^e(k)$ is the exchange operator.

$\psi_i(k,x)$ can be expanded as the linear combination of Bloch functions

$$\psi_i(k,x) = \sum_\alpha c_{i\alpha} \Phi_\alpha(k,x) \tag{14}$$

where the Bloch function $\Phi_\alpha(\mathbf{k},\mathbf{r})$ can be constructed from the atomic basis functions. Inserting eqn(14) into the Hartree-Fock equation and varying the coefficients $c_{i\alpha}$ yields the Hartree-Fock-Roothaan equation

$$F(\mathbf{k})\ \mathbf{c}_i = \varepsilon_i(\mathbf{k})S(\mathbf{k})\mathbf{c}_i \tag{15}$$

where $F(\mathbf{k})$, $S(\mathbf{k})$ are, respectively, the Fock and overlap matrices with the Bloch functions $\{\Phi_\alpha(\mathbf{k},\mathbf{r})\}$ as the basis, and $\mathbf{c}_i$ and $\varepsilon_i(\mathbf{k})$ are eigenvectors and eigenvalues of Hartree-Fock-Roothaan equation. The i-th energy band is constructed from all of the eigenvalues $\{\varepsilon_i(\mathbf{k})\}$ with the $\mathbf{k}$ values of the first Brillouin zone.

After the Hartree-Fock-Roothaan equations are solved, the charge density is constructed as

$$\rho(\mathbf{r}) = \sum_i^{occ} \int d\sigma \int_{\varepsilon_i(k)\le\varepsilon_F} d\mathbf{k}\ \psi_i(\mathbf{k},\mathbf{x})\psi_i^*(\mathbf{k},\mathbf{x}) \tag{16}$$

where the summation is over the occupied bands, the integral $\int d\sigma$ is over the spin component, and the other integral is over the reciprocal regime in the first Brillouin zone for those $\mathbf{k}$ that the eigenvalue $\varepsilon_i(\mathbf{k})$ is less than the Fermi energy ε_F. If we assume every single-particle state $\psi_i(\mathbf{k},\mathbf{r})$ is occupied by two electrons with opposite spin, then we can integrate out the spin part of eqn(16). This yields

$$\rho(\mathbf{r}) = 2\sum_i^{occ} \int_{\varepsilon_i(k)\le\varepsilon_F} d\mathbf{k}\ \psi_i(\mathbf{k},\mathbf{r})\psi_i^*(\mathbf{k},\mathbf{r}) \tag{17}$$

Inserting eqn (14) into the density expression eqn(17) and noting that the Bloch functions are constructed by the atomic basis functions (eqn(6)) yields

$$\rho(\mathbf{r}) = \sum_{gl} \sum_{\alpha\beta} P_{\alpha\beta}^{g-l} \varphi_\alpha(\mathbf{r}-\mathbf{R}_g) \varphi_\beta^*(\mathbf{r}-\mathbf{R}_l) \qquad (18)$$

where the first summation is over the lattice points, the second one is over the atomic basis functions in a cell, and $P_{\alpha\beta}^{g-l}$ is the density matrix given by

$$P_{\alpha\beta}^{g-l} = 2N^{-1} \sum_{i}^{occ} \int_{\varepsilon_i(k)\le\varepsilon_F} d\mathbf{k}\ c_{i\alpha}(\mathbf{k}) c_{i\beta}^*(\mathbf{k})\ exp(i\mathbf{k}\cdot(\mathbf{R}_l-\mathbf{R}_g)) \qquad (19)$$

3.2.3 Details of the Calculations

In this chapter and next chapter we will concentrate on the studies of the crystal systems: diamond, silicon and zinc blende compounds: AlP, BN, BP, and SiC. The experimental lattice parameters listed in the second column of table 3-1 are used in the determinations of the charge density for these crystals. The charge densities are calculated from program CRYSTAL 88 (Dovesi, Pisani, Roetti, Causà and Saunders, 1989). The Gaussian type functions {1(s-type); x,y,z(p-type); x^2,y^2,z^2,xy,yz(d-type)} $exp(-\alpha r^2)$ are used to contract the atomic basis sets. The basis set 621G* (Hehre, et al, 1986; Orlando, et al, 1990) is adopted in the calculations. In this basis set, 6 Gaussian functions are used to represent the atomic core, two valence orbitals for an atom are used: one is expressed in terms of two Gaussian functions, the other of one Gaussian function. The star in the notation 621G* denotes the inclusion of a d-type Gaussian functions for the calculation. The standard Gaussian exponentials and expansion coefficients (Hehre, et al, 1986) for the core atomic orbitals are used. The Gaussian exponentials and expansion coefficients for the valence orbitals including the d orbital are listed in Table 3-1. These basis sets have been shown to yield good optimized geometry, binding energy (Orlando, et al, 1990).

Table 3-1 the Experimental Lattice Parameter a and the valence Basis Sets Used in the Calculations (Orlando, et al, 1990).

System	a (Å)	α(sp)	c(s)	c(p)	α(sp)	α(d)	
C[a]	3.567	3.6645,0.77054	-0.39590,1.2158	0.23646,0.86062	0.226	0.8	
BN[a]	3.615	2.2819,0.46525	-0.36866,1.1994	0.23115,0.86676	0.197	0.8	B
		5.4252,1.1491	-0.41330,1.2244	0.23797,0.85895	0.297	0.8	N
SiC[b]	4.360	3.6650,0.77054	-0.39590,1.2158	0.23646,0.86062	0.184	0.8	C
		1.0791,0.30242	-0.37611,1.2516	0.067103,0.95688	0.180	0.5	Si
BP[a]	4.528	2.2819,0.46525	-0.36866,1.1994	0.23115,0.86676	0.140	0.8	B
		1.2186,0.39555	-0.37150,1.2710	0.091582,0.93492	0.160	0.43	P
Si[a]	5.431	1.0791,0.30242	-0.37611,1.2516	0.067103,0.95688	0.130	0.5	
AlP[a]	5.451	1.164,0.268	-0.17574,0.25280	-0.0021333,0.009958	0.110	0.37	Al
		1.2186,0.39555	-0.37150,1.2710	0.09158,0.93492	0.151	0.48	P

(a) The lattice parameter a is from Weast, Astle and Beyer (1987).

(b) The lattice parameter is from Chang and Cohen (1987).

3.2.4 X-Ray Diffraction Method for the Determination of the Charge Density

Let $\rho(\mathbf{r})$ be the charge density of scattering matter at point $\mathbf{r}=(x,y,z)$ of the crystal, the axes being parallel to the primitive translations **a**, **b**, and **c**, and not necessarily rectangular. The periodic distances are a, b, and c, respectively, in direction **a**, **b**, and **c**. Generally, any periodic function, say T(x), can be expanded in the basis set $\{\exp(-2\pi inx/a),\ n=0, \pm1, \pm2,\ldots\}$ in the form of eqn (20)

$$T(x) = \sum_{-\infty}^{\infty} \{c_n \exp(-2\pi inx/a)\} \qquad (20)$$

The coefficients $\{c_n\}$ can be obtained through the orthogonal relations

$$\int_0^a dx \exp(2\pi imx/a) = a\delta_{m0} \qquad (21)$$

Therefore one has

$$c_n = a^{-1}\int_0^a dx \exp(2\pi i n x/a) T(x) \qquad (22)$$

One has a similar equation for the three-dimensional periodic charge density function $\rho(\mathbf{r})$

$$\rho(\mathbf{r}) = \sum_{-\infty}^{\infty}\sum_{-\infty}^{\infty}\sum_{-\infty}^{\infty} \{c_{hkl}\exp(-2\pi i(hx/a + ky/b + lz/c)\} \qquad (23)$$

where the coefficient c_{hkl} is given by

$$c_{hkl} = (abc)^{-1}\int_0^a\int_0^b\int_0^c dxdydz\rho(\mathbf{r})\exp(2\pi i(hx/a + ky/b + lz/c)) \qquad (24)$$

For rectangular coordinates, the volume element dv is dxdydz, and for non-rectangular lattices, x,y,z can be expressed as the linear combinations of the rectangular coordinates, therefore dv= Cdxdydz, where C is a constant. So eqn (24) can be expressed in terms of the volume element

$$c_{hkl} = (V)^{-1}\int_\Omega dv\rho(\mathbf{r})\exp(2\pi i(hx/a + ky/b + lz/c)) \qquad (25)$$

where we have used the fact that the volume of the unit cell is V=Cabc, and the integral is over the unit cell.

The scattering factor or amplitude of a crystal is defined by

$$F_{hkl} = \int_\Omega dv\rho(\mathbf{r})\exp(2\pi i(hx/a + ky/b + lz/c)) \qquad (26)$$

From this definition of the scattering factor, we have

$$c_{hkl} = (V)^{-1}F_{hkl} \qquad (25a)$$

Therefore the charge density is related to the diffraction factors by the Fourier transformation

$$\rho(\mathbf{r}) = V^{-1} \sum_{-\infty}^{\infty} \sum_{-\infty}^{\infty} \sum_{-\infty}^{\infty} \{F_{hkl} \exp(-2\pi i(hx/a + ky/b + lz/c)\} \qquad (27)$$

Experimentally, the scattering cross sections, which are proportional to the $|F_{hkl}|^2$, are measured. There are three problems regarding the use of eqn (27) to obtaining the charge density. The first is the famous phase problem. That is one can know the absolute value of F_{hkl} but not the phase. As far as the author knows, this problems can be solved in three ways. The first way is to use the free atomic models to estimate the phases and do the least square fitting between the model and experimental F_{hkl}. The second way is the so called direct method (Hauptman, 1972; Srinivasan and Parthasarathy, 1976) which makes use of point charge model and the structure invariance and seminvariance of the phase relationships. The third way is to use the model we propose in chapter 4 which takes the atomic size and shape into consideration. The other two problems for the use of eqn (27) are the finite number of F_{hkl} and their imperfection which is due to the errors of experiments. By the Bragg law,

$$2d(hkl)\sin\theta = \lambda \qquad (28)$$

where $d(hkl)$ is the spacing between two adjacent planes of a set (hkl), we have

$$\frac{\sin\theta}{\lambda} = \frac{1}{2d(hkl)} \leq \frac{1}{\lambda} \qquad (29)$$

Therefore the number of (hkl) is limited for a fixed X-ray wavelength λ. With this limitation, the charge density determined from X-ray is

$$\rho^{E}(\mathbf{r}) \cong V^{-1} \sum_{exp} \{F_{hkl} \exp(-2\pi i(hx/a + ky/b + lz/c)\} \qquad (30)$$

where the summation is over the measured the structure factors. It is obvious that the charge density estimated in this way will not be necessarily positive.

Recently, a maximum entropy method (Collins, 1982; Sakata and Sato, 1990; Sato, 1992) has been developed to obtain the electron density from the experimental structure factors. This method provides the most unbiased representation of a system for a given finite and imperfect set of experimental data. By maximizing functional $Q[\rho(\mathbf{r})]$ with respect to $\rho_n(\mathbf{r})$

$$Q = -\sum_{\mathbf{r}} \rho'_n(\mathbf{r}) \ln[\rho'_n(\mathbf{r})/\rho'_{n-1}(\mathbf{r})] - \frac{\lambda'}{2} \sum_{hkl} |F_{hkl} - F^{n-1}_{hkl}|^2/\sigma^2_{hkl} \qquad (32)$$

one obtains the iterative charge density formula

$$\rho_n(\mathbf{r}) = \exp\left\{\ln\rho_{n-1}(\mathbf{r}) + N\lambda' \sum_{hkl} (F^{n-1}_{hkl} - F_{hkl}) \exp(-2\pi i \mathbf{k}\cdot\mathbf{r})/\sigma^2_{hkl}\right\} \qquad (33)$$

where the summation is over the hkl (and (-h,-k,-l)) which the structure factors F_{hkl} have been observed, $\rho'_n(\mathbf{r}) = \rho_n(\mathbf{r})/\sum_{\mathbf{r}} \rho_n(\mathbf{r})$, N is electron number in the unit cell, F^n_{hkl} is calculated from eqn (26) with $\rho_n(\mathbf{r})$ and λ' is a disposable constant. The convergent function $\rho_n(\mathbf{r})$ is the desired electron density. This is a powerful technique for the determination of the charge density from experiment. Sakata and Sato (1990) used this method to determine the charge density of silicon crystal, for which the structure factors have been most accurately measured so far, and found that the R-factor between experimental and calculated structure factors is 0.05%!

3.3 The Geometrical Structures of Diamond and Zinc-Blende

3.3.1 Diamond and Its Geometrical Structure

The crystalline forms of carbon which have been recognized for a long

time are diamond, hexagonal graphite, and rhombohedral graphite. Under normal condition (room temperature and atmospheric pressure) graphite is stable, diamond is metastable. Under certain conditions a hexagonal polymorph of carbon with wurtzite structure (lonsdaleite) can be produced (Bundy and Kasper, 1967). This type of carbon crystal is also found in meteorites. Diamond occurs naturally and can also be synthesized under high pressure or at low pressure by chemical vapor deposition methods (Angus and Hayman, 1988; Robertson, 1991; Wei, et al, 1992). The great interest in diamond stems from its extreme properties. Diamond has the highest atom number density of any material at terrestrial pressures (Angus, 1986), (A possible exception is the superdense carbon phase reported by Matyusenko et al, 1979.). Diamond is the least compressible substance known (Field, 1979) and has the highest bulk modulus and hardness of any material (a possible exception is β-C_3N_4, Liu and Cohen, 1990). The thermal conductivity of diamond at 300 K is higher than that of any other materials (Field, 1979).

The structural difference between diamond and graphite is obvious. In diamond a carbon atom has strong interactions with its four nearest neighbor atoms and therefore has a tetrahedral environment. However, graphite is a layer structure, a carbon atom strongly interacts with its three nearest neighbour atoms within the layer and weakly interacts with the atoms of its neighbouring layers. In this section the geometrical structure and the conventional chemical structure of diamond will be illustrated. The conventional chemical structure, which shows the bonds between the atoms, is obtained by empirically assigning bonds between the atoms based on the observed geometry. A precise definition of a bond will be given in section

3.4. The geometrical and chemical structural difference between diamond and lonsdaleite is given in section 3.3.3 and this difference is used to illustrate the relative stability of these two tetrahedral carbon crystals.

Figure 3-1 shows one way of looking at the diamond structure, the space group of the structure is $Fd3m$ (O_h^7), No. 227 in the International Tables for Crystallography. We will denote this group as $Fd3m$ (O_h^7, 227) in the rest of the thesis. Table 3-2 shows the relevant page of the International Tables for X-Ray Crystallography. The two atoms in the primitive cell lie at the positions a which have fractional coordinates (1/8, 1/8, 1/8) and (7/8, 7/8, 7/8) or (-1/8, -1/8,- 1/8). The origin on this table is chosen at the midpoint of a pair of nearest neighbour atoms. Another way to choose the origin in the International Tables for X-Ray Crystallography is to place it at a nucleus. If not specifically stated in the rest of the thesis, we will use the origin chosen in Table 3-2. Other elements that crystallize with this structure are Si, Ge and α-Sn.

From Table 3-2 we know that the possible point symmetries (called site symmetries) for the space group $Fd3m$ (O_h^7, 227) are T_d, D_{3d}, C_{3v}, C_{2v}, C_s and C_2. The Bravais lattice of diamond is face-centered cubic (fcc) with two atoms in a primitive unit cell. The primitive translational vectors ($\mathbf{a}_l$) for the fcc lattice can be taken to be

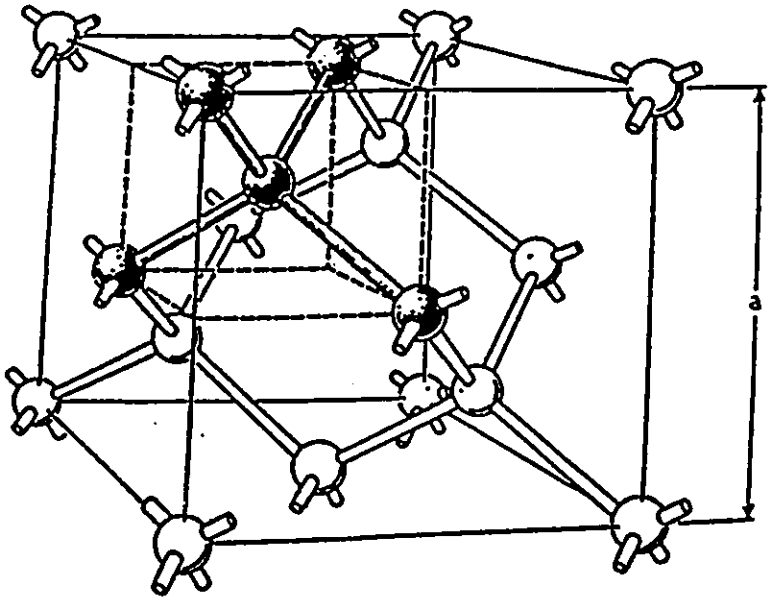

Fig. 3-1 Diamond crystal structure indicating the tetrahedal coordination

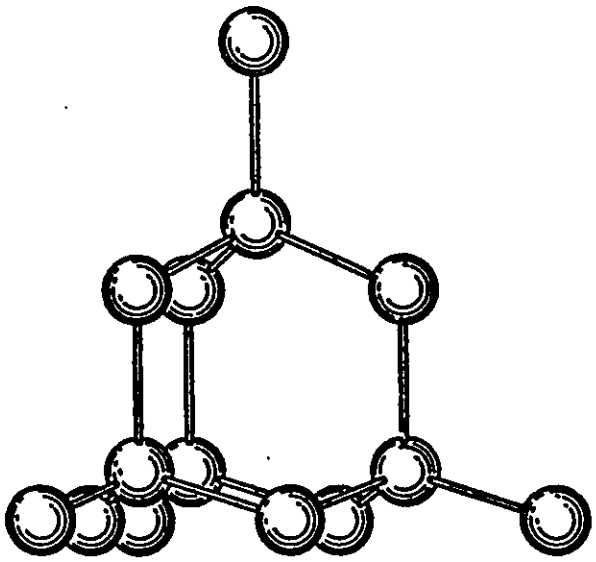

Fig. 3-2 (111) Direction of Diamond

Table 3-2 The Table of Space Group *Fd3m* (O_h^7, 227)

(from *International Tables for X-Ray Crystallography*, 1965)

Cubic $m\,3\,m$ — $F\,4_1/d\,\bar{3}\,2/m$ — No. 227 — $Fd3m$ O_h^7

Origin at centre ($\bar{3}m$), at $\frac{1}{8},\frac{1}{8},\frac{1}{8}$ from $\bar{4}3m$ (compare previous page for alternative origin)

Number of positions, Wyckoff notation, and point symmetry			Co-ordinates of equivalent positions	Conditions limiting possible reflections
			$(0,0,0;\ 0,\frac{1}{2},\frac{1}{2};\ \frac{1}{2},0,\frac{1}{2};\ \frac{1}{2},\frac{1}{2},0)+$	
				General:
192	*i*	1	x,y,z; $x,\frac{1}{2}-y,\frac{1}{2}-z$; $\frac{1}{2}-x,y,\frac{1}{2}-z$; $\frac{1}{2}-x,\frac{1}{2}-y,z$; z,x,y; $z,\frac{1}{2}-x,\frac{1}{2}-y$; $\frac{1}{2}-z,x,\frac{1}{2}-y$; $\frac{1}{2}-z,\frac{1}{2}-x,y$; y,z,x; $y,\frac{1}{2}-z,\frac{1}{2}-x$; $\frac{1}{2}-y,z,\frac{1}{2}-x$; $\frac{1}{2}-y,\frac{1}{2}-z,x$; x,z,y; $x,\frac{1}{2}-z,\frac{1}{2}-y$; $\frac{1}{2}-x,z,\frac{1}{2}-y$; $\frac{1}{2}-x,\frac{1}{2}-z,y$; y,x,z; $y,\frac{1}{2}-x,\frac{1}{2}-z$; $\frac{1}{2}-y,x,\frac{1}{2}-z$; $\frac{1}{2}-y,\frac{1}{2}-x,z$; z,y,x; $z,\frac{1}{2}-y,\frac{1}{2}-x$; $\frac{1}{2}-z,y,\frac{1}{2}-x$; $\frac{1}{2}-z,\frac{1}{2}-y,x$; $\bar{x},\bar{y},\bar{z}$; $\bar{x},\frac{1}{2}+y,\frac{1}{2}+z$; $\frac{1}{2}+x,\bar{y},\frac{1}{2}+z$; $\frac{1}{2}+x,\frac{1}{2}+y,\bar{z}$; $\bar{z},\bar{x},\bar{y}$; $\bar{z},\frac{1}{2}+x,\frac{1}{2}+y$; $\frac{1}{2}+z,\bar{x},\frac{1}{2}+y$; $\frac{1}{2}+z,\frac{1}{2}+x,\bar{y}$; $\bar{y},\bar{z},\bar{x}$; $\bar{y},\frac{1}{2}+z,\frac{1}{2}+x$; $\frac{1}{2}+y,\bar{z},\frac{1}{2}+x$; $\frac{1}{2}+y,\frac{1}{2}+z,\bar{x}$; $\bar{x},\bar{z},\bar{y}$; $\bar{x},\frac{1}{2}+z,\frac{1}{2}+y$; $\frac{1}{2}+x,\bar{z},\frac{1}{2}+y$; $\frac{1}{2}+x,\frac{1}{2}+z,\bar{y}$; $\bar{z},\bar{y},\bar{x}$; $\bar{z},\frac{1}{2}+y,\frac{1}{2}+x$; $\frac{1}{2}+z,\bar{y},\frac{1}{2}+x$; $\frac{1}{2}+z,\frac{1}{2}+y,\bar{x}$.	*hkl*: $h+k,k+l,(l+h)=2n$ *hhl*: $(l+h=2n)$; C 0*kl*: $(k,l=2n)$; $k+l=4n$ C
				Special: as above, plus
96	*h*	2	$0,x,\bar{x}$; $0,\frac{1}{2}-x,\frac{1}{2}+x$; $\frac{1}{2},x,\frac{1}{2}+x$; $\frac{1}{2},\frac{1}{2}-x,\bar{x}$; $\bar{x},0,x$; $\frac{1}{2}+x,0,\frac{1}{2}-x$; $\frac{1}{2}+x,\frac{1}{2},x$; $\bar{x},\frac{1}{2},\frac{1}{2}-x$; $x,\bar{x},0$; $\frac{1}{2}-x,\frac{1}{2}+x,0$; $x,\frac{1}{2}+x,\frac{1}{2}$; $\frac{1}{2}-x,\bar{x},\frac{1}{2}$; $0,\bar{x},x$; $0,\frac{1}{2}+x,\frac{1}{2}-x$; $\frac{1}{2},\bar{x},\frac{1}{2}-x$; $\frac{1}{2},\frac{1}{2}+x,x$; $x,0,\bar{x}$; $\frac{1}{2}-x,0,\frac{1}{2}+x$; $\frac{1}{2}-x,\frac{1}{2},\bar{x}$; $x,\frac{1}{2},\frac{1}{2}+x$; $\bar{x},x,0$; $\frac{1}{2}+x,\frac{1}{2}-x,0$; $\bar{x},\frac{1}{2}-x,\frac{1}{2}$; $\frac{1}{2}+x,x,\frac{1}{2}$.	no extra conditions
96	*g*	*m*	x,x,z; $x,\frac{1}{2}-x,\frac{1}{2}-z$; $\frac{1}{2}-x,x,\frac{1}{2}-z$; $\frac{1}{2}-x,\frac{1}{2}-x,z$; z,x,x; $z,\frac{1}{2}-x,\frac{1}{2}-x$; $\frac{1}{2}-z,x,\frac{1}{2}-x$; $\frac{1}{2}-z,\frac{1}{2}-x,x$; x,z,x; $x,\frac{1}{2}-z,\frac{1}{2}-x$; $\frac{1}{2}-x,z,\frac{1}{2}-x$; $\frac{1}{2}-x,\frac{1}{2}-z,x$; $\bar{x},\bar{x},\bar{z}$; $\bar{x},\frac{1}{2}+x,\frac{1}{2}+z$; $\frac{1}{2}+x,\bar{x},\frac{1}{2}+z$; $\frac{1}{2}+x,\frac{1}{2}+x,\bar{z}$; $\bar{z},\bar{x},\bar{x}$; $\bar{z},\frac{1}{2}+x,\frac{1}{2}+x$; $\frac{1}{2}+z,\bar{x},\frac{1}{2}+x$; $\frac{1}{2}+z,\frac{1}{2}+x,\bar{x}$; $\bar{x},\bar{z},\bar{x}$; $\bar{x},\frac{1}{2}+z,\frac{1}{2}+x$; $\frac{1}{2}+x,\bar{z},\frac{1}{2}+x$; $\frac{1}{2}+x,\frac{1}{2}+z,\bar{x}$.	
48	*f*	*mm*	$x,\frac{1}{8},\frac{1}{8}$; $\bar{x},\frac{7}{8},\frac{7}{8}$; $\frac{1}{4}-x,\frac{1}{8},\frac{1}{8}$; $\frac{3}{4}+x,\frac{7}{8},\frac{7}{8}$; $\frac{1}{8},x,\frac{1}{8}$; $\frac{7}{8},\bar{x},\frac{7}{8}$; $\frac{1}{8},\frac{1}{4}-x,\frac{1}{8}$; $\frac{7}{8},\frac{3}{4}+x,\frac{7}{8}$; $\frac{1}{8},\frac{1}{8},x$; $\frac{7}{8},\frac{7}{8},\bar{x}$; $\frac{1}{8},\frac{1}{8},\frac{1}{4}-x$; $\frac{7}{8},\frac{7}{8},\frac{3}{4}+x$.	*hkl*: $h+k+l=2n+1$ or $4n$
32	*e*	3*m*	x,x,x; $x,\frac{1}{2}-x,\frac{1}{2}-x$; $\frac{1}{2}-x,x,\frac{1}{2}-x$; $\frac{1}{2}-x,\frac{1}{2}-x,x$; $\bar{x},\bar{x},\bar{x}$; $\bar{x},\frac{1}{2}+x,\frac{1}{2}+x$; $\frac{1}{2}+x,\bar{x},\frac{1}{2}+x$; $\frac{1}{2}+x,\frac{1}{2}+x,\bar{x}$.	no extra conditions
16	*d*	$\bar{3}m$	$\frac{1}{2},\frac{1}{2},\frac{1}{2}$; $\frac{1}{2},0,0$; $0,\frac{1}{2},0$; $0,0,\frac{1}{2}$.	*hkl*: $h=2n+1$, $k=2n+1$, $l=2n+1$
16	*c*	$\bar{3}m$	$0,0,0$; $0,\frac{1}{2},\frac{1}{2}$; $\frac{1}{2},0,\frac{1}{2}$; $\frac{1}{2},\frac{1}{2},0$.	$4n+2$ or $4n+2$ or $4n+2$ — $4n$ or $4n$ or $4n$
8	*b*	$\bar{4}3m$	$\frac{3}{8},\frac{3}{8},\frac{3}{8}$; $\frac{1}{8},\frac{1}{8},\frac{1}{8}$.	*hkl*: $h+k+l=2n+1$ or $4n$
8	*a*	$\bar{4}3m$	$\frac{7}{8},\frac{7}{8},\frac{7}{8}$; $\frac{5}{8},\frac{5}{8},\frac{5}{8}$.	

$$\mathbf{a}_1 = (\mathbf{i} + \mathbf{j})/\sqrt{2}$$
$$\mathbf{a}_2 = (\mathbf{i} + \mathbf{k})/\sqrt{2} \qquad (34)$$
$$\mathbf{a}_3 = (\mathbf{j} + \mathbf{k})/\sqrt{2}$$

This structure can be described as two interpenetrating face-centered cubic structures that are displaced relative to one another along the main diagonal by $(a/4, a/4, a/4)$, where a is the side of the cubic cell. From this way of looking at the structure, we see that it has fcc Bravais lattice structure with two atoms per lattice point (primitive unit cell), and therefore there are eight atoms in one cubic cell (conventional cell). If we assume the structure is constructed by spherical atoms, the fraction of the volume filled by the atoms is $8 \cdot 4\pi/3 \cdot (a \cdot \sqrt{3}/8)^3/a^3 = \pi\sqrt{3}/16 = 0.340$. This value is much lower than the filled fraction of the closest packing structure (0.742). Therefore, if spheres attempting close packing would never arrange themselves in the diamond structure (Slater, 1965). The positions where the nuclei locate have T_d site symmetry. This indicates that a carbon atom has tetrahedral environment and therefore shows that the tetrahedral bonds can be assigned to the carbon atom.

Another way of illustrating the structure shows the carbon tetrahedra more directly. This is to take the crystal, and orient it so that the 111 direction is vertical. Then we have a set of tetrahedra, erected on top of each other, as shown in the Fig.3-2. In this figure we see plainly the fact that there are two atoms per primitive cell: the atoms in one plane in the figure have bonds extending vertically upward to the next higher plane, while the atoms in the other plane have bonds extending vertically downward. The atoms of one type cannot be obtained from those of the other type by a simple

translation, which would be required if they were in equivalent positions in the crystal. Rather, one can get an atom of one type from that of the other type by an inversion about the atom, followed by a translation carrying this atom to the nearest neighbor. Alternatively, one can get an atom of one type from that of the other type by an inversion about the midpoint between the two atoms.

3.3.2 The Zinc Blende Structure

The zinc blende structure (ZnS) is closely related to the diamond structure, but now the two interpenetrating fcc structures contain different atoms. As in the diamond structure, one type of atoms is tetrahedrally bonded to the atoms of the other type. Many important semiconductors, for example GaAs, GaP and InSb, crystallize in this structure (Cohen and Chelikowsky, 1989). The crystals AlP, BN, BP and SiC, which are chosen as examples for the present study, are the zinc blende structure.

The space group of the zinc blende structure is $F\bar{4}3m$ (T_d^2, 216). The relevant page of the International Crystallography Tables is given in Table 3-3. The site symmetries in this space group are T_d, C_{3v}, C_{2v} and C_s. One type of atoms occupy on position a, and the other on position c. The fractional coordinates of the atoms in the primitive unit cell are (0, 0, 0)($\in a$) and (1/4, 1/4, 1/4)($\in c$), respectively.

Table 3-3 The Table of Space Group $F\bar{4}3m$ (T_d^2, 216)

(from *International Tables for X-Ray Crystallography*, 1965)

Cubic $\bar{4}\,3\,m$ — $F\bar{4}\,3\,m$ — No. 216 — $F\bar{4}3m$ T_d^2

Origin at $\bar{4}3m$

Number of positions, Wyckoff notation, and point symmetry			Co-ordinates of equivalent positions (0,0,0; 0,½,½; ½,0,½; ½,½,0)+	Conditions limiting possible reflections
				General:
96	*i*	1	x,y,z; z,x,y; y,z,x; x,z,y; y,x,z; z,y,x; $x,\bar{y},\bar{z}$; $z,\bar{x},\bar{y}$; $y,\bar{z},\bar{x}$; $x,\bar{z},\bar{y}$; $y,\bar{x},\bar{z}$; $z,\bar{y},\bar{x}$; $\bar{x},y,\bar{z}$; $\bar{z},x,\bar{y}$; $\bar{y},z,\bar{x}$; $\bar{x},z,\bar{y}$; $\bar{y},x,\bar{z}$; $\bar{z},y,\bar{x}$; $\bar{x},\bar{y},z$; $\bar{z},\bar{x},y$; $\bar{y},\bar{z},x$; $\bar{x},\bar{z},y$; $\bar{y},\bar{x},z$; $\bar{z},\bar{y},x$.	*hkl*: $h+k,k+l,(l+h)=2n$ *hhl*: $(h+l=2n)$ C
				Special: as above only
48	*h*	*m*	x,x,z; z,x,x; x,z,x; $\bar{x},x,\bar{z}$; $\bar{z},x,\bar{x}$; $\bar{x},z,\bar{x}$; $x,\bar{x},\bar{z}$; $z,\bar{x},\bar{x}$; $x,\bar{z},\bar{x}$; $\bar{x},\bar{x},z$; $\bar{z},\bar{x},x$; $\bar{x},\bar{z},x$.	
24	*g*	*mm*	$x,\frac{1}{4},\frac{1}{4}$; $\frac{1}{4},x,\frac{1}{4}$; $\frac{1}{4},\frac{1}{4},x$; $\bar{x},\frac{3}{4},\frac{3}{4}$; $\frac{3}{4},\bar{x},\frac{3}{4}$; $\frac{3}{4},\frac{3}{4},\bar{x}$.	
24	*f*	*mm*	$x,0,0$; $0,x,0$; $0,0,x$; $\bar{x},0,0$; $0,\bar{x},0$; $0,0,\bar{x}$.	
16	*e*	$3m$	x,x,x; $x,\bar{x},\bar{x}$; $\bar{x},x,\bar{x}$; $\bar{x},\bar{x},x$.	
4	*d*	$\bar{4}3m$	$\frac{3}{4},\frac{3}{4},\frac{3}{4}$.	
4	*c*	$\bar{4}3m$	$\frac{1}{4},\frac{1}{4},\frac{1}{4}$.	
4	*b*	$\bar{4}3m$	$\frac{1}{2},\frac{1}{2},\frac{1}{2}$.	
4	*a*	$\bar{4}3m$	0,0,0.	

3.3.3 The Basic Structural Elements in Diamond and Zinc Blende Structures: Ring and Cage

An atom in both diamond and zinc-blende crystals has a tetrahedral environment and can be thought to be tetrahedrally bonded to its four nearest neighbour atoms. The point (site) symmetry at the position of a nucleus is T_d. Two neighboring atoms in these crystals are staggered. For a simple organic molecule, for example ethane, the staggered form structure (see Fig. 3-3(a)) is more stable than other conformations, for example, the eclipsed form in Fig. 3-3 (b) (Loudon, 1984). There are two kinds of six-atom rings according to the conventional bonding model: boat and chair type which are shown in Fig. 3-3 (c) and (d). The chair form in cyclohexane is more stable than the boat structure because of the greater steric interaction in the latter (Loudon, 1984). It is the chair structure that is used to build the diamond and zinc blende crystals. The chair structure has point symmetry D_{3d} in diamond and C_{3v} in zinc blende. Fig. 3-3(e) shows the cage structure in diamond which is built from three chair rings. The whole crystal of diamond is constructed only from one kind of cage, one kind of ring (chair), and all the C-C bonds are staggered! In zinc blende structure there is also only one kind of ring, but there are two kinds of cages which are shown in Fig. 3-4. Cage I in Fig. 3-4 is constructed from four A atoms, which have three bonds in the cage, and six B atoms, which have only two bonds. We denote this kind of cage as (4A,6B). Cage II, denoted as (4B,6A), is obtained by the exchange of A and B in cage I. All the cages in diamond and zinc blende compounds have the same point symmetry T_d.

(a)

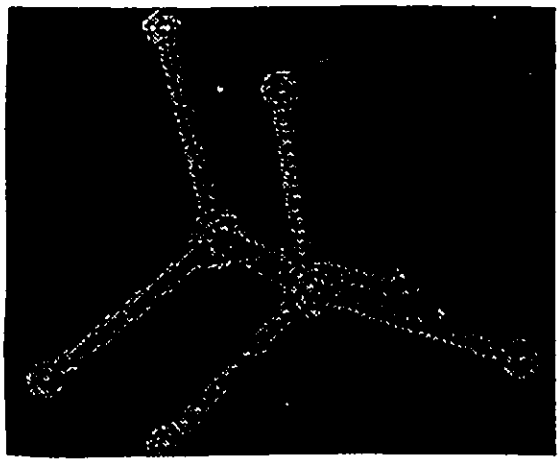

(b)

(c)

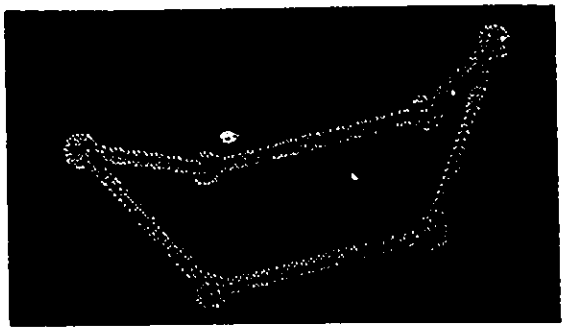

(d)

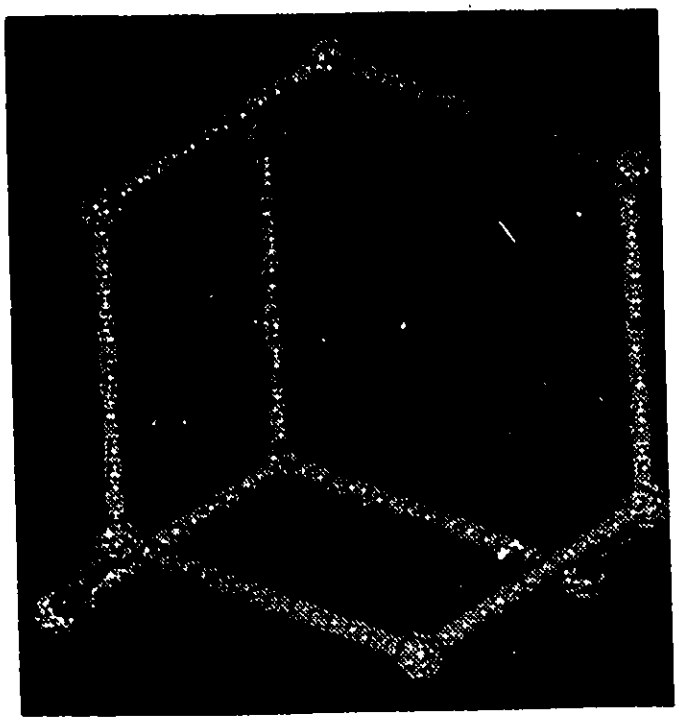

(e)

Fig. 3-3 Conformations of Ethane, Cyclohexane and the Cage in diamond: (a) staggered form of ethane, (b) eclipsed form of ethane, (c) chair form of cyclohexane, (d) boat form of cryclohexane, (e) the cage structure in diamond.

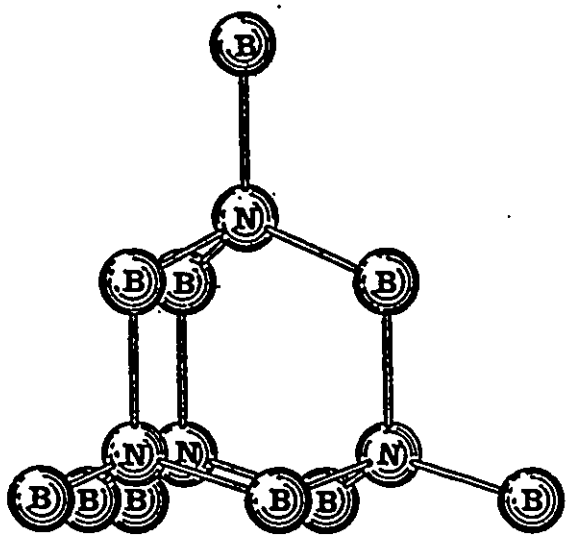

I

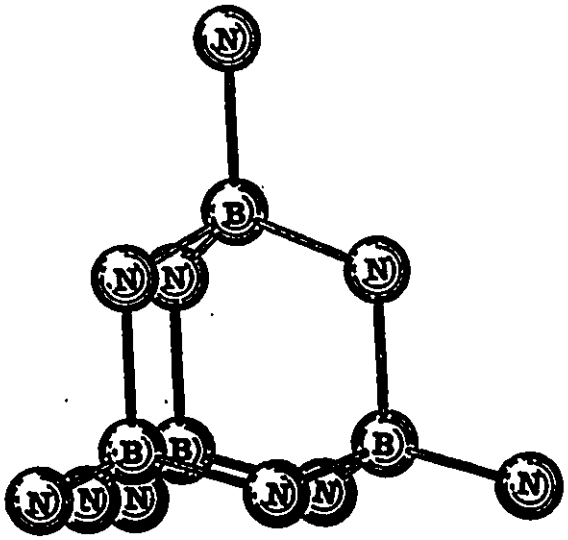

II

Fig. 3-4 Two kinds of Cages in BN: (I) (4N,6B) and (II) (4B,6N).

The structural difference between diamond or zinc blende and lonsdaleite or wurtzite is that there are two kinds of ring (chair and boat) in lonsdaleite and wurtzite, and there is only one kind of rings in diamond and zinc blende. The cage in lonsdaleite or wurtzite structures is constructed from three boat and two chair rings. Some of the bonds in lonsdaleite are eclipsed. From the consideration of steric interaction of simple organic molecules, the eclipsed C-C conformations and the boat form six-atom rings are not as stable as the staggered and chair form structures. Therefore we can infer that the lonsdaleite is not as stable as diamond.

3.4 Topological Analysis of the Charge Density $\rho(\mathbf{r})$ in a Crystal

Conventionally, the chemical and many physical properties of a molecule or a crystal are related to the structural concepts: atom, bond, ring and cage. The basic structural elements are atoms and bonds. The atoms are represented by points in a conventional molecule graph, and the bonds show the connectivities between the atoms and are represented by lines. The geometrical ring and cage follow by the arrangement of the points and lines in space. Conventionally, the existence of a bond between two atoms is often empirically identified and justified by relative energy difference between the free and bonded atoms or bond length. However, what experiment and theory determine for a molecule or crystal are the nuclear positions and the charge distribution in three dimensional space. How can one unambiguously identify the conventional concepts from an experimentally observed or theoretically calculated charge distribution? The topological analysis of the charge density gives unique and precise definitions to these concepts. In this section the central points of the topological analysis for a charge density

will be demonstrated.

The dominant topological feature of the electronic charge density——that it exhibits local maxima at the positions of the nuclei——is illustrated in Fig. 3-5 (a) which gives a display of $\rho(\mathbf{r})$ for diamond. The plane shown contains the carbon nuclei on the (110) plane in a cubic unit cell (Fig. 3-1). The density exhibits a maximum at the position of a nucleus for any plane containing the nucleus. This behaviour of the charge density is to be contrasted with that exhibited at the mid-point of a C-C inter nuclear axis. The charge density has the appearance of a saddle at this point for the two neighboring carbon nuclei in the plane of Fig. 3-5 (a), but appears as a maximum in ρ at the corresponding point between the two carbon nuclei lying above and below the plane shown in the figure. Knowledge of ρ in one or two dimensions is insufficient to characterize three dimensional form. What is needed is a method for summarizing in a succinct manner the principal topological features of a charge distribution.

3.4.1. Critical Points and Their Classification

Each topological feature of $\rho(\mathbf{r})$, whether it be a maximum, a minimum or a saddle, has associated with it a point in space called a *critical point*, where the first derivative of $\rho(\mathbf{r})$ vanishes. Thus at such a point, denoted by the position vector $\mathbf{r}_{cp}$,

$$\nabla\rho(\mathbf{r})\,|_{\mathbf{r}=\mathbf{r}_{cp}} = 0 \qquad (35)$$

where $\nabla\rho$ denotes the operation

$$\nabla\rho = \mathbf{i}\partial\rho/\partial x + \mathbf{j}\partial\rho/\partial y + \mathbf{k}\partial\rho/\partial z$$

Whether a function is a maximum or a minimum at an extreme is, of course, determined by the sign of its second derivative or curvature at this point.

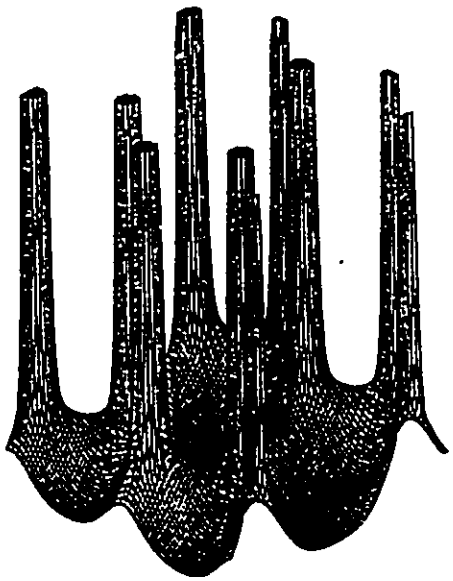

(a)

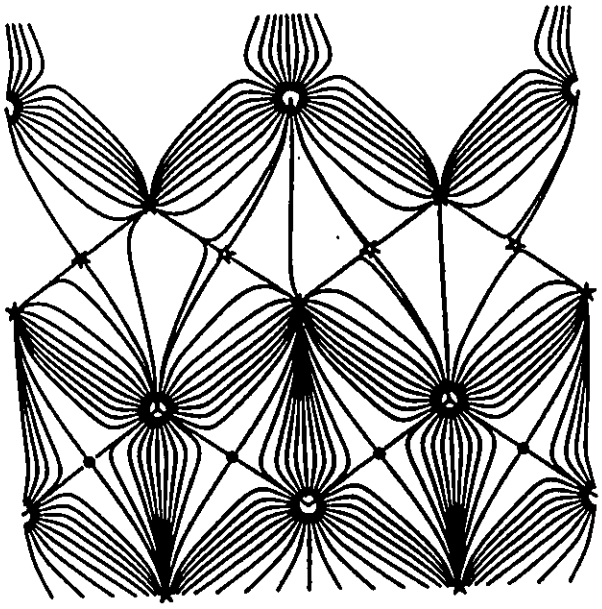

(b)

(c)

Fig. 3-5 (a) Relief map of the charge density ρ for diamond in (110) plane; (b) map showing the trajectories traced out by the gradient vectors of the charge density for the same plane as (a); (c) a carbon atom in diamond.

In general, for an arbitrary choice of coordinate axis, one will encounter nine second derivatives of the form $\partial^2\rho/\partial x\partial y$ in the determination of the curvatures of ρ at a point in space. Their ordered 3x3 array is called the Hessian matrix of the charge density, or simply, the Hessian of ρ. This is a real, symmetric matrix and as such it can be diagonalized with a real unitary matrix. The new coordinate axes, in which the Hessian is diagonal, are called the principal axes of curvature. The trace of the Hessian matrix, the sum of its diagonal elements, is invariant to the rotation of the coordinate system. Thus the value of the quantity $\nabla^2\rho$, called the Laplacian of ρ,

$$\nabla^2\rho = \partial^2\rho/\partial x^2 + \partial^2\rho/\partial y^2 + \partial^2\rho/\partial z^2$$

is invariant to the choice of coordinate axes. The principal axes and their corresponding curvatures at a critical point in ρ are obtained as the eigenvectors and corresponding eigenvalues in the diagonalization of the Hessian matrix of ρ. While all of the eigenvalues of the Hessian matrix of ρ at a critical point are real, they may equal to zero. The rank of a critical point, denoted by ω, is equal to the number of non-zero eigenvalues or non-zero curvatures of ρ at the critical point. The signature, denoted by σ, is simply the algebraic sum of the sign of the eigenvalues, i.e. of the signs of the curvatures of ρ at the critical point. The critical point is labelled by

$$(\omega,\sigma).$$

With few exceptions, the critical points of charge distributions for molecules and solids at or in the neighborhoods of energetically stable geometrical configurations of the nuclei are all of rank three. It is in terms of the properties of critical points with $\omega = 3$ that the elements of molecular elements are defined. A critical point with $\omega < 3$, i.e. with at

least one zero curvature, is said to be degenerate. Such a critical point is unstable in the sense that a small change in the charge density, as caused by a displacement of the nuclei, causes it to either vanish or to bifurcate into a number of non-degenerate or stable (ω = 3) critical points. Since structure is generic in the sense that a given structure or arrangement of bonds persists over a range of nuclear configurations, the observed limited occurrence (Bader, 1990) of degenerate critical points is not surprising. One correctly anticipates that the appearance of a degenerate critical point in a molecular charge distribution denotes the onset of structural change.

There are just four possible signature values for critical points of rank three. They are:

(1) (3,-3), denoted by $\mathbf{r}_n$, all curvatures are negative and ρ is a local maximum at $\mathbf{r}_{cp}$;

(2) (3,-1), denoted by $\mathbf{r}_b$, two curvatures are negative and ρ is a maximum at $\mathbf{r}_b$ in the plane defined by their corresponding axes. ρ is a minimum at $\mathbf{r}_b$ along the third axis which is perpendicular to this plane;

(3) (3,+1), denoted by $\mathbf{r}_r$, two curvatures are positive and ρ is a minimum at $\mathbf{r}_r$ in the plane defined by the corresponding axes. ρ is a maximum at $\mathbf{r}_r$ along the third axis which is perpendicular to this plan;

(4) (3,+3) all curvatures are positive and ρ is a local minimum.

3.4.2. Relation between Structural Elements of a crystal and Gradient Vector Field and Critical Points of the Charge Density

A complete theory of molecular and crystal structures is brought to the fore in the gradient vector field of the electronic charge density. This theory recovers all of the elements of structure in a manner that is totally

independent of any information other than that contained within the observable quantity charge density $\rho(\mathbf{r})$ (Bader, Nguyen-Dang and Tal, 1981; Bader, 1990; Bader and Zou, 1992), which can be determined from both theory and experiments. The boundary condition of a quantum subsystem is also stated in terms of this field (Bader and Beddall, 1972; also see Paper *I* appended in chapter 1).

The gradient vector field of the charge density is represented through a display of the trajectories traced out by the vector $\nabla\rho$. A trajectory of $\nabla\rho$, also called a gradient path, starting at some arbitrary point $\mathbf{r}_0$ is obtained by calculating $\nabla\rho(\mathbf{r}_0)$, moving a distance $\Delta\mathbf{r}$ away from this point in the direction indicated by the vector $\nabla\rho(\mathbf{r}_0)$ and then repeating this procedure until the path so generated terminates. Such a trajectory is a solution of equation

$$\frac{d\mathbf{r}(s)}{ds} = \nabla\rho(\mathbf{r}) \qquad (36)$$

with the initial condition $\mathbf{r}(0) = \mathbf{r}_0$. Fig. 3-5(b) shows the gradient vector field in the (110) plane of diamond. The appearance of the structural elements in this figure will be demonstrated in the following.

(1) *Atom*

The gradient paths which terminate at a given nucleus are shown as ending at the boundary of a circle of arbitrary radius. The coulomb potential becomes infinitely negative when an electron and a nucleus coalesce and, because of this, the state function and charge density for an atom or molecule or crystal must exhibit a cusp at a nuclear position (kato, 1957). However, this is not a problem of practical import and the nuclear positions behave

topologically as do (3,-3) critical points in the charge density at the positions of the nuclei, and hereafter they will be referred to as such. Because ρ is a local maximum at each nuclear position, each nucleus or (3,-3) critical point serves as the terminus of all the gradient paths starting from and contained in some neighborhood of the nucleus and it behaves as an *attractor* in the gradient vector field of the charge density. Associated with each attractor is a *basin*, the space traversed by all the gradient paths which terminate at the attractor. Fig. 3-5(b) shows the carbon nuclei in diamond acting as attractors.

Since (3,-3) critical points in a many-electron charge distribution are generally found at the positions of the nuclei, the nuclei act as the attractors of the gradient field of ρ. The result of this identification is that the space of a molecular or crystalline charge distribution, real space, is partitioned into disjoined regions, the basins, each of of which contains one point attractor or nucleus. *An atom, free or bound, is defined as the union of an attractor and its associated basin.*

Alternatively, an atom can be defined in terms of its boundary (Bader, 1990). The atomic basin is separated from neighboring atoms by inter atomic surfaces. The existence of an inter atomic surface S_{AB} denotes the presence of a (3,-1) critical point: the surface S_{AB} consists of all gradient paths which terminate at the (3,-1) critical point. It is generated by the two eigenvectors ω_1 and ω_2 associated with the negative eigenvalues of the Hessian matrix of such a critical point. Indeed, in a sufficiently small neighbourhood of the critical point at $\mathbf{r}_b$ (the (3,-1) critical point), the inter atomic surface coincides with its tangent plane at $\mathbf{r}_b$, which is linearly

spanned by ω_1 and ω_2. The entire inter atomic surface can be obtained by solving the differential equation eqn (36), for initial conditions $\mathbf{r}_0 = \mathbf{r}(0)$ such that each $\mathbf{r}_0$ belongs to the intersection of the surface with the above neighbourhood of $\mathbf{r}_b$ and is thus expressible as a linear combination of ω_1 and ω_2. The *atomic surface* S_A of an atom A is defined as the boundary of its basin. Generally this boundary comprises the union of a number of inter atomic surfaces, separating two neighbouring basins, and some portions which may be infinitely distant from the attractor for an atom in a molecule. The inter atomic surfaces as well as the surfaces found at infinity are the only closed surface S of real space which satisfy the equation (Bader, Nguyen-Dang and Tal, 1981)

$$\nabla\rho(\mathbf{r})\cdot\mathbf{n}(\mathbf{r}) = 0 \quad \forall\ \mathbf{r} \in S \tag{37}$$

where $\mathbf{n}(\mathbf{r})$ is the unit vector normal to the surface at $\mathbf{r}$. A surface which satisfies eqn (37) is called a *zero-flux surface*. Thus, an atom is a region of real space which contains a single nuclear attractor and which is bounded by a zero-flux surface. Fig. 3-5(c) shows a carbon atom in diamond. This figure shows that the atom occupies a finite region and has T_d symmetry. The atomic surface comprises four interatomic surfaces.

(2) *Bond*

For the two nearest neighbouring carbon nuclei in the (110) plane shown in Fig. 3-5(a), the charge density exhibits one positive and one negative curvature at the critical point between the neighboring carbon nuclei and it has the appearance of a saddle. For the plane perpendicular to the inter nuclear axis, the corresponding critical point exhibits two negative curvatures and appears as a maximum in this particular plane. Thus the

critical points between the nearest neighboring carbon nuclei are (3,-1) critical points. It is important to note that since the charge density is maximum at the (3,-1) critical point in the plane perpendicular to the inter nuclear axis, electronic charge is accumulated in the region between the nuclei (Fig. 3-5(a)). Such a critical point is found between every pair of nuclei which are considered to be linked by a chemical bond (Bader, Nguyen-Dang and Tal, 1981).

Reference to the gradient vector field shown for diamond illustrates that no trajectories cross from one atomic basin to another across an interatomic surface. It is recalled that $\nabla\rho$ vanishes at a critical point and the lines shown linking neighboring nuclei are not trajectories which cross the surface, but rather pairs of trajectories each of which originates at a (3,-1) critical point where $\nabla\rho = 0$. Each such pair of trajectories is defined by the eigenvector associated with the single positive eigenvalue of a (3,-1) critical point. These two unique gradient paths define a line through the charge distribution linking the neighboring nuclei along which $\rho(\mathbf{r})$ is a maximum with respect to any neighbouring line. Such a line is found between every pair of nuclei whose atomic basins share a common interatomic surface, and in general case it is referred to as an *atomic interaction line*.

The existence of a (3,-1) critical point and its associated atomic interaction line indicates that electronic charge density is accumulated between the nuclei that are so linked. Both theory and observation concur that the accumulation of electronic charge between a pair of nuclei is a necessary condition if two atoms are to be bonded to one another. This accumulation of charge is also a sufficient condition when the forces on the

nuclei are balanced and the system possesses a minimum energy equilibrium internuclear separation. Thus the presence of an atomic interaction line in such an equilibrium geometry satisfies both the necessary and sufficient conditions that the atoms be bonded to one another. In this case the line of the maximum charge density linking the nuclei is called a *bond path* and the (3,-1) critical point referred to as a *bond critical point*.

For a given configuration in nuclear configuration space, a *molecular* or *crystalline graph* is defined as the union of the closures of the bond paths. Pictorially the graph is the network of bond paths linking pairs of neighbouring nuclear attractors. A molecular or crystalline graph is a direct result of the principal topological properties of a molecular charge distribution: that the only local maxima, (3,-3) critical points, generally occur at the positions of the nuclei thereby defining the atoms, and that (3,-1) critical points are found to link certain, but not all, pairs of nuclei in a molecule or crystal. The network of bond paths thus obtained is found to *coincide* with the network generated by linking together those pairs of atoms which are assumed to be bonded to one another on the basis of chemical considerations. For example, a carbon atom in diamond is linked by bond paths to its four nearest neighbouring atoms. Therefore the network of diamond of Figs. 3-1 or 3-2 is the network of bond paths generated by all the (3,-1) critical points in the crystal.

(3) *Ring and Cage*

The remaining critical points of rank three occur as consequences of particular arrangements of bond paths and they define the remaining elements of molecular and crystal structure——rings and cages. If the bond paths are

linked so as to form a ring of bonded atoms, then a (3,+1) critical point is found in the interior of the ring. The eigenvectors associated with the two positive eigenvalues of the Hessian matrix of ρ at this critical point generate an infinite set of gradient paths which originate at the critical point and define a surface, called the ring surface.

If the bond paths are so arranged as to enclose the interior of a molecule with ring surfaces, then (3,+3) or cage critical point is found in the interior of the resulting cage. The charge density is a local minimum at a cage critical point. Trajectories only originate at such a critical point and terminate at nuclei, and at bond and ring critical points, thereby defining a bounded region of space. A cage contains at least two rings such that the union of the ring surfaces bounds a region in real space R^3 which contains a (3,+3) critical point. The precise definitions of ring and cage can be found in the references Bader, Nguyen-Dang and Tal, 1981 or Bader, 1990.

For the case of diamond, we have pointed out the rings and cages of the network of bonds of the crystal in section 3.3.3. The ring critical point of a ring is at the centre of it. The ring critical points of the crystal are located at the positions labelled *d* in the International Tables for Crystallography. From table 3-2 we can see that the site symmetry of positions *d* is D_{3d}. This is the symmetry of a ring in diamond (see Fig. 3-3(c)). The cage critical points in diamond are at those positions of *b* in table 3-2. The site symmetry of *b* is T_d which is the symmetry of a cage in diamond (see Fig.3-3(e)). This example shows a correspondence between the critical points and the arrangements of bond paths in space.

3.4.3. The Pointcarè-Hopf Relationship for A Crystal and Its Applications

Since the ring and cage critical points follow from the special arrangement of the critical points of (3,-3) (corresponding to the nuclei in the molecular graph) and (3,-1) (the bonds) in the space, this implies that the numbers of (3,-3), (3,-1), (3,+1) and (3,+3) are not independent. Actually, for a finite molecular system, the Pointcaré-Hopf relation exists

$$n - b + r - c = 1 \qquad (38)$$

where n is the number of atomic ((3,-3)) critical points in the system, b, the number of bond critical points, r, the number of ring critical points, and c, the number of cage critical points (Collard and Hall, 1977). However, for a crystal, there are an infinite number of critical points, the relation (38) is no longer satisfied for the description of the dependence between the numbers of different kinds of critical points. Instead the following equation holds for a crystalline system

$$n - b + r - c = 0 \qquad (39)$$

where n, b, r and c have the same meaning as eqn (38) except that here they refer to the corresponding numbers of critical points in the primitive unit cell for the crystal.

Proof: Equation (39) can be proven directly from eqn (38). Since a crystal can be represented by periodically repeating lattice points and every lattice point represents the same physical contents, we have

$$n - b + r - c = \alpha \qquad (40)$$

where α is a finite constant because the critical points in a lattice point must be finite. Now consider a part of the crystal which consists of N lattice points and of the representing physical contents. The Poincarè-Hopf

relation for a molecule eqn (38) must be satisfied for the molecule constructed from the N lattice points. We can divide the molecule into two parts: the part represented by the boundary lattice points, and the part represented by the interior lattice points. The critical point distribution in the interior of the molecule is the same as the crystal. We assume there are N_1 lattice points in the interior, therefore there are N_1n atomic critical points, N_1b bond critical points, N_1r ring critical points and N_1c cage critical points in this part of the molecule. The critical point distribution of the part represented by the boundary lattice points is different from the distribution in crystal. We assume that there are n_2 atoms, b_2 bonds, r_2 rings and c_2 cages on the boundary part, these numbers n_2, b_2, r_2 and c_2 should be in the order of the boundary lattice points. According to eqns (38) and (40), we have

$$N_1\alpha + n_2 - b_2 + r_2 - c_2 = 1 \qquad (41)$$

If α was not equal to 0, then $N_1\alpha$ would be the order of $(N^{1/3})^3$ for large N in three-dimensional case. However $n_2 - b_2 + r_2 - c_2$ is at most of the order of $(N^{1/3})^2$. Therefore when $N \longrightarrow \infty$, eqn (41) is no longer satisfied because the first term and the remaining terms on lhs of eqn (41) are not in the same order. This proves α has to be 0. For one and two dimensional cases, one can make the same conclusion. #

As an example of Poincaré-Hopf relationship for a crystalline system: eqn (39), we will consider the critical points in diamond and BN crystals. In these two crystals, the atom is tetrahedrally bonded to its nearest neighbor atoms and there are two nuclei in a primitive unit cell. The nuclear positions are the local maximums of the electronic charge density, therefore

n=2 for these two crystals. Since a bond connects two nuclei, we can conclude that there are four bonds in a primitive unit cell, this yields b=4. Every two bonds in an atom can form two six atom rings (see Fig. 3-1 or 3-2), therefore one atom is connected to twelve rings. This implies that there are four rings in a primitive unit cell, therefore we have r=4. An atom plays two kinds of role to the cages: one is only two of the four bonds of the atom are used to construct a cage, in the other three of the bonds contribute to a cage. Relative to one atom, there are total six cages of the first kind, and four for the second kind. Therefore one atom contributes to ten ten-atom cages, and this yields two cages 2(6/10 + 4/10) in a primitive lattice cell, this yields c=2. It is obvious eqn (39) is satisfied in this topological structure, $n-b+r-c = 2-4+4-2=0$.

Generally, it is not easy to find and locate all the critical points in a crystal without using symmetry, although, in the case of diamond and BN, the atomic and bond critical points are relatively easy to locate. Similar to the use of the International Tables for Crystallography in the determination of a crystal structure, we can use the same tables to locate all the critical points of a crystal and determine the numbers of critical points in a primitive cell. For example, in diamond, two nuclei in a primitive cell are located at positions a (see Table 3-2) of the space group $Fd3m(O_h^7,\ 227)$ in the International Tables for Crystallography, four bond critical points at positions c, four ring critical points at d and two cage critical points at b. In BN, the atoms B and N are located, respectively, at positions a and c (see Table 3-3) of the space group $F\bar{4}3m(T_d^2,\ 216)$ table, bonds and rings at positions e with different parameter x (with x=0.0791 for bonds and x=0.613

for rings by the calculations given in section 3.2.3), cages at *b* and *d*. The cage critical points *b* correspond to cage (4N,6B) shown in Fig. 3-4(I), and *d* to (4B,6N) of Fig.3-4(II). Using the numbers of the special positions listed in the International Tables for Crystallography, we can easily see that the topological rule eqn (39) holds for diamond and BN crystals.

For a given space group of a crystal, the International Tables for Crystallography can be used to locate the critical points and determine the point symmetries of the structural elements. The number of special positions given in the Tables and the Poincarè-Hopf relationship can be used to check whether all the critical points have been found. Table 3-4 lists all the critical points in diamond, silicon, AlP, BN, BP and SiC. For example, in silicon, from table 3-2 and (3-4 we know the number of the critical points is: 24 (8+16) for (3,-3), 32 for (3,-1), 16 for (3,+1) and 8 for (3,+3) in a unit cubic cell. Therefore we have 24-32+16-8 =0. The site symmetries of the special positions are the symmetries of the corresponding structure elements. In the case of silicon, for example, the positions *a* have point symmetry T_d which is the symmetry of the silicon atom in the crystal. The ring critical points *d* and cage critical points *b* have point group D_{3d} and T_d, respectively. These point symmetries correspond to the point groups of the ring and cage structures in the crystal. For the crystal BN, the atoms (positions *a* and *c*) and cages (*b* and *d*) have the same point symmetry T_d. The rings (*e*) have C_{3v} symmetry.

Table 3-4 Critical Points in Diamond, Silicon and Zinc Blende Compounds

	C	Si	AlP	BN	BP	SiC
(3,-3)	*a**	*a*(Si),*c*	*a*(Al),*c*(P)	*a*(B),*c*(N)	*a*(B),*c*(P)	*a*(Si),*c*(C)
(3,-1)	*c*	*e*(0.0380)†	*e*(0.0872)	*e*(0.0791)	*e*(0.0759)	*e*(0.155)
(3,+1)	*d*	*d*	*e*(0.621)	*e*(0.613)	*e*(0.616)	*e*(0.633)
(3,+3)	*b*	*b*	*b*, *d*‡	*b*, *d*	*b*, *d*	*b*, *d*

* The symbols *a*, *b*, *c*, *d* and *e* refer to Table 3-2 for diamond and silicon or Table 3-3 for zinc blende compounds.

† The number in the bracket is the x value of Table 3-2 or 3-3.

‡ For a zinc blende compound AB, *b* is (4A,6B) cage and *d* is (4B,6A).

3.5 Electronic Charge Structures of Diamond, Si, AlP, BN, BP and SiC

In this section, the electronic charge structures of diamond, silicon and zinc blende compounds: AlP, BN, BP and SiC will be profiled through the properties of the critical points and the gradient vector field, the Laplacian density of the charge density and the charge density itself on a (110) plane.

3.5.1 The Bonding Nature of the Crystals

A bond in a crystal is defined by the bond paths connecting two nuclei and generated from a (3,-1) critical point. A charge density along a bond path attains its minimum value at the bond critical point $\mathbf{r}_b$ and the associated curvature or eigenvalue of the Hessian of ρ at the bond critical point is such positive. The charge density ρ_b and the Laplacian $\nabla^2\rho_b$ at a bond critical point are two important properties for characterizing the nature of the corresponding chemical bond. The value of ρ_b at a bond critical point provides a useful measure of bond strength for all types of bonds (Bader, 1990). The Laplacian of ρ, $\nabla^2\rho$, is the sum of its three principal curvatures at each point in space. When $\nabla^2\rho<0$, the value of the charge density at point

$\mathbf{r}$ is greater than the value of $\rho(\mathbf{r})$ averaged over all neighbouring points in space, and when $\nabla^2\rho>0$, $\rho(\mathbf{r})$ is less than this averaged value. Thus one may think of $\nabla^2\rho(\mathbf{r})$ as providing a measure of the extent to which the charge density is locally compressed or locally expanded. The charge is locally depleted at the bond critical point relative to neighboring points on the bond paths. The charge density in the interatomic surface, on the other hand, attains its maximum value at $\mathbf{r}_b$ and the two associated curvatures of the Hessian, those directed along axes perpendicular to the bond path, are such negative. The charge density at this point is locally concentrated at $\mathbf{r}_b$ in the interatomic surface. Therefore a chemical bond requires the creation of a (3,-1) critical point which has two negative and one positive curvatures. Mechanisms involving both charge concentrations and charge depletions are brought into play in the formation of a chemical bond. The formation is a result of two competing effects: the radial contraction of the charge density towards the bond paths, leading to its concentration at $\mathbf{r}_b$ and in the interatomic surface, as opposed by a parallel expansion of ρ which removes charge density from $\mathbf{r}_b$ and from interatomic surface and results in its separate accumulation in each of the atomic basins (Bader, 1990). Which of the two effects dominates a given interaction is determined by the sign of the Laplacian of ρ at $\mathbf{r}_b$.

The charge concentration effect is dominant in the covalent bond, for example C-C bond in diamond, and therefore the Laplacian $\nabla^2\rho$ at the bond critical point is negative. The parallel curvature $\lambda_{\parallel}$, the positive eigenvalue of the Hessian at $\mathbf{r}_b$, is relatively small. This is shown in table 3-5. The parallel curvatures of silicon and diamond are smaller than the

other values listed in the table. Table 3-6 shows that the Laplacians $\nabla^2\rho_b$ at the bond critical points for these two crystals are negative. Therefore the C-C bond in diamond and the Si-Si bond in crystal silicon are classified as covalent bonds.

Table 3-7 lists the total charge Q of the atoms in the crystals: diamond, silicon, AlP, BN, BP and SiC. The total charge is calculated as the sum of the positive nuclear charge Z and the negative electronic charge in the atom

$$Q = Z - \int_{\Omega} d\mathbf{r}\rho(\mathbf{r})$$

where the integral is over the atomic basin Ω. From this table we can see that the 'ionicity' order for the zinc-blende compounds is SiC > AlP ≅ BN > BP which is consistent with the empirical population analysis(Orlando, et al, 1990; Christensen et al, 1987).

When there is substantial charge transfer across an interatomic surface, electronic charge is separately accumulated in the basins of the two atoms and, as a result, the parallel curvature of ρ at $\mathbf{r}_b$, is large and its sign dominates the value of $\nabla^2\rho_b$. This can be seen from the properties of the crystals BN, SiC and AlP. Table 3-5 shows the relatively large parallel curvatures for the bonds in these three crystals and table 3-7 shows the relative large charge transfer (all > 2.3). The Laplacians $\nabla^2\rho_b$ for the these crystals are positive as shown in Table 3-6. The charge transfer in crystal BP is smaller (< 1.6) than BN, SiC and AlP, therefore the parallel curvature is smaller. The charge concentration effect is dominant in BP and therefore the Laplacian $\nabla^2\rho_b$ is negative. Table 3-8 shows that the values of

Table 3-5 The Bond Parallel Curvature

	Diamond	BN	SiC	BP	Si	AlP
$\lambda_{\parallel}$	0.119	0.832	0.608	0.139	0.0776	0.301

Table 3-6 Critical Point Properties

	C	BN	SiC	BP	Si	AlP
ρ_b	0.263	0.152	0.111	0.130	0.092	0.056
$\nabla^2\rho_b$	-0.880	0.185	0.310	-0.206	-0.089	0.183
$\rho_r\times10^2$	2.060	1.793	1.197	0.947	0.434	0.449
$\nabla^2\rho_r\times10$	1.020	1.062	0.474	0.366	0.155	0.141
$\rho_{c_1}\times10^2$	1.281	1.153	0.742	0.600	0.237	0.247
$\nabla^2\rho_{c_1}\times10^2$	7.493	8.383	3.655	2.566	0.915	1.022
$\rho_{c_2}\times10^2$		0.898	0.621	0.501		0.235
$\nabla^2\rho_{c_2}\times10^2$		6.506	3.107	2.159		0.788
ρ_n					0.093	
$\nabla^2\rho_n$					-0.170	

Table 3-7 Net charge of an atom in crystal

Atom	C	Si*	Al in AlP	B in BN	B in BP	Si in SiC
Net Charge	0.	1.92	2.42	2.37	1.57	3.07

* There exists a pseudo atom between two nearest neighbor silicon atom, therefore the silicon appears a positive charge.

Table 3-8 The Relation between Ionicity and Laplacian

Atom	Si in SiC	Al in AlP	B in BN	B in BP
Net Charge	3.07	2.42	2.37	1.57
Laplacian $\nabla^2\rho_b$	0.310	0.183	0.185	-0.206

the Laplacian of ρ at the bond critical points for the zinc blende compounds have the same order as the 'ionicity', that is SiC > AlP ≅ BN > BP.

3.5.2 The Charge Density Structures

The charge density itself contains a lot of information. As we have shown in section 3.4, many chemically interesting features are revealed in the charge density map (zero derivative of $\rho(\mathbf{r})$), the gradient vector field of ρ (the first order derivative of $\rho(\mathbf{r})$) and the Laplacian of ρ (the second order derivative of $\rho(\mathbf{r})$). The charge density map gives the electronic density distribution in space, the gradient vector field shows the structural elements of the crystal and the Laplacian of ρ demonstrates the shell structures of atoms and the information about the charge transfer between the bonding atoms. Therefore in this section, the charge density structures of the crystals will be illustrated through the maps of the zero-, first- and second-order derivatives of ρ.

The most chemically interesting topological properties of the charge density of diamond and zinc blende compounds can be most easily shown through the (110) plane of the crystals. All four kinds of critical points can be found on the diagonal line (x = y = z) which lies in this plane. Fig. 3.6 (a) and (b) show, respectively, the charge density and the Laplacian of ρ in (110) plane of diamond. The gradient field of ρ for the same plane of this system is shown in Fig. 3-5(b). The second column of Table 3-6 gives the electronic charge density and Laplacian values at the bond, ring and cage critical points of diamond. The gradient vector field (Fig. 3-5(b)) clearly shows the critical points which correspond to the structural elements: nucleus, atom, bond, ring and cage. The two nearest neighbor atoms are

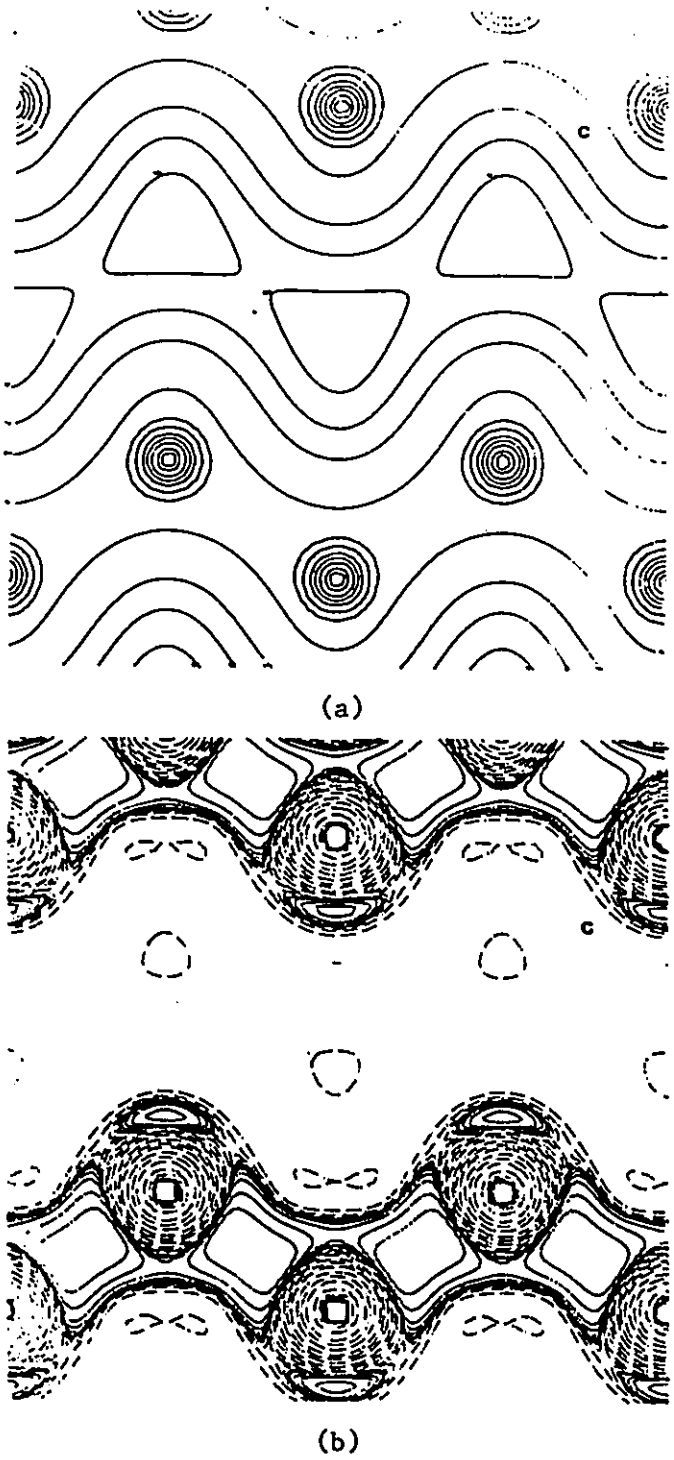

Fig. 3-6 The charge density (a) and the Laplacian (b) of the charge density on the (110) plane in diamond. In (b), solid lines represent negative values of $\nabla^2\rho$ where the electron charge density is locally concentrated, dashed lines, positive values of $\nabla^2\rho$ where the charge density is locally depleted.

connected through the bond paths generated by the bond critical point. On the diagonal line, the critical points are distributed as

$$\cdots(3,-3)-(3,-1)-(3,-3)-(3,+3)-(3,+1)-(3,+3)-(3,-3)\cdots$$

The charge minimum (the (3,+3) critical point, see the value ρ_c in table 3-6) is at the centre of the cubic unit cell.

The Laplacian of ρ recovers the shell structure of an atom by displaying a corresponding number of shells of charge concentration ($\nabla^2\rho < 0$) and charge depletion ($\nabla^2\rho > 0$) (Bader and Essen, 1984). Fig. 3-6(b) shows there exist two shells for a carbon atom in diamond. The negative values of $\nabla^2\rho$ in the neighbourhood of the bond critical point show the charge concentration in the bonding region and, therefore, a strong covalent bonding nature.

The electronic charge density map, the gradient vector field and the Laplacian of the electronic charge density on (110) plane of silicon crystal are shown in Fig. 3-7 (a),(b) and (c), respectively. The bonding charge density of silicon is one order less than that of diamond (see Table 3-6). From the gradient field picture Fig. 3-7(b) we can see that there is a (3,-3) attractor between two nearest neighbour silicon atoms. This attractor does not have a nucleus at the centre and therefore is referred to as non-nuclear attractor. The appearance of non-nuclear attractors in silicon crystal is one of the profound features for silicon. The topological structure of silicon is different from diamond even though both of them share the same space group. In silicon, the two nuclei, and the ring and cage critical points in the primitive cell are located at the same special positions in the International Crystallography Tables as in diamond. The atomic critical points (3,-3) for the non-nuclear attractors, which do not exist in diamond, are located at c,

the bonds at e with x=0.0380. The appearance of the charge density maximum at the inversion centre behaves topologically as though there is a nucleus at the centre. Therefore the non-nuclear attractor is referred to as a pseudo atom which separates the chemically bonded silicon atoms. Even though the charge density in the pseudo atom is very low ($\rho(\mathbf{r}) \leq 0.093$ for $\mathbf{r} \in$ pseudo atom), however, one pseudo atom has approximately 0.96 electron which almost has as many electron as a free hydrogen atom does. In chapter 4 we will show that the pseudo atoms of silicon play an important role in the (222) diffraction intensity and the phase of the corresponding scattering amplitude. On the diagonal line of the (110) plane, the critical points are distributed as

$\cdots$-Si(3,-3)-(3,-1)-*N*(3,-3)-(3,-1)-Si(3,-3)-(3,+3)-(3,+1)-(3,+3)-Si(3,-3)$\cdots$

where Si(3,-3) denotes nuclear position and *N*(3,-3), the (3,-3) critical point of the non-nuclear attractor. The three shell structure for the silicon atom is shown in the Laplacian diagram.

Fig.3-8 to 3-11 show the electronic charge density maps, the gradient vector fields, and Laplacian maps of the electronic charge densities of AlP, BN, BP and SiC. The critical point distributions on the (110) plane of these zinc blende compounds are the same as those in diamond. However, there exists charge transfer in these compounds which is clearly shown in the Laplacian diagram. For example, a comparison between the Laplacian of Si crystal and SiC shows that the third shell of silicon vanishes in SiC and therefore the electrons of that shell have been transferred to its neighbouring carbon atoms. The Laplacians of other zinc-blende compounds also show the similar the trends of electronic charge transfer.

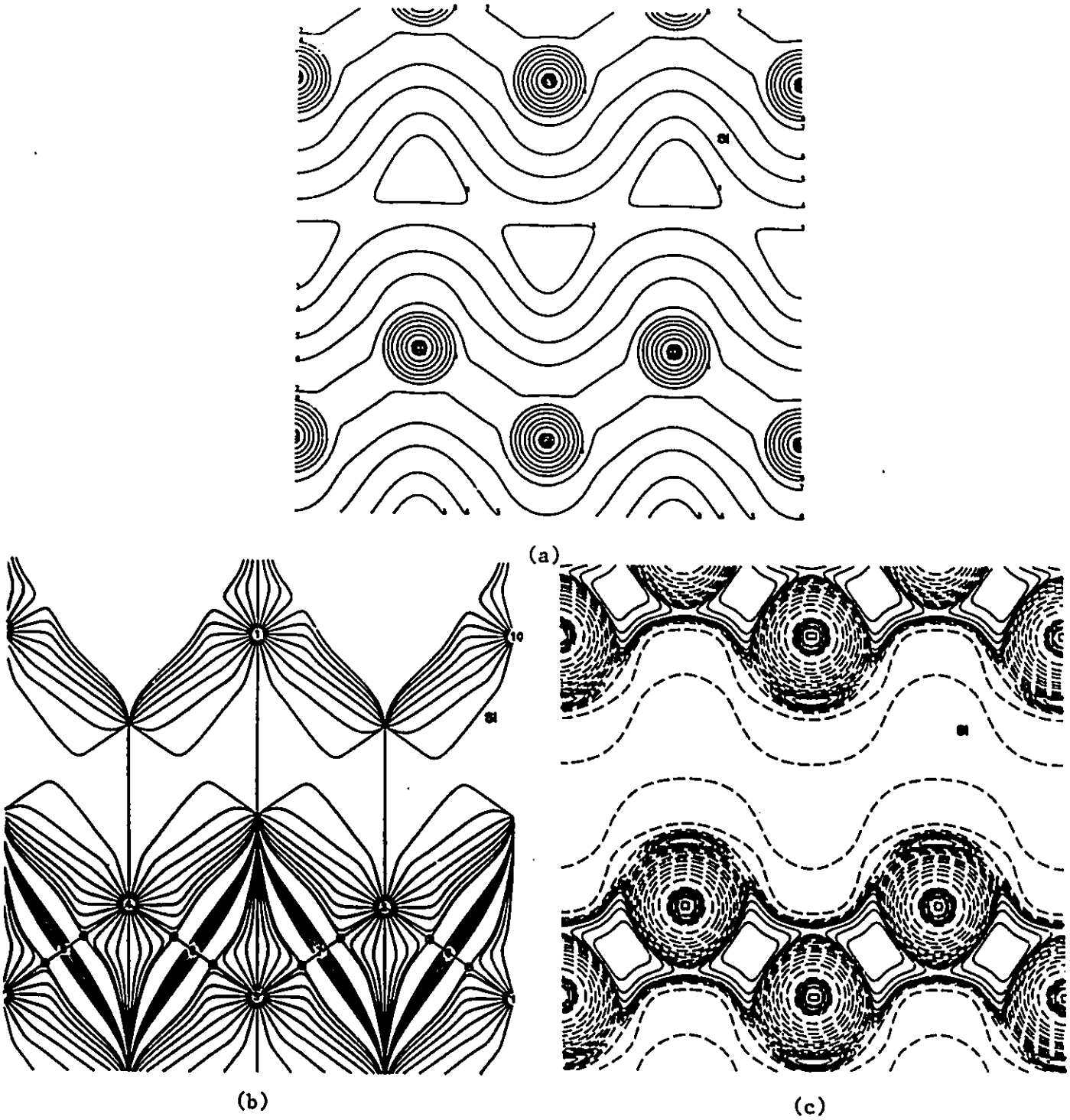

Fig. 3-7 The charge density (a), the gradient vector field (b) and the Laplacian (c) of the charge density on the (110) plane in silicon.

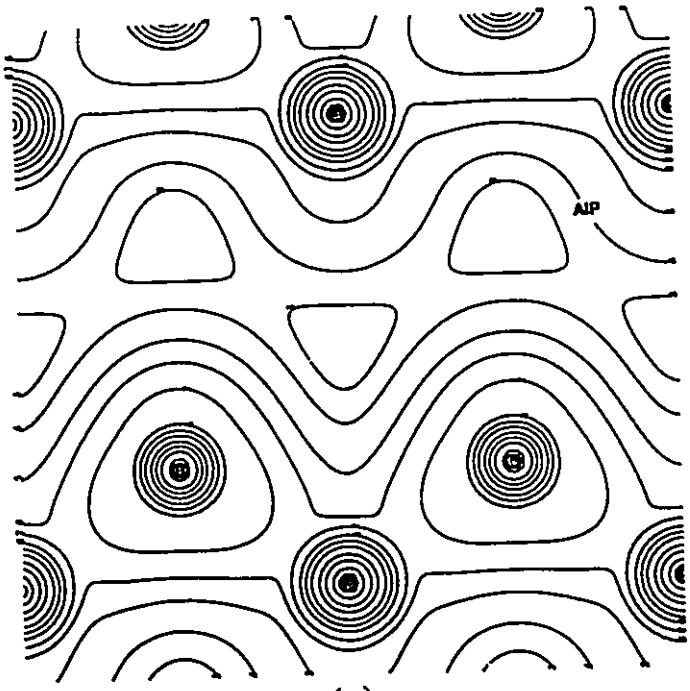

(a)

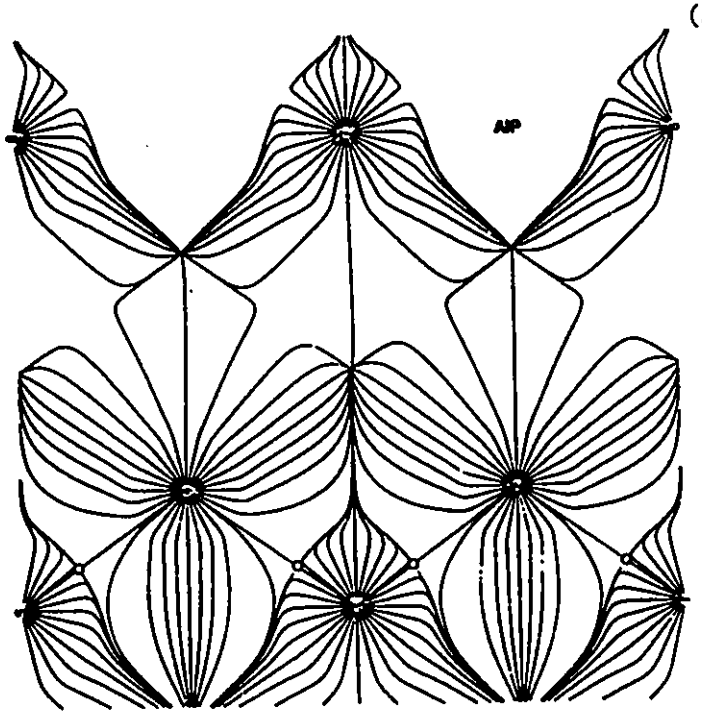

(b)

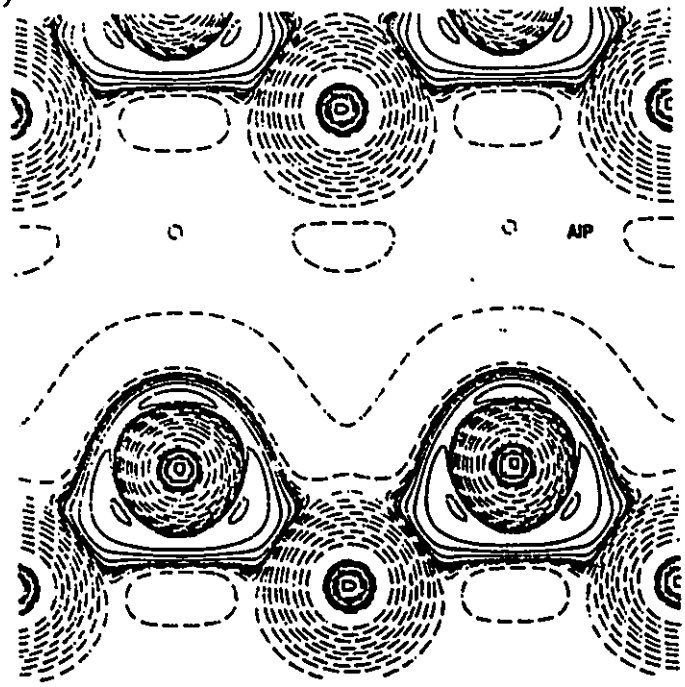

(c)

Fig. 3-8 The charge density (a), the gradient vector field (b) and the Laplacian (c) of the charge density on the (110) plane in AlP.

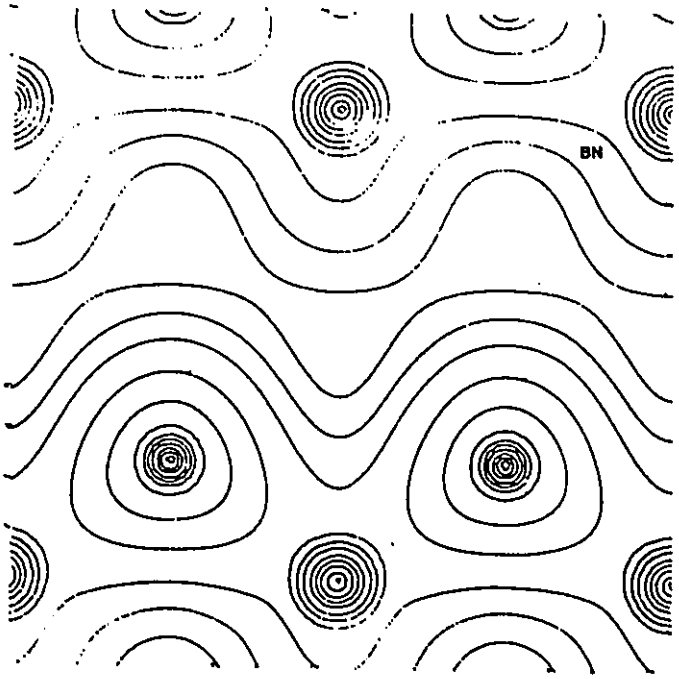

(a)

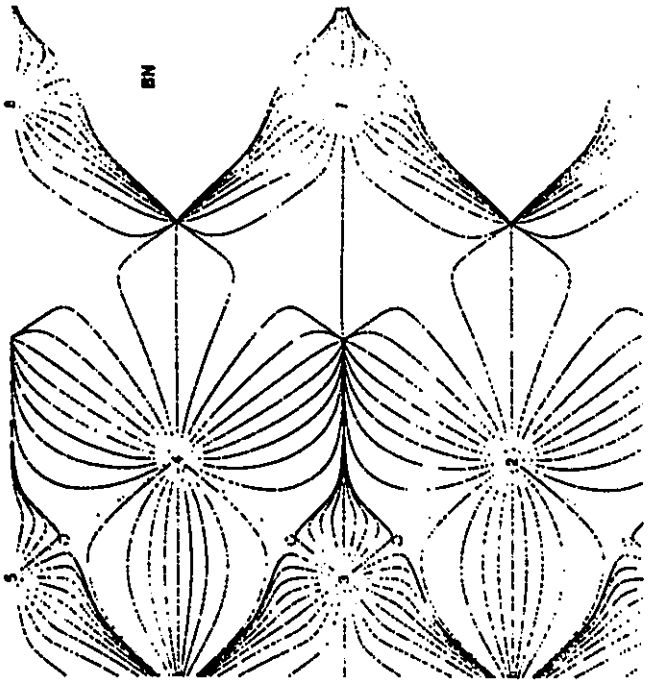

(b)

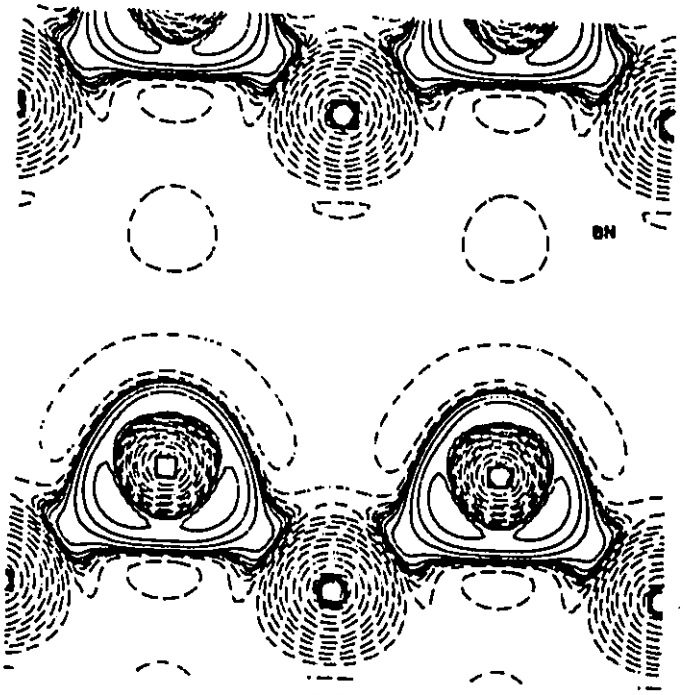

(c)

Fig. 3-9 The charge density (a), the gradient vector field (b) and the Laplacian (c) of the charge density on the (110) plane in BN.

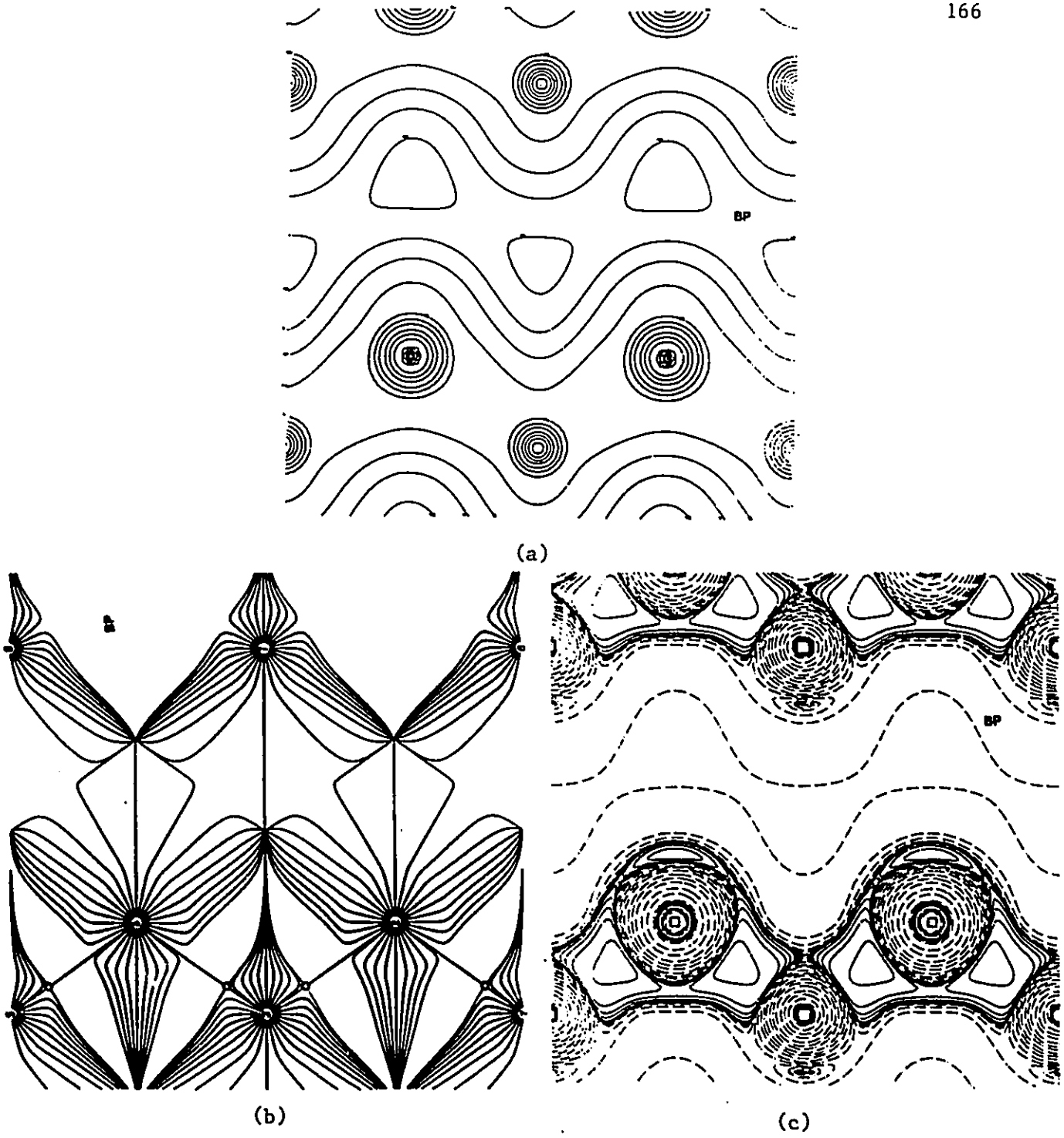

Fig. 3-10 The charge density (a), the gradient vector field (b) and the Laplacian (c) of the charge density on the (110) plane in BP.

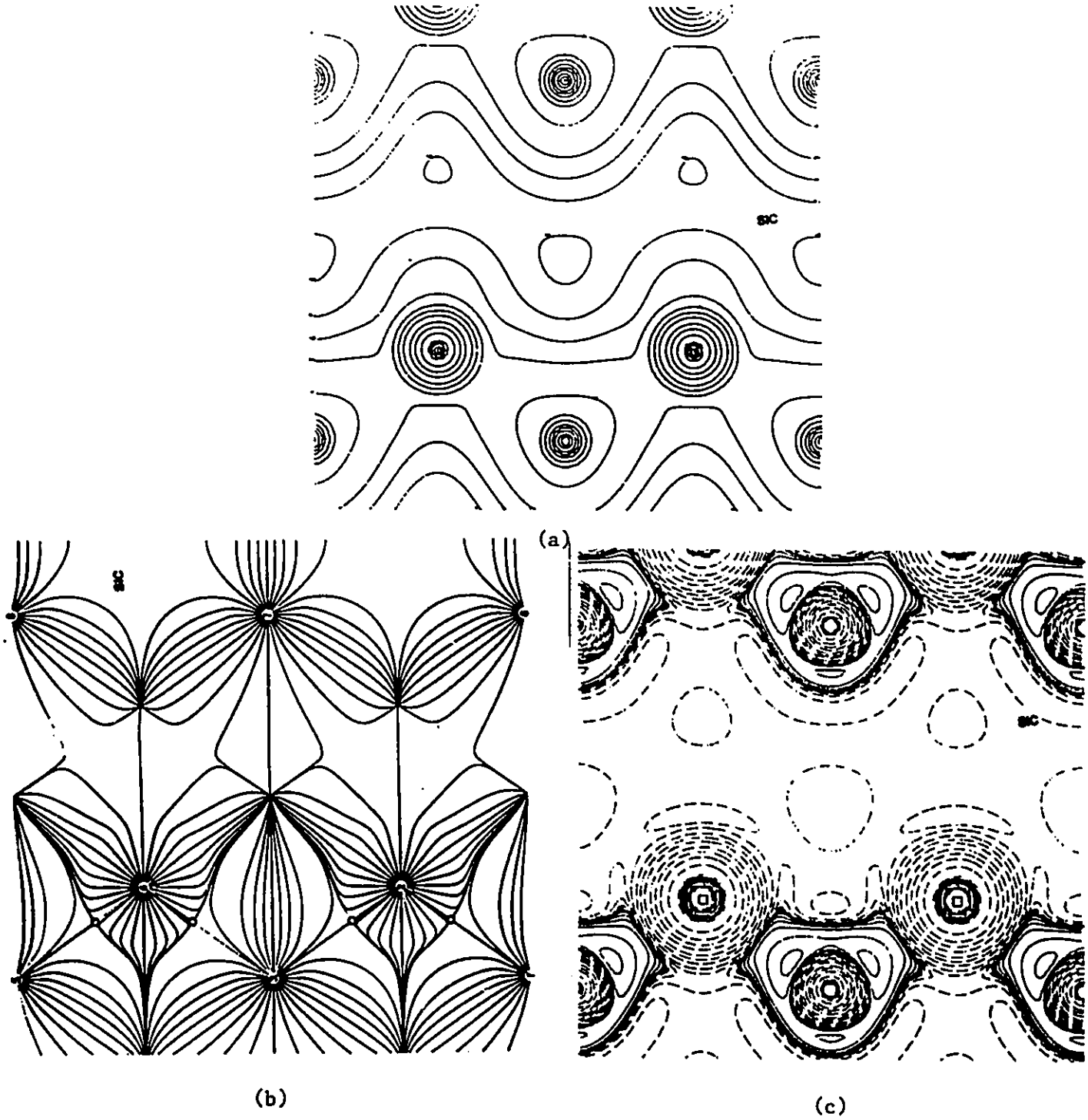

Fig. 3-11 The charge density (a), the gradient vector field (b) and the Laplacian (c) of the charge density on the (110) plane in SiC.

3.5.3 Comparison Between Crystal and Molecular Topological Properties

Table 3-9 shows the similarity of the C-C bond in diamond crystal and the molecules shown in Fig. 3-12. The central carbon atom in neo-pentane (Fig. 3-12(a)) has a similar tetrahedral environment as the carbon in diamond. The cage in adamantane $C_{10}H_{16}$ shown in Fig. 3-12(b) has a structure similar to the cage in diamond. It is interesting to note that the charge density and Laplacian at the C-C bond critical point are almost the same for both molecules and diamond when the charge density is calculated with the same basis set 621G* described in section 3.2.3. The bond critical point properties for both molecules, neo-pentane and adamantane $C_{10}H_{16}$, are also almost the same when the same basis set (631++G**) is used for the calculation. Table 3-10 gives a similar comparison for silicon crystal and molecule $Si(SiH_3)_4$.

Table 3-11 lists the charge density and Laplacian at the bond, ring and cage critical points for diamond and molecule $C_{10}H_{26}$. Both of table 3-10 and 3-11 show that the critical point properties change little when the same basis set is used for both molecule and crystal. This demonstrates that the long range interaction in diamond crystal has little effect on the charge density at the critical points. Therefore the charge distribution of an atom in a crystal is mainly determined by the interaction between the nearest and second nearest neighbouring atoms. The relatively invariant property of the charge distribution between an atom in a crystal and the atom in a relevant molecule provides a way to model solid state properties from atoms in molecules. In next chapter, we will demonstrate this by modelling the scattering properties of diamond with the central carbon atom in molecule neo-pentane.

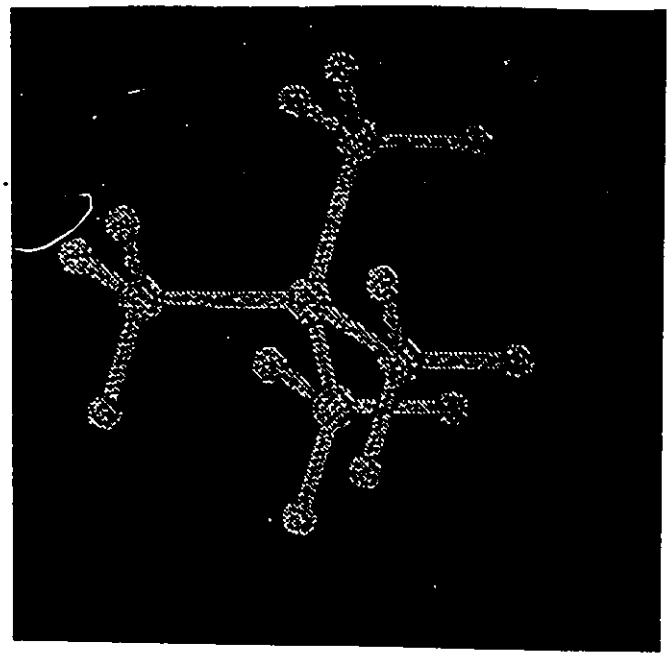

(a)

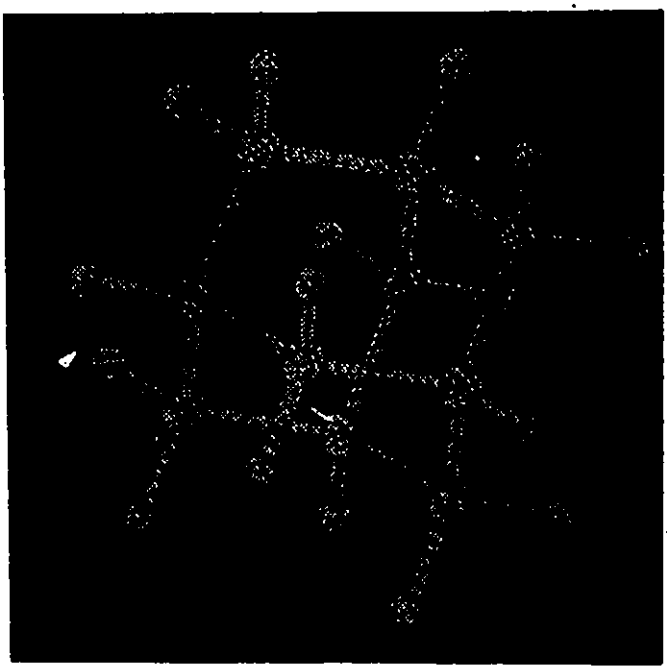

(b)

Fig. 3-12 Structures of (a) $C(CH_3)_4$ (b) $C_{10}H_{16}$. Both molecules have symmetry $\mathcal{T}_d$. The large spheres represent carbon atoms and the small ones denote the hydrogen atoms.

Table 3-9 Properties of C-C Bond Critical Point in Diamond, Neo-pentane and Cage $C_{10}H_{16}$

	ρ_b	$\nabla^2\rho_b$	$\lambda_1=\lambda_2$	λ_3
Diamond	0.263	-0.880	-0.500	0.119
$C(CH_3)_4$*(a)	0.262	-0.899	-0.502	0.104
Cage $C_{10}H_{16}$(b)	0.263	-0.905	-0.503	0.101
$C(CH_3)_4$*(b)	0.251	-0.647	-0.474	0.300
Cage $C_{10}H_{16}$(b)	0.251	-0.648	-0.474	0.299

* The C-C bond length in the molecules = 1.545Å which is as the same as the C-C bond length of diamond. The bond length of C-H is chosen to be 1.09Å which is the approximation of the C-H bond length in methane. The point symmetry of both the molecules in the table is T_d. The basis set for hydrogen is 631++G**. (a) The basis set for the C atoms in the molecule is the same as for diamond. (b) The basis set is 631++G**. The charge density is calculated from Gaussian 92.

Table 3-10 Si-Si Bond Critical Point in Silicon Crystal and Molecule $Si(SiH_3)_4$, the values in bracket of silicon are the properties for the (3,-3)critical points.

	ρ_b	$\nabla^2\rho_b$	$\lambda_1=\lambda_2$	λ_3
Silicon	0.0922(0.0935)	-0.0889(-0.17)	-0.0833(-0.085)	0.0776(-0.0002)
$Si(SiH_3)_4$*	0.0955	-0.176	-0.0928	0.0101

* The bond length of Si-Si in the molecule is chosen as the same as the Si-Si in silicon crystal. The Si-H bond length is taken to be 1.485Å which is the approximated bond length of SiH_4The point group of the molecule is T_d. The basis set for the molecule is 631G**.

Table 3-11 Comparison of the Critical Point Properties between Cage $C_{10}H_{26}$ and Diamond (notes (a) and (b) are the same as Table 3-9)

	ρ_b	$\nabla^2\rho_b$	ρ_r	$\nabla^2\rho_r$	ρ_c	$\nabla^2\rho_c$
Diamond	0.263	-0.880	0.0206	0.102	0.0128	0.0749
Cage $C_{10}H_{16}$(a)	0.263	-0.905	0.0194	0.101	0.0122	0.0716
Cage $C_{10}H_{16}$(b)	0.251	-0.648	0.0799	0.186	0.0128	0.0792

3.6 Correlation Between Physical and Topological Properties of the Crystal

Many physical and chemical properties are found to be empirically related to the charge density at the critical points for the molecular systems (Wiberg, et al, 1987; Bader, 1990). In metals, Eberthart et al (1991) found that the choice of a metal between bcc structure or fcc structure is related to the topological properties of the charge density, and the bulk modulus for the metal is related to the Laplacian of the charge density at the bond critical points. In this section, we will demonstrate that the binding energies, transverse frequencies, bulk moduli, and cleavage planes of diamond and zinc blende crystals can be related to the topological properties of ρ at the bond and cage critical points of the crystals.

3.6.1 Binding Energy and the Charge Density at the Bond critical Points

The binding energy of a crystal is defined as the difference between the total energies of the bulk and of the isolated atoms. Therefore the binding energy measures bonding strength in a crystal and should directly relate to the charge density ρ_b at the bond critical points. Table 3-12 shows that the larger the charge density at the bond critical point is, the larger the binding energy for the compounds considered here. Figure 3-13 show the same relation as Table 3-12. The interesting point in this figure is that the strong covalent compounds: diamond, BN and the relatively large ionic system SiC are on one straight line, the weak covalent silicon and relatively small ionic (see Table 3-7) and weak covalent interaction bonding systems: AlP and BP are on another line. This suggests that not only the bond charges relate to the bonding energy but also the ionicity.

Table 3-12 Binding Energies and The Charge Density at the Bond Critical Points

	C	BN	SiC	BP	Si	AlP
Binding Energy*	0.555	0.498	0.475	0.383	0.345	0.317
$\rho_b \times 10$	2.63	1.52	1.11	1.30	0.935	0.562

* The experimental binding energy is from Orlando, et al(1990).

3.6.2 Transverse Optical Frequencies and the Charge Density at Bond Critical Points

The vibrational frequency with respect to bond stretch is called the transverse optical frequency. The vibrational constant k is given by the the second derivative of the energy with respect to the bond displacement from its equilibrium. In the 'frozen-phonon' harmonic approximation it is given as

$$\nu = h^{-1}(m_e k/\mu)^{-1/2} \qquad (42)$$

where m_e and μ are the electron mass and the reduced mass of the unit cell respectively, h is Plank constant.

Table 3-13 shows the relation between the charge densities at the bond critical points and the frequencies of the crystals. As in the case of binding energies, the larger the charge density at the bond critical point, the larger is the frequency. The stretching force constant parallel to a bond in a crystal is proportional to the strength of the bond. Therefore, the stronger the bond, the larger the bond vibrational frequency.

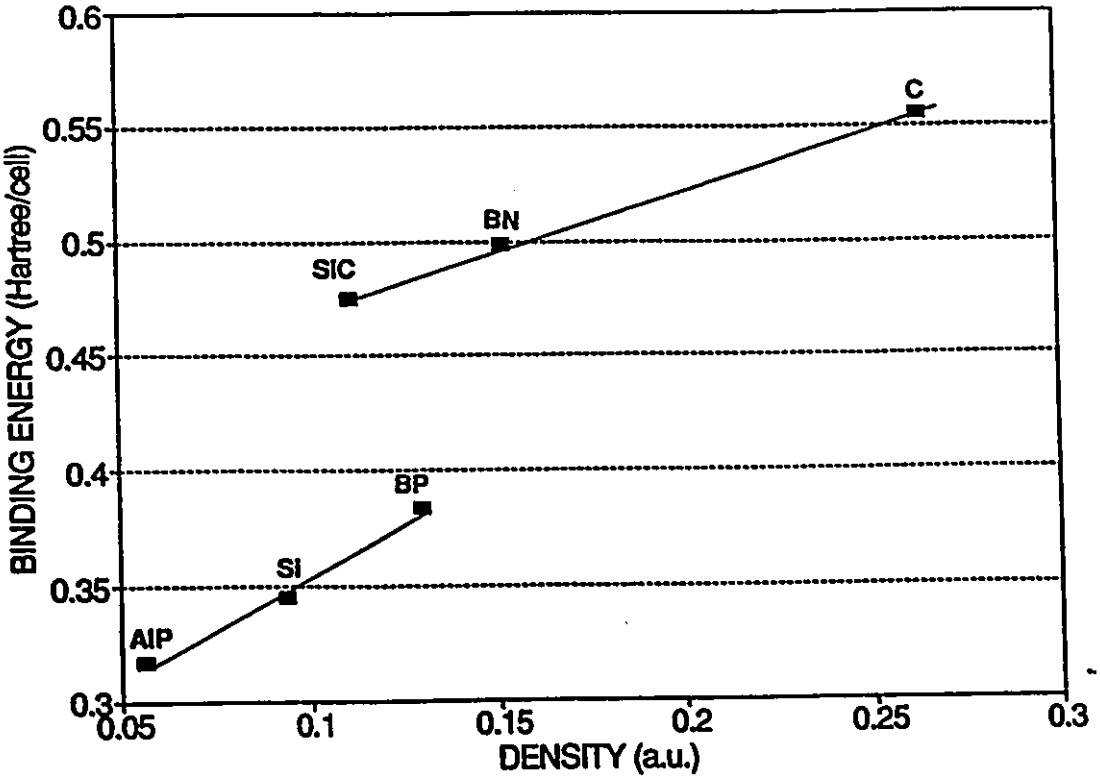

Figure 3-13 Binding energy vs charge density at the bond critical point

Table 3-13 Transverse Optical Frequencies and the Charge Densities at the Bond Critical Points

	C	BN	SiC	BP	Si	AlP
Frequency	39.9[a]	31.62[a]	23.86[a]	23.9[b]	15.53[a]	13.17[a]
$\rho_b \times 10$	2.63	1.52	1.11	1.30	0.935	0.562

[a] From Weyrich, et al (1988), [b] from Wentzcovitch, et al (1986).

3.6.3 Bulk Modulus and Laplacian of ρ

The bulk modulus or the modulus of volume elasticity is defined as the reciprocal of the coefficient of compressibility. Explicitly, it can written as

$$B = \frac{P_1 - P_2}{(V_1 - V_2)/V_1} \qquad (43)$$

where P_1, P_2; V_1, V_2 are the initial and final pressure and volume respectively. At zero temperature, the differential form of eqn (43) is (Cohen, 1985)

$$B = -VdP/dV = Vd^2E/dV^2 \qquad (44)$$

where V and E are the volume and energy, respectively, P is the pressure in crystal. In the cubic systems, B is related to the elastic constants by

$$B = (C_{11} + 2C_{12})/3$$

Bulk modulus is an important parameter for high-performance engineering materials (Liu and Cohen, 1989 and 1990). It determines the hardness of a cubic crystal.

Eberhart et al found that there exists a linear relation between the

parallel curvature of ρ at the metal-metal bond critical point in a metal and the bulk modulus of the metal. The metals which Eberhart et al have studied are closest packed structure, therefore the charge density at the bond critical point will play the dominant role in response to the external force on the crystal. However in diamond or zinc blende type structures, there exists more space inside the crystals. Therefore we would expect that the bulk moduli of these crystals would relate not only to the bonds but also to the cages in the crystals. Table 3-14 lists the bulk moduli, the Laplacian at the cage critical points and the charge densities at the bond critical points of the charge distributions in the crystals. This table shows the same trend of change for the bulk modulus and the Laplacian at cage critical point. Even though the physical mechanism is not clear , the studies of Eberhart et al and the present calculations do show there exists a close relation between the bulk modulus and the Laplacian of the charge distribution at critical points. The charge densities at the bond critical points and bulk moduli show the similar trend of change except for the order of SiC and BP. The large ionicity in SiC may account for the larger modulus of SiC than BP.

Table 3-14 Relation of the charge density at the bond critical point, the Laplacian of ρ at the Cage Critical point and Bulk Modulus

	C	BN	SiC	BP	Si	AlP
Bulk Modulus	443[a]	367[b]	224[a]	173[b]	99[a]	86[c]
$\nabla^2\rho_c\times100$	7.493	2.169	1.218	0.720	0.305	0.263
$\rho_b\times10$	2.63	1.52	1.11	1.30	0.935	0.562

a From Chang and Cohen (1987), b from Wentzcovitch, et al (1986), c from Zhang and Cohen (1987).

3.6.4 The Cleavage Planes of Diamond and Zinc Blende Compounds

Under an external force a crystal is split into two pieces. Usually a crystal exhibits a preferential cleavage plane. The cleavage property of a crystal is primarily determined by its crystal structure and is only secondarily related to chemical composition (Newnham, 1975). For example the cleavage plane for any closest packed metal is (110). However, for a metal with bcc structure, it is the (100) plane. The cleavage plane of diamond or silicon is (111), and for the zinc-blende compounds it is the (110) plane.

Based on the consideration of energy, there are three basic principles to determine the preferential cleavage plane. (1) The number of bonds to be broken should be as few as possible. (2) The charge density in the cleavage plane should be as low as possible. (3) The charges of the cleaved pieces should be neutral. From fig. 3-2, we can easily see that (111) plane must be the cleavage plane for diamond because (1) only one bond is broken per surface atom; (2) the (111) plane passing through the bond critical points has the lowest average charge density for the crystal because the plane contains the highest number of ring and cage critical points; (3) the neutral condition is obviously satisfied if the cleavage plane is the plane of minimum charge density. If (100) was the cleavage plane for diamond, then two bonds must be broken per surface atom. This does not satisfy principle (1). On the other hand, if (110) was the cleavage plane, the average charge density on this plane is higher than that on the (111) plane. This point can be seen clearer from fig. 3-14 (a). Points A(1/4,1/4,0), B(1/2,0,1/2) and C(0,1/2,1/2) (the origin is chosen as Table 3-2) are on the (110) plane $y=1/2 - x$. This plane does not pass through the ring or cage critical points. Therefore the charge

density must be higher than the (111) plane which passes the bond, ring and cage critical points.

For the polar zinc blende compounds, the situation is very different. Fig 3-14 (b) shows a BN cage structure unit. If the (111) plane is cleaved, the first principle is satisfied. However if the neutral condition is satisfied, then the condition of low charge density on the cleavage plane is not satisfied. If the low density condition is satisfied, then three same charged surface atoms are bonded to one atom beneath the surface (see fig. 3-14(b)), the energy of this structure should be high and therefore certainly should not be a stable structure. On the other hand, if zinc blende compounds cleave on (110) plane as shown in fig. 3-14 (c), both B and N atoms will appear on the cleaved surface and therefore the energy will be lower than the (111) cleaved surface. This shows that (110) plane should be the cleaved plane.

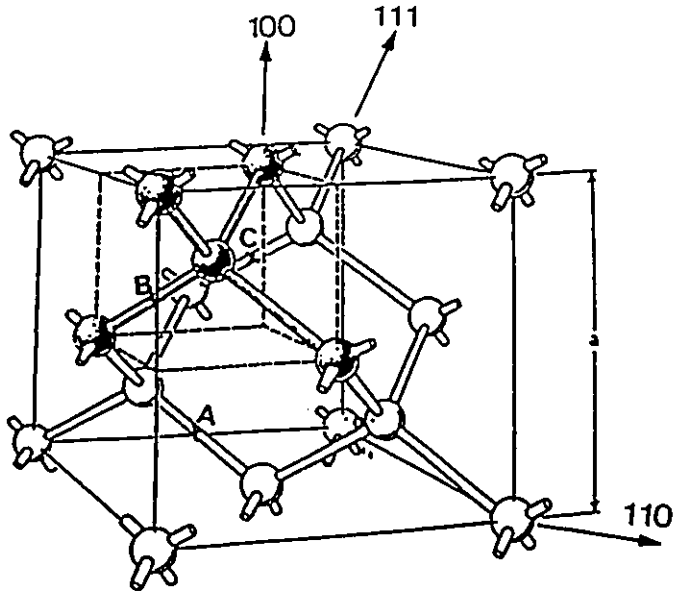

(a)

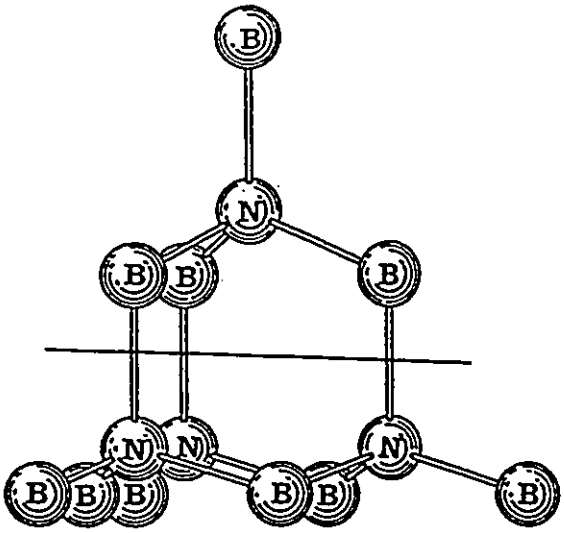

(b)

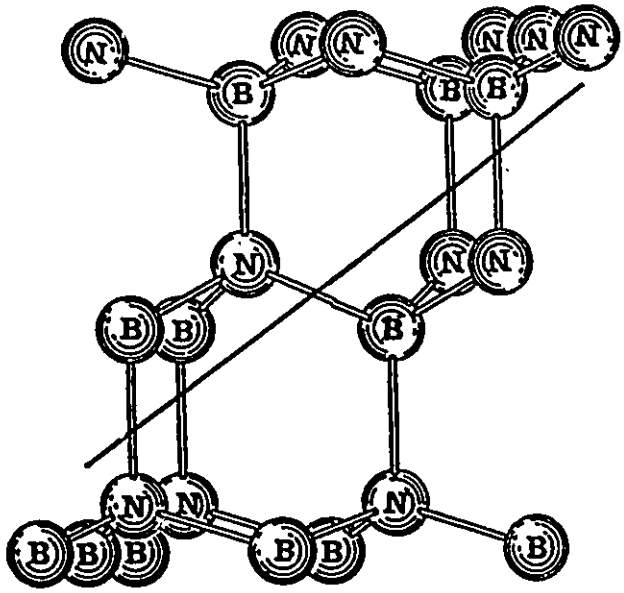

(c)

Fig. 3-14 (a) shows the directions of (100), (110) and (111) planes, points A, B and C are on a (110) plane; (b) (111) cleavage plane and (c) (110) cleavage plane.

3.7 Weak Interactions in Crystals

The properties of ρ at the bond critical points are not only able to classify the strong chemical interactions in crystals, they are also able to describe weak interactions, for example, second neighbor bonds and the bonds between molecules in a molecular crystal. We will demonstrate these interactions with ionic crystal LiF and molecular crystal CO_2. The structure of LiF crystal is shown in Fig. 3-15 which has the same type of structure of NaCl (rock salt). Fig 3-16 presents the gradient vector field on (100) plane of LiF. The first neighbor bond Li-F shown in this figure is strong ionic bonding. The characteristic properties for a ionic interaction bonding critical point are relatively small charge density and relatively large Laplacian. This can be seen from table 3-15. The electronic charge density at the nearest neighbor bond critical point is 0.019 which is smaller than ρ_b for those compounds listed in table 3-6. The positive Laplacian of ρ_b at this point shows that the depletion is dominant. The second neighbor bond shown in Fig. 3-16 is the bond between the neighboring fluorine atoms. The charge density (0.0092) at this bond critical point is very low as shown in Table 3-15 and therefore it represents a weak interaction between the fluorines. The Laplacian value (0.0612) and the parallel curvature (0.0781) at the second neighbor bond critical point are very close, therefore the charge depletion effect dominates in this weak interaction. A similar weak interaction exists in molecular crystals. Fig. 3-17 presents the gradient vector field of CO_2 molecular crystal for a plane on which the first- and second-neighbor bonds are shown. It is clear that the second neighbor bond is between the oxygens in two neighboring molecules. Table 3-16 lists the charge density and

Laplacian at the bond critical points. As a comparison, the corresponding properties for the single-molecule CO_2 are also listed in the table. We can see that the properties of C-O (1-st neighbor bond) are very similar between single-molecule and crystal. The second neighbor bond (O-O bond in crystal) is weak and the depletion is dominant as the fluorine-fluorine bond in LiF crystal.

Table 3-15 The Density and Laplacian of Ionic Crystal LiF at the Bond Critical Points. The charge density is calculated with the standard 621G basis set for F and the basis set from reference Dovesi, et al (1983) for Li. The geometry a = 4.02Å is from experiment (Wyckoff, 1965). The space group is $Fm3m$ (O_h^5, 225).

	1-st Neighbor Bond			2-nd Neighbor Bond		
	$\rho(\mathbf{r}_b)$	$\nabla^2\rho(\mathbf{r}_b)$	$\lambda_\parallel$	$\rho(\mathbf{r}_b)$	$\nabla^2\rho(\mathbf{r}_b)$	$\lambda_\parallel$
	0.0190	0.186	0.258	0.00915	0.0612	0.0781

Table 3-16 The Density and Laplacian of CO_2 Crystal and Molecule at the Bond Critical Points. Both molecule and crystal are calculated with the standard 621G basis set and with the experimental geometry (a=5.624Å). The space group of crystal CO_2 is $Pa\bar{3}$(T_h^6, 205)

	1-st Neighbor Bond			2-nd Neighbor Bond		
	$\rho(\mathbf{r}_b)$	$\nabla^2\rho(\mathbf{r}_b)$	$\lambda_\parallel$	$\rho(\mathbf{r}_b)$	$\nabla^2\rho(\mathbf{r}_b)$	$\lambda_\parallel$
Crystal	0.448	-0.554	1.91	0.00420	0.0284	0.0346
Molecule	0.449	-0.575	1.89			

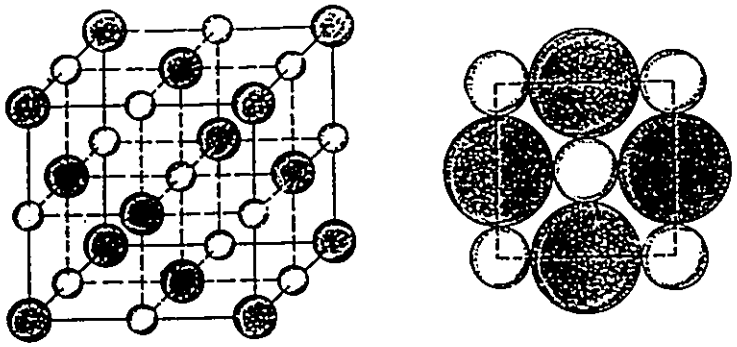

Fig. 3-15 The lithium fluoride structure. The dark spheres represent fluorine atoms while the light spheres represent Li. The panel to the right shows (100) plane containing the nuclei.

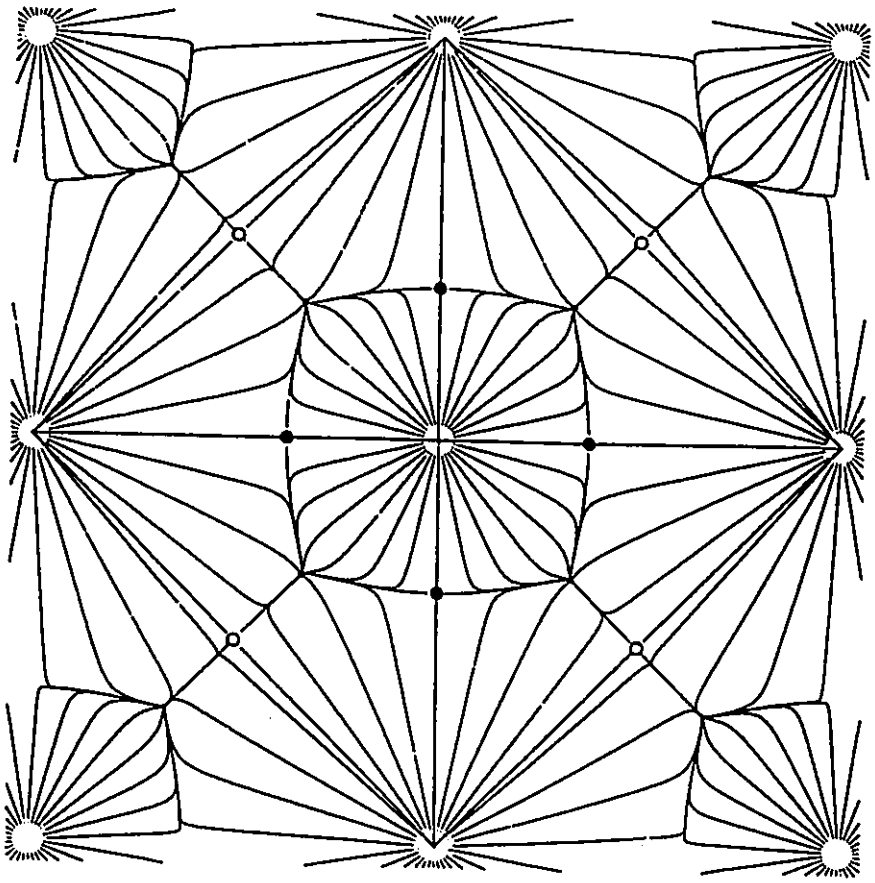

Fig. 3-16 The gradient vector field of lithium fluoride in the (100) plane shown in Fig. 3-15. The nearest neighbouring bond critical points are denoted by dots, the next nearest neighbouring bond critical points by small open circles. The nuclei are within the large open circles.

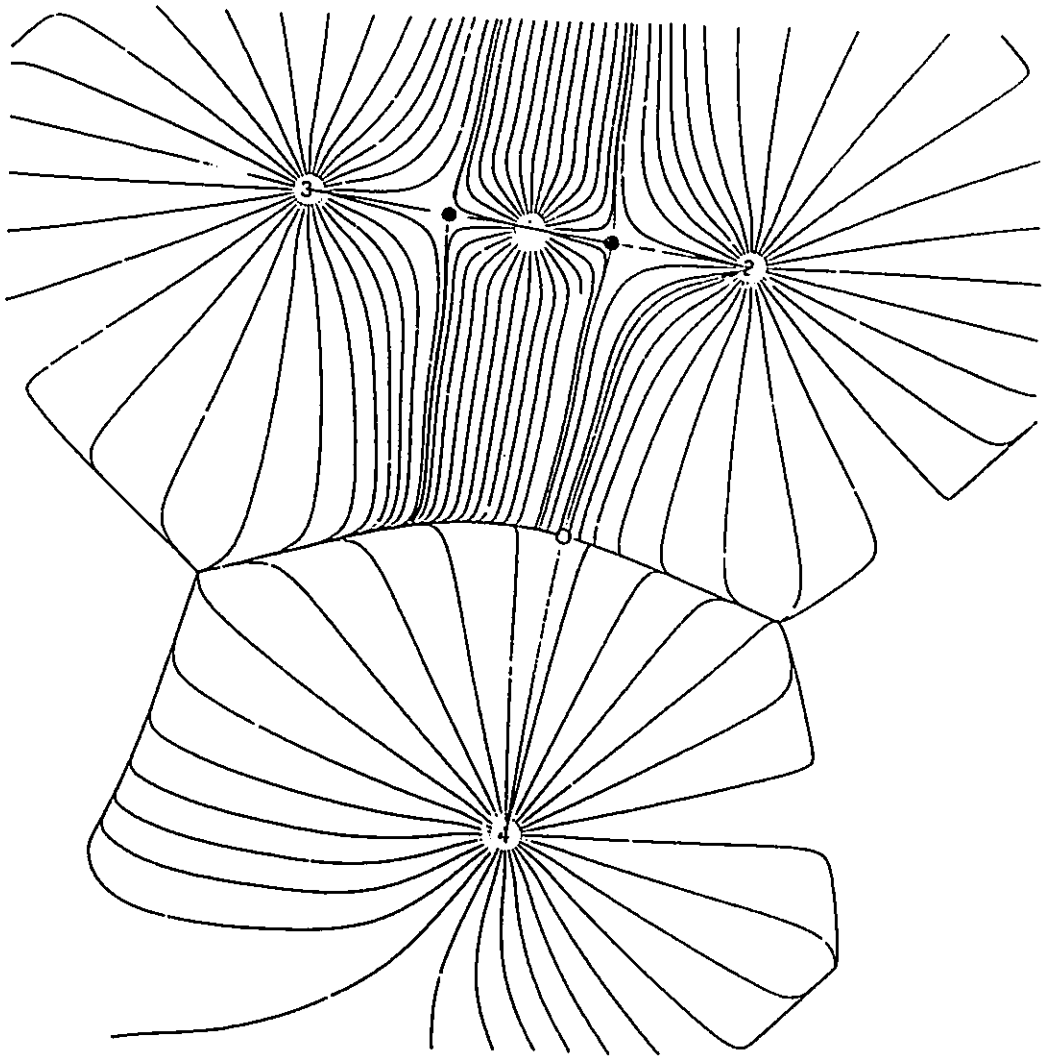

Fig. 3-17 The projected gradient vector field of crystal CO_2 shows the first neighbouring bond C-O and the second neighbouring bond O-O. The nearest neighbouring bond critical points are denoted by dots, the next nearest neighbouring bond critical points by small open circles. The number 1 labers the C nucleus, and the numbers 2 to 4 label oxygen nuclei. Trajectories from the basin of the carbon atom separate the oxygen atoms 3 and 4.

4. THE ATOMIC SCATTERING FACTOR OF CRYSTAL

Here the wave theory of X rays and the atomic theory of crystals come together, one of those surprising events to which physics owes its powers of conviction.

——Max von Laue, *History of Physics*

4.1. Introduction

When atoms are chemically bonded to one another, they have specific equilibrium separations and a corresponding electronic charge distribution that is determined by minimizing the total energy. In solid systems, these minimum energy states can be realized through the periodic arrangement of certain chemical "building blocks" such as atoms or chemical groups. To explore the structures of these crystalline states we require waves that interact with atoms and have wavelength comparable to the size of the atoms in the crystals. Nowadays a direct imaging of atomic structures is possible using the high-resolution electron microscope, the field ion microscope, or

the electron tunneling microscope. Nonetheless, when one wishes to determine an unknown structure, or make exact measurements of structural parameters, it is necessary to rely on diffraction experiments. To perform diffraction experiments one can make use of X-rays, electrons, neutrons or atoms. These various probes differ widely with respect to their interaction with the solid, and hence their areas of application are also different. Atoms and electrons are mainly used to probe surface structures because these material waves only interact with the surface atoms. Neutrons are scattered from the nuclei and therefore can be used for the determination of the nuclear arrangement of a crystal, particularly the positions of protons. However it is difficult not only to obtain the neutron beams but also to detect the scattered beams(Ibach and Luth, 1990), therefore the application is limited. X-ray photons are scattered from the charged particles, primarily the electrons in a solid and therefore can be used to determine both the atomic configurations as well as the electronic charge density of a crystal. Since it is easy to obtain the X-ray beams and straightforward to measure the diffracted waves, this method is widely used in practice.

A determination of a crystal structure by means of X-rays is a determination of the distribution of diffracting matter in the unit cell. At each point in the crystal there is a charge density $\rho(\mathbf{r})$ as the scattering source. A crystal structure is essentially a repeating pattern of electronic charge density and therefore the density function $\rho(\mathbf{r})$ can be expressed as the sum of a suitable Fourier series (eqn (27) of chapter 3):

$$\rho(\mathbf{r}) = \frac{1}{V} \sum_{-\infty}^{\infty} F(h,k,l) exp(-2\pi i \mathbf{H}\cdot\mathbf{r})$$

where h,k,l are integers, the summation is referred to the H=(h,k,l), and V is the volume of the unit cell. The Fourier component F(h,k,l) is called the structure factor whose modulus can be determined from the X-ray diffraction experiments. However, for the purpose of a Fourier analysis the value of the phase angle $\alpha(h,k,l)$ of the structure factor F(h,k,l), relative to the agreed origin, must also be known as accurately as possible. The phase angle $\alpha(h,k,l)$ depends on the nature and arrangement of the scattering source and on the direction of scattering. Even though many efforts were made for the experimental measurement of relative phase values (Bird, et at, 1987), they cannot be directly determined by experiment except in certain limited circumstances. Theory plays a vital role in not only the understanding of the diffraction phenomenon but also in the estimation of the phase angles of structure factors.

Two essential concepts of atoms in crystals and the periodic arrangements of the atoms enter the theory for the interpretation of the X-ray diffraction patterns and intensities. The arrangement of the atoms in a primitive unit cell of the real space determines the diffraction intensities and the interferences between the units determine the patterns. The key concept for the understanding of the X-ray diffraction by a crystal is *atom*. The observed scattered wave is considered as the supposition of the scattered waves from the individual atoms in the crystal. Therefore the structure factor can be decomposed into the atomic scattering factors. An atomic scattering factor, also called the atomic form factor, is a measure of the amplitude scattered by an atom when radiation of a given amplitude falls upon it. It is expressed in terms of the amplitude scattered by a single classical electron under the same

conditions, that is, by an electron scattering according to the Thomson formula (James, 1965; Sakurai, 1987). For the detailed determination of structures, comparison between the observed intensities of the spectra and those calculated from some assumed atomic arrangement plays an essential role; and such calculations cannot be made unless the atomic scattering factors of the atoms concerned in the structure are known.

In practice, the free spherical atomic scattering factors, listed in the International Crystallography Tables, are often used to estimate the scattering amplitudes F(h,k,l) and obtain the crystal structure. For most of the cases, the charge distribution in the core region changes very little between the free atom and the atom in a crystalline environment, and most of the scattering processes occur in this region, therefore the free atomic model can give a reasonable estimation to the phase values. Nevertheless this model does not take the atomic forms present in the crystal into account, and therefore it fails to explain those reflections with nonspherical effects, for example the (222) diffraction of diamond or silicon. Bragg (1915) stressed the necessity of taking into account the effect of the distribution of electrons over a region whose dimensions are comparable with the wavelength of the radiation employed, that is, an atomic dimension. He later made the following statement relating to the then recently observed (222) reflection in the diamond structure which is forbidden by the spherical atom model (Bragg, 1921): "It is necessary, therefore, to suppose that the attachment of one atom to the next is due to some directed property, and the carbon atom has four such special directions: as indeed the tetravalency of the atom might suggest." In this chapter we will establish an X-ray diffraction theory based

upon the theory of atoms in crystals. Our approach takes the atomic form and size into consideration and therefore eliminates the approximations in the conventional theory and provides an accurate interpretation of X-ray diffraction by a crystal. At the same time it also gives a precise meaning to the atoms in a crystal in X-ray diffraction theory.

The atom in our theory is defined as a basin in the real space bounded by the zero flux of the gradient vector field of the charge density in the crystal, as we have given in chapter one. The atom defined in this way not only has variational basis, as demonstrated in chapter one, but also preserves the local symmetry in the crystal. The total space can be filled by the translation of the atoms in a primitive unit cell. These properties of atoms in crystals will be illustrated in section 4.2. The transferability of atoms for the similar environmental systems will give this approach a practical value in modelling crystal properties. For example, the phases for the weak diffractions can be accurately estimated, whereas the free atomic models have difficulty with these estimations.

The quantum mechanical treatment of X-ray diffraction from a crystal is given in section 4.3. The relationship between charge distribution of a crystal and the X-ray diffraction intensity is derived from first principles. The lattice diffraction rules of the Laue equations and Bragg's law are obtained by the use of the translational symmetry of the crystal. In section 4.4, the conventional free atomic model is reviewed and a new approach based upon atoms in crystals is proposed. How to estimate the phase of a structure factor within our theory is also given in this section. Detailed comparisons of atomic form factors obtained from the free atomic model and atoms in

crystals are given in section 4.5. The last section is the conclusion. The possible future applications for the atoms in crystals are also discussed in this section.

4.2 Atoms in Crystals

Any decomposition of the space of a crystal which preserves the translational invariance of the lattice and which exhausts all of space is a mathematically acceptable partitioning. Physically however, and from the point of view of imposing boundary conditions in solving Schrödinger's equation for a periodic lattice, further constraints are required. This is exemplified in the classic study of metallic sodium by Wigner and Seitz (1933) who accomplished these goals by being the first to define an atom in a crystal. To obtain the wave function for the single valence electron in each sodium atom in this bcc crystal, they satisfied both the mathematical and physical requirements by surrounding each nucleus (in this case, each lattice point) by a space-filling polyhedron which had the additional desirable property of reflecting the local symmetry of the cubic point group. This was done by constructing planes at the midpoints of and perpendicular to the lines linking one nucleus to its two sets of equivalent neighbours. Because of the translational symmetry of the crystal, the derivative of the ground state wave function of a free electron must vanish perpendicular to each plane of the resulting fourteen-sided polyhedron representing the crystalline sodium atom, the condition $\nabla\psi\cdot\mathbf{n} = 0$. These atomic polyhedra generate the unit cell which most closely approximates a sphere and Wigner and Seitz imposed the boundary condition that $\partial\psi/\partial r = 0$ at the surface of the sphere of equal volume in obtaining the solutions to the radial wave equation for a spherically

symmetric potential. Slater (1934) later extended the method of Wigner and Seitz to take into account the actual shape of the crystal polyhedra.

For the nodeless one-electron ground state wave function, the periodic boundary condition satisfied by the polyhedric Wigner-Seitz cell, and indeed the condition defining the cell, can be alternatively stated in terms of the charge density $\rho(\mathbf{r})$ as

$$\nabla\rho(\mathbf{r})\cdot\mathbf{n}(\mathbf{r}) = 0 \qquad \forall\ \mathbf{r} \in S(\mathbf{r}) \tag{1}$$

where $\mathbf{n}(\mathbf{r})$ is the unit vector normal to the surface $S(\mathbf{r})$. This "zero-flux" surface condition is also the definition of an atom in a molecule (Bader, 1990) where $\rho(\mathbf{r})$ is, in general, the charge density of an N-electron system

$$\rho(\mathbf{r}) = N\int d\tau'\psi^*\psi \tag{2}$$

The integration symbol $\int d\tau'$ in eqn (2) implies a summation over all spin coordinates and the integration over the spatial coordinates of all electrons but one, whose coordinate is denoted by $\mathbf{r}$. This zero-flux surface condition leads to an exhaustive partitioning of the space of any system into a collection of mono-nuclear, that is, atomic fragments because of the dominant topological property exhibited by the electronic charge distribution - that in general (Bader, et al, 1981; Bader, 1990), it exhibits local maxima only at the positions of the nuclei, Fig. 3-5(a). Thus a nucleus acts as an attractor in the gradient vector field of the charge density (see, for example, Fig. 3-5(b)), leading to the definition of an atom as the the union of the attractor and its basin, the region of space traversed by the trajectories of $\nabla\rho$ terminating at the nucleus.

Equally important, eqn (1) is the boundary condition for the variational

definition of an open quantum subsystem, one that can undergo transfer of charge and energy across the surface separating it from the environment. The generalization of the energy functional used by Schrödinger (1926) to derive his "wave equation" to a subsystem denoted by Ω is (Bader and Nguyen-Dang, 1981; Bader, 1990)

$$\mathcal{S}[\psi,\Omega] = \int_\Omega d\mathbf{r}\int d\tau'\left\{ (\hbar^2/2m)\sum_i \nabla_i\Psi^*\cdot\nabla_i\Psi + (\hat{V} - E)\Psi^*\Psi \right\} \qquad (3)$$

where -E is substituted for the Lagrange multiplier required for the conservation of the norm. Variation of $\mathcal{S}[\psi,\Omega]$ including a variation of the surface bounding the subsystem Ω, subject to the natural boundary condition that

$$\nabla_i\psi\cdot\mathbf{n}(\mathbf{r}_i) = 0 \quad \text{or} \quad \nabla_i\psi^*\cdot\mathbf{n}(\mathbf{r}_i) = 0 \qquad \forall \ \mathbf{r}_i = \infty \qquad (4)$$

and to the variational constraint that

$$\delta\left\{ -(\hbar^2/4m)\int_\Omega \nabla^2\rho(\mathbf{r})d\mathbf{r} \right\} = 0 \qquad (5)$$

which is equivalent to imposing the surface condition of zero flux eqn (1) at every stage of the variation (Bader, 1990), yields Schrödinger's equations

$$\hat{H}\psi^* - E\psi^* = 0 \quad \text{or} \quad \hat{H}\psi - E\psi = 0 \qquad (6)$$

and the result (cc denotes complex conjugate)

$$\delta\mathcal{S}[\psi,\Omega] = (\hbar^2/4m)\oint dS(\Omega,\mathbf{r})\int d\tau'\left\{ \nabla\psi^*\delta\psi - \psi^*\delta\nabla\psi \right\}\cdot\mathbf{n}(\mathbf{r}) + cc \qquad (7)$$

The resultant variation in the functional may be re-expressed in terms of the flux in the variation of the vector current density $\mathbf{j}(\mathbf{r})$ where

$$\mathbf{j}(\mathbf{r}) = (\hbar/2mi)\int d\tau'\,(\psi^*\nabla\psi - (\nabla\psi^*)\psi) \qquad (8)$$

The flux through the surface bounding the atom is related to $\delta\mathcal{G}[\psi,\Omega]$ by

$$\delta\mathcal{G}[\psi,\Omega] = -(i\hbar/2)\oint dS(\Omega,\mathbf{r})\,\delta_\psi \mathbf{j}(\mathbf{r})\cdot\mathbf{n}(\mathbf{r}) + cc \qquad (9)$$

where $\delta_\psi \mathbf{j}$ denotes a variation of the current with respect to ψ. Satisfaction of eqn (9) for all $\delta\psi$ ensures that the energy is a minimum through the satisfaction of Schrödinger's equations, eqn (6).

The variational result for a subsystem given in eqn (9) is equivalent to earlier expressions obtained by Slepian (1949) and Kohn (1952) for the special problem of finding the propagating one-electron solutions to Schrödinger's equation in a periodic lattice. Slepian was able to show, by working in the domain of real pericdic trial functions ϕ, that one can minimize the integral $I(\phi,\Omega)$ defined as the expectation value of the Hamiltonian $\hat{H}$ over a region Ω,

$$I(\phi,\Omega) = \langle\phi,\hat{H}\phi\rangle_\Omega / \langle\phi,\phi\rangle_\Omega \qquad (10)$$

that the variation in $I(\phi,\Omega)$ was given by the one-electron version of the RHS of eqn (7) or (9). Since Slepian constrained the $\delta\psi$ to satisfy the same periodic boundary conditions as ψ and $\nabla\psi$, the surface flux in the variation of the current density vanishes and the energy is a minimum. The drawback of this approach, as pointed out by Kohn, is that it is restricted to the use of periodic trial functions. Kohn overcame this restriction by suggesting that the sum of $I(\phi,\Omega)$ and the surface integral of the variation in the vector current density, symmetrized with respect to the periodic boundaries, be made stationary. He was able to show that the unrestricted variation of this sum would vanish for the exact solution, but in this method the exact energy of the problem no longer provides a bound for $I(\phi,\Omega)$. Srebrenik (1975) was able to demonstrate that if the region Ω is bounded by a zero-flux surface as in eqn (1), then the variation of $\mathcal{G}[\phi,\Omega]$ for the one-electron case yields an

upper bound to the true ground state energy with no restrictions on ϕ other than it be square integrable and single-valued. More recent variational methods for cellular models have been developed by Ferreira and Leite (1978) and by Nesbet (1988) for space-filling cells of arbitrary shape. In Nesbet's approach the matching of the wave function external to the cell is accomplished using a linear operator $\mathcal{R}$ that produces function values on the surface when acting on gradients normal to the surface.

Cells satisfying the zero-flux boundary condition clearly possess special variaticnal properties. The general variational result given in eqn (9) demonstrates that these properties are not restricted to systems exhibiting the translational symmetries of crystals, but apply to all systems, that is, to any assembly of atoms. It can be demonstrated without difficulty that eqn (9) is in fact an extension of Schwinger's principle of stationary action (Schwinger, 1951) to a subsystem (Bader and Nguyen-Dang, 1981; Bader, 1990). If one identifies, as Schwinger does, the variations in ψ on the space-like boundaries of the system with the action of generators of infinitesimal unitary transformations, that is

$$\delta\psi = -(i\varepsilon/\hbar)\hat{G}\psi \quad \text{and} \quad \delta\psi^* = (i\varepsilon/\hbar)\hat{G}\psi^* \tag{11}$$

where $\hat{G} \equiv \hat{G}(\mathbf{r})$, then the variational principle can be expressed as

$$\delta\mathcal{G}[\psi,\Omega] = -(\varepsilon/2)\left\{ \oint dS(\mathbf{r}) j_G(\mathbf{r})\cdot\mathbf{n}(\mathbf{r}) + cc \right\} \tag{12}$$

where the current for the property G is given by

$$j_G(\mathbf{r}) = (\hbar/2mi)\int d\tau' \left\{ \psi^*\nabla(\hat{G}(\mathbf{r})\psi) - (\nabla\psi^*)\hat{G}(\mathbf{r})\psi \right\} . \tag{13}$$

The atomic statement of the Heisenberg equation of motion for the average value of the generator $\hat{G}$ is

$$(1/2)\{(i/\hbar)\langle\Psi|[\hat{H},\hat{G}]|\Psi\rangle_\Omega + cc\} = (1/2)\oint dS(\mathbf{r})\{\mathbf{j}_\Omega(\mathbf{r})\cdot\mathbf{n}(\mathbf{r}) + cc\} \quad (14)$$

and through its use one obtains the atomic statement of the principle of stationary action for a system in a stationary state

$$\delta\mathcal{G}[\Omega,\psi] = -(\varepsilon/2)\{(i/\hbar)\langle\Psi|[\hat{H},\hat{G}]|\Psi\rangle_\Omega + cc\} \quad (15)$$

where the averaging implied by $\langle\ \rangle_\Omega$ is the same as that given in eqn (3). In the time dependent case the variational principle is expressed in terms of the atomic Lagrangian $\delta\mathcal{L}[\Omega,\Psi,t]$ (Bader and Nguyen-Dang, 1981; Bader, 1990) as

$$\delta\mathcal{L}[\Omega,\Psi,t] = (\varepsilon/2)\{(i/\hbar)\langle\Psi|[\hat{H},\hat{G}]|\Psi\rangle_\Omega + cc\} \quad (16)$$

which can include systems in the presence of an electromagnetic field (Bader, 1989). In the Heisenberg representation, Schwinger's principle of stationary action can be expressed in the form of a variational statement of the Heisenberg equation of motion for the generator $\hat{G}$, as is evident from eqn (16). Eqns (15) and (16) apply to any region of space bounded by a zero-flux surface, a condition satisfied by the total system as well as by its constituent atoms. The Lagrangian and action integrals vanish for a system described by Schrödinger's equations. The atomic Lagrangian and action integrals share this same property, as a consequence of the zero-flux boundary condition eqn (1), and it is for this reason that the action integrals for the total system and for the atoms it contains exhibit similar variational properties (Bader and Nguyen-Dang, 1981; Bader, 1989; Bader, 1990).

The atomic variation principle, eqn (15) or (16) , determines that the subsystem expectation value of a Hermitian operator $\hat{A} = (i/\hbar)[\hat{H},\hat{G}]$ be given by

$$\lambda(\Omega) = (N/2)\{\langle\Psi,\hat{A}\Psi\rangle_\Omega + \langle\hat{A}\Psi,\Psi\rangle_\Omega\} = N\int_\Omega d\mathbf{r}\int d\tau'\,(1/2)\{\Psi^*\hat{A}\Psi + (\hat{A}\Psi)^*\Psi\} \quad (17)$$

that is, by taking the subsystem average of $N\mathrm{Re}\{\Psi^*\hat{A}\Psi\}$. Atomic properties are

additive. The sum of $A(\Omega)$ over all the atoms in a molecule yields the molecular average of the property A, including properties induced by applied external fields. The mechanics of an atom in a molecule are determined by the atomic variation principles. Important atomic theorems obtained using the following generators in eqns (15) or (16) are (Bader, 1990; Bader and Popelier, 1992); $\hat{G} = \hat{\mathbf{p}}$, generates a rigid translation of the coordinates of an electron over the basin of atom Ω and yields an expression which states that the Ehrenfest force acting on the electronic charge over the basin of the atom is balanced by the pressure exerted on each element of the atomic surface, where the pressure is determined by the quantum stress tensor; $\hat{G} = \hat{\mathbf{r}}\times\hat{\mathbf{p}}$, generates a rigid rotation of the coordinates over the atomic basin and yields the atomic torque theorem; $\hat{G} = \hat{\mathbf{r}}\cdot\hat{\mathbf{p}}$, generates a scaling of the coordinates over the atomic basin and yields the atomic virial theorem, enabling one to define an additive atomic energy; $\hat{G} = \hat{\mathbf{r}}$, generates a gauge transformation which demonstrates that the conservation of current over each atom is a consequence of gauge invariance when the system is in the presence of a magnetic field and yields the atomic current theorem.

Thus the special variational properties of atoms in a crystal or atoms in a molecule defined by the "zero-flux" surface lead to their identification as quantum subsystems. It is proposed that atoms in a crystal represent a generalization of the concept embodied in the original definition of a "Wigner-Seitz cell" and that this name be applied to a region of space in a solid satisfying the zero-flux boundary condition stated in eqn (1). This identification of a cell with a physical property of the system obviates a difficulty associated with the original construction of the polyhedric cell in

that it did not lead to a physically unique decomposition in cases where more than a single atom occupies a lattice point.

The shape of a Wigner-Seitz cell in diamond is illustrated in Fig. 4-1. The cell contains two carbon atoms. A carbon atom is defined by its four interatomic surfaces. Although it is possible to use the same recipe of bisecting the distances to the nearest neighbour lattice points, twelve in number for a fcc lattice, with perpendicular planes for the construction of a Wigner-Seitz cell (Slater, 1965), this construction does not reflect the form of the charge distribution nor the basic symmetry of the system at the atomic level. Each of the four interatomic surfaces which separates the basin of a given carbon atom of $\mathcal{T}_d$ symmetry from its four bonded neighbours is seen to be curved with the form of a chaise-longue, as are the six such surfaces bounding the linked pair of atoms that constitute the unit cell, where a *primitive unit cell, a Wigner-Seitz cell,* is now defined as *the smallest connected set of atomic basins which preserves the translational invariance of the lattice.* As a consequence of this definition, each atom exhibits the basic local symmetry of the crystal, while the symmetry of the cell reflects the translational invariance of the group of atoms which comprise the cell. Thus each carbon atom in diamond is of $\mathcal{T}_d$ symmetry while the Wigner-Seitz cell is of $\mathcal{D}_{3d}$ symmetry with the inversion centre at the bond critical point linking the two atoms of the cell. Diamond is assigned to the space group O_h^7 implying an octahedral symmetry (Slater, 1965). However, this assignment, obtained by placing the origin at a nucleus, necessitates the inclusion of a nonprimitive translation to carry one nucleus into the other, and the operations of $\mathcal{T}_d$ are subsequently converted into those of O_h by the inversion operation. Placing

the origin at the centre of symmetry obviates the need for the inclusion of nonprimitive translations and the point group reflecting only the spatial symmetry of the Wigner-Seitz cell is obtained, $\mathcal{D}_{3d}$ in the case of diamond. The definition of a Wigner-Seitz cell given here will always reflect the physical symmetry imposed on the cell by the distribution of charge throughout the crystal, a symmetry that will differ from that given by the space group, if the space group contains nonprimitive translations.

The word *connected* appearing in the definition of a unit cell is used in the usual sense to imply that the set of atoms comprising the cell are bonded to one another (Bader, Nguyen-Dang and Tal,1981; Bader, 1990). The separatrix shared by the basins of neighbouring atoms contains a critical point in ρ, $\nabla\rho(\mathbf{r}_c) = 0$, at which the Hessian of ρ possesses one positive and two negative eigenvalues, a (3,-1) critical point. The eigenvectors associated with the two negative eigenvalues (curvatures of ρ) define a two-dimensional manifold, the zero-flux interatomic surface, composed of the trajectories of $\nabla\rho$ which terminate at the critical point at $\mathbf{r}_c$, the point at which $\rho(\mathbf{r})$ attains its maximum value in the surface, Fig. 4-1. The single eigenvector associated with the positive eigenvalue defines a unique pair of trajectories, perpendicular to the surface at $\mathbf{r}_c$ and along which ρ is a minimum at $\mathbf{r}_c$, each terminating at a nucleus of one of the neighbouring atoms. They define a line linking the nuclei of the two atoms sharing a common surface along which the charge density is a maximum with respect to any neighbouring line, Fig. 3-5. Such a line when present in an equilibrium geometry is called a bond path and its presence fulfills the necessary and sufficient conditions that two atoms so linked be bonded to one another (Bader, 1990). The network of bond paths

so generated, the molecular structure, has been shown to recover the bonded structures of molecules. In the diamond structure, each carbon nucleus is linked to four neighbouring nuclei by bond paths, as anticipated by Bragg (1921).

The trajectories defining the interatomic surface originate at cage and ring critical points, (3,+3) and (3,+1) critical points respectively. One easily shows using the Poincaré-Hopf relation governing the type and number of critical points which can co-exist for an extended system, that an atom at a bcc lattice point is linked by bond paths to the six next nearest neighbours as well as to its eight nearest neighbours. This structure would yield an atom bounded by fourteen interatomic surfaces in agreement with the original definition of a Wigner-Seitz cell for a bcc lattice. Eberhart et al (1991) have found this pattern of bond paths, that is, this *structure*, to be predicted by the calculated charge distributions of bcc transition metals and have also demonstrated the absence of bond paths to second nearest neighbours in metals possessing the fcc lattice, a result again in agreement with the Poincaré-Hopf relation. These same authors find relationships between the local properties of the charge density at the bond critical point and bulk properties of the metal. The details of the topological analysis of a crystal charge density is the subject of another paper, what is important here is that the topology defines quantum subsystems and their connectivity.

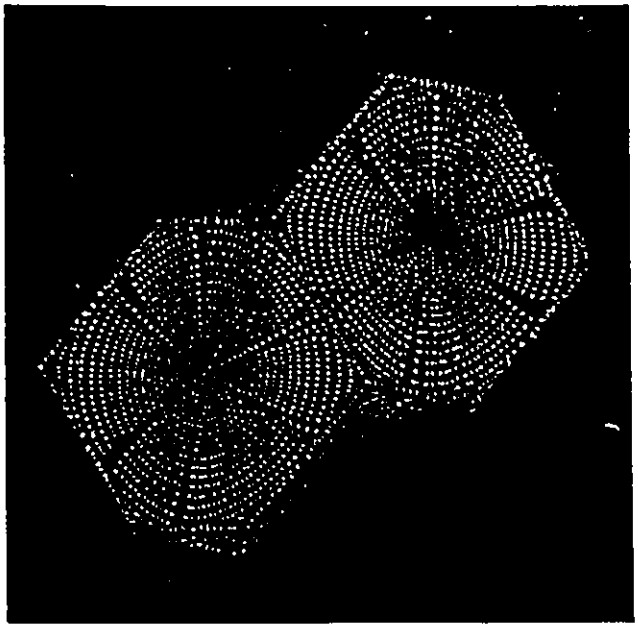

(a)

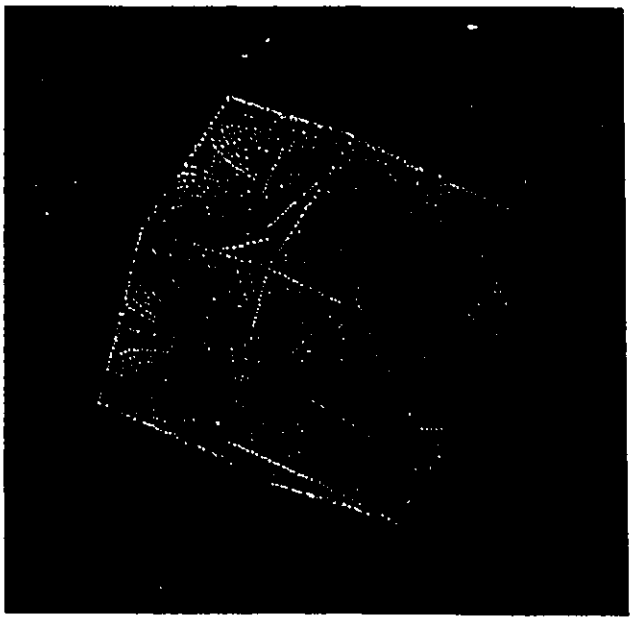

(b)

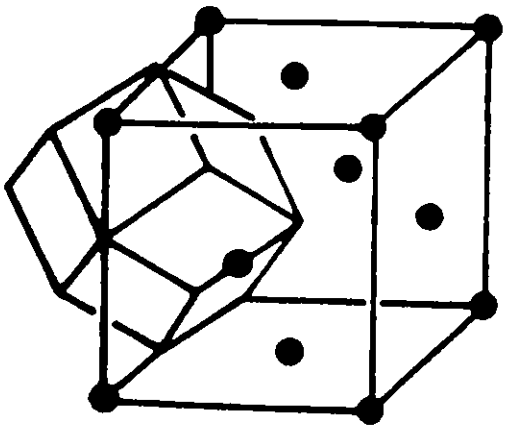

(c)

Fig. 4-1 Wigner-Seitz cells: (a) a primitive cell in diamond, (b) the superposition of the two carbon atoms in a primitive cell, (c) the Wigner-Seitz cell of fcc lattice (from reference Burns and Glazer, 1990).

4.3. Quantum Treatment of X-Ray Scattering from Crystal

The classical treatment of X-ray scattering from a crystal can be found in many X-ray crystallography text books, for example, James' book (1965). Chang (1984) had an excellent review on the developments of X-ray diffraction theory and experiment in his book "*Multiple Diffraction of X-Rays in Crystals*". The conventional quantum treatment (James, 1965; Chang, 1984) of X-ray diffraction takes the scattering electrons as quantum particles and treats the X-rays as a classical electromagnetic field. In this section, we will treat both electrons of a crystal and the X-ray photons as quantum particles.

The interaction between the electrons in a crystal and X-rays can be written as

$$H_{int} = \sum_i \left\{ -\frac{e}{2mc}\{\mathbf{p}_i\cdot\mathbf{A}(\mathbf{x}_i,t) + \mathbf{A}(\mathbf{x}_i,t)\cdot\mathbf{p}_i\} + \frac{e^2}{2mc^2}\mathbf{A}(\mathbf{x}_i,t)\cdot\mathbf{A}(\mathbf{x}_i,t) \right\} \qquad (18)$$

where $\mathbf{p}_i$, e and m are, respectively, the momentum operator, charge and mass of electron i; $\mathbf{A}$ is the vector potential operator of X-ray which can be expressed as (Sakurai, 1987)

$$\mathbf{A}(\mathbf{x},t) = \frac{1}{\sqrt{V}}\sum_k\sum_\alpha c\sqrt{\frac{\hbar}{2\omega}}[a_{k,\alpha}\boldsymbol{\varepsilon}^{(\alpha)}e^{i\mathbf{k}\cdot\mathbf{x}-i\omega t} + a^+_{k,\alpha}\boldsymbol{\varepsilon}^{(\alpha)}e^{-i\mathbf{k}\cdot\mathbf{x}+i\omega t}] \qquad (19)$$

where the quantization of $\mathbf{A}$ is according to the periodic boundary conditions enclosed in a box taken to be a cube with side $L = V^{1/3}$; α (α = 1 or 2) denotes polarization, $\boldsymbol{\varepsilon}^{(\alpha)}$ and $\hbar\mathbf{k}$ are, respectively, polarization vector and momentum of a photon in state $|\mathbf{k},\alpha\rangle$; $\omega = |\mathbf{k}|c$; $a_{k,\alpha}$ and $a^+_{k,\alpha}$ are annihilation and creation operators of photons in state $|\mathbf{k},\alpha\rangle$. The polarization vectors $\{\boldsymbol{\varepsilon}^{(1)}, \boldsymbol{\varepsilon}^{(2)}\}$ are the two directions orthogonal to the propagation direction of

light $\mathbf{k}/|\mathbf{k}|$.

The single photon state of the incident X-ray and the electronic state of the crystal before scattering are assumed, respectively, as $|\mathbf{k},\alpha\rangle$ and $|\Psi\rangle$. Therefore the initial state of the scattering system can be written as $|i\rangle = |\mathbf{k},\alpha;\Psi\rangle$. According to the perturbation theory, at time t after the interaction H_{int}, the amplitude of the system in state $|f\rangle = |\mathbf{k}',\alpha';\Psi'\rangle$ can be approximated by (to first order)

$$c_f^{(1)} = 1/(i\hbar)\int_0^t dt'\langle f|H_{int}|i\rangle\, e^{i\tilde{\omega}t'} \qquad (20)$$

where $|i\rangle = |\mathbf{k},\alpha;\Psi\rangle$, and $\tilde{\omega} = (E_f - E_i)/\hbar$.

In this section only elastic scattering will be considered. For the elastic scattering, $|\Psi'\rangle = |\Psi\rangle$ and $|\mathbf{k}'| = |\mathbf{k}|$, that is no photon will be absorbed by the crystal during scattering. There is no contribution for the first two terms of H_{int} in eqn (18) to the first order amplitude $c_f^{(1)}$, because these two terms are related to the photon absorption or emission of the crystal. This yields

$$c_f^{(1)} = \frac{e^2}{2i\hbar mc^2}\int_0^t dt'\langle f|\sum_i \mathbf{A}(\mathbf{x}_i,t')\cdot\mathbf{A}(\mathbf{x}_i,t')|i\rangle\, e^{i\omega t'}$$

$$= \frac{e^2}{2i\hbar mc^2}\int d\mathbf{x}\rho(\mathbf{x})\int_0^t dt' e^{i\omega t'}\langle \mathbf{k}',\alpha'|\ \mathbf{A}(\mathbf{x},t')\cdot\mathbf{A}(\mathbf{x},t')|\mathbf{k},\alpha\rangle \qquad (21)$$

$\mathbf{A}(\mathbf{x},t)\cdot\mathbf{A}(\mathbf{x},t)$ has typical terms aa, aa^+, a^+a, a^+a^+. The non-zero terms of $\langle \mathbf{k}',\alpha'|\ \mathbf{A}(\mathbf{x},t)\cdot\mathbf{A}(\mathbf{x},t)|\mathbf{k},\alpha\rangle$ are $\langle \mathbf{k}',\alpha'|\ a_{k,\alpha}a^+_{k',\alpha'}\ |\mathbf{k},\alpha\rangle$ (= 1), $\langle \mathbf{k}',\alpha'|\ a^+_{k',\alpha'}a_{k,\alpha}\ |\mathbf{k},\alpha\rangle$ and $\langle \mathbf{k}',\alpha'|\ a^+_{k'',\alpha''}a_{k'',\alpha''} + a_{k'',\alpha''}a^+_{k'',\alpha''}\ |\mathbf{k},\alpha\rangle$ which only contributes to the nonscattering process, that is $|\mathbf{k}',\alpha'\rangle = |\mathbf{k},\alpha\rangle$. Therefore the scattering amplitude given by eqn (21) is

$$c_f^{(1)} = \frac{e^2}{2i\hbar mc^2}\int d\mathbf{x}\rho(\mathbf{x})\int_0^t dt' e^{i\omega t'}$$

$$\langle \mathbf{k}',\alpha' | \frac{\hbar c^2}{2V\sqrt{\omega'\omega}} \varepsilon^{(\alpha')}\cdot\varepsilon^{(\alpha)} e^{i(\mathbf{k}-\mathbf{k}')\cdot\mathbf{x}-i(\omega-\omega')t'} a^+_{\mathbf{k}',\alpha'} a_{\mathbf{k},\alpha} + a_{\mathbf{k},\alpha} a^+_{\mathbf{k}',\alpha'} | \mathbf{k},\alpha$$

$$= \frac{e^2}{2i\hbar mc^2}\int d\mathbf{x}\rho(\mathbf{x})\int_0^t dt' e^{i\omega t'} \frac{2\hbar c^2}{2V\sqrt{\omega'\omega}} \varepsilon^{(\alpha')}\cdot\varepsilon^{(\alpha)} e^{i(\mathbf{k}-\mathbf{k}')\cdot\mathbf{x}-i(\omega-\omega')t'}$$

$$= \frac{e^2}{2iVm\sqrt{\omega'\omega}} \mathcal{F}(\mathbf{k}-\mathbf{k}')\varepsilon^{(\alpha')}\cdot\varepsilon^{(\alpha)}\int_0^t dt' e^{i(\omega-(\omega-\omega'))t'} \qquad (22)$$

where

$$\mathcal{F}(\mathbf{k}-\mathbf{k}') = \int d\mathbf{x}\rho(\mathbf{x}) e^{i(\mathbf{k}-\mathbf{k}')\cdot\mathbf{x}} \qquad (23)$$

is the Fourier transformation of the charge distribution of the crystal. The probability to transfer from state $|\mathbf{k},\alpha;\Psi\rangle$ to $|\mathbf{k}',\alpha';\Psi\rangle$ is

$$|c_f^{(1)}|^2 = 2\pi\left[\frac{e^2}{2Vm\sqrt{\omega'\omega}}\right]^2 |\mathcal{F}(\mathbf{k}-\mathbf{k}')\varepsilon^{(\alpha')}\cdot\varepsilon^{(\alpha)}|^2 t\delta(\omega-(\omega-\omega')) \qquad (24)$$

where the formula

$$\lim_{\alpha\to 0} 1/\pi \frac{\sin^2(\alpha x^2)}{\alpha x^2} = \delta(x)$$

has been used.

For the scattered X-ray, the allowed photon states(degeneracy) in an energy interval $[\hbar\omega, \hbar(\omega+d\omega)]$ at the solid angle element $d\Omega$ is (Sakurai, 1987)

$$\rho(\hbar\omega)d\Omega = \frac{V\omega^2 d\Omega}{(2\pi)^3\hbar c^3} \qquad (25)$$

Therefore the total transition probability per unit time into a solid angle element is

$$P d\Omega = \int d(\hbar\omega)\,|c_f^{(1)}|^2/t\rho_{(\omega)}\,d\Omega$$

$$=2\pi\left[\frac{e^2}{2Vm\sqrt{\omega'\omega}}\right]^2 |\mathcal{F}(\mathbf{k}-\mathbf{k}')\varepsilon^{(\alpha')}\cdot\varepsilon^{(\alpha)}|^2\frac{V\omega^2 d\Omega}{(2\pi)^3c^3} \qquad (26)$$

The differential cross section is obtained by the total transition probability in a unit solid angle $P=P(\Omega)$ divided by the photon flux, which is c/V since there is one photon in the normalization box of volume V

$$d\sigma/d\Omega=P/(c/V)$$

$$=\left[\frac{e^2}{4\pi c^2 m}\right]^2 |\mathcal{F}(\mathbf{k}-\mathbf{k}')\varepsilon^{(\alpha')}\cdot\varepsilon^{(\alpha)}|^2$$

$$=T_0\ |\mathcal{F}(\mathbf{k}-\mathbf{k}')|^2 \qquad (27)$$

where

$$T_0 = \left[\frac{e^2}{4\pi c^2 m}\right]^2 |\varepsilon^{(\alpha')}\cdot\varepsilon^{(\alpha)}|^2 \qquad (28)$$

is Thomson scattering differential cross section (Sakurai, 1987), which is assumed that the electromagnetic wave scattered by one electron sitting at the origin. Equation (27) states that the scattered X-ray strength is proportional to the square of $|\mathcal{F}(\mathbf{S})|=|\mathcal{F}(\mathbf{k}-\mathbf{k}')|$ where $\mathbf{S}=\mathbf{k}-\mathbf{k}'$. $\mathcal{F}(\mathbf{S})$ is the Fourier transformation of the charge distribution of the crystal. For a crystal, the Bravais lattice points are related through translation

$$\mathcal{T}(lmn)=l\mathbf{a}+m\mathbf{b}+n\mathbf{c} \qquad (29)$$

where l,m,n are integers. Therefore $\mathcal{F}(\mathbf{S})$ can be divided into the contributions by the periodically repeating units related by symmetry translation $\mathcal{T}(lmn)$

$$\mathcal{F}(\mathbf{S}) = \sum_{lmn}\int_{\Omega_{lmn}} d\mathbf{x}\rho(\mathbf{x})\,e^{i\mathbf{S}\cdot\mathbf{x}} \qquad (30)$$

If we assume

$$F(\mathbf{S}) = \int_{\Omega_{000}} d\mathbf{x}\rho(\mathbf{x})e^{i\mathbf{S}\cdot\mathbf{x}} \tag{31}$$

Then by the symmetry, eqn (30) can be rewritten as

$$\mathcal{F}(\mathbf{S}) = F(\mathbf{S})\sum_{lmn} e^{i\mathbf{S}\cdot(l\mathbf{a}+m\mathbf{b}+n\mathbf{c}\mathbf{x})} \tag{32}$$

The summation in eqn (15) can be worked out, this yields

$$\mathcal{F}(\mathbf{S}) = F(\mathbf{S})\frac{1-exp(iN_1\mathbf{S}\cdot\mathbf{a})}{1-exp(i\mathbf{S}\cdot\mathbf{a})}\frac{1-exp(iN_2\mathbf{S}\cdot\mathbf{b})}{1-exp(i\mathbf{S}\cdot\mathbf{b})}\frac{1-exp(iN_3\mathbf{S}\cdot\mathbf{c})}{1-exp(i\mathbf{S}\cdot\mathbf{c})} \tag{33}$$

where the total lattice points $N=N_1N_2N_3$ are assumed. Multiplying eqn(33) by its conjugate expression, we obtain

$$|\mathcal{F}(\mathbf{S})|^2 = |F(\mathbf{S})|^2\frac{\sin^2(N_1\mathbf{S}\cdot\mathbf{a}/2)}{\sin^2(\mathbf{S}\cdot\mathbf{a}/2)}\frac{\sin^2(N_2\mathbf{S}\cdot\mathbf{b}/2)}{\sin^2(\mathbf{S}\cdot\mathbf{b}/2)}\frac{\sin^2(N_3\mathbf{S}\cdot\mathbf{c}/2)}{\sin^2(\mathbf{S}\cdot\mathbf{c}/2)} \tag{34}$$

The value of the fraction $\dfrac{\sin^2(N_1\mathbf{S}\cdot\mathbf{a}/2)}{\sin^2(\mathbf{S}\cdot\mathbf{a}/2)}$ changes from N_1^2 to zero when $\mathbf{S}\cdot\mathbf{a}$ changes from $h\pi$ to $h\pi\pm\pi/N_1$. Between each pair of main maxima corresponding to successive integral values of h are $N_1 - 2$ subsidiary maxima. The other maxima fall off very rapidly(James, 1965). In practical cases, N_1 is at least several thousand, therefore the fraction has appreciable values only for values of $\mathbf{S}\cdot\mathbf{a}$ that are very nearly integral multiples of π. This yields the conditions for $|\mathcal{F}(\mathbf{S})|^2$ with a maximum value

$$\begin{aligned}\mathbf{S}\cdot\mathbf{a} &= 2h\pi\\ \mathbf{S}\cdot\mathbf{b} &= 2k\pi\\ \mathbf{S}\cdot\mathbf{c} &= 2l\pi\end{aligned} \tag{35}$$

where h,k and l are integers. These three condition equations, also called

Laue equations, directly lead to the Bragg equation

$$2d(hkl)\sin\vartheta = \lambda \qquad (36)$$

where d(hkl) is the distance of the lattice plane, ϑ is half of the angle between the incident and scattered waves, and $\lambda = 2\pi/|\mathbf{k}|$ is the wavelength of the X-ray. The Bragg equation is used to determine the lattice structure of a crystal. The structure within the primitive unit cell is determined by $F(\mathbf{S})$. By the conditions in eqn (35), the structure factor on the diffraction direction, $F(\mathbf{H})$, can be written as,

$$F(\mathbf{H}) = F(hkl) = \int_{\Omega_{000}} d\mathbf{x}\rho(\mathbf{x})e^{2\pi i(hx+ky+lz)} \qquad (37)$$

Ω_{000} is the region of the unit cell (0,0,0).

4.4. Atomic Form Factor in a Crystal

4.4.1 Conventional Models

In a practical implementation, the structure factor given in eqn (37) is generally replaced by some general discrete-atom version, that is $F(\mathbf{S})$ is expressed in terms of the atomic contributions from the atoms in the unit cell. The conventional treatment follows by expressing the charge distribution as a supposition of 'atomic' distributions referred to the j-th nucleus in the unit cell. By specifying the reference nuclear positions as $\mathbf{r}_j$ and the associated 'atomic' electronic charge densities as ρ_j', the total distribution is assumed to be the supposition of ρ_j'

$$\rho(\mathbf{r}) = \sum_j \rho_j'(\mathbf{r} - \mathbf{r}_j) \qquad (38)$$

Using (38), eqn (37) yields

$$F(\mathbf{H}) = \sum_j f_j(\mathbf{H}) \exp(2\pi i \mathbf{H}\cdot\mathbf{r}_j) \qquad (39)$$

where $\mathbf{r}_j$ has fractional coordinates and $f_j(\mathbf{H})$ is identified as the atomic scattering factor.

$$f_j(\mathbf{H}) = \int \rho_j'(\mathbf{r}) \exp(2\pi i \mathbf{H}\cdot\mathbf{r}) d\mathbf{r} \qquad (40)$$

The approximation of replacing the integral domain from a translational unit cell to the whole space has been made for deriving eqns (39) and (40).

In the usual least square refinements, the continuous electron density of the crystal is resolved into neutral and spherical atomic contributions

$$\rho_0(\mathbf{r}) = \sum \rho_j^a(\mathbf{r}-\mathbf{r}_j) \qquad (41)$$

where the summation is over all the atoms and $\rho_j^a(\mathbf{r})$ is the electron density of atom j which is considered as a free atom in vacuum. With $\rho_0(\mathbf{r})$, one can calculate the theoretical scattering factor F_T by eqns (39) and (40). By fitting the calculated F_T to the experimental scattering factor F_E, the equilibrium configuration of the crystal can be obtained. Since the strong diffractions are caused by the scattering of X-ray from the core regions of the atoms in crystals, the free spherical atomic model is reasonable for these strong diffractions. However the spherical model cannot explain those diffractions from the nonspherical part of the charge distribution in the crystal, it is this part that is the most chemically and physically interesting. To reveal the asphericity of the valence electron density due to chemical bonding, one needs to calculate the deformation density

$$\delta\rho(\mathbf{r}) = \rho_E(\mathbf{r}) - \rho_0(\mathbf{r}) \qquad (42)$$

where $\rho_E(\mathbf{r})$ is the charge density calculated from the observed diffraction factors.

Another model used to reveal the aspherical atoms in crystal, called the multipole model, directly assumes that the charge distribution $\rho_i^a(\mathbf{r})$ is not spherical and that the aspherical part has some flexibility to be refined (Dawson, 1967; Stewart, 1969-1976). Many procedures have been proposed to implement the refinement, for example, the Pop procedure (Epstein, et al, 1982; Craven, et al, 1987), the Molly procedure (Hansen and Coppens, 1978) and the Hirshfeld's implementation (Hirshfeld, 1971 and 1977). Generally, the charge density of an atom in the crystal is written as

$$\rho^a(\mathbf{r}) = \rho_s^a(\mathbf{r}) + \delta\rho^a(\mathbf{r}) \qquad (43)$$

where $\rho_s^a(\mathbf{r})$ and $\delta\rho^a(\mathbf{r})$ are either the core density and the refinable nonspherical valence density or the free atom total density and the deviations from this density. In each case, $\delta\rho^a(\mathbf{r})$ can be written as the product of radial functions $R_n(r)$ with a set of orientation dependent functions $A_n(\vartheta,\phi)$ defined on the local axis centered at the atom

$$\delta\rho^a(\mathbf{r}) = \sum_n c_n R_n(r) A_n(\vartheta,\phi) \qquad (44)$$

The parameters c_n and the parameters in the radial functions $R_n(r)$ need to be refined.

One of the advantages of the multipole model is that this method allows one to estimate the phases of the structure factors so that the difference between the experimental and calculated structure factors is as small as one desires for any crystal. It is obvious from eqn (44) that the more accurate the phases need to be, the more parameters it is necessary to be refined.

Despite the success of free atomic models in practice, they are conceptually unsatisfactory: (1) An atom in a crystal should occupy a finite region in real space. However all the models used in the treatment of X-ray diffraction assume that the atom occupy the total space; (2) The symmetry of the atoms in crystals are all considered to be spherical in the spherical model, however, the actual point symmetry for the atom is usually much lower than the spherical symmetry; (3) There exists arbitrariness in choosing the radial functional form and the refinable parameters. Our model based on the theory of atoms in crystals and given in the next section (4.4.2) eliminates all these undesirable features.

4.4.2 Atomic Scattering Factor of Atoms in Crystals

The atom in a crystal is defined as the zero flux surface of the gradient vector field of the charge density. The atoms defined in this way satisfy not only the space filling condition for the supposition of atoms into a crystal, but also the subspace variational principle and local point symmetry of the crystal. The atomic scattering factor of an atom in crystal is defined as

$$f_a = \int_{\Omega_a} \rho(\mathbf{r}')\exp\{2\pi i \mathbf{S}\cdot\mathbf{r}'\}d\mathbf{r}' \qquad (45)$$

where ρ is the charge density of crystal, $\mathbf{r}'$ is the coordinates originated at the nucleus of atom a, and the integral is over the basin of atom a. In terms of the atomic scattering factors, eqn (37) can be written as

$$F(\mathbf{S}) = \sum_a \int_{\Omega_a} \rho(\mathbf{r})\exp\{2\pi i \mathbf{S}\cdot\mathbf{r}\}d\mathbf{r} = \sum_a f_a \exp\{2\pi i \mathbf{S}\cdot\mathbf{r}_a\} \qquad (46)$$

This is the desired expression for the structure factor with reflection direction $\mathbf{S}$. This expression for the structure factor differs from that used

in the conventional treatment wherein the charge distribution over the unit cell is expressed as a superposition of atomic contributions, contributions which not only overlap one another within the cell but extend over into neighbouring cells. The expression given in terms of the atomic contributions in eqn (46) preserves the number of electrons not only within the cell but within each atom of the cell. The form of eqn (46) is a consequence of the topology of the charge density partitioning a crystal into a set of quantum subsystems. This topology is itself a consequence of the balancing of the Ehrenfest force over each atomic basin and of the vanishing of the Hellamnn-Feynman forces acting on the nuclei and the decomposition of the total scattering amplitude into atomic contributions given in eqn (46) is physically meaningful and unique.

4.4.3 Determination of Phases from Atoms in Crystals

Since the shapes of the atoms in a crystal are taken into consideration, the atomic form factors defined in section 4.4.2 are not necessarily real, and for the same kind of atom, if they are oriented in different direction, they will give different scattering power. An example is the two carbons in the primitive cell, the atomic scattering factor for one atom is the complex conjugate of the other because of the centre symmetry between them. Therefore, generally, we can write down the atomic scattering factor as

$$f_a = A_a + iB_a \qquad (47)$$

where A_a and B_a are the real and imaginary part of the form factor for atom a in a crystal. With this expansion for an atomic form factor, the structure factor of diffraction **S** can be written as

$$F(\mathbf{S}) = \sum_a (A_a + iB_a)\exp(2\pi i\mathbf{S}\cdot\mathbf{r}_a) = \sum_a (A_a\cos(2\pi i\mathbf{S}\cdot\mathbf{r}_a) - B_a\sin(2\pi i\mathbf{S}\cdot\mathbf{r}_a)) +$$

$$i\sum_a (A_a\sin(2\pi i\mathbf{S}\cdot\mathbf{r}_a) + B_a\cos(2\pi i\mathbf{S}\cdot\mathbf{r}_a)) \qquad (48)$$

From eqn (48) we obtain the phase for the structure factor F(S)

$$\Phi(\mathbf{S}) = \tan^{-1}\left\{ \sum_a [A_a\sin(2\pi i\mathbf{S}\cdot\mathbf{r}_a) + B_a\cos(2\pi i\mathbf{S}\cdot\mathbf{r}_a)] \right.$$

$$\left. / \sum_a [A_a\cos(2\pi i\mathbf{S}\cdot\mathbf{r}_a) - B_a\sin(2\pi i\mathbf{S}\cdot\mathbf{r}_a)] \right\} \qquad (49)$$

In terms of the experimental measurable quantity $|F(\mathbf{S})|$ and the estimated phase of eqn (49), The structure factor is

$$F(\mathbf{S}) = |F(\mathbf{S})|\exp\{i\Phi(\mathbf{S})\} \qquad (50)$$

It is worthwhile to point out that in the free spherical atom model, the same kind of atoms in a crystal have the same real atomic form factor even though they may have different orientations in the real space. In that case the summation over atoms in the unit cell can be separated into two parts: the type of atoms and the equivalent positions, the latter part depends only upon the geometry and is given in the International Crystallography Tables.

4.5. Free Atomic Form Factor vs Atomic Form Factor in Crystal

In this section we give a detailed comparison between the free atomic model and the model based upon atoms in molecules or crystals. The atomic form factors of Al, B, C, N, P and Si atoms obtained from crystals are also reported in this section.

Table 4-1 lists the atomic form factors of a free carbon atom, of a carbon atom in crystal diamond and in SiC and of the central carbon atom in

molecule $C(CH_3)_4$. The free atomic form factors are calculated from the following approximate analytical expression

$$f(s) = c + \sum_{1}^{4} a_i \exp(-b_i s^2) \qquad (51)$$

where $s = \sin\theta/\lambda = \sqrt{h^2 + k^2 + l^2}/(2a)$, a is the lattice parameter of cubic system. The coefficients $\{a_i, b_i,\ i=1,4\}$ are obtained from the International Tables for Crystallography (1973). The charge densities of diamond and crystal SiC and of molecule $C(CH_3)_4$ are calculated as in Chapter 3. That is 621G* is used for the calculation of the crystals and 631++G** for the molecule.

The quantity f(0,0,0) or A(0,0,0) in Table 4-1 is the total electronic charge of the atom which should be 6 for free carbon atom and the carbon in diamond. The deviation from the the accurate value 6 is due to the numerical error of the approximation formula eqn (51) or the determination of inter-atomic surface and integral method. Table 4-1 shows that even though the four carbons have very different environments, especially the carbon in SiC which has more than 9 electrons , the form factors for the same $\sin\theta/\lambda$ are very close to each other except for those with small $\sin\theta/\lambda$. This shows that for the relatively large $\sin\theta/\lambda$, the diffracted X-rays comes primarily from the core region. The most interesting feature in this table is the similarity between the carbon in diamond and the central carbon in neo-pentane. The difference between A(h,k,l) or B(h,k,l) of carbon in diamond and the corresponding values of the carbon in neo-pentane is less than 0.05 for $(h,k,l) \neq 0$. This similarity does not exist between the other pair of carbon

atoms. Therefore we can conclude that, compared to the spherical atomic model, the central carbon atom in neo-pentane is a better atomic model for the treatment of X-ray diffraction of diamond. This is because the new model takes the actual form of an atom in a crystal into consideration. The similarity of the atomic form factors between the carbon in diamond and the central carbon in neo-pentane shows the transferable properties between the two carbons. Another feature of Table 4-1 is that it shows the relative large difference of the atomic form factors with h=k=l between spherical free carbon atom and the carbon atom in diamond or in neo-pentane.

Table 4-1 Carbon Atomic Form Factor

(The shapes of the atoms in the crystals are shown in Fig. 4-2)

(h k l)	Free C	C in Diamond		C in SiC[a]		C in $C(CH_3)_4$	
	f_C	A	B	A	B	A	B
0 0 0	5.99920	5.99758	0.00000	9.04069	0.00000	5.87071	0.00000
1 1 1	3.02788	3.39665	-0.15503	2.96879	-0.13927	3.40023	-0.16634
2 0 0	2.65579	3.02593	0.00000	2.63140	0.00000	3.03594	0.00027
2 2 0	1.96081	1.90939	0.00000	1.78225	0.00000	1.96156	-0.00017
3 1 1	1.75829	1.64304	0.01208	1.71774	-0.16912	1.67858	0.00842
2 2 2	1.71368	1.44225	0.15082	1.94560	-0.14729	1.46003	0.13282
4 0 0	1.58860	1.53448	0.00000	1.52005	0.00000	1.55700	-0.00089
3 3 1	1.52384	1.45005	0.11257	1.49881	0.02998	1.44586	0.10120
4 2 0	1.50514	1.45155	0.00000	1.48619	0.00000	1.45723	-0.00029
4 2 2	1.43890	1.44011	0.13865	1.40685	0.04234	1.43883	0.13657
5 1 1	1.39501	1.36507	0.02198	1.39413	-0.00850	1.37164	0.02212
3 3 3	1.39501	1.54798	0.15753	1.26083	-0.04236	1.54391	0.18002
4 4 0	1.32827	1.32003	0.00000	1.37155	0.00000	1.33517	0.00012
5 3 1	1.29088	1.28777	0.01014	1.27317	0.01108	1.29486	0.01818
6 0 0	1.27878	1.25217	0.00000	1.25345	0.00000	1.26377	-0.00132
4 4 2	1.27878	1.33281	0.00033	1.26984	-0.03579	1.34321	0.02199
6 2 0	1.23192	1.21153	0.00000	1.21819	0.00000	1.22233	-0.00068
5 3 3	1.19827	1.23130	-0.06267	1.21318	-0.02423	1.24898	-0.04969
6 2 2	1.18732	1.18106	0.00111	1.15105	-0.00575	1.19231	0.00223
4 4 4	1.14477	1.10047	-0.15007	1.16432	0.07070	1.14026	-0.15262
7 1 1	1.11411	1.08837	0.00059	1.08977	0.00062	1.09975	0.00163
5 5 1	1.11411	1.09246	-0.00380	1.07271	-0.02003	1.10163	-0.00789
6 4 0	1.10411	1.08601	0.00000	1.06880	0.00000	1.09651	0.00001

6	4	2	1.06526	1.03342	-0.00886	1.04597	-0.00347	1.05502	-0.01186
7	3	1	1.03724	1.00828	-0.00101	1.00886	-0.00438	1.02334	-0.00054
5	5	3	1.03724	0.96346	-0.03223	0.99052	0.01335	0.99189	-0.04297
8	0	0	0.99259	0.95947	0.00000	0.95089	0.00000	0.97735	-0.00036
7	3	3	0.96697	0.92356	-0.01155	0.94102	0.00743	0.94027	-0.00799
8	2	0	0.95862	0.92728	0.00000	0.91500	0.00000	0.94360	-0.00083
6	4	4	0.95862	0.85811	0.01246	0.89494	-0.00414	0.87459	-0.00273
6	6	0	0.92614	0.89447	0.00000	0.88151	0.00000	0.91587	0.00003
8	2	2	0.92614	0.89348	-0.00096	0.88798	0.00003	0.91157	-0.00164
7	5	1	0.90271	0.86744	-0.00402	0.88066	0.00004	0.88422	-0.00033
5	5	5	0.90271	0.79554	0.10008	0.88173	-0.05841	0.79306	0.08316
6	6	2	0.89508	0.86252	0.00083	0.85909	0.03112	0.87593	0.00525
8	4	0	0.86537	0.83588	0.00000	0.81555	0.00000	0.85046	-0.00081
9	1	1	0.84395	0.81666	-0.00007	0.83675	-0.00171	0.82775	0.00019
7	5	3	0.84395	0.80765	0.00863	0.80601	-0.00669	0.81897	0.00524
8	4	2	0.83697	0.80955	0.00209	0.79659	0.00725	0.82045	-0.00080
6	6	4	0.80980	0.79041	0.04346	0.80271	-0.00689	0.78530	0.04431
9	3	1	0.79021	0.76231	-0.00118	0.79166	-0.00416	0.77455	0.00119
8	4	4	0.75899	0.73821	0.01525	0.73805	-0.00901	0.74605	0.01342
7	7	1	0.74107	0.71338	0.00294	0.74398	-0.00645	0.72409	-0.00156
9	3	3	0.74107	0.70968	-0.00040	0.71912	-0.00001	0.72611	0.00109
7	5	5	0.74107	0.76156	0.03910	0.72751	0.01770	0.76577	0.04420
10	0	0	0.73523	0.70691	0.00000	0.65475	0.00000	0.72232	0.00001
8	6	0	0.73523	0.71580	0.00000	0.69563	0.00000	0.72296	-0.00060
10	2	0	0.71252	0.68634	0.00000	0.63295	0.00000	0.70071	-0.00044
8	6	2	0.71252	0.69018	0.00235	0.66600	-0.01275	0.70110	0.00232
9	5	1	0.69614	0.66802	0.00160	0.69984	0.01217	0.68344	0.00096
7	7	3	0.69614	0.67245	0.00457	0.69626	-0.02273	0.68781	-0.00158
10	2	2	0.69080	0.66714	0.00511	0.64086	0.00442	0.67860	-0.00057
6	6	6	0.69080	0.76719	-0.01950	0.62932	0.03255	0.78003	0.01023
9	5	3	0.65504	0.62937	0.00393	0.65405	-0.00860	0.64380	0.00148
10	4	0	0.65016	0.63204	0.00000	0.59661	0.00000	0.63911	-0.00124
8	6	4	0.65016	0.63524	-0.00733	0.62347	0.02281	0.64719	0.00428
10	4	2	0.63116	0.61664	-0.00219	0.57810	-0.00585	0.62146	0.00000
7	7	5	0.61746	0.62188	-0.02812	0.59376	-0.01090	0.63928	-0.02017
8	8	0	0.59562	0.57575	0.00000	0.54394	0.00000	0.58950	0.00040

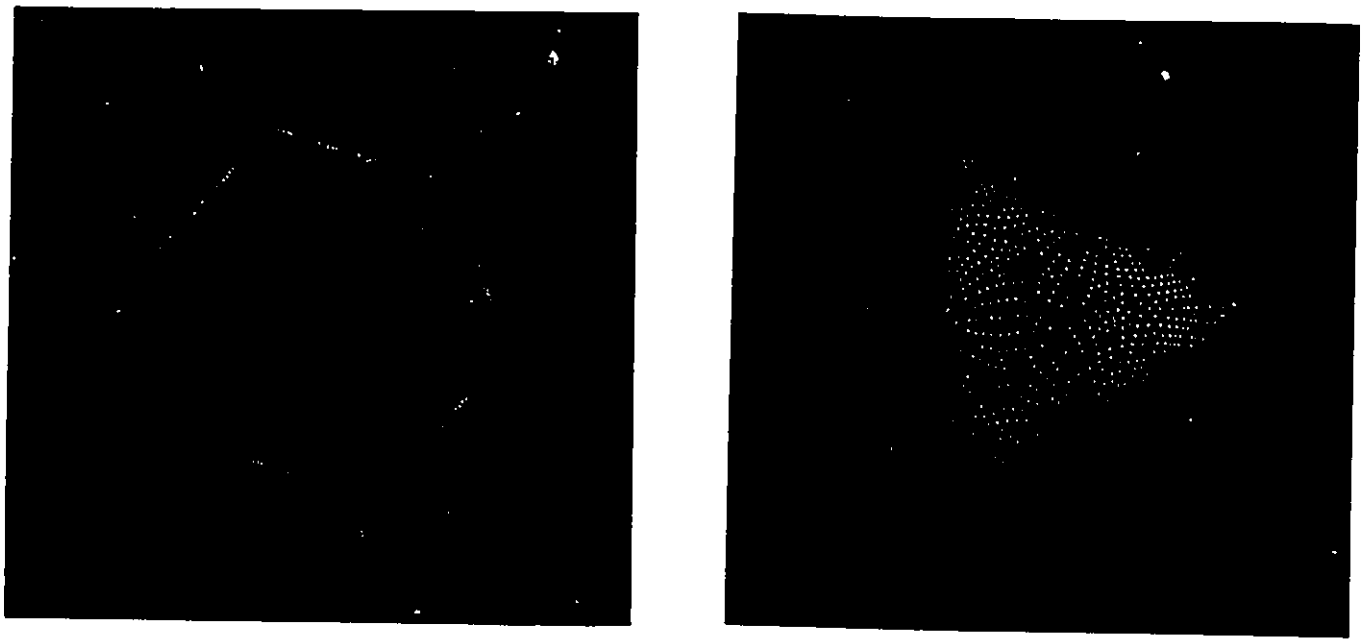

(a) (b)

Fig. 4-2 (a) A carbon atom in diamond, (b) a carbon atom in SiC.

Table 4-2 gives the X-ray scattering amplitudes obtained from the carbon atomic form factors listed in Table 4-1. The R-factors for these atomic models are also given in the table. The R-factor measures the deviations between the theoretical estimated amplitudes and experimental values and is defined by

$$R = \Sigma|F_{exp} - F_{cal}|/\Sigma|F_{exp}|$$

where F_{exp} and F_{cal} are, respectively, experimental and estimated amplitudes, the summation is over all the measured (h,k,l). Since the form of the carbon atom in neo-pentane is considered, the R-factor obtained from this atomic model is 0.023 which is as good as the R-factor derived from the carbon in diamond. The R-factors calculated from other works with the Hartree-Fock method are 0.024 (Euwema et al, 1973 and 1975), 0.028 (Heaton and Lafon, 1978) and 0.023 (Dovesi, et al, 1980). The R-factors obtained from the free carbon atom and the carbon in SiC are 2~3 times larger than those derived from C in diamond and the C in neo-pentane. From table 4-2 we can see that the free atomic model fails to predict the appearance of (222) diffraction, and the other atomic models in the table give excellent estimations. This shows that the atomic models from atoms in molecules or atoms in crystals have advantages over the free atomic models with regards to the estimation of weak diffractions.

Table 4-2 The Theoretical Estimated and Experimental Scattering Amplitudes of X-Ray from Diamond

(h k l)	Free Atom	C in Diamond	C in SiC	C in $C(CH_3)_4$	Experiment
0 0 0	47.99360	47.98068	72.32551	46.96568	
1 1 1	-17.12826	-18.33733	-17.58184	-18.29364	18.80000
2 2 0	-15.68644	-15.27510	-14.25798	-15.69248	15.81000
3 1 1	-9.94640	-9.22614	-8.76031	-9.44785	9.42600

2 2 2	0.00000	1.20655	1.17829	1.06256	1.20800
4 0 0	-12.70877	-12.27588	-12.16038	-12.45600	11.86500
3 3 1	8.62015	8.83952	8.30896	8.75149	8.96300
4 2 2	11.51118	11.52092	11.25483	11.51064	11.58800
5 1 1	7.89138	7.84634	7.93448	7.88430	8.05600
3 3 3	7.89138	7.86556	6.89271	7.71533	8.05600
4 4 0	10.62613	10.56023	10.97239	10.68136	
5 3 1	7.30233	7.22733	7.26481	7.22199	
4 4 2	0.00000	-0.00268	-0.28634	-0.17592	
6 2 0	9.85536	9.69226	9.74556	9.77864	
5 3 3	-6.77846	-6.61076	-6.99983	-6.78421	
6 2 2	0.00000	-0.00887	-0.04600	-0.01784	
4 4 4	-9.15813	-8.80379	-9.31457	-9.12208	
7 1 1	6.30233	6.15343	6.16816	6.21190	
5 5 1	-6.30233	-6.15842	-6.18150	-6.18713	
6 4 2	-8.52206	-8.26737	-8.36774	-8.44016	
7 3 1	-5.86751	-5.69797	-5.73177	-5.78583	
5 5 3	-5.86751	-5.63244	-5.67875	-5.85405	
8 0 0	7.94069	7.67576	7.60712	7.81880	
7 3 3	-5.47000	-5.28979	-5.36528	-5.36417	
6 4 4	0.00000	0.09967	0.03315	-0.02184	
6 6 0	-7.40909	-7.15575	-7.05209	-7.32696	
8 2 2	-7.40909	-7.14783	-7.10383	-7.29256	
7 5 1	-5.10650	-4.92975	-4.98202	-5.00377	
5 5 5	5.10650	5.06644	5.31825	4.95665	
6 6 2	0.00000	0.00663	-0.24894	0.04200	
8 4 0	-6.92297	-6.68706	-6.52443	-6.80368	
9 1 1	-4.77410	-4.61933	-4.74308	-4.68354	
7 5 3	4.77410	4.61757	4.59734	4.66244	
8 4 2	0.00000	0.01669	-0.05803	-0.00640	
6 6 4	6.47843	6.32330	6.42166	6.28240	
9 3 1	-4.47012	-4.31893	-4.45480	-4.37478	
8 4 4	6.07190	5.90564	5.90440	5.96840	
7 7 1	4.19214	4.05215	4.24508	4.08725	
9 3 3	4.19214	4.01230	4.06803	4.11366	
7 5 5	4.19214	4.08683	4.21551	4.08182	
10 2 0	-5.70014	-5.49073	-5.06358	-5.60568	
8 6 2	5.70014	5.52144	5.32803	5.60880	
9 5 1	3.93794	3.78795	3.89006	3.87155	
7 7 3	3.93794	3.77809	3.81002	3.89978	
10 2 2	0.00000	0.04085	-0.03539	-0.00456	
6 6 6	0.00000	0.15602	0.26041	-0.08184	
9 5 3	3.70547	3.53800	3.65126	3.63351	
8 6 4	0.00000	0.05861	0.18246	-0.03424	
10 4 2	5.04928	4.93310	4.62477	4.97168	
7 7 5	-3.49288	-3.35878	-3.42049	-3.50222	
8 8 0	4.76497	4.60600	4.35152	4.71600	
R-FACTOR	0.05456	0.02347	0.06434	0.02328	

Table 4-3 lists the X-ray scattering amplitudes of silicon crystal and the contributions from pseudo-atoms and silicon atoms. The contributions from the pseudo-atoms is relatively small compared to the contributions from the silicon atoms to amplitudes in most of the diffraction directions (h,k,l). However, for the forbidden diffraction (222), the contribution from the pseudo-atoms is larger than that from the silicon atoms. The phase value of this forbidden diffraction is determined by the pseudo-atoms.

Table 4-3 Calculated X-Ray Scattering Amplitudes of Silicon Crystal and the Contributions from the Pseudo-atoms and Silicon Atoms (The shapes of silicon atom and pseudo-atom are shown in Fig. 4-3).

(h k l)	pseudo-atom	Silicon	Total
(1 1 1)	-2.87562	-57.93116	-60.80677
(2 0 0)	0.00000	0.00000	0.00000
(2 2 0)	2.24307	-71.18950	-68.94642
(3 1 1)	2.53662	-47.70259	-45.16597
(2 2 2)	3.60978	-2.02955	1.58023
(4 0 0)	1.44699	-61.06608	-59.61910
(3 3 1)	1.06901	39.99947	41.06847
(4 2 0)	0.00000	0.00000	0.00000
(4 2 2)	1.02589	52.80339	53.82928
(5 1 1)	0.10956	36.39889	36.50845
(3 3 3)	1.65939	34.66718	36.32657
(4 4 0)	0.14353	48.52041	48.66394
(5 3 1)	0.14344	32.80330	32.94674
(6 0 0)	0.00000	0.00000	0.00000
(4 4 2)	0.60782	-0.59258	0.01525
(6 2 0)	0.05204	43.65630	43.70834
(5 3 3)	0.56749	-30.28155	-29.71406
(6 2 2)	-0.10420	-0.11118	-0.21538
(4 4 4)	0.51407	-40.39104	-39.87696
(7 1 1)	0.21734	27.10446	27.32179
(5 5 1)	-0.22016	-27.07386	-27.29402
(6 4 0)	0.00000	0.00000	0.00000
(6 4 2)	-0.15940	-36.28767	-36.44706
(7 3 1)	0.03525	-24.88843	-24.85317
(5 5 3)	-0.02516	-24.84200	-24.86716
(8 0 0)	0.16783	33.38771	33.55554
(7 3 3)	0.24065	-22.95412	-22.71347
(8 2 0)	0.00000	0.00000	0.00000

(6 4 4)	-0.19805	0.06508	-0.13297
(6 6 0)	0.61738	-31.09222	-30.47484
(8 2 2)	-0.05266	-30.92085	-30.97351
(7 5 1)	0.19492	-21.33358	-21.13866
(5 5 5)	-0.23683	21.40095	21.16412
(6 6 2)	0.09606	0.07208	0.16813
(8 4 0)	-0.24168	-28.76677	-29.00845
(9 1 1)	0.10216	-19.77459	-19.67243
(7 5 3)	-0.00298	19.93242	19.92944
(8 4 2)	-0.31779	-0.04708	-0.36488
(6 6 4)	-0.54651	27.24094	26.69443
(9 3 1)	-0.11439	-18.52202	-18.63642
(8 4 4)	-0.29727	25.22371	24.92644
(7 7 1)	-0.05692	17.27127	17.21436
(9 3 3)	0.09952	17.32379	17.42331
(7 5 5)	-0.57877	17.83884	17.26007
(10 0 0)	0.00000	0.00000	0.00000
(8 6 0)	0.00000	0.00000	0.00000
(10 2 0)	0.58416	-23.67939	-23.09522
(8 6 2)	0.31178	23.63575	23.94753
(9 5 1)	-0.15757	16.35317	16.19560
(7 7 3)	-0.05886	16.54654	16.48769
(10 2 2)	0.06707	-0.02213	0.04494
(6 6 6)	-0.46186	0.69110	0.22925
(9 5 3)	-0.07309	15.56701	15.49393
(10 4 0)	0.00000	0.00000	0.00000
(8 6 4)	-0.03672	0.28655	0.24983
(10 4 2)	0.04065	21.24576	21.28642
(7 7 5)	-0.43477	-14.22058	-14.65534
(8 8 0)	0.49711	20.28769	20.78479

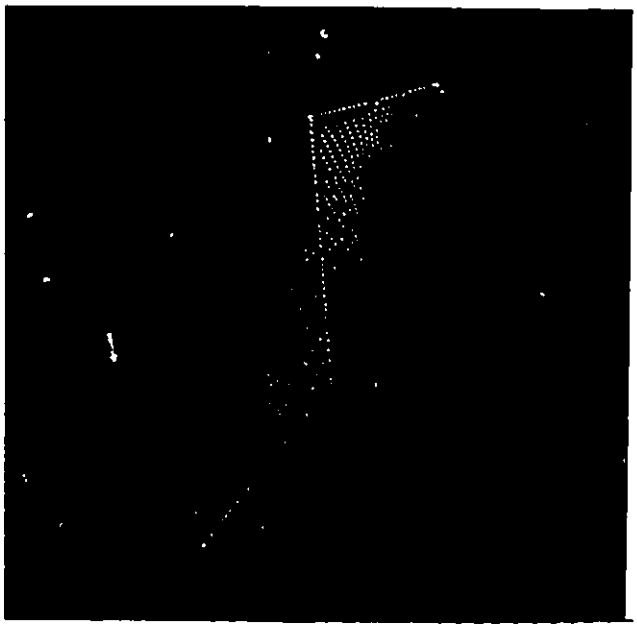

(a)

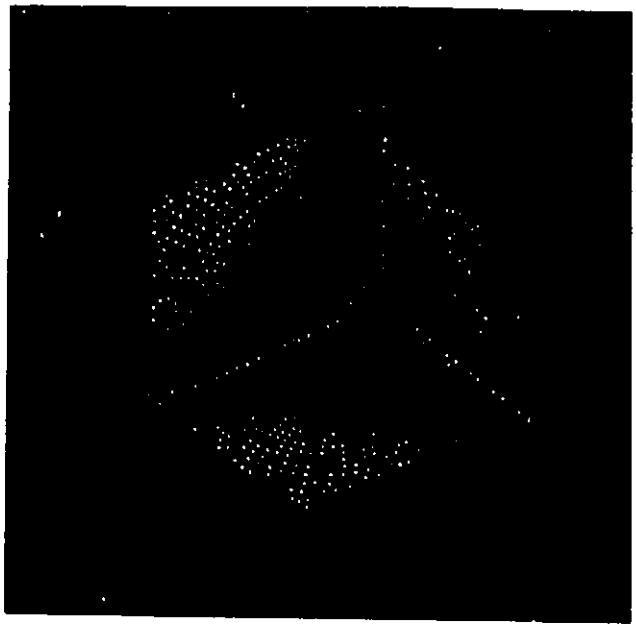

(b)

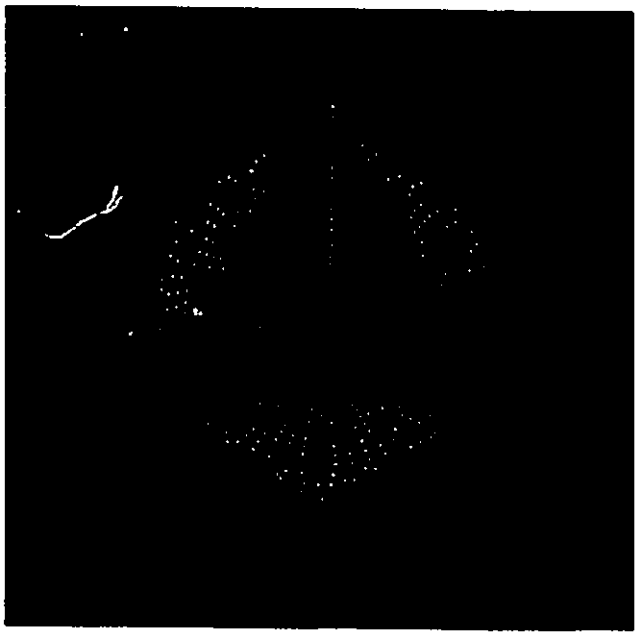

(c)

Fig. 4-3 (a) A pseudo atom in silicon, (b) a silicon atom in silicon crystal, (c) Si in SiC.

Table 4-4 gives the comparisons of the X-ray scattering amplitudes for a silicon crystal obtained from experiments and from different atomic models. Because of the interest in semiconducting materials, the scattering factors of silicon crystal has been most accurately measured in experiment (Aldred and Hart, 1973; Teworte and Bonse, 1984; Saka and Kato; 1986). At least 18 scattering factors are now known to the millielectron (10^{-3}) per atom level of accuracy, better by one or more order of magnitude than any other crystal (Deutsch, 1992). Spackman (1986), Cummings and Hart (1988), and Deutsch (1991, 1992) have made careful analysis and explanation on the accurately measured data. Cummings and Hart (1988) have consolidated five data sets obtained in three independent experiments, (Aldred and Hart, 1973; Teworte and Bonse, 1984; Saka and Kato; 1986), examing carefully the internal consistencies after corrections for anomalous dispersion (using measured wavelength-dependent f') and nuclear scattering. Many theoretical works have been dedicated for the comparison between theory and experiment. The charge density has been calculated by a number of methods, for example, empirical or first principle pseudopotential methods (Chelikowsky and Cohen, 1974; Haman, 1979; Baldereschi, et al, 1981; Yin and Cohen, 1982), ab initio methods (Wang and Klein, 1981; Dovesi, et al 1981; Pisani, et al, 1992; Lu and Zunger, 1992). In a recent work, Lu and Zunger (1992) used the linearized augmented plane wave implementation (Wei and Krakauer, 1985) of the local density theory (Hohenberg and Kohn, 1965; Kohn and Sham, 1965). Their R-factor for the 18 structure factors is 0.21% which is in excellent agreement between experiment and theory. Another recent ab initio calculation (Pisani, et al, 1992) used Gaussian type functions as basis and obtained even smaller R-factor 0.11%.

The experimental data listed in Table 4-4 is from Cumming and Hart (1988) except the 222 reflection which is obtained from Alkire, Yelon and Schneider, 1982. The data have been corrected to 0 K. The correction for the thermal motion uses formula

$F(\sin\theta/\lambda) = F_e(\sin\theta/\lambda)\exp(B\sin^2\theta/\lambda^2)$

where F_e is the scattering factor with thermal motion, the Debye-Waller factor B is taken to be 0.4632 (Spackman,1986). The R-factors for the theoretical estimations are also given in Table 4-4. The R-factor measures the general goodness for the theoretically estimated scattering amplitudes. From the table we can see that the amplitudes from the model of Si atom in the molecule $Si(SiH_3)_4$ (R=0.187%) are much better than those from the free atomic model (R=0.812%). The R-factor from the model of Si in $Si(SiH_3)_4$ is as good as the recent reported best values of 0.11-0.25% which are obtained from the charge density calculated from an optimized basis set (Pisani, et al, 1992) or from a different ab initio method (Lu and Zunger, 1992). Again, the amplitude of forbidden diffraction (222) is predicted from the model of atoms in molecules. The charge density of silicon crystal is calculated from 621G*. The R-factor from this basis set is 0.41% which is larger than that from Si in $Si(SiH_3)_4$. The reason for this is that the calculated charge density of the molecule with 631G** basis set is better than the calculated charge density of silicon crystal with 621G*.

Table 4-4 The Theoretical Estimated and Experimental X-Ray Scattering Amplitudes of Silicon Crystal

(h k l)	Crystal	Free Si	Si in $Si(SiH_3)_4$*	Experiment
(1 1 1)	-60.80677	-59.59949	-60.75642	-60.68730
(2 2 0)	-68.94642	-69.74194	-69.32944	-69.24560
(3 1 1)	-45.16597	-46.21305	-45.34908	-45.37020
(2 2 2)	1.58023	0.00000	1.69048	1.52640
(4 0 0)	-59.61910	-60.10016	-59.71736	-59.59440
(3 3 1)	41.06847	40.66425	41.01123	40.99690
(4 2 2)	53.82928	53.66731	53.76184	53.72960
(5 1 1)	36.50845	36.46441	36.52840	36.41940
(3 3 3)	36.32657	36.46441	36.33199	36.35660
(4 4 0)	48.66394	48.34278	48.46584	48.36960
(5 3 1)	32.94674	32.91744	32.89789	
(4 4 2)	0.01525	0.00000	-0.21112	
(6 2 0)	43.70834	43.78492	43.82480	
(5 3 3)	-29.71406	-29.87142	-29.98150	
(6 2 2)	-0.21538	0.00000	-0.03816	
(4 4 4)	-39.87696	-39.86027	-39.89144	-39.83280
(7 1 1)	27.32179	27.24598	27.24895	
(5 5 1)	-27.29402	-27.24598	-27.26304	-27.19360
(6 4 2)	-36.44706	-36.47300	-36.53712	-36.43840
(7 3 1)	-24.85317	-24.97834	-24.97552	
(5 5 3)	-24.86716	-24.97834	-25.11010	
(8 0 0)	33.55554	33.54372	33.52128	33.41120
(7 3 3)	-22.71347	-23.01579	-23.04546	
(6 4 4)	-0.13297	0.00000	-0.08392	
(6 6 0)	-30.47484	-31.00520	-31.00272	-30.93040
(8 2 2)	-30.97351	-31.00520	-30.98560	
(7 5 1)	-21.13866	-21.31366	-21.30569	
(5 5 5)	21.16412	21.31366	21.25235	21.26920
(6 6 2)	0.16813	0.00000	-0.04008	
(8 4 0)	-29.00845	-28.80039	-28.77696	
(9 1 1)	-19.67243	-19.83398	-19.81319	
(7 5 3)	19.92944	19.83398	19.72375	
(8 4 2)	-0.36488	0.00000	-0.02904	
(6 6 4)	26.69443	26.88082	26.74192	
(9 3 1)	-18.63642	-18.54452	-18.53468	
(8 4 4)	24.92644	25.20530	25.15712	25.08000
(7 7 1)	17.21436	17.41786	17.37814	
(9 3 3)	17.42331	17.41786	17.38317	
(7 5 5)	17.26007	17.41786	17.37039	
(10 2 0)	-23.09522	-23.73881	-23.72224	
(8 6 2)	23.94753	23.73881	23.71864	
(9 5 1)	16.19560	16.43072	16.40906	
(7 7 3)	16.48769	16.43072	16.40097	
(10 2 2)	0.04494	0.00000	-0.00240	
(6 6 6)	0.22925	0.00000	0.00216	

(9 5 3)	15.49393	15.56327	15.53955	
(8 6 4)	0.24983	0.00000	-0.05432	
(10 4 2)	21.28642	21.31827	21.29880	
(7 7 5)	-14.65534	-14.79865	-14.87374	
(8 8 0)	20.78479	20.31733	20.30568	20.26480
R-FACTOR	0.00410	0.00812	0.00187	

* The geometry and basis set for the determination of charge density are the same as in chapter 3.

Tables 4-5 to 4-10 list the calculated atomic form factors of atoms: Al in crystal AlP, B in BN and BP, C in SiC, N in BN, P in BP and AlP and of Si in SiC. As a comparison, the free atomic form factors obtained from the International Crystallography Tables are also listed in our tables. From these tables we can see that the difference between the value of A in the table and the corresponding free atomic form factor is very small. Therefore we can conclude that the scattering amplitudes obtained from the free atomic model and from our atoms in crystals model will not have much difference for the strong diffractions.

Table 4-5 Atomic Form Factors of Al in Crystal AlP

(The shape of Al atom is shown in Fig. 4-4)

(h k l)	Free Al	Al in AlP		(h k l)	Free Al	Al in AlP	
	f_{Al}	A	B		f_{Al}	A	B
0 0 0	12.99370	10.58099	0.00000				
1 1 1	9.87427	9.69150	0.03456	6 6 0	3.34571	3.36278	0.00000
2 0 0	9.42775	9.42642	0.00000	8 2 2	3.34571	3.35180	-0.00150
2 2 0	8.35231	8.52615	0.00000	7 5 1	3.24799	3.25779	0.01030
3 1 1	7.82211	7.95882	0.03403	5 5 5	3.24799	3.30298	-0.02323
2 2 2	7.66830	7.76431	0.08711	6 6 2	3.21676	3.22205	0.01063
4 0 0	7.12209	7.18545	0.00000	8 4 0	3.09818	3.10447	0.00000
3 3 1	6.76275	6.77474	0.03246	9 1 1	3.01546	3.01796	0.00118
4 2 0	6.65013	6.66824	0.00000	7 5 3	3.01546	3.02877	0.00633
4 2 2	6.22930	6.18601	0.01654	8 4 2	2.98900	2.99707	0.00754
5 1 1	5.94080	5.91331	0.00125	6 6 4	2.88838	2.92107	0.00704
3 3 3	5.94080	5.84511	0.00047	9 3 1	2.81805	2.81938	0.00198
4 4 0	5.50421	5.48864	0.00000	8 4 4	2.70974	2.72328	0.01418
5 3 1	5.26598	5.23237	-0.00389	7 7 1	2.64964	2.65111	0.01155
6 0 0	5.19020	5.15848	0.00000	9 3 3	2.64964	2.65502	0.00522

4 4 2	5.19020	5.13039	-0.01852	7 5 5	2.64964	2.67787	0.02062
6 2 0	4.90405	4.87948	0.00000	10 0 0	2.63037	2.63030	0.00000
5 3 3	4.70607	4.65930	-0.04085	8 6 0	2.63037	2.63922	0.00000
6 2 2	4.64304	4.61640	-0.01447	10 2 0	2.55685	2.55747	0.00000
4 4 4	4.40477	4.36855	-0.07187	8 6 2	2.55685	2.54939	0.01336
7 1 1	4.23969	4.22810	-0.00392	9 5 1	2.50524	2.50256	0.00267
5 5 1	4.23969	4.23790	0.00374	7 7 3	2.50524	2.49348	0.00799
6 4 0	4.18708	4.18796	0.00000	10 2 2	2.48866	2.48700	0.00290
6 4 2	3.98804	3.98324	-0.01205	6 6 6	2.48866	2.51599	0.04298
7 3 1	3.84993	3.85064	-0.00239	9 5 3	2.38074	2.37458	0.00666
5 5 3	3.84993	3.85475	-0.03363	10 4 0	2.36641	2.36145	0.00000
8 0 0	3.63905	3.63948	0.00000	8 6 4	2.36641	2.35785	0.01532
7 3 3	3.52310	3.53406	-0.00848	10 4 2	2.31153	2.30410	-0.00008
8 2 0	3.48608	3.48807	0.00000	7 7 5	2.27281	2.26719	0.02749
6 4 4	3.48608	3.51304	-0.02982	8 8 0	2.21252	2.21166	0.00000

Table 4-6 Atomic Form Factors of B in Crystals BN and BP

(The shapes of the atoms are shown in Fig. 4-5.)

(h k l)	Free B	B in BN		Free B	B in BP	
	f_B	A	B	f_B	A	B
0 0 0	4.99860	2.63041	0.00000	4.99860	3.42590	0.00000
1 1 1	2.34107	2.27870	0.03374	2.79786	2.74729	0.10471
2 0 0	2.09695	2.17955	0.00000	2.50089	2.59065	0.00000
2 2 0	1.69733	1.88152	0.00000	1.92944	2.14218	0.00000
3 1 1	1.58351	1.71201	0.03574	1.75608	1.91908	0.09401
2 2 2	1.55531	1.63975	0.09252	1.71768	1.77656	0.21877
4 0 0	1.46051	1.51419	0.00000	1.61009	1.71199	0.00000
3 3 1	1.39836	1.40531	0.04071	1.55378	1.58000	0.09494
4 2 0	1.37861	1.39293	0.00000	1.53727	1.59997	0.00000
4 2 2	1.30346	1.26029	0.03101	1.47737	1.41562	0.06322
5 1 1	1.25065	1.22464	0.00567	1.43644	1.43841	0.01293
3 3 3	1.25065	1.15489	0.02245	1.43644	1.26822	0.01388
4 4 0	1.16870	1.15593	0.00000	1.37264	1.39466	0.00000
5 3 1	1.12290	1.08765	0.00404	1.33637	1.31041	0.02233
6 0 0	1.10817	1.07533	0.00000	1.32457	1.30787	0.00000
4 4 2	1.10817	1.04200	-0.00176	1.32457	1.22651	0.00014
6 2 0	1.05174	1.02359	0.00000	1.27875	1.26271	0.00000
5 3 3	1.01192	0.94742	-0.02806	1.24574	1.15863	-0.05871
6 2 2	0.99911	0.96178	-0.00880	1.23499	1.19934	-0.00485
4 4 4	0.95000	0.88388	-0.06036	1.19317	1.12954	-0.13129
7 1 1	0.91531	0.89199	-0.00367	1.16302	1.13652	-0.00276
5 5 1	0.91531	0.89958	0.00675	1.16302	1.14330	0.02288
6 4 0	0.90414	0.89345	0.00000	1.15319	1.15442	0.00000
6 4 2	0.86131	0.83468	-0.01175	1.11496	1.07040	-0.01230
7 3 1	0.83103	0.81627	-0.00284	1.08739	1.06705	-0.00157
5 5 3	0.83103	0.80425	-0.03644	1.08739	1.04750	-0.07611

8 0 0	0.78382	0.76883	0.00000	1.04343	1.02018	0.00000
7 3 3	0.75732	0.74568	-0.01509	1.01820	1.00113	-0.02058
8 2 0	0.74877	0.73524	0.00000	1.00997	0.99051	0.00000
6 4 4	0.74877	0.74346	-0.04353	1.00997	1.01751	-0.06811
6 6 0	0.71595	0.71914	0.00000	0.97795	0.99090	0.00000
8 2 2	0.71595	0.70573	-0.00577	0.97795	0.96044	-0.00712
7 5 1	0.69269	0.68793	0.00861	0.95483	0.94605	0.01514
5 5 5	0.69269	0.71497	-0.04701	0.95483	1.02005	-0.05703
6 6 2	0.68518	0.67213	0.00378	0.94729	0.90921	-0.00408
8 4 0	0.65633	0.64991	0.00000	0.91795	0.90420	0.00000
9 1 1	0.63586	0.62590	0.00002	0.89676	0.88127	-0.00126
7 5 3	0.63586	0.63231	-0.00708	0.89676	0.88432	-0.02314
8 4 2	0.62925	0.62434	0.00142	0.88985	0.87364	-0.00673
6 6 4	0.60381	0.62068	-0.01720	0.86293	0.89931	-0.02718
9 3 1	0.58574	0.57673	-0.00032	0.84349	0.82917	0.00122
8 4 4	0.55740	0.56445	0.00061	0.81243	0.81587	-0.00214
7 7 1	0.54139	0.53803	0.01056	0.79458	0.78500	0.02460
9 3 3	0.54139	0.54099	-0.00110	0.79458	0.78323	0.00402
7 5 5	0.54139	0.56619	-0.00295	0.79458	0.83419	0.01047
10 0 0	0.53621	0.52874	0.00000	0.78875	0.77391	0.00000
8 6 0	0.53621	0.54136	0.00000	0.78875	0.79191	0.00000
10 2 0	0.51623	0.51042	0.00000	0.76604	0.75150	0.00000
8 6 2	0.51623	0.50485	0.01030	0.76604	0.74328	0.00547
9 5 1	0.50200	0.49504	0.00151	0.74962	0.73609	0.00262
7 7 3	0.50200	0.48828	0.00047	0.74962	0.74182	-0.01763
10 2 2	0.49739	0.49093	0.00182	0.74426	0.73244	0.00028
6 6 6	0.49739	0.53258	0.01700	0.74426	0.78171	0.05483
9 5 3	0.46689	0.46132	0.00267	0.70825	0.70143	-0.00211
10 4 0	0.46277	0.45435	0.00000	0.70331	0.69574	0.00000
8 6 4	0.46277	0.45956	0.00761	0.70331	0.70992	0.00005
10 4 2	0.44685	0.43808	-0.00083	0.68407	0.67517	0.00332
7 7 5	0.43546	0.44465	0.01943	0.67014	0.68724	0.04101
8 8 0	0.41747	0.41939	0.00000	0.64785	0.65523	0.00000

Table 4-7 Atomic Form Factors of C in Crystal SiC

(The shape of the atom is shown in Fig. 3-2)

(h k l)	Free C	C in SiC		(h k l)	Free C	C in SiC	
	f_C	A	B		f_C	A	B
0 0 0	5.99920	9.04069	0.00000				
1 1 1	3.57853	4.14596	-0.05640	6 6 0	1.14281	1.09772	0.00000
2 0 0	3.18237	3.58230	0.00000	8 2 2	1.14281	1.11897	0.00240
2 2 0	2.32197	2.03621	0.00000	7 5 1	1.12222	1.09245	-0.00370
3 1 1	2.02545	1.84544	-0.18700	5 5 5	1.12222	1.14007	0.07572
2 2 2	1.95789	1.91220	-0.36046	6 6 2	1.11546	1.08727	-0.01805
4 0 0	1.77288	1.67742	0.00000	8 4 0	1.08892	1.06837	0.00000
3 3 1	1.68600	1.72577	-0.10227	9 1 1	1.06954	1.05853	-0.00022

4	2	0	1.66270	1.61263	0.00000	7	5	3	1.06954	1.06531	0.00579
4	2	2	1.58707	1.67667	-0.03130	8	4	2	1.06317	1.04575	-0.00903
5	1	1	1.54233	1.52378	-0.04897	6	6	4	1.03819	0.99630	0.02647
3	3	3	1.54233	1.60858	0.11104	9	3	1	1.01993	1.00590	0.00192
4	4	0	1.48033	1.47883	0.00000	8	4	4	0.99041	0.97417	0.01638
5	3	1	1.44778	1.45509	0.01505	7	7	1	0.97322	0.97192	-0.00572
6	0	0	1.43746	1.41272	0.00000	9	3	3	0.97322	0.96172	-0.00317
4	4	2	1.43746	1.38730	0.03372	7	5	5	0.97322	0.91421	0.00109
6	2	0	1.39824	1.40596	0.00000	10	0	0	0.96757	0.93830	0.00000
5	3	3	1.37051	1.30394	-0.01424	8	6	0	0.96757	0.96199	0.00000
6	2	2	1.36152	1.36020	0.01690	10	2	0	0.94541	0.91878	0.00000
4	4	4	1.32667	1.28159	-0.10772	8	6	2	0.94541	0.95016	-0.00147
7	1	1	1.30151	1.30130	-0.00367	9	5	1	0.92922	0.90434	-0.00225
5	5	1	1.30151	1.32007	0.01529	7	7	3	0.92922	0.91775	0.01818
6	4	0	1.29329	1.31332	0.00000	10	2	2	0.92390	0.89720	-0.00029
6	4	2	1.26116	1.24126	-0.00893	6	6	6	0.92390	0.87873	-0.05796
7	3	1	1.23779	1.23062	0.00848	9	5	3	0.88777	0.86769	0.01250
5	5	3	1.23779	1.26378	-0.03856	10	4	0	0.88276	0.87193	0.00000
8	0	0	1.20010	1.18156	0.00000	8	6	4	0.88276	0.85425	-0.00700
7	3	3	1.17820	1.16524	-0.02239	10	4	2	0.86310	0.85350	-0.00743
8	2	0	1.17101	1.15995	0.00000	7	7	5	0.84873	0.85104	-0.02518
6	4	4	1.17101	1.21237	-0.00250	8	8	0	0.82549	0.80422	0.00000

Table 4-8 Atomic Form Factors of N in Crystal BN

(The shape of the atom is shown in Fig. 4-6)

(h k l)	Free N	N in BN		(h k l)	Free N	N in BN	
	f_N	A	B		f_N	A	B
0 0 0	6.99460	9.35119	0.00000				
1 1 1	3.96387	4.35526	0.18635	6 6 0	1.11086	1.07214	0.00000
2 0 0	3.48168	3.68169	0.00000	8 2 2	1.11086	1.09350	0.00396
2 2 0	2.45265	2.20993	0.00000	7 5 1	1.08970	1.07339	0.00889
3 1 1	2.09576	1.94631	0.19231	5 5 5	1.08970	1.03148	-0.03563
2 2 2	2.01373	2.04377	0.29614	6 6 2	1.08278	1.06533	0.00676
4 0 0	1.79001	1.66180	0.00000	8 4 0	1.05570	1.03351	0.00000
3 3 1	1.68802	1.73088	0.03121	9 1 1	1.03601	1.02602	-0.00181
4 2 0	1.66140	1.65054	0.00000	7 5 3	1.03601	1.01534	-0.00607
4 2 2	1.57761	1.60106	-0.01598	8 4 2	1.02957	1.02058	-0.00178
5 1 1	1.52982	1.51402	0.02018	6 6 4	1.00435	0.96402	0.01968
3 3 3	1.52982	1.48814	-0.06310	9 3 1	0.98601	0.97805	0.00399
4 4 0	1.46483	1.45782	0.00000	8 4 4	0.95649	0.92878	-0.00067
5 3 1	1.43082	1.41525	-0.01683	7 7 1	0.93938	0.93927	-0.00848
6 0 0	1.42003	1.39180	0.00000	9 3 3	0.93938	0.92645	-0.00398
4 4 2	1.42003	1.35735	0.01466	7 5 5	0.93938	0.92460	0.03186
6 2 0	1.37885	1.38543	0.00000	10 0 0	0.93378	0.91396	0.00000
5 3 3	1.34961	1.32074	0.05274	8 6 0	0.93378	0.93555	0.00000
6 2 2	1.34013	1.31566	-0.00556	10 2 0	0.91183	0.88568	0.00000

4 4 4	1.30328	1.34138	0.06591	8 6 2	0.91183	0.90224	-0.00452
7 1 1	1.27669	1.27218	-0.00747	9 5 1	0.89584	0.87920	-0.00356
5 5 1	1.27669	1.28361	0.00164	7 7 3	0.89584	0.88085	-0.00748
6 4 0	1.26801	1.26616	0.00000	10 2 2	0.89061	0.87199	-0.00124
6 4 2	1.23414	1.23510	0.01034	6 6 6	0.89061	0.91990	0.01991
7 3 1	1.20959	1.19815	0.00273	9 5 3	0.85513	0.83573	0.00160
5 5 3	1.20959	1.23994	-0.01406	10 4 0	0.85023	0.83918	0.00000
8 0 0	1.17020	1.15888	0.00000	8 6 4	0.85023	0.84291	0.00618
7 3 3	1.14743	1.15166	0.00540	10 4 2	0.83101	0.81764	0.00071
8 2 0	1.13998	1.12708	0.00000	7 7 5	0.81700	0.82357	-0.01633
6 4 4	1.13998	1.13836	-0.03595	8 8 0	0.79438	0.77991	0.00000

Table 4-9 Atomic Form Factors of P in Crystals BP and AlP

(The shapes of the atoms is shown in Fig. 4-7)

(h k l)	Free P	P in BP		Free P	P in AlP	
	f_P	A	B	f_P	A	B
0 0 0	14.99930	16.55793	0.00000	14.99930	17.43472	0.00000
1 1 1	10.54285	10.79046	0.38798	11.37603	11.77166	0.21450
2 0 0	9.88776	9.87061	0.00000	10.72412	10.93565	0.00000
2 2 0	8.45403	8.13706	0.00000	9.17942	8.86657	0.00000
3 1 1	7.87365	7.64409	0.29838	8.54508	8.34967	0.24843
2 2 2	7.71763	7.75638	0.55707	8.38143	8.39219	0.41330
4 0 0	7.18639	6.99279	0.00000	7.85919	7.72273	0.00000
3 3 1	6.84440	6.99515	0.02929	7.54972	7.61364	0.08874
4 2 0	6.73729	6.81016	0.00000	7.45587	7.44605	0.00000
4 2 2	6.33544	6.41334	-0.06461	7.11117	7.20249	0.02388
5 1 1	6.05783	6.08186	-0.00463	6.87572	6.89739	0.04531
3 3 3	6.05783	6.03134	-0.14713	6.87572	6.91070	-0.06265
4 4 0	5.63388	5.62112	0.00000	6.51358	6.57635	0.00000
5 3 1	5.40047	5.37718	-0.02325	6.31087	6.35776	-0.02536
6 0 0	5.32592	5.31715	0.00000	6.24545	6.25431	0.00000
4 4 2	5.32592	5.22776	0.00933	6.24545	6.22594	-0.00727
6 2 0	5.04292	5.04986	0.00000	5.99367	6.05242	0.00000
5 3 3	4.84574	4.79228	0.07558	5.81463	5.80565	0.04308
6 2 2	4.78271	4.74881	-0.00411	5.75671	5.77789	-0.01592
4 4 4	4.54332	4.58194	0.11888	5.53346	5.58661	0.08575
7 1 1	4.37636	4.36619	-0.01172	5.37446	5.40872	-0.00423
5 5 1	4.37636	4.39303	0.00548	5.37446	5.41066	-0.00688
6 4 0	4.32296	4.32260	0.00000	5.32299	5.36188	0.00000
6 4 2	4.11999	4.13231	0.01002	5.12451	5.14383	0.01310
7 3 1	3.97829	3.96150	0.00387	4.98306	5.00224	-0.00583
5 5 3	3.97829	4.03720	-0.02745	4.98306	5.04609	0.00746
8 0 0	3.76045	3.74691	0.00000	4.76057	4.77424	0.00000
7 3 3	3.63988	3.64218	-0.00759	4.63459	4.66067	0.01572
8 2 0	3.60127	3.57886	0.00000	4.59379	4.61267	0.00000
6 4 4	3.60127	3.60495	-0.06597	4.59379	4.64112	-0.03142

6	6	0	3.45428	3.40261	0.00000	4.43633	4.41967	0.00000
8	2	2	3.45428	3.43538	0.00399	4.43633	4.43909	-0.00038
7	5	1	3.35142	3.32109	0.00260	4.32401	4.32911	0.01102
5	5	5	3.35142	3.28071	-0.08437	4.32401	4.30741	-0.06420
6	6	2	3.31846	3.27937	-0.00332	4.28762	4.30093	0.00907
8	4	0	3.19285	3.16859	0.00000	4.14715	4.14631	0.00000
9	1	1	3.10483	3.09238	0.00047	4.04689	4.05978	-0.00335
7	5	3	3.10483	3.06553	-0.01057	4.04689	4.06000	-0.01664
8	4	2	3.07661	3.06291	-0.00210	4.01441	4.02901	0.00142
6	6	4	2.96894	2.89908	0.02492	3.88894	3.86191	-0.00753
9	3	1	2.89338	2.88400	0.00077	3.79935	3.81055	0.00318
8	4	4	2.77653	2.74821	0.00400	3.65811	3.65311	-0.01652
7	7	1	2.71145	2.71982	-0.00478	3.57795	3.59666	-0.00475
9	3	3	2.71145	2.69941	-0.00744	3.57795	3.58956	-0.00302
7	5	5	2.71145	2.68974	0.04951	3.57795	3.56005	0.02215
10	0	0	2.69055	2.67107	0.00000	3.55196	3.55305	0.00000
8	6	0	2.69055	2.70065	0.00000	3.55196	3.56839	0.00000
10	2	0	2.61063	2.58993	0.00000	3.45149	3.44767	0.00000
8	6	2	2.61063	2.61151	-0.00212	3.45149	3.46594	-0.00829
9	5	1	2.55437	2.54118	-0.00482	3.37967	3.38293	-0.00173
7	7	3	2.55437	2.55875	0.00071	3.37967	3.37655	-0.01707
10	2	2	2.53628	2.52116	0.00086	3.35637	3.35703	-0.00214
6	6	6	2.53628	2.57888	0.05412	3.35637	3.38772	0.03734
9	5	3	2.41822	2.40160	0.00019	3.20185	3.20186	-0.00809
10	4	0	2.40250	2.39728	0.00000	3.18094	3.18966	0.00000
8	6	4	2.40250	2.41580	0.00326	3.18094	3.17972	0.01088
10	4	2	2.34228	2.33310	-0.00006	3.10004	3.10975	0.00110
7	7	5	2.29974	2.33167	-0.03125	3.04214	3.07820	0.00018
8	8	0	2.23344	2.21358	0.00000	2.95059	2.95935	0.00000

Table 4-10 Atomic Form Factors of Si in Crystals Silicon and SiC

(The shapes of the atoms is shown in Fig. 4-3)

(h k l)	Free Si	Si in Silicon		Free Si	Si in SiC	
	f_{Si}	A	B	f_{Si}	A	B
0 0 0	13.99760	12.08605	0.00000	13.99760	10.93196	0.00000
1 1 1	10.53580	10.42740	-0.18652	9.70060	9.65298	-0.07351
2 0 0	9.98741	10.07032	0.00000	9.16904	9.31371	0.00000
2 2 0	8.71774	8.89869	0.00000	7.96192	8.17279	0.00000
3 1 1	8.16939	8.30231	-0.13040	7.39333	7.50676	-0.05474
2 2 2	8.02007	7.94038	-0.25369	7.22799	7.23910	-0.12023
4 0 0	7.51252	7.63326	0.00000	6.63474	6.65278	0.00000
3 3 1	7.18849	7.15556	-0.08459	6.24129	6.19321	-0.03171
4 2 0	7.08737	7.14599	0.00000	6.11808	6.09479	0.00000
4 2 2	6.70841	6.60042	-0.01441	5.66039	5.55845	0.00632
5 1 1	6.44606	6.44638	-0.01190	5.35061	5.29703	0.00193
3 3 3	6.44606	6.25466	0.12631	5.35061	5.19826	0.06826

4 4 0	6.04285	6.06505	0.00000	4.89025	4.87651	0.00000
5 3 1	5.81904	5.78851	-0.01035	4.64396	4.60549	0.00491
6 0 0	5.74722	5.72851	0.00000	4.56640	4.52615	0.00000
4 4 2	5.74722	5.65686	0.07407	4.56640	4.50138	0.04081
6 2 0	5.47311	5.45704	0.00000	4.27706	4.25205	0.00000
5 3 3	5.28057	5.24597	0.10710	4.08028	4.05070	0.06884
6 2 2	5.21874	5.18635	0.01390	4.01824	3.99521	0.01716
4 4 4	4.98253	5.04888	0.14408	3.78642	3.80747	0.09629
7 1 1	4.81645	4.79272	0.00128	3.62838	3.60959	0.00432
5 5 1	4.81645	4.80133	-0.01530	3.62838	3.62363	-0.01800
6 4 0	4.76309	4.76926	0.00000	3.57849	3.58241	0.00000
6 4 2	4.55913	4.53596	0.02720	3.39171	3.38412	-0.00007
7 3 1	4.41559	4.40116	-0.00147	3.26405	3.25588	-0.00200
5 5 3	4.41559	4.45791	0.06642	3.26405	3.28312	0.02657
8 0 0	4.19296	4.17346	0.00000	3.07227	3.06153	0.00000
7 3 3	4.06866	4.06623	0.00848	2.96848	2.97725	-0.00301
8 2 0	4.02867	4.01485	0.00000	2.93560	2.92429	0.00000
6 4 4	4.02867	4.09386	0.00813	2.93560	2.97609	0.00024
6 6 0	3.87565	3.88653	0.00000	2.81203	2.82315	0.00000
8 2 2	3.87565	3.86511	-0.00145	2.81203	2.80468	-0.00039
7 5 1	3.76776	3.75693	-0.01435	2.72706	2.72140	-0.01786
5 5 5	3.76776	3.85401	-0.07082	2.72706	2.79064	-0.03405
6 6 2	3.73304	3.71806	0.00901	2.70009	2.67390	-0.01409
8 4 0	3.60005	3.59585	0.00000	2.59849	2.58401	0.00000
9 1 1	3.50619	3.49616	-0.00047	2.52840	2.51684	-0.00179
7 5 3	3.50619	3.52620	-0.00262	2.52840	2.51520	-0.01424
8 4 2	3.47596	3.46895	-0.00589	2.50611	2.49064	-0.00314
6 6 4	3.36010	3.40512	-0.05959	2.42194	2.42682	-0.03293
9 3 1	3.27824	3.27119	-0.00307	2.36365	2.34755	-0.00342
8 4 4	3.15066	3.15296	-0.01891	2.27477	2.26144	-0.02084
7 7 1	3.07907	3.06580	-0.01264	2.22590	2.20790	-0.01990
9 3 3	3.07907	3.07138	-0.00894	2.22590	2.20736	-0.00948
7 5 5	3.07907	3.07998	-0.07351	2.22590	2.21089	-0.04540
10 0 0	3.05599	3.04781	0.00000	2.21030	2.19215	0.00000
8 6 0	3.05599	3.05591	0.00000	2.21030	2.20366	0.00000
10 2 0	2.96735	2.95992	0.00000	2.15107	2.13505	0.00000
8 6 2	2.96735	2.95447	0.00153	2.15107	2.11951	-0.00562
9 5 1	2.90457	2.89604	-0.00518	2.10975	2.08693	0.00026
7 7 3	2.90457	2.91901	-0.00603	2.10975	2.08179	0.00724
10 2 2	2.88431	2.87681	-0.00277	2.09653	2.07947	-0.00164
6 6 6	2.88431	2.82583	-0.08639	2.09653	2.05327	-0.06180
9 5 3	2.75122	2.74267	-0.00922	2.01096	1.99043	0.00308
10 4 0	2.73339	2.72646	0.00000	1.99966	1.98497	0.00000
8 6 4	2.73339	2.72868	-0.03582	1.99966	1.96971	-0.00089
10 4 2	2.66478	2.65572	-0.00443	1.95654	1.93863	-0.00132
7 7 5	2.61606	2.56599	-0.05212	1.92623	1.88568	-0.01639
8 8 0	2.53967	2.53596	0.00000	1.87922	1.87500	0.00000

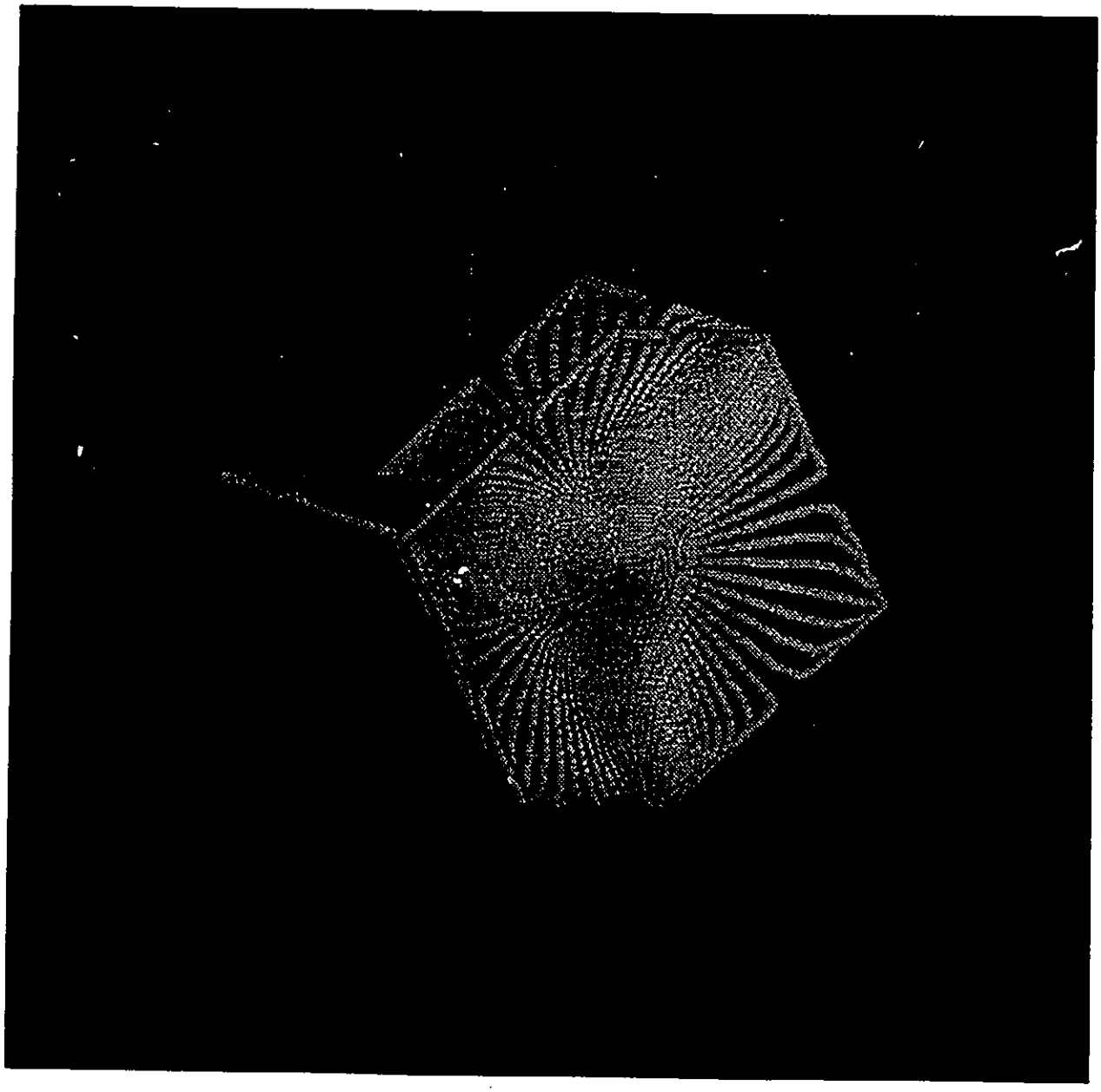

Fig. 4-4 Al in AlP.

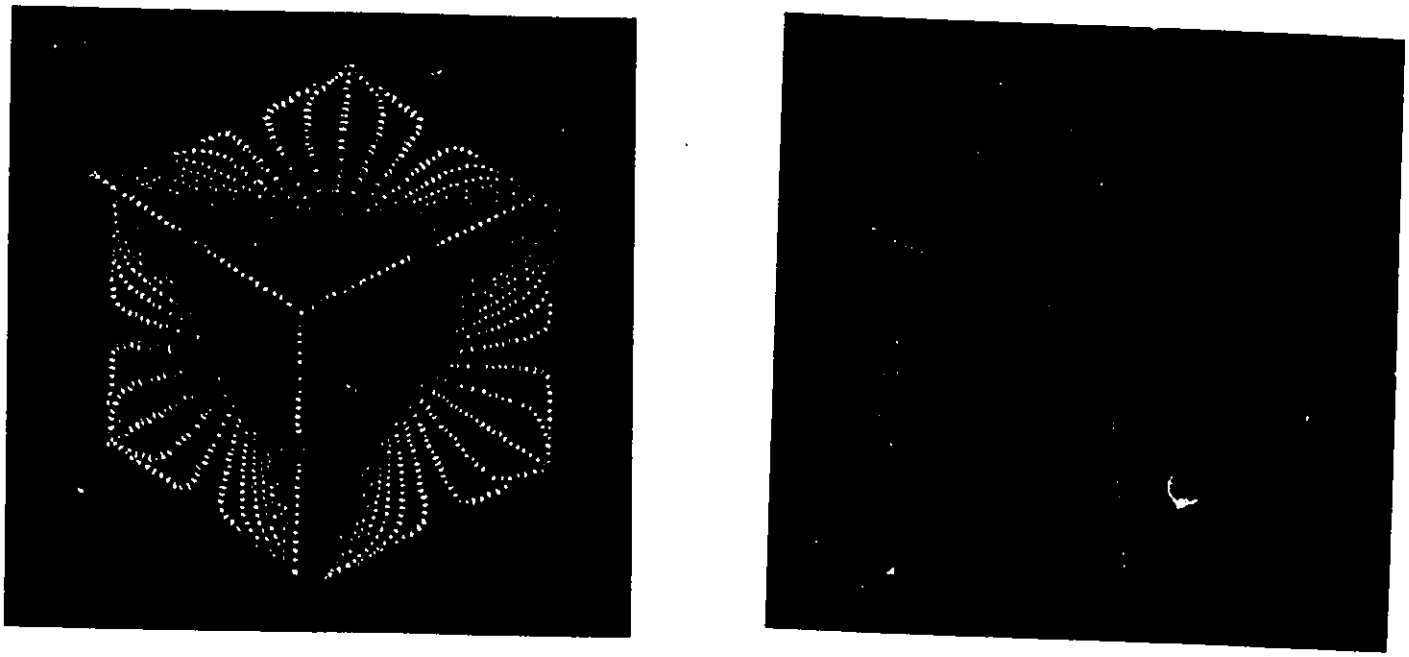

(a) (b)

Fig. 4-5 (a) B in BN, (b) B in BP.

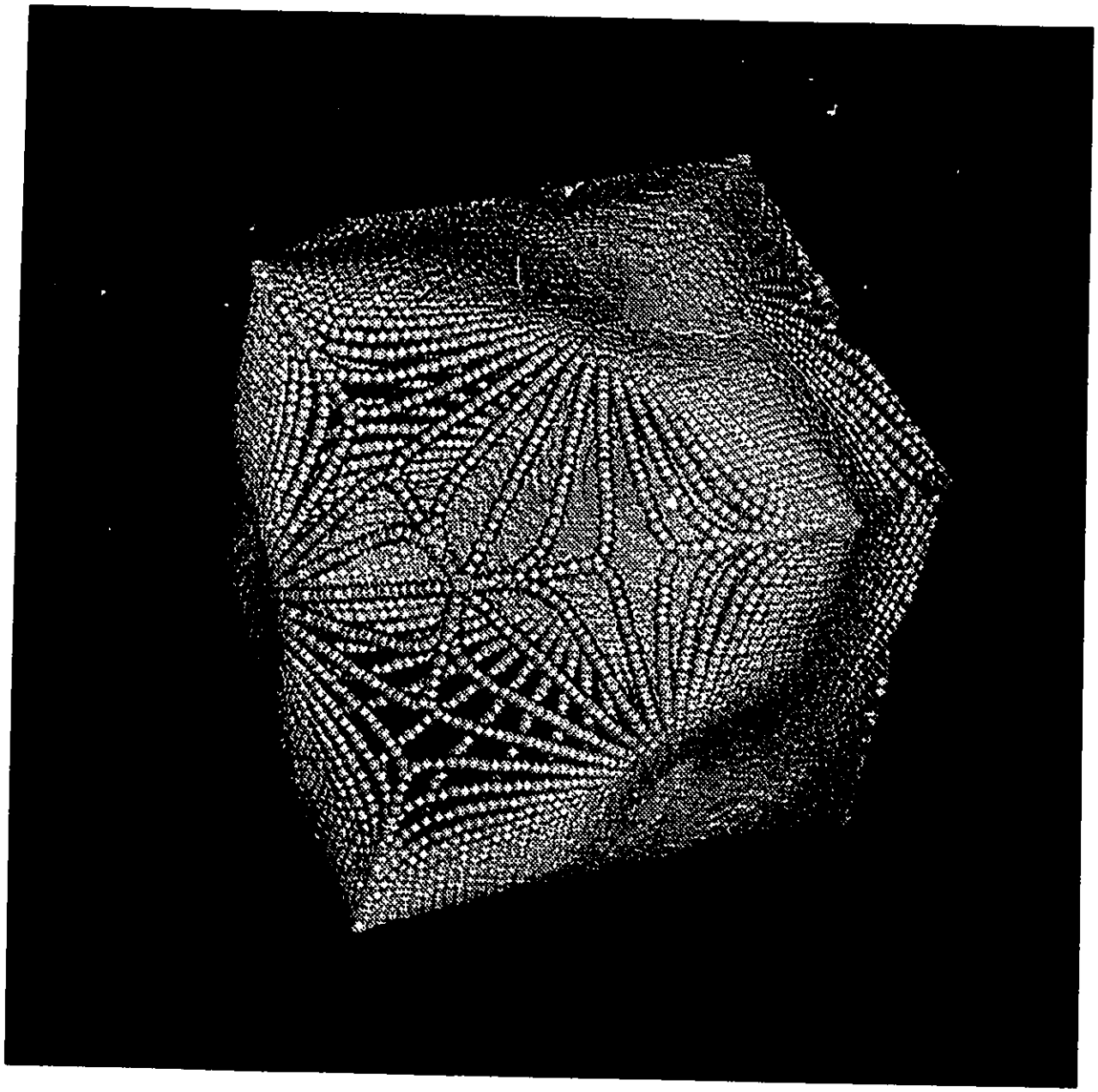

Fig. 4-6 N in BN

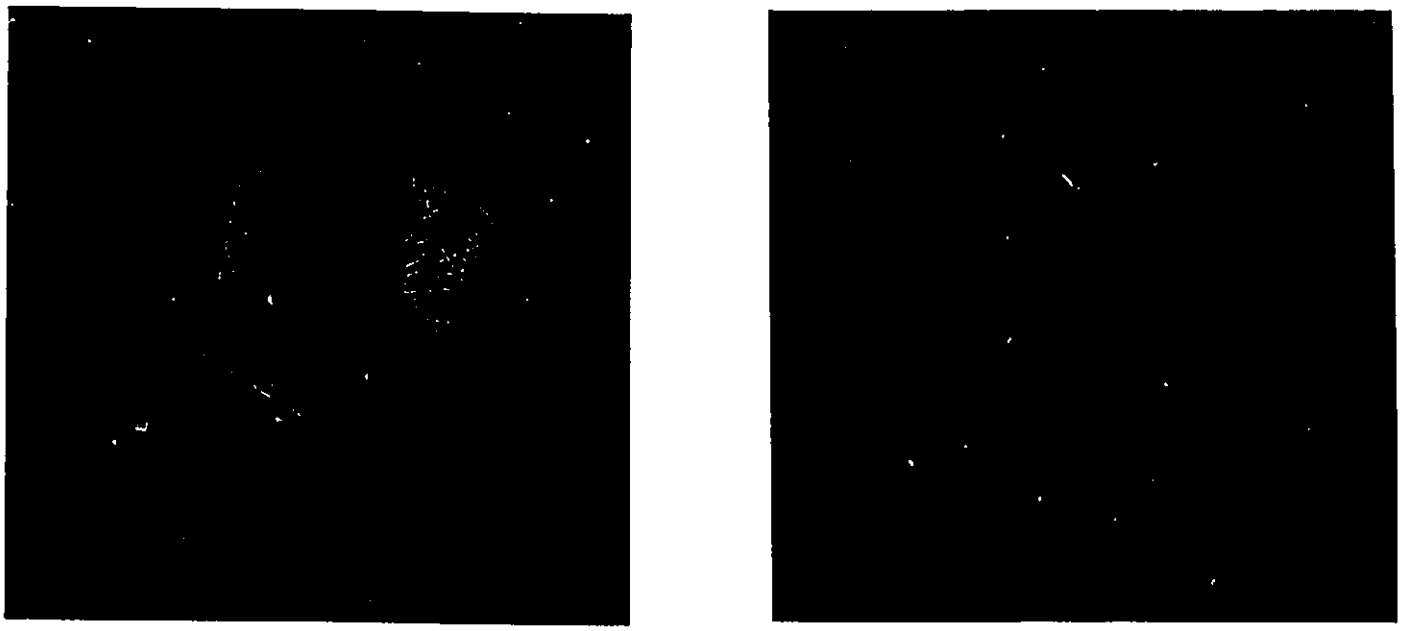

(a) (b)

Fig. 4-7 (a) P in AlP, (b) P in BP.

4.6. Electron Diffraction from a Crystal

Parallel to the development of the theory of elastic scattering of X-rays from a crystal, we will show in this section that the scattering amplitudes for high energy electron scattering can also be expressed in terms of contributions from the atomic form factors. These atomic form factors are determined by the atoms in crystals. The relationship between the x-ray and electron scattering factors will also be given in the present section. High energy for the incident electrons is assumed so that the elastic treatment can be used (Bonham and Fink, 1974).

The initial state for the incident electron and the electrons of the crystal is assumed as

$$|i\rangle = \exp(i\mathbf{k}\cdot\mathbf{r})\ \Psi(\mathbf{x}_1,\mathbf{x}_2,\ldots,\mathbf{x}_n) \tag{52}$$

where $\mathbf{k}$ refers to the wave vector of the incident electron and Ψ stands for the electron state of the crystal, $\mathbf{x}$ refers to the spin-space coordinates. The final state is

$$|f\rangle = \exp(i\mathbf{k}'\cdot\mathbf{r})\ \Psi'(\mathbf{x}_1,\mathbf{x}_2,\ldots,\mathbf{x}_n) \tag{53}$$

for the elastic scattering, $\Psi'=\Psi$. Here complications which are caused by the identity of the incident electron with one of the electrons in the crystal are ignored in eqns (52) and (53). This treatment is legitimate for a relatively fast electron (Bonham and Fink, 1974) because there is little overlap between the bound-state electron and the incident electron in the momentum space.

The interaction potential between the incident electron and crystal can be written as

$$V = -\sum_{\alpha}\frac{Z_\alpha e^2}{|\mathbf{r}-\mathbf{R}_\alpha|} + \sum_{i}\frac{e^2}{|\mathbf{r}-\mathbf{r}_i|} \tag{54}$$

where the first term on rhs is the interaction between the incident electron and the nuclei in the crystal, so the summation over α means over all the nuclei in the crystal, and the second term is the interaction between the incident electron and the electrons in the crystal.

In order to calculate the differential cross section for the elastic scattering of electrons by a crystal, one needs to evaluate the matrix element $\langle i|V|f\rangle$ =

$$\int d\mathbf{r}\exp(i\mathbf{q}\cdot\mathbf{r})\int\cdots\int d\mathbf{x}_1\Psi^*(\mathbf{x}_1,\mathbf{x}_2,\ldots,\mathbf{x}_n)\left\{-\sum_\alpha\frac{Z_\alpha e^2}{|\mathbf{r}-\mathbf{R}_\alpha|}+\sum_i\frac{e^2}{|\mathbf{r}-\mathbf{r}_i|}\right\}\Psi(\mathbf{x}_1,\mathbf{x}_2,\ldots,\mathbf{x}_n) \quad (55)$$

where $\mathbf{q}=\mathbf{k}'-\mathbf{k}$, the first integral is for the coordinates of the incident electron, the other integrals are for the spin-space coordinates of the electrons of the crystal. The electron-nucleus interaction term can be directly integrated because this term does not contain any coordinates of the crystal electrons

$$\int d\mathbf{r}\exp(i\mathbf{q}\cdot\mathbf{r})\int\cdots\int d\mathbf{x}_1\Psi^*(\mathbf{x}_1,\mathbf{x}_2,\ldots,\mathbf{x}_n)\left\{-\sum_\alpha\frac{Z_\alpha e^2}{|\mathbf{r}-\mathbf{R}_\alpha|}\right\}\Psi'(\mathbf{x}_1,\mathbf{x}_2,\ldots,\mathbf{x}_n)$$

$$= -\int d\mathbf{r}\exp(i\mathbf{q}\cdot\mathbf{r})\sum_\alpha\frac{Z_\alpha e^2}{|\mathbf{r}-\mathbf{R}_\alpha|} = -\frac{4\pi}{q^2}\sum_\alpha Z_\alpha\exp(i\mathbf{q}\cdot\mathbf{R}_\alpha) \quad (56)$$

where the integral formula $\int d\mathbf{r}\exp(i\mathbf{q}\cdot\mathbf{r})/r = 4\pi/q^2$ has been used. The electron-electron interaction term can be expressed in terms of the electronic charge distribution of crystal, therefore we have

$$\langle i|V|f\rangle = -\frac{4e^2\pi}{q^2}\sum_\alpha Z_\alpha\exp(i\mathbf{q}\cdot\mathbf{R}_\alpha)+e^2\int d\mathbf{r}\exp(i\mathbf{q}\cdot\mathbf{r})\int d\mathbf{r}'\rho(\mathbf{r}')/|\mathbf{r}-\mathbf{r}'|$$

$$= -\frac{4e^2\pi}{q^2}\sum_\alpha Z_\alpha\exp(i\mathbf{q}\cdot\mathbf{R}_\alpha)+\frac{4e^2\pi}{q^2}\int d\mathbf{r}\exp(i\mathbf{q}\cdot\mathbf{r})\rho(\mathbf{r})$$

$$= \frac{4e^2\pi}{q^2} F_{el}(\mathbf{q}) \tag{57}$$

where

$$F_{el}(\mathbf{q}) = \left\{ -\sum_{\alpha} Z_{\alpha} \exp(i\mathbf{q}\cdot\mathbf{R}_{\alpha}) + \int d\mathbf{r} \exp(i\mathbf{q}\cdot\mathbf{r})\rho(\mathbf{r}) \right\} \tag{58}$$

The differential cross section (Sakurai, 1985) is

$$d\sigma/d\Omega = \left| \frac{m}{2\pi\hbar^2} \langle i|V|f\rangle \right|^2 \tag{59}$$

Substituting eqn (57) into eqn (59) and noting the translational invariance of a crystal, the Laue diffraction equation can be derived and the differential cross section is found

$$d\sigma/d\Omega \propto |Q(\mathbf{H})|^2 \tag{60}$$

where $Q(\mathbf{H})$ is the electron scattering structure factor which can be written as

$$Q(\mathbf{H}) = \frac{2e^2m}{\hbar^2q^2} \left\{ \sum_{\alpha_0} Z_{\alpha_0} \exp(2\pi i\mathbf{H}\cdot\mathbf{R}_{\alpha_0}) - \int_{\Omega_0} d\mathbf{r} \exp(2\pi i\mathbf{H}\cdot\mathbf{r})\rho(\mathbf{r}) \right\} \tag{61}$$

where the summation α_0 is over the nuclei in the Bravais lattice unit cell where the origin is located and the integral is over the cell. Similar to the discussion given in section 4.4.2, eqn (61) can be written as the atomic contribution as

$$Q(\mathbf{H}) = \sum_{j} q_{j(\mathbf{H})} \exp(2\pi i\mathbf{H}\cdot\mathbf{R}_j) \tag{62}$$

where the electron atomic scattering factor $q_{j(\mathbf{H})}$ is given by

$$q_{j(\mathbf{H})} = \frac{2e^2m}{\hbar^2q^2} \{Z_j - f_j(\mathbf{H})\} \tag{63}$$

Equation (63) is the extension of the famous Mott-Bethe equation (Zuo, Spence and O'keeffe, 1988) which gives the relationship between the x-ray scattering

factor $f_j(\mathbf{H})$ and the electron scattering factor $q_j(\mathbf{H})$ in the situation of scattering by a free atom. In the case of forbidden reflections, the electron atomic scattering factors can be considered as contributed only by the electrons since the contributions of the scattering from the nuclei are cancelled out, thus we have

$$q_j^{\text{forbidden}}(\mathbf{H}) = -\frac{2e^2m}{\hbar^2q^2} f_j^{\text{forbidden}}(\mathbf{H}) \qquad (64)$$

Another feature about eqn (64) is that since Z_j is a point charge, and most of f_j contributes from the spherical portion, the difference will magnify the aspherical part. We can conclude that the electron scattering structure factors are more strongly influenced by the aspherical nature of the atomic charge distribution in the crystal than X-ray scattering from a crystal, that is the spherical model may not be a very good approximation for the treatment of experimental electron scattering data.

4.7. Conclusion

The atoms in molecules or crystals not only provide a theory to interpret the X-ray diffraction from a crystal but also enable us to quantitatively predict the diffraction intensities and their phase values. This new approach is especially valuable for estimating the amplitudes of *weak* diffractions which the spherical atomic model fails and much effort is needed for the other "fitting" models for the understanding. Both our new model and the spherical atom model will not have significant difference for the estimated amplitudes in the strong diffractions. At present, the extension of our elastic scattering theory to nonelastic scattering of both X-rays and electrons is

under study. The nonelastic scattering theory is the key to understand multiple scattering phenomenon (Chang, 1984; Van Hove, et al, 1986), for example LEED (Pendry, 1974; Van Hove, et al, 1986). The theory of atoms in crystals can not only provide a physical basis to qualitatively understand the phenomenon, but also yield a model to quantitatively estimate the diffraction intensities.

Defining a Wigner-Seitz cell in terms of the atoms in a crystal extends its usefulness and increases our understanding of the properties of crystals. Every property of an atom in a crystal is defined and each makes an additive contribution to the corresponding property of the total system. In accordance with the expectations of density functional theory (Hohenberg and Kohn, 1964), it is found that when the charge distribution of an atom is the same within two different systems or alternatively, at two different sites within a crystal, the atom makes the same additive contribution to the total value of every property in both systems (Riess and Münch, 1981; Bader and Becker, 1988). This behaviour is also found for field induced properties. Thus it has been demonstrated that the atoms of theory recover the volumes, energies, magnetic susceptibilities and polarizabilities (Wiberg, et al, 1987; Bader, et al, 1992a; Keith and Bader, 1992) of atoms in molecules that are measurable in those limiting situations where a series of molecules exhibits additivity relationships, thereby confirming that the atoms of theory are the atoms of chemistry. The atoms of theory are, by their very definition and by demonstration, the most transferable pieces of matter that can be defined in an exhaustive partitioning of real space (Bader, 1990; Chang and Bader, 1992; Bader, et al, 1992b). Thus the form factors for atoms and functional

groupings of atoms can be determined theoretically in calculations on relatively small systems and subsequently used in structure determinations of crystals containing the same functional groups. Even atoms in model systems can be used for this purpose. Thus as shown above, the charge density of the central carbon atom in *neo*-pentane, whose form is homeomorphic with that of a carbon atom in a crystal, can be used to estimate the phase and intensity of the forbidden (222) reflection in diamond. The method of atoms in crystals offers the opportunity of comparing directly the form and properties of an atom or group as it occurs in different systems. The tabulation of the properties of Wigner-Seitz cells in terms of their atomic contributions makes possible the quantitative determination of the degree of similarity between systems and their properties as determined by the distribution of charge at the atomic level. The similarity between atoms in a crystal and the atoms in the modelling molecules can be employed to predict the properties of the crystal, for example the cohesive energy.

While many properties are determined by $\rho(\mathbf{r})$ itself, there are increasingly successful attempts to obtain the first-order density matrix $\Gamma^{(1)}(\mathbf{r},\mathbf{r}')$ from experimentally measured structure factors (Massa, et al, 1985; Aleksandrov, 1989; Schmider, et al, 1992). The quantum stress tensor is determined by $\Gamma^{(1)}$ and this tensor totally determines the mechanics of an atom in a crystal (Bader, 1990), including the kinetic and potential energies of the electrons. The kinetic energy can in particular be obtained in this manner and by using the atomic virial theorem as obtained from eqn (15) with $\hat{G} = \mathbf{r}\cdot\mathbf{p}$, one can determine the energy of each atom in an equilibrium configuration of a crystal from the relation $E(\Omega) = -T(\Omega)$ and the total energy

of the crystal from their sum.

The zero-flux boundary always defines the physically relevant pieces of some total system; an amino acid fragment in a polypeptide, a molecule in a molecular crystal, precise specifications of Schottky and Frenkel defects and the change in the shapes of the the atoms bordering a vacancy. All quantum subsystems obey an equation of motion which is the analog of the one used in classical continuum mechanics, wherein the average Ehrenfest force exerted on the subsystem is expressed in terms of a stress tensor and current density (Bader, 1990). The theory of an atom in a crystal identifies models employed in the study of the solid state with bounded regions of real space and makes possible a quantum description of their behaviour.

REFERENCES

Aldred, P.J.E. and M. Hart, Proc. R. Soc. London Ser. A 332, 223 and 239(1973).

Aleksandrov,Y. V., V. G. Tsirelson, I. M. Reznik and R. P. Ozerov, Phys. Stat. Sol. 155, 201 (1989).

Alkire, R.W., W.B. Yelon and J.R. Schneider, Phys. Rev. B, 26, 3097(1982).

Angus, J.C., Thin Solid Films 142, 145(1986).

Angus, J.C. and C.C. Hayman, Science, 241, 913(1988).

Aurbach A., S. Kivelson and D. Nicole, Phys. Rev. Lett. 53, 411(1984); (E) 53, 2275(1984).

Auerbach A. and S. Kivelson, Nucl. Phys. B257, 799(1985).

Bader, R.F.W. and P.M. Beddall, J. Chem. Phys., 56, 3320(1972).

Bader, R.F.W. and T.T. Nguyen-Dang, Adv. Quantum Chem., 14, 63(1981).

Bader, R.F.W., T.T. Nguyen-Dang and Y. Tal, Rep. Prog. Phys., 44, 893(1981).

Bader, R.F.W. and H. Essen, J. Chem. Phys., 80, 1943(1984).

Bader, R.F.W., P.J. MacDougall and C.D.H. Lau, J. Am. Chem. 106, 1594(1984).

Bader, R. F. W., and Becker, P., Chem. Phys. Letters, 148, 452(1988).

Bader, R. F. W., J. Chem. Phys. 91, 6989 (1989).

Bader, R.F.W., *Atoms in Molecules - A quantum Theory*, Oxford University Press, Oxford, UK, 1990.

Bader, R. F. W., T. A. Keith, K. M. Gough and K. E. Laidig, Mol. Phys. 75, 1167 (1992a).

Bader, R.F.W., P. L. A. Popelier and C. Chang, J. Mol. Struct. (theochem) 255, 145 (1992b).

Bader, R.F.W. and P. A. L. Popelier, *Int. J. Quantum Chem.* 45, 189(1992).

Bader, R.F.W. and P.F. Zou, Chem. Phys. Lett., 191,54(1992).

Baldereschi, A., K. Maschke, A. Milchev, R. Pickenhain and K. Unger, Phys. Status Solidi B 108, 511(1981).

Benesh, G.A. and J.E. Inglesfield, J. Phys. C: Solid State Phys., 17, 1595(1984).

Berezin, F.A., *The Method of Second Quantization*, Academic Press, New York, 1966.

Bird, D.M., R. James and A.R. Preston, Phys. Rev. Lett. 59, 1216(1987)

Bonham R. A. and M. Fink, *High Energy Electron Scattering*, Van Nostrand Reinhold Company, New York, 1974.

Born, M. and E. Wolf, *Principles of Optics*, Pergamon Press, Oxford, 6th edition, 1980.

Bragg, W.H., Phil. Trans. Roy. Soc., A, 215, 153(1915).

Bragg, W.H., The intensity of X-ray reflection by diamond, Proceedings of the Physical Society of London 33, 301(1921).

Bundy, F.P. and J.S. Kasper, J. Chem. Phys., 46, 3437(1967).

Burke, P.G., C.J. Gillan and L. A. Morgan, in *Aspects of Electron-Molecule Scattering and Photoionization*, A. Herzenberg, ed., American Institute of Physics, New York, 1990.

Burke, P.G. and W.D. Robb, Adv. At. Mol. Phys., 11, 143(1975)

Burns, G. *Solid State Physics*, Academic Press, New York, 1985

Burns, G. and A.M. Glazer, *Space Groups for Solid State Scientists*, Boston, Academic Press, 1990.

Büttiker M., Y. Imry, R. Landauer and S. Pinhas, Phys. Rev. B **31**, 6207(1985).

Chang, S.-L., *Multiple Diffraction of X-Rays in Crystals*, Springer-Verlag, New

York, 1984

Chang, K.J. and M. L. Cohen, Phys. Rev. B 35, 8196(1987).

Chelikowsky, J. R. and M. L. Cohen, Phys. Rev. B, 10, 5095(1974).

Chang, C. and R. F. W. Bader, J. Phys. Chem. 96, 1654 (1992).

Change, L. L., L. Esaki, and R. Tsu, Appl. Phys. Lett. 2, 593(1974).

Chester, G. V., Rep. Prog. Phys. 26, 411(1963).

Christensen, N.E., S. Satpathy and Z. Pawlowska, Phys. Rev. B, 36, 1032(1987).

Cohen, M.L., Phys. Rev. B, 32, 7988(1985).

Cohen, M.L. and J.R. Chelikowsky, *Electronic Structure and Optical Properties of Semiconductors*, Springer-Verlap, New York, 1989.

Collard K. and Hall G.G., Int. J. Quantum Chem., 12, 623(1977).

Collins, D. M., Nature, 298, 49(1982)

Connerade J.P. and A.M. Lane, in *Aspects of Electron-Molecule Scattering and Photoionization*, A. Herzenberg, ed., American Institute of Physics, New York, 1990.

Craven, B.M., H.P. Weber and X. He, Tech. Report TR-87-2, Department of Crystallography, University of Pittsburgh, PA 15260 (1976).

Cummings, S. and M. Hart, Aust. J. Phys., 41, 423(1988)

Davies, E. B. , *Quantum Theory of Open System*, Academic, London, 1976.

Dawson, B., Proc. Roy. Soc. A 298, 255 and 264(1967)

de Broglie, L., *Heisenberg's Uncertainties and the Probabilistic Interpretation of Wave Mechanics*, Kluwer Academic Publishers, Boston, 1990.

Deutsch, M., Phys. Lett. A, 153, 368(1991).

Deutsch, M., Phys. Rev. B, 45, 646(1992).

Dirac, P.A.M. *Principles of Quantum Mechanics*, 1958, Clarendonn, Oxford.

Dovesi, R., M. Causa and G. Angonoa, Phys. Rev. B, 24, 4177(1981).

Dovesi, R., E. Ferrero, C. Pisani and C. Roetti, Z. Phys. B-Condensed Matter, 51, 195(1983).

Dovesi, R., C. Pisani, C. Roetti, M. Causà and V.S. Saunders, The Manual of *CRYSTAL 88*, QCPE Program No. 577, Department of Chemistry, Indiana University, Bloomington, IN, 1989.

Dykstra, C.E. and B. Kirtman, Annu. Rev. Phys. Chem.,41, 155(1990).

Eberhart, M.E., M.M. Donovan, J.M. Maclaren and D.P. Clougherty, Prog. Surface Science, 36, 1(1991)

Eberhart, M.E., M.M. Donovan and R.A. Outlaw, Phys. Rev. B, 46, 12744(1992)

Economou, E.N., *Green's Functions in Quantum Physics*, Springer-Verlag, New York, 1979.

Epstein, J., J.R. Ruble and B.M. Craven, Acta Cryst. B38, 140 (1982).

Ferraz A. C., M. I. T. Chagas, E. K. Takahashi, and J. R. Leite, Phys. Rev. B, 29, 7003(1984).

Ferraz, A.C., E. K. Takahashi, and J. R. Leite, Phys. Rev. B, 26, 690(1982).

Ferreira, L.G. and J. R. Leite, Phys. Rev. A 18, 335 (1978).

Feynman, R.P., Rev. Mod. Phys., 20, 367(1948)

Feynman, R.P., Phys. Rev., 76, 749(1949).

Feynamn, R.P., in *Variational Calculations in Quantum Field Theory*, eds. L. Polley and D.E.L. Pottinger, World Scientific, Singapore, 1988.

Field, J.E., *Properties of Diamond*, Academic Press, London, 1979.

Frensley, W.R., Phys. Rev. Lett. **57**, 2853(1986), (E) **60**, 1589(1986).

Frensley, W.R., Phys. Rev. B **36**, 1570(1987), (E) **37**, **10379**(1987).

Frensley, W.R., Rev. Mod. Phys. **62**, 745(1990).

Gillespie, R.J. and R.S. Nyholm, Quart. Rev. Chem. Soc., 11, 239(1957)

Gillespie, R.J., *Molecular Geometry*, Van Nostrand Reinhold, London, 1972.

Glauber, R.J., Phys. Rev. 131, 2767(1963)

Gordon, J. P., Phys. Rev. 161, 367(1967).

Greiner, A. and G. Mahler, Phys. Rev. 46, 7132(1992)

Haken, H., Rev. Mod. Phys. 47, 67(1975).

Haman, D.R., Phys. Rev. Lett. 42, 662(1979).

Hansen, N.K. and P. Coppens, Acta Cryst. A34, 909(1978).

Hehre, W.J., L. Radom, P.v. R. Schleyer and J. A. Pople, *Ab Initio Molecular Orbital Theory*, Wiley, New York, 1986.

Hirshfeld, F.L., Acta Cryst. B27, 769(1971).

Hirshfeld, F.L., Isr J. Chem. 16, 198(1977).

Hohenberg, P. and W. Kohn, Phys. Rev. 136, B864(1965).

Holden, A., *The Nature of Solids*, Columbia University Press, 1965.

Inglesfield, J.E. , J. Phys. C: Solid State Phys.4, L14(1971).

Inglesfield, J.E., J. Phys. C 14, 3795(1981).

Inglesfield, J.E., Rep. Prog. Phys. 45, 223(1982).

Inglesfield, J.E. and G. A. Benesh, Phys. Rev. B37,6682(1988) .

International Tables for X-Ray Crystallography, vol. I, The Kynoch Press, Birmingham, England, 1969; vol. IV, 1974. New edition: *International Tables for Crystallography*, vol. I, D. Riedel Publishing Company, Boston, 1983.

Ising, E., Z. Physik, 31, 253(1925).

Itzykson, C. and J.-M., Drouffe, *Statistical Field Theory*, vol. 1, Cambridge University Press, New York, 1989.

James, R.W., *The Optical Principles of the Diffraction of X-Rays*, Cornell

University Press, Ithaca, New York, 1965

Kato, W.A., Commun. Pure Appl. Math., 10, 151(1957).

Keith, T. A. and R. F. W. Bader, Chem. Phys. Letters 194, 1 (1992).

Khandekar, D.C. and S.V. Lawande, Phys. Rep., 137, 115(1986).

Kittel, C. *Introduction to Solid State Physics*, 6th ed., John Wiley & Sons, New York, 1986.

Klauder, J. R., Ann. Phys. 11, 123(1960).

Kohn, W., Phys. Rev. 87, 472 (1952).

Kohn, W. and L.J. Sham, Phys. Rev. 140, A1133(1965).

Koster G.F., in *Solid State Physics*, Eds. F. Seitz and D. Turnbull, vol. 5, 1957.

Kvam, E.W., J. Mol. Struct. THEOCHEM 213, 334(1991).

Landauer, R., Philos. Mag. **21**, 863(1970).

Lane, A. M. and R.G. Thomas, Rev. Mod. Phys., 30, 257(1958).

Lannoo, M. and J. Bourgoin, *Point Defects in Semiconductors*, vols. I and II, Springer-Verlag, New York, 1981.

Lax, M., Phys. Rev. 85, 621(1952).

Lax, M., *Symmetry Principles in Solid State and Molecular Physics*, Wiley, New York, 1974.

Lebowitz, J. I., Phys. Rev. 114, 1192(1959).

Lewis, G.N., J. Am. Chem. Soc., 38, 762(1916).

Li, K. H., Phys. Rep. 134, 1(1986).

Lino A. T., J. R. Leite, A. C. Ferraz, and E. K. Takahashi, J. Phys. Chem. Solids 48, 911(1987).

Liu, A.Y. and M.L. Cohen, Science 245, 841(1989).

Liu, A.Y. and M.L. Cohen, Phys. Rev. B 41, 10727(1990).

Loudon, G.M., *Organic Chemistry*, Addison-Wesley Publishing Company, Reading, Massachusetts, 1984.

Louisell, W. H., *Quantum Statistical Properties of Radiation*, Wiley, New York, 1973.

Lu, Z.W. and A. Zunger, Acta Cryst. A48, 545(1992).

Mandl F. and Shaw G., *Quantum Field Theory*, John Wiley & Sons, New York, 1990.

March, N.H. and B.M. Deb, *The Single-Particle Density in Physics and Chemistry*, Academic Press, New York, 1987.

Massa, L. J., M. Goldberg, C. A. Frishberg, R. F. Boehme, and S. I. La Placa, Phys. Rev. 55, 622 (1985).

Matyusenko, N.N. and V.E. Strel'nitskii, J. Exp. Theor. Phys. Lett. 30, 199 (1979).

Nesbet, R. K., Phys. Rev. B 30, 4230(1984).

Nesbet, R. K., Phys. Rev. B 33, 8027(1986).

Nesbet, R. K. and T. Sun, Phys. Rev. B 36, 6351(1987).

Nesbet, R. K., Phys. Rev. A 38, 4955(1988).

Newnham, R. E., *Structure-Property Relations*, Springer-Verlag, New York, 1975

Nieto-Vesperinas, M. *Scattering and Diffraction in Physical Optics*, John Wiley & Sons, New York, 1991.

Oppenheim, I., K. E. Shuler, and G. H. Weiss, *Stochasic Processes in Chemical Physics: The Master Equation*, MIT,Cambridge, MA, 1977

Onsager, L., Phys. Rev. 65, 117(1944).

Orlando, R. R. Dovesi, C. Roetti and V.R. Saunders, J. Phys.: Condens. Matter 2, 7769(1990).

Palatnik, L.S. , M.B. Guseva, V.G. Babaev, N.F. Savchenko and I.I. Fal'ko, Sov. Phys. JETP 60, 520(1984).

Parr, R.G. and W. Yang, *Density-Functional Theory of Atoms and Molecules*, Oxford University Press, New York, 1989.

Pauling, L., *The Nature of the Chemical Bond*, Cornell University Press, New York, 1960.

Pendry, J.B., *Low Energy Electron Diffraction*, Academic Press, New York, 1974.

Pisani, C., R. Dovesi and C. Roetti, *Hartree-Fock Ab Initio Treatment of Crystalline Systems*, Springer-Verlag, New York, 1988.

Planck, M., "Das Prinzip der kleinston Wirkung," (from Kultur der Gegenwart(1915)). The quoted paragraphy is from Yourgrau W. and S. Mandelstam, *Variational Principles in Dynamics and Quantum Theory*, Dover Publications, New York, 1979, on page 164.

Riess, J., and Münch, W., *Theoret.Chim. Acta*, 58, 295(1981).

Robertson, J., Prog. Solid St. Chem., 21, 199(1991).

Saka, T. and N. Kato, Acta Cryst. A42, 469(1986).

Sakata, M. and M. Sato, Acta Cryst. A46, 263 (1990).

Sakurai, J. J., *Advanced Quantum Mechanics*, Addison-Wesley Publishing Company, New York, 1987.

Sakurai, J. J., *Modern Quantum Mechanics*, Addison-Wesley Publishing Company, New York, 1985.

Sato T., Acta Cryst. A 48, 842 (1992).

Schlosser, S. and P. M. Marcus, Phys. Rev. 131, 2529(1963).

Schmider, H., V. H. Smith and W. Weyrich, J. Chem. Phys. 96, 8986 (1992).

Schrödinger, E., *Ann. d. Phys.* 79, 361 (1926).

Schwinger, J., Phys. Rev. 74, 1439(1948).

Schwinger, J., Phys. Rev. 82, 914(1952).

Schwinger, J., *Particles, Sources, and Fields*, vols. I-III, Addison-Wesley, New York, 1989.

Scully, M. O. and Lamb, W. E., Jr., Phys. Rev. 159, 208(1967).

Slater,J. C., Phys. Rev. 45, 794 (1934).

Slater, J.C., *Quantum Theory of Molecules and Solids*, vol. 2, McGraw-Hill, New York, 1965.

Slepian, D., thesis, Harvard University (1949).

Sollner, T. C. L. G., W. D. Goodhue, P. E. Tannenwald, C. D. Parker, and D. D. Peck, Appl. Phys. Lett. 43, 588(1983).

Spackman, M. A., Acta Cryst. A42, 271(1986).

Srebrenik, S., Int. J. Quantum Chem. Symp. 9, 375 (1975).

Srebrenik, S. and R.F.W. Bader, J. Chem. Phys. 63, 3945(1975).

Srebrenik, S., R.F.W. Bader and T.T. Nguyen-Dang , J. Chem. Phys. 63, 3945(1975).

Srinivasan, R. and S. Parthasarathy, *Some Statistical Applications in X-ray Crystallography*, Pergamon Press, New York, 1976.

Stewart, R.F., J. Chem. Phys. 51, 4569(1969).

Stewart, R.F., J. Chem. Phys. 58, 1668(1973).

Stewart, R.F., Acta Cryst. A32, 565(1976).

Stone, A.D. and A. Szafer, IBM J. Res. Dev. **32**, 384(1988).

Sun,T. and R.K. Nesbet, Phys. Rev. B 36, 6356(1987).

Szafer, A. and A. D. Stone, Phys. Rev. Lett. **62**, 300(1989).

Teworte, R. and U. Bonse, Phys. Rev. B 29, 2102(1984).

Van Hove, M.A., W.H. Weinberg and C.M. Chan, *Low-Energy Electron Diffraction*, Springer-Verlag, New York, 1986.

Wang, C. S. and D. M. Klein, Phys. Rev. B 24, 3393(1981).

Weast, R.C., M.J. Astle and W.H. Beyer, *Handbook of Chemistry and Physics* 67th ed., West Palm Beach, FL: CRC, 1987.

Webster, F. and J.C. Light, J. Chem. Phys.90,265(1989) and reference there.

Wei, S.H. and H. Krakauer, Phys. Rev. Lett. 55, 1200(1985).

Wei, J., J.M. Chang and Y. Tzeng, Thin Solid Films, 212, 91(1992).

Wentzcovitch, R.M., K.J. Chang and M.L. Cohen, Phys. Rev. B, 34, 1071(1986).

Weyrich, K.H., L. Brey and N.E. Christensen, Phys. Rev. B, 37, 1392(1988).

Wiberg, K. B., R. F. W. Bader and C. D. H. Lau, J. Am. Chem. Soc. 109, 1001 (1987).

Wigner E. and F. Seitz, Phys. Rev. 43, 804(1933).

Wolf, E. in *Coherence and Quantum Optics*, L. Mandel and E. Wolf, eds., Plenum Press, New York, 1973.

Wyckoff, R.W.G., *Crystal Structures*, 2nd edition, vol.1, Interscience Publishers, New York, 1965.

Yin, M.T. and M. L. Cohen, Phys. Rev. B 37, 26, 5668(1982).

Yin, M.T. and M. L. Cohen, Phys. Rev. Lett. 50, 1172(1983).

Yourgrau W. and S. Mandelstam, *Variational Principles in Dynamics and Quantum Theory*, Dover Publi tions, New York, 1979.

Zhang, S.B. and M.L. Cohen, Phys. Rev. B, 35, 7604(1987).

Zuo, J.M., J.C.H. Spence and M. O'Keeffe, Phys. Rev. Lett., 61, 353(1988).